DISSERTATION

ASSOCIATIONS BETWEEN WHITE MATTER MICRO- AND MACROSTRUCTURAL INTEGRITY, NEUROPHYSIOLOGY, AND MOTOR FUNCTION IN PEOPLE WITH MULTIPLE SCLEROSIS

Submitted by

Christopher Michael Patrick

Department of Health and Exercise Science

In partial fulfillment of the requirements

For the Degree of Doctor of Philosophy

Colorado State University

Fort Collins, Colorado

Summer 2025

Doctoral Committee:

Advisor: Brett W. Fling

Tod R. Clapp
Thomas J. LaRocca
Brian L. Tracy

ABSTRACT

ASSOCIATIONS BETWEEN WHITE MATTER MICRO- AND MACROSTRUCTURAL INTEGRITY, NEUROPHYSIOLOGY, AND MOTOR FUNCTION IN PEOPLE WITH MULTIPLE SCLEROSIS

Movement is one of the most fundamental expressions of brain function. From “simple” movements like reaching and walking to the most complex aerial gymnastic stunts, voluntary movement emerges from the seamless integration of sensory input, motor planning, and execution. Such integration relies on a symphony of widespread, dynamic communication across cortical, subcortical, brainstem, and spinal regions orchestrated to produce smooth, purposeful movement. In this way, the brain does not merely support movement, it is shaped by and for it. However, when the integrity of these neural systems is disrupted, as in neurodegenerative conditions like multiple sclerosis (MS), the consequences can be life altering, leading to impaired mobility, loss of independence, and diminished quality of life.

MS is a chronic disease of the central nervous system (CNS) that results in neural injury, impairing communication within neural networks. Damage to neurons and their connections gives rise to a range of heterogeneous symptoms, among which challenges with balance and mobility are among the most common and impactful. Understanding how MS-related damage to the CNS contributes to functional impairment requires tools that can capture different aspects of neural integrity and motor performance. This dissertation integrates biomechanical, neurophysiological, and neuroimaging approaches to characterize the state of the CNS in people with MS and to link these metrics to real-world movement abilities.

Using biomechanical techniques, the first study found that individuals with MS control their bodyweight differently during a sit-to-stand transfer movement, producing less force and power than neurotypical controls, with power helping to distinguish fallers from non-fallers. Building on this, the second study examined corticospinal integrity using neurophysiological measures, finding that altered excitability and prolonged conduction were associated with reduced force during both isolated muscle contractions and a sit-to-stand transfer movement, linking corticospinal function to movement performance. The third study used advanced neuroimaging techniques, including diffusion tensor imaging, diffusion kurtosis imaging, and fixel-based analysis, to assess corticospinal tract integrity in people with MS, revealing white matter alterations throughout the corticospinal tract. Among these methods, fixel-based metrics demonstrated the strongest associations with clinical measures of balance, disability, and neurophysiological outcomes. Finally, recognizing that the corticospinal tract is not the sole motor pathway, the fourth study examined the corticoreticulospinal tract and found that fiber density in this pathway correlates with balance and walking performance in people with MS.

Together, these studies illustrate the complex ways in which neural damage in MS disrupts the intricate networks essential for effective movement. By employing a multimodal approach, this work enhances understanding of how structural and functional changes across multiple motor pathways contribute to motor function. These insights may help inform future efforts to assess and manage mobility impairments in people with MS.

ACKNOWLEDGEMENTS

This journey was long, with twists and turns,
but I never walked alone.
Each stride was met with steady hands
that helped to guide my own.

To friends, to colleagues,
to the ones, always at my side.
Your strength became a guiding force
through every changing tide.

My mentors shared their wisdom's flame,
a lantern in the night.
While family kept me anchored firm
through days both heavy and light.

The journey's end was made complete
by those who saw me through.
This milestone isn't mine alone,
I owe it to ALL of you!

TABLE OF CONTENTS

CHAPTER 1 – REVIEW OF STRUCTURAL NEUROIMAGING TECHNIQUES IN MULTIPLE SCLEROSIS

Introduction

In the complex landscape of neurodegenerative diseases, multiple sclerosis (MS) presents a unique challenge. MS is a chronic, multifaceted neurological disorder that manifests in a wide range of symptoms, complicating both diagnosis and disease management. The disease is primarily driven by an immune-mediated inflammatory response resulting in hallmark lesions throughout the central nervous system (CNS). Within these lesions, immune cells attack and damage myelin, the protective sheath surrounding nerve fibers, disrupting communication between neurons in the brain and spinal cord.[1,2] While axons are relatively preserved in the early stages of MS pathology, axonal degeneration develops as the disease progresses.[3] The interplay between inflammation, demyelination, and neurodegeneration is highly individual, not only differing in severity but in the specific areas of the CNS affected and the degree of impact on function.[4,5] Variability in the extent and site of damage leads to highly diverse clinical presentations and trajectories of symptom progression, making MS especially challenging to study, understand, diagnose, predict, and manage effectively.

Variability in disease presentation is reflected in the wide range of symptoms experienced by individuals with MS. Common symptoms include fatigue, cognitive dysfunction, depression, muscle weakness and strength asymmetries, balance and mobility difficulties, visual impairment, bladder and bowel dysfunction, and sensory disturbances. [5–7] Symptoms can appear in isolation or in combination, fluctuating in severity or steadily progressing as MS advances.[5] The first diagnosis a patient typically receives is clinically isolated syndrome, which marks the first neurological

episode. Although clinically isolated syndrome is not a definitive diagnosis of MS, it can be an early indicator of the initial onset of MS.[8]

Clinically, MS is categorized into several subtypes primarily based on the pattern of disease progression. The most common form is relapsing-remitting MS, making up 85-90% of all diagnosed cases. Relapsing-remitting MS is characterized by episodes of symptom flare-ups that develop over hours or days and persist for weeks, followed by periods of partial or complete recovery.[9] Complete recovery is more common in the early stages of MS, however, as relapses and neural damage accumulate over time, partial recovery becomes more typical.[7,10] Notably, relapsing-remitting MS is three times more prevalent in females compared to males, and the average age of diagnosis is in the early 30s.[11,12] This relatively early onset in life contributes to MS being the leading neurodegenerative disease causing long-term disability in young adults.[13] Around 20% of individuals with relapsing-remitting MS will develop persistent neurological decline known as secondary progressive MS, typically 15-20 years following initial symptom onset.[7,14] Secondary progressive MS is marked by a steadier accumulation of impairment with the absence of remitting phases.[15] A smaller portion of MS diagnoses, roughly 5-15%, are categorized as primary progressive MS, marked by progressive decline from the onset of symptoms.[7,15]

In addition to these more common forms, progressive-relapsing MS represents a rare subtype found in less than 5% of patients in which both steady progression of symptoms and intermittent relapses with worsening symptoms are present without remission.[15] Even rarer, radiologically isolated syndrome, found in less than 1% of patients, describes individuals who possess identifiable CNS lesions via brain scans but do not have clinical symptoms.[16,17] Radiologically isolated syndrome has been suggested as a preclinical stage of MS, as half of those diagnosed will go on to develop relapsing-remitting or primary progressive MS, however, the other

half will remain asymptomatic.[18] Taken all together, MS presents with a wide range of symptoms that vary in severity level, and its progression spans a spectrum from relapsing-remitting to more aggressive forms. Given these complexities, significant efforts have been made to develop techniques and assessments that provide clinicians and researchers with reliable information to better diagnose, manage, and study the disease.

Currently, a single definitive diagnostic test for MS does not exist.[9] Instead, a comprehensive diagnosis is typically made by combining clinical evaluations, neuroimaging, and laboratory evidence following the McDonald criteria. The McDonald criteria are based on evidence of dissemination in time (evidence of MS across at least two different time points) and space (evidence in at least two different CNS locations).[19] Neuroimaging, particularly T2-weighted and gadolinium-enhanced magnetic resonance imaging (MRI), is used to detect lesions and specify their location in the CNS. Laboratory tests often include a lumbar puncture to analyze cerebrospinal fluid for the presence of oligoclonal bands, which are proteins that indicate the presence of neuroinflammation.[19]

First established in 2001, the McDonald criteria have been revised multiple times, most recently in 2017, with the goal of making the guidelines more accessible for clinicians to apply and allow for earlier diagnoses.[19,20] With substantial progress in the formation and discovery of disease-modifying therapies, early diagnosis has become a pressing issue in MS. Studies have shown that delayed administration of disease-modifying therapies is associated with an increased risk of disability. However, disease-modifying therapies also present unnecessary risks and are linked to morbidity in misdiagnosed patients. Together, these outcomes apply pressure on physicians to make decisions quickly while simultaneously weighing the risks and benefits of early

treatment.[21,22] Despite efforts to establish clear and distinct guidelines to aid the medical community in their evaluation of MS, the variability of the disease presents a formidable barrier.

Studies evaluating the 2017 McDonald criteria revisions have shown improvements in diagnostic sensitivity, ranging from 68 to 100%, but also highlight a decrease in specificity, ranging from 14 to 63%, compared to previous versions.[20,23] While increased sensitivity is beneficial for early diagnosis, improvements in technologies and approaches may hold the key to an optimal balance between early detection and limiting the number of misdiagnoses. To that end, the 40th Congress of the European Committee for Treatment and Research in Multiple Sclerosis recently proposed revisions to the 2017 version that aim to leverage advancements in imaging and molecular biomarkers with the explicit goal of enabling earlier diagnosis, facilitating timely treatment, and reducing misdiagnoses. As such, there is strong motivation within the neurodegenerative research community to develop and refine techniques that enhance our understanding of MS pathophysiology and offer insight into the neural substrates underlying clinical symptoms.

This review examines neuroimaging techniques used in MS research, with an emphasis on their ability to reveal structural abnormalities, such as lesions and microstructural damage, and their associations with clinical outcomes. The use of neuroimaging has several advantages: 1) it is non-invasive, thus mitigating patient risk; 2) it provides direct visualization of tissue and functional changes; and 3) it provides insights into both global and focal changes, as opposed to molecular biomarkers, which tend to only reflect systemic processes. While developments in biochemical biomarkers, such as oligoclonal bands, kappa free light chain, and serum neurofilament light chain, have shown promise as indicators of MS disease mechanisms and provide valuable complementary information, they fall outside the scope of this review. For recent discussions on biochemical

biomarkers, scholars are encouraged to consult these recent publications, Rocca et al. 2024 and Chertcoff et al. 2024.[24,25] This review aims to provide a comprehensive understanding of established and emerging non-invasive techniques used in MS that are central to efforts to better evaluate, manage, and understand MS.

Structural Imaging Techniques in MS

In 1868, Jean-Martin Charcot provided the first detailed description of MS, connecting clinical manifestations to the presence of multiple sclerotic plaques in the CNS. Using postmortem tissue samples, Charcot was responsible for identifying key histological properties, such as loss of myelin, that helped establish MS as a distinct disease.[26] Since direct examination of the brain is typically reserved for after death, the ability to view the brain for diagnostic and prognostic purposes is at the forefront of MS and other neurological disorders. Although it's important to note that no imaging technique directly measures underlying disease processes, structural neuroimaging, mainly through MRI, has become an essential tool heavily relied on in medical practice and research.

Conventional MRI techniques, such as T1-weighted and T2-weighted imaging, have become fundamental for identifying macroscopic lesions and quantifying physical metrics, including lesion load and brain atrophy. Advanced techniques such as diffusion tensor imaging, magnetization transfer imaging, and myelin water imaging enable more detailed assessments of white matter structural integrity, offering researchers valuable tools to investigate microstructural changes that may contribute to the pathophysiology and clinical heterogeneity of MS. Imaging biomarkers like the central vein sign can aid in diagnosing MS and paramagnetic rim lesions may be useful indicators of clinical outcomes. Finally, emerging imaging technologies, such as 7T MRI, are establishing new bounds for imaging resolution and may hold the key to improved diagnostic

accuracy. This section will explore these various structural imaging methods and their clinical and research applications in MS.

Conventional Imaging

Basics

Magnetic resonance imaging leverages the nuclear spin of hydrogen atoms (i.e., protons) to generate detailed images of the body's internal structures.[27] MRI is particularly well-suited for capturing brain images due to the brain's high water content and, thus, a large abundance of hydrogen atoms.[28,29] A standard 1.5T MRI system generates a magnetic field that is roughly 30,000 times stronger than Earth's.[30] In the presence of such a strong magnetic field, the intrinsic magnetic field of protons, which are naturally randomly oriented (Figure 1.1a), divides into two energy states – aligned parallel or antiparallel to the applied magnetic field (Figure 1.1b). The energy state aligned parallel to the strong magnetic field has a slightly lower energy level and is thus the slightly preferred energy state, creating an overall net magnetization aligned in the same direction as the strong magnetic field.[30]

Once a static magnetization alignment is established, a transient radiofrequency pulse is applied, knocking the protons out of the established alignment and into an orthogonal orientation (Figure 1.1c). As the protons return to the original static alignment state, they release energy, which is detected by MRI sensors (Figure 1.1d).[30] The signals collected from proton energy vary depending on the type of tissue, as gray matter, white matter, and cerebrospinal fluid each cause protons to return to their aligned state at different rates.[31–33] This process is repeated several times at different field strengths and frequencies to capture detailed images slice by slice, which are ultimately compiled into a three-dimensional image volume.[34,35]

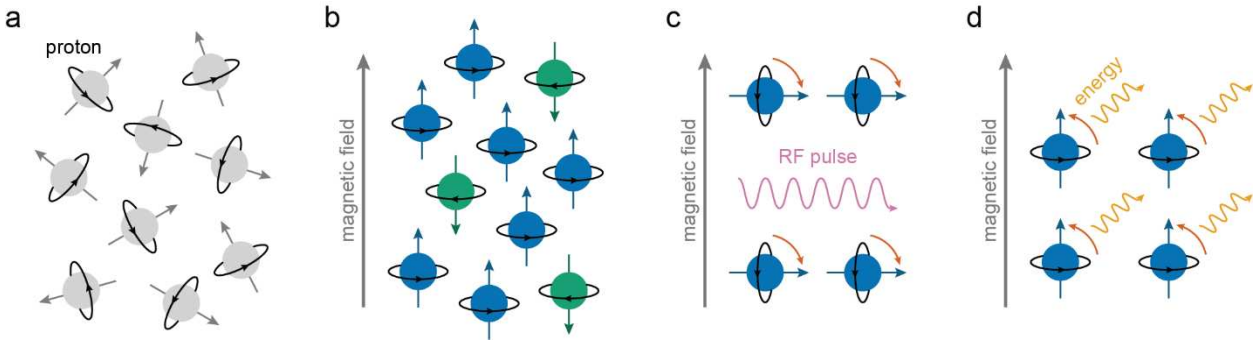

Figure 1.1. Basic Principles of Magnetic Resonance Imaging Signal Generation. Schematic of the fundamental steps involved in MRI. a) In the absence of a magnetic field, hydrogen protons in the body are randomly oriented. b) In the presence of a strong external magnetic field, protons align parallel or antiparallel to the field. c) A radiofrequency (RF) pulse temporarily tips the aligned protons into an orthogonal plane. d) As the protons return to alignment with the magnetic field, they release energy, which is detected and used to construct MR images.

T1- and T2-Weighted Images

The typical imaging protocol recommended for MS wields two fundamental MRI techniques, T1- and T2-weighted imaging (Figure 1.2).[36] These methods provide different contrasts based on the type of spin relaxation and the tissue environment surrounding the protons. T1-weighted imaging measures the time it takes for protons to realign with the applied static magnetic field after being bumped out of alignment by the radiofrequency pulse. During this process, known as T1 relaxation or longitudinal relaxation, the disrupted protons transfer their energy to surrounding molecules.[30] In myelin-rich areas, such as white matter, where there is a high presence of lipids and macromolecules, T1 times are short. Short T1 times are primarily due to the transient bonds formed between water molecules and surrounding macromolecules.[33] The formation of these bonds allows for efficient transfer of energy and rapid spin realignment, resulting in a bright contrast in T1-weighted images. Conversely, energy transfer is far less efficient in cerebrospinal fluid, where water is less restricted, and macromolecules are less abundant, resulting in longer T1 relaxation time and darker contrast in T1-weighted images (Figure 1.2a).[37,38]

T2-weighted imaging measures the time it takes for protons to lose spin coherence in the transverse plane following radiofrequency pulse excitation. Unlike T1, which reflects energy loss, T2 time refers to the loss of spin coherence, where nearby protons gradually fall out of phase with each other.[30] Similar to T1, T2 times also vary depending on the tissue environment. In white matter, proton movement is more restrictive, resulting in rapid dephasing and short T2 times. In areas with cerebrospinal fluid where water is less restricted, proton dephasing is more gradual, resulting in longer T2 times. The difference in how quickly protons fall out of phase creates the contrast in T2-weighted images, with areas of free water appearing bright and lipid-rich tissues appearing darker.[29,37,38] Importantly, neither T1- nor T2-weighted imaging directly measures specific cellular components. Rather, the detailed tissue contrast provided by both methods is a result of the interaction between the tissue environment and the nuclear spin of hydrogen atoms.

T1 and T2 imaging are critical tools in assessing MS, offering distinct yet complementary insights into key clinical and diagnostic markers. These imaging methods can quantify disease outcomes such as lesion count, volume, and location, as well as measures of brain atrophy. T2-weighted imaging is commonly used for the quantification of lesions in MS. Both acute and chronic lesions appear as hyperintensities due to the presence of increased water content in the affected areas, which is linked to pathological changes such as inflammation, edema, demyelination, gliosis, or axonal loss.[39,40] To enhance the visibility of lesions, most clinical MRI protocols include a Fluid Attenuated Inversion Recovery (FLAIR) sequence for MS patients. FLAIR sequences suppress the bright signal from cerebrospinal fluid, making lesions more easily identifiable, especially those located superficially. Studies have demonstrated that using FLAIR sequences enables the detection of up to four times as many lesions compared to standard T2-weighted imaging (Figure 1.2b).[41]

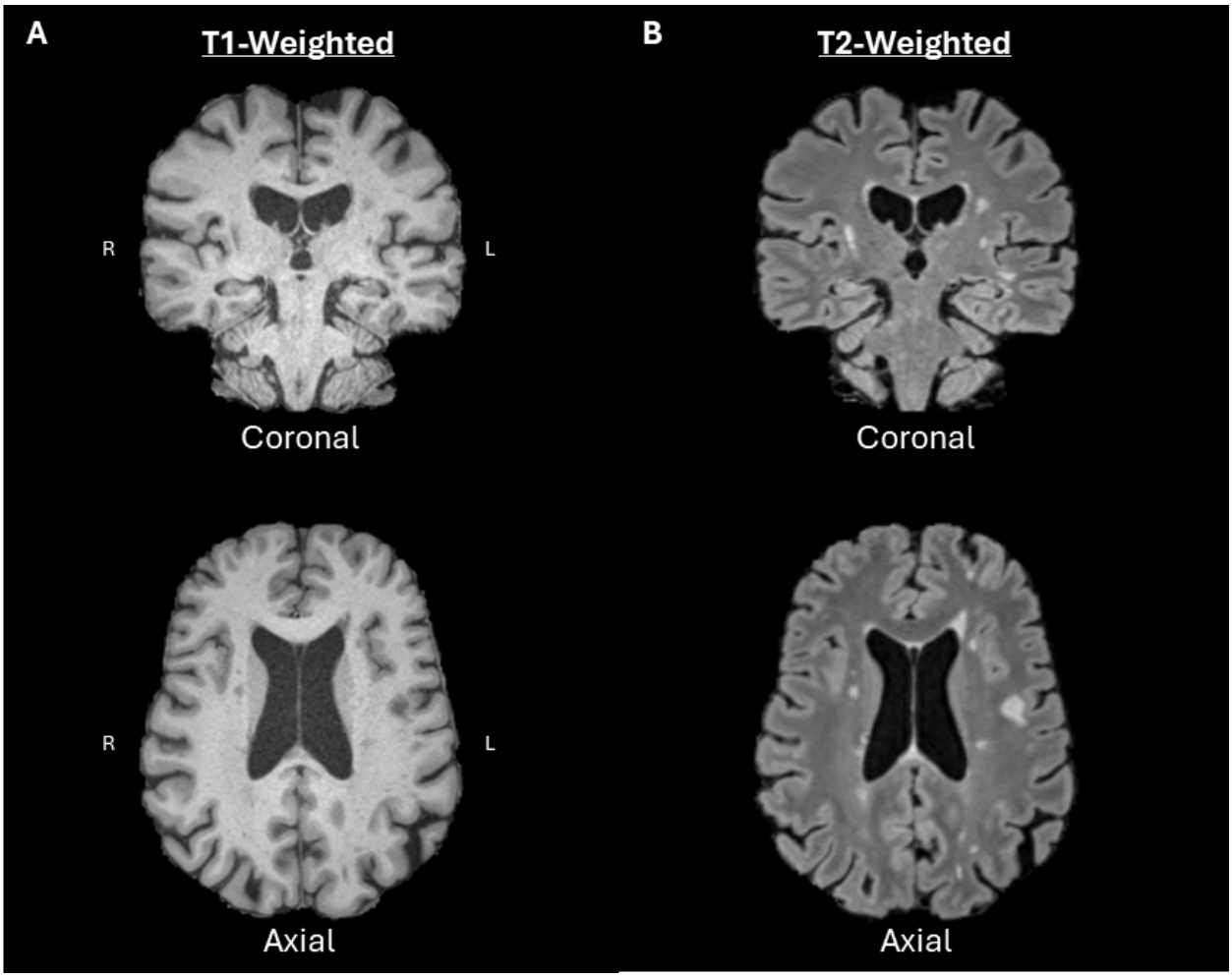

Figure 1.2. Example T1- and T2-Weighted MRIs in Multiple Sclerosis. Structural brain images highlighting differences in tissue contrast between MRI sequences. a) T1-weighted image from an individual with MS, shown in coronal (top) and axial (bottom) views, with lesions appearing hypointense. b) T2-weighted FLAIR image from the same individual, shown in coronal (top) and axial (bottom) views, with MS lesions appearing hyperintense.

Although these hyperintensities in T2 images are highly effective for flagging lesions, they are limited in that they cannot reliably distinguish between the severity or age of a lesion.[42] Approximately 10 – 20% of areas appearing hyperintense on T2-weighted images are also detectable on T1-weighted sequences, allowing for further classification of lesions based on their characteristics.[39] Lesions on T1-weighted images may appear as isointensities or as hypointensities, often referred to as "black holes". These hypointensities have been associated with significant tissue destruction and axonal loss, indicating areas of severe injury.[43] In addition to

severity, T1 images can also be used to characterize newly formed lesions with the aid of a contrasting agent, typically a gadolinium-based agent.[44] Gadolinium is a paramagnetic ion known for its high relaxivity, which significantly shortens nuclear spin relaxation times upon introduction to tissue.[45] This property makes gadolinium valuable in enhancing contrast for MRI, especially for T1 imaging.[46]

Gadolinium enhances the visibility of newly formed lesions in MRI due to its ability to cross a disrupted blood-brain barrier and is associated with active inflammation.[47,48] Blood-brain barrier dysfunction is an early mechanism of new lesion formation, occurring prior to the onset of symptoms and other MRI markers.[49–51] This disruption enables gadolinium to accumulate in areas of tissue damage, particularly in lesions where there is increased vascular permeability. As a result, newly formed lesions exhibit heightened contrast on T1-weighted images, aiding in their detection and characterization. Notably, only newly formed lesions are contrast-enhancing, and this enhancement fades as the lesions age.[46] This allows for tracking lesion development over time and distinguishes those that recover from those that evolve into persistent "black holes".

In summary, T1- and T2-weighted MRI are foundational techniques for detecting, characterizing, and quantifying lesions in MS. T2 imaging is highly sensitive to both acute and chronic lesions, revealing areas of inflammation and demyelination, while T1-weighted imaging, particularly with gadolinium enhancement, highlight active, newly forming lesions and can be tracked to identify chronic "black holes", indicative of severe tissue damage. Together, these imaging modalities provide essential insights into lesion burden, disease activity, and progression, making them indispensable for the diagnosis and monitoring of MS.

Clinico-Radiologic Paradox

Despite the ubiquitous use of T1- and T2-weighted imaging for diagnosing and monitoring MS, lesion load or total lesion volume has historically shown an inconsistent relationship with clinical outcomes. This discrepancy largely arises from the inherent variability in MS, as some patients may have many lesions without apparent signs of clinical manifestation. In contrast, others may display severe symptomology yet minimal lesion evidence. This disconnect between imaging findings and physical and cognitive symptoms is referred to as the clinico-radiologic paradox.[52–54]

Studies measuring T2 lesion volume have shown a wide range of correlation strengths with the Expanded Disability Status Scale (EDSS), a widely accepted clinical measure of disability in MS.[55] Reported correlation values range from 0.17 to 0.60 in cross-sectional studies and from 0.18 to 0.72 in longitudinal studies, reflecting the substantial variability in MS research outcomes.[56] Some studies have observed a plateau in the relationship between T2 lesion volume and EDSS scores above 4.5, suggesting that lesion load may lose its predictive value at higher levels of disability. However, other publications have not found a similar trend.[57,58] Further longitudinal studies have identified that T2 lesion volume captured early in MS correlates with long-term disability and clinical outcome.[59,60] Taken together, T2 lesion volume measured early in disease progression, when EDSS scores are low, may be a valuable tool for assessing and predicting future disability. However, its predictive value may diminish in patients with chronic disease, where lesion volume may no longer closely correspond with clinical outcomes.

T1 imaging with contrast is used to identify active lesions and is a strong predictor of future relapse, but the measured level of burden differs across clinical subtypes. Studies have reported that higher burden of enhanced lesions in relapsing-remitting and secondary-progressive MS

compared to primary-progressive MS.[61–63] T1 mapping of the accumulation of "black hole" lesions has been shown to correlate more strongly with disability than T2 lesion load, particularly in progressive forms of MS.[64] This suggests that evaluating "black hole" lesions may provide the most valuable insights into the disability experienced by patients.

The clinico-radiologic paradox in MS highlights the complex relationship between imaging findings and clinical symptoms. Several factors have been postulated for reasons underscoring the paradox: 1. Conventional MRI techniques are limited to identifying macroscopic lesions and cannot quantify damage in normal-appearing brain tissue. 2. Conventional imaging cannot readily distinguish the cause of the focal intensity in the image (edema, degeneration, inflammation, etc.). 3. Absence of spinal cord imaging. 4. MS lesions are dynamic and may regress or repair over time. 5. Total lesion volume over looks regional brain injury outcomes. 6. Clinical outcome measures, specifically the EDSS, may be limited.[56] Additionally, the timing of imaging assessments relative to disease progression and the specific imaging modalities used can further complicate the interpretation of lesion burden in relation to clinical outcomes. Given these challenges, there is a need to research and develop advanced imaging techniques and biomarkers that can more accurately reflect the underlying disease processes and their impact on patient outcomes.

Lesion Location

While total lesion volume may not be the strongest correlate of clinical outcomes in MS, due to the regionality of brain functions, efforts to connect lesion location to specific outcomes have shown promise. MS lesions can appear in any region of the CNS and typically populate both hemispheres of the brain. However, compared to other white matter disorders, MS tends to impact specific areas more frequently, including periventricular and juxtacortical white matter, the brainstem, the corpus callosum, and the cervical segment of the spinal cord.[65] These regions are

central to the McDonald criteria, which utilizes lesion location as a critical factor in confirming MS diagnoses through MRI, by helping to distinguish MS from other neurological disorders.[19] In addition to being relied on for diagnosing protocols, studies have shown that the specific location of lesions within the CNS plays a role in shaping clinical manifestations and may help explain the variability in symptom presentation among patients.

Research indicates that lesion locations in MS correspond to experienced symptoms, with lesions in specific areas leading to different clinical outcomes. For example, lesion locations associated with cognitive disabilities are distinct from those linked to physical disabilities.[66] Cognitive and motor outcomes in MS have been associated with lesion accumulation in anatomically plausible regions relating to brain function. Motor disability has been linked to lesions in the internal capsule, cerebellar peduncles, and pyramidal periventricular white matter.[66,67] Cognitive disability has been associated with commissural fiber tracts, putative superior longitudinal fascicle, and gray-white matter junctions of associative, limbic, and prefrontal cortex.[66–68] Studies comparing individuals with MS who experience cognitive impairment to those who do not strengthen the rationale for incorporating lesion mapping alongside lesion quantification. While patients with cognitive deficits often show a higher overall lesion load, their lesions tend to be more regionally concentrated. In contrast, individuals without cognitive impairment typically have a more widespread distribution of lesions. These findings suggest that the location of lesions, not just their total volume, plays a critical role in cognitive function.[68]

Although they are more challenging to detect, gray matter lesions are common in MS, despite the lower relative abundance of myelin in gray matter.[69,70] Most gray matter lesions are mixed lesions, affecting both white and gray matter at their junctions, however, lesions also present

as isolated within the cortex.[71] Cortical lesions are significantly challenging to visualize using MRI due to their subtlety and location. Many cortical lesions are missed even when a FLAIR sequence is employed.[72] Further intensity suppression can be achieved using a double-inversion recovery sequence, which quiets the white matter signals to improve lesion detection. However, many small cortical lesions remain elusive compared to findings in postmortem analyses.[73,74] Despite the challenges in detecting cortical lesions on MRI, they hold significant clinical relevance. Cortical lesions have been shown to have significant correlations with physical and cognitive impairments and can often be detected early in the disease course.[75–77] Some studies suggest that clinical outcomes may be more closely linked to the presence of cortical lesions than to those in deep white matter.[78] Further, research indicates that gray and white matter lesions may develop independently, each providing distinct information about disease progression and outcomes.[78,79] Collectively, the identification of both gray and white matter lesions is crucial for a comprehensive understanding of MS and its clinical implications.

Focal lesion formation is not confined solely to the brain, spinal cord lesions can also significantly contribute to clinical manifestations. Most patients with MS exhibit spinal cord hyperintensities, which tend to be more symptomatic than brain lesions and show strong correlations with physical disability.[80–82] Spinal cord lesions are valuable for diagnosis and prognosis. Although not formally included in the McDonald criteria as a diagnostic lesion location, they can still be used as evidence of dissemination in space and are uncommon in other neurological disorders, making them useful for distinguishing MS.[19,83] These lesions are also strong predictors of long-term disability and are particularly effective in identifying individuals at high risk of progressing from clinically or radiologically isolated syndrome to MS.[84–86] Despite their importance, spinal cord imaging is not always part of standard clinical practice and has

historically been challenging due to the cord's smaller size, complex anatomy, and added imaging time.[87,88] Currently, spinal cord imaging is recommended in the presence of spinal cord-related symptoms, when considering MS in a population where MS is less prevalent, or when additional information is needed to increase diagnostic confidence.[19]

Atrophy

Multifocal lesions are well-known as the primary physiological hallmark of MS. However, other neurodegenerative traits are commonly observed and should be quantified to understand disease outcomes better. Specifically, brain atrophy, characterized by a reduction in brain volume, has been associated with disease progression. The global brain atrophy rate in MS is significantly higher than in healthy controls, with estimates ranging from 0.5% to 1.35% per year, compared to 0.1% to 0.3% per year, respectively.[89] While the atrophy rate may slow with the use of disease-modifying therapies, it occurs across all stages of the disease, including in patients with clinically isolated syndrome, and is most pronounced in progressive subtypes as atrophy accumulates.[90–93] Measures of brain volume obtained from early scans provide predictive value for short-, mid-, and long-term declines in function.[94–97]

Atrophy has been associated with neurodegenerative biomarkers and axonal loss and is correlated with overall disability, as well as physical and cognitive impairments.[98–101] Moreover, with advancements in computational technology, measuring brain atrophy can now leverage semi-automated processes, making it feasible and efficient for research and clinical use. Multiple software packages are available that provide tools for quick, precise, and repeatable assessments that are relatively easy to implement.[102]

The mechanisms underlying atrophy are still being unraveled, as conflicting reports exist regarding its association with lesions. Evidence suggests separate mechanisms might be at play,

as atrophy can develop in the absence of lesion formation, and some research has shown a lack of association between active lesions and brain volume.[103,104] Other studies have found associations between lesion load and atrophy, particularly in the early stages of MS, but also suggest that this relationship may diminish over time.[105] Comparisons between lesion load and atrophy may also be limited by the shortcomings of traditional lesion measurements, as current imaging techniques often miss smaller, microscopic injuries and cortical lesions. Overall, the relationship between lesion load and atrophy is likely dynamic and not entirely independent of each other.

Caution should be exercised when interpreting measures of global atrophy, as numerous confounding factors, including age, lifestyle, cardiovascular disease, diabetes, genetics, and medication, can influence brain volume.[106] Additionally, like global lesion measurements, global atrophy measures may lack the sensitivity of more localized, regional analyses. Atrophy occurs in both gray and white matter of the brain and spinal cord, and the rates of atrophy are not uniform across the CNS. Atrophy in the brain's white matter is common in the corpus callosum, corticospinal tract, and longitudinal fibers.[107,108] In gray matter, several studies have documented differences across various brain cortices, suggesting that atrophy may occur in a specific order, depending on the disease phenotype and duration. For example, in relapsing-remitting MS, initial atrophy has been observed in the posterior cingulate cortex and precuneus, with subsequent involvement of the middle cingulate cortex, brainstem, and thalamus.[109] When modeling physical dysfunction, the best results were achieved by including the cortical thickness of the bilateral sensorimotor cortices and the bilateral insula. In the same study, the most accurate model for cognitive dysfunction included the bilateral posterior cingulate cortex and the bilateral temporal pole.[110]

In addition to cortical changes, alterations in deep gray matter structures are associated with MS progression. Atrophy has been observed in regions such as the caudate, putamen, pallidum, nucleus accumbens, and thalamus.[111] Among these, thalamic atrophy is particularly notable, indicating that the thalamus is a key region where structural decline closely aligns with clinical symptoms.[112] Thalamic atrophy may hold prognostic value, as it is observed in individuals with clinically isolated syndrome and is predictive of conversion to MS.[113,114] Additionally, thalamic volume has been linked to overall disability, cognitive impairment, and even aerobic fitness level.[112,114–116]

Spinal cord atrophy, similarly, shows a strong association with disability and, in particular, physical impairment. MS patients tend to have smaller spinal cord cross-sectional areas compared to healthy controls, with those experiencing greater disability and longer disease duration exhibiting more pronounced atrophy.[80,117] Additional evidence supports spinal cord atrophy as a significant feature in MS, with studies reporting axonal density losses of up to 65%.[118] Further, spinal cord volume is associated with disability in MS independently of brain atrophy and lesion load.[119] Altogether, tracking region-specific atrophy from the early stages of MS through the course of the disease may offer insights into patient symptomology and disability progression.

Imaging Normal-Appearing Brain Tissue

So far in this review, we have covered lesions and atrophy observed at the macroscopic, regional, and global scale in MS. However, postmortem histopathological studies show that MS also causes diffuse neurodegeneration in non-lesion locations, termed normal-appearing brain tissue, which is not easily detectable using conventional MRI techniques. Signs such as inflammatory infiltrates, microedema, diffuse microglial, widespread axonal damage, and gliosis are observed in this seemingly unaffected tissue.[79] Depending on the severity and extent, these

processes can disrupt neural communication and lead to neural injury.[79,120,121] Research suggests that these areas of dysfunction may precede new lesion development, forming preactive lesions, and their study may offer deeper insights into the underpinnings of clinical outcomes in MS.[122,123]

Traditional MRI, with imaging resolutions and sensitivities typically in the range of 1-3 mm, can miss these microstructural changes, thereby limiting our ability to fully understand the extent of neuronal damage. The lack of sensitivity in standard imaging methods means that these subtle changes in normal-appearing brain tissue go unmeasured. Given these limitations, researchers have turned to advanced MRI techniques, such as diffusion weighted imaging and magnetization transfer imaging, to better understand non-lesional damage and its relationship to clinical outcomes in MS.

Diffusion Weighted Imaging

Basics

With conventional MRI, images of brain structures are captured based on the density and relaxation properties of hydrogen protons, providing contrast between tissue types and macroscopic structures. Diffusion MRI (dMRI) extends this capability by leveraging the directional movement of water molecules, or diffusion, to provide insights into tissue's microstructural properties. Outside the body, water molecules, without restrictions, exhibit constant, random Brownian motion, representing uninhibited or free diffusion (Figure 1.3a). In contrast, water movement within biological tissues is typically restricted due to interactions with cell membranes and other macromolecules (Figures 1.3b and c).[124] Whether in extracellular, intracellular, or intravascular spaces, the surrounding cellular architecture affects the extent and direction of water molecule diffusion, ultimately defining the dMRI signal.[125] Accordingly, the degree of diffusion restriction is inversely correlated with cell density and membrane integrity in

biological tissue (Figures 1.3b and c).[126] Notably, the typical water displacement distance during diffusion measurement is estimated at 8–10μm, roughly the average size of cells in the human body. This suggests that, in principle, dMRI has the sensitivity to probe cellular microstructure in vivo.[127]

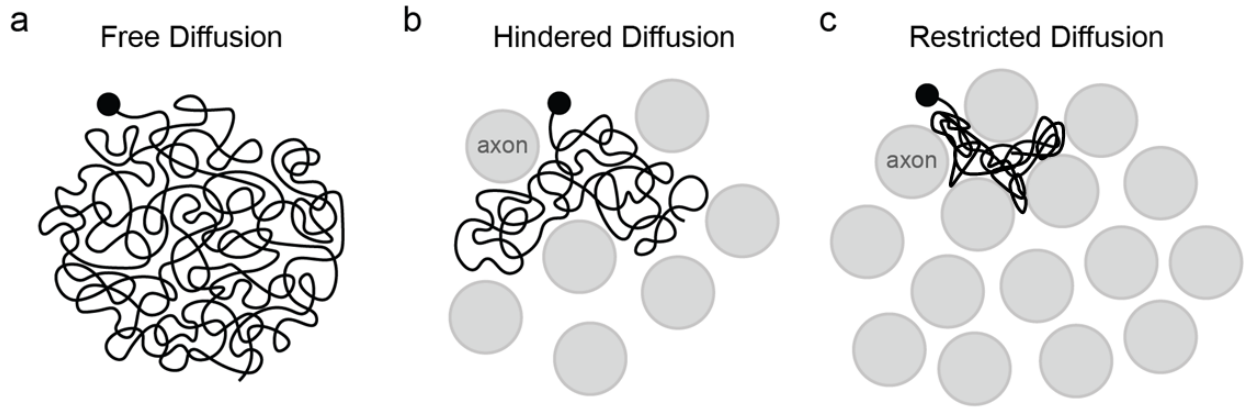

Figure 1.3. Representation of Water Diffusion. Schematic illustrating how extracellular water molecule movement varies across different microstructural environments, forming the basis of dMRI. a) Free diffusion, water molecules move randomly without barriers, as in cerebrospinal fluid. b) Hindered diffusion, water movement is partially constrained by cellular structures such as sparsely distributed axons. c) Restricted diffusion, water is tightly confined by densely packed axons, limiting displacement and producing strong diffusion anisotropy.

The dMRI sequence is largely adapted from T2-weighted MRI sequences. In dMRI, two diffusion-sensitizing gradients are added around radiofrequency pulses to identify water movement within tissues.[128] These two applied gradients shift the alignment, or phase, of proton spins, depending on their motion. For example, water molecules that are highly restricted and stationary are largely unaffected as the two gradients cancel, and high signal intensity is preserved during both gradient applications. However, for less restricted water molecules, the first gradient shifts their phase, and then, because the molecules have moved in space by the time the second gradient is applied, their phase isn't fully restored, leading to a drop in signal.[128–130] By applying gradients in multiple directions within an MRI acquisition, dMRI provides a map of diffusion strength and direction across the brain. The differing phase responses of unrestricted and restricted

water molecules enable the measurement of cellular density and structural integrity differences in various tissues and between populations.

Within the CNS, myelin acts as a strong barrier to water motion, and especially in white matter where myelinated axons are aligned, it creates a non-uniform water diffusion direction distribution called anisotropic diffusion.[131] Contrastingly, in the ventricles, where cerebrospinal fluid is present without many cells or surrounding structure, diffusion more closely resembles free diffusion, which is a uniform movement distribution across all directions, or isotropic.[132] Gray matter fits in the middle of this spectrum as it contains high cell density but also lacks uniform direction and contains unique structures, such as cell bodies that return more isotropic signals. [132–134]

By understanding the distinct diffusion characteristics of different brain tissues and regions, dMRI can highlight subtle microstructural alterations associated with early disease stages or minor injury, including differences in normal-appearing white matter. Abnormal diffusion patterns can signal compromised tissue, as seen in stroke, tumors, traumatic brain injury, and neurodegenerative conditions such as MS, where diffusion characteristics deviate significantly from typical healthy patterns.[124,135–139] Through its sensitivity to microstructure, dMRI has become a valuable tool for assessing brain health and structural connectivity, providing researchers with insights into regions and pathways that may appear unaffected on conventional MRI.

Diffusion Tensor Imaging

To fully harness the power of dMRI, models are needed to help quantify and interpret the complex data captured during imaging. One of the most widely used models is diffusion tensor imaging (DTI), which quantifies the diffusion of water molecules by representing them as tensors. A tensor is a multi-dimensional array that encapsulates directional information, allowing DTI to

capture the degree and directionality of water diffusion within each imaging voxel (Figure 1.4).[140] To obtain a reliable diffusion tensor within a 3D space, DTI imaging sequences must capture data across at least six directions in addition to an image with no diffusion weighting.[141] In DTI, the diffusion of water is modeled as an ellipsoid, where the principal axes correspond to the predominant directions of water movement. This tensor ellipsoid can be characterized by three eigenvectors, representing the extent of diffusion along three orthogonal axes, providing a comprehensive picture of water diffusion within the voxel (Figure 1.4).[132] When the eigenvalues associated with these vectors are similar in magnitude, diffusion is isotropic, occurring equally in all directions (Figure 1.4a). In contrast, diffusion is anisotropic when one eigenvalue is significantly larger than the other two, indicating a preferred direction of water movement (Figure 1.4b).[132]

From the tensor representation, several metrics can be derived to describe the underlying water movement and subsequent interpretation of microstructure. The most commonly used metrics are mean diffusivity (MD), axial diffusivity (AD), radial diffusivity (RD), and fractional anisotropy (FA).[142] MD is the average of all three eigenvalues and represents a directionless measure of the average rate of water diffusion within a voxel. MD is often used as a general measure of tissue integrity in white matter, where lower MD values correlate with more intact tissue and higher values with tissue damage.[142] AD measures diffusion along the primary direction and is often associated with axonal integrity in white matter, where lower AD values are correlated with axonal loss.[143,144] RD quantifies diffusion perpendicular to the primary direction and is calculated as the average of the secondary and tertiary eigenvalues. RD has been linked to structural organization and demyelination, where higher values generally indicate reduced structural integrity.[145–147]

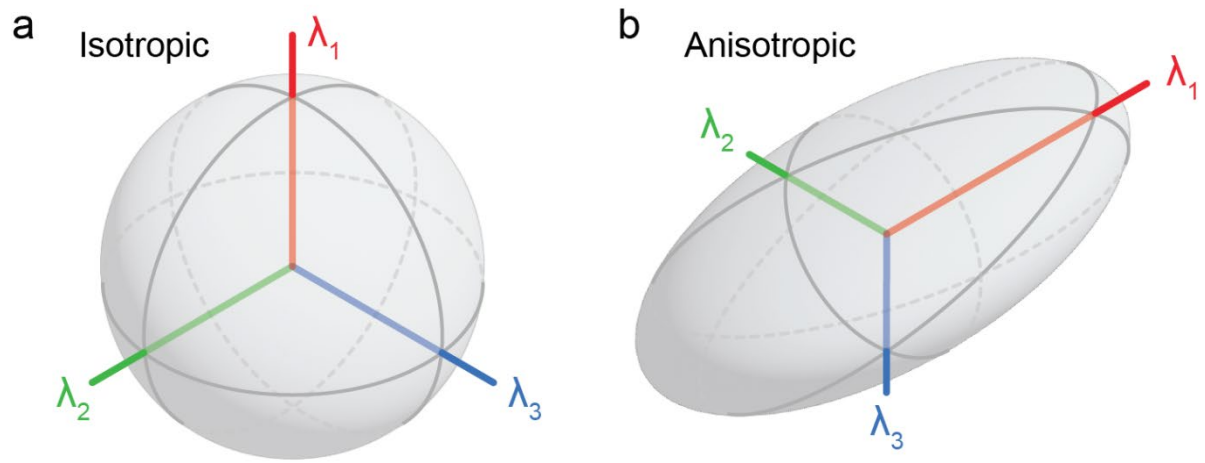

Figure 1.4. Diffusion Tensors. Tensors model the direction and magnitude of diffusion. a) An isotropic tensor, visualized as a sphere, represents equal diffusion in all directions. The associated eigenvectors are of roughly equal length, indicating no primary direction of diffusion. b) An anisotropic tensor, shown as an elongated ellipsoid, reflects directional diffusion. One of the associated eigenvectors is significantly longer, indicating greater diffusion along the principal direction.

FA measures the degree of anisotropy of water diffusion calculated on a scale of 0 to 1, where 0 is isotropic and 1 is anisotropic. FA is the most frequently used DTI metric and is primarily used as a summary metric for structural integrity, where higher values indicate better integrity.[142] Studies have recommended the utility of analyzing all 4 metrics collectively to distinguish diffusion patterns and infer underlying physiology.[148,149] Although DTI is one of the most widely used diffusion models and histopathologic correlations have been explored for its metrics, it's crucial to recognize that, like conventional MRI, DTI does not directly measure cellular structures. Changes in DTI metrics can result from a variety of underlying factors and may be misleading.[150] Therefore, caution should be used when interpreting these imaging metrics in isolation.

In MS research, DTI has become a widely used tool for quantifying microstructural changes in the CNS, with over 300 studies published as of 2019.[151] Given that MS is marked by demyelination and axonal loss, which disrupts neural architecture, DTI is particularly well-suited for investigating these pathological changes and their clinical associations. Early studies in the

field revealed that MD and FA were reduced in both white matter lesions and normal-appearing white matter in MS patients compared to controls, indicating both focal and diffuse structural differences. Additionally, lower MD and FA values were observed in hypointense T1 lesions compared to isointense lesions, suggesting that these DTI metrics may be useful indicators of lesion severity.[152,153] In a separate study, lesion FA was only weakly correlated with EDSS score across all MS phenotypes and moderately correlated in progressive forms. [154]

With evidence that DTI can detect structural abnormalities in normal-appearing white matter, tract-based DTI analyses have become a prominent approach in MS research. Using regional DTI analysis, metrics extracted from the corticospinal tract and corpus callosum have been found to correlate with motor disability in MS patients, while metrics from the parietal, frontal, and temporal white matter are associated with cognitive dysfunction.[155–157] Altogether, tract-based DTI analysis has shown strong associations with clinical outcomes, likely because it captures structural damage in regions that appear unaffected on conventional imaging.[158]

DTI studies of the spinal cord in MS patients have demonstrated that DTI metrics can distinguish between patients with high and low disability levels, even among those with low lesion counts.[159] Furthermore, spinal cord DTI metrics have been shown to correlate with sensorimotor impairment across MS phenotypes, with altered DTI metrics observed in patients with more progressive forms of the disease.[160]

This brief overview highlights only some of the research in MS using DTI to detect and quantify structural changes. With demonstrated correlations between DTI metrics and both physical and cognitive disability, DTI has established itself as a valuable research tool for investigating the neural basis of MS-related impairments.

Despite its popularity as a model and widespread usage in MS research, DTI is accompanied by several important considerations. First, DTI is based on the assumption that water diffusion in biological tissue follows a Gaussian distribution, which is only true in the case of isotropic, unrestricted diffusion.[161] In the complex cellular environment of neural tissue, intracellular and extracellular water molecules encounter various structural barriers, such as membranes and organelles, which lead to highly heterogeneous diffusion patterns. As a result, diffusion within neural tissue rarely fits a true Gaussian model, leading to deviations that can limit the accuracy of DTI measurements.[161,162] This assumption, while simplifying modeling, can lead to potential inaccuracies, particularly in regions with complex microstructures.

Another major limitation of DTI is that it assumes only one primary diffusion process per voxel, which can lead to erroneous quantification in regions containing multiple fiber orientations.[163] This is a significant issue, as recent estimates suggest that between 63-90% of white matter contains crossing fibers.[164] In such regions, DTI struggles to accurately represent the true diffusion patterns, as the ellipsoid tensor model oversimplifies fiber architecture by reducing multiple fiber tracts within a voxel to a single pathway. This simplification can lead to incomplete or misleading interpretations of the integrity of underlying neural pathways.

Another challenge arises from the fluid-filled areas surrounding blood vessels in the brain, known as perivascular spaces, which have been shown to influence DTI metrics. Studies indicate that increased fluid in these spaces leads to increased MD values and decreased FA values, potentially introducing bias in measurements.[165] Lastly, DTI metrics lack specificity when used in isolation. For example, while FA measures anisotropy, it is an aggregate metric, meaning that changes in FA could result from demyelination, axonal loss, edema, changes in axonal orientation, or a combination of these factors. These considerations highlight the importance of exercising

caution when interpreting DTI findings in isolation and suggest that, while DTI has demonstrated considerable potential, more advanced imaging techniques may provide a more comprehensive and accurate characterization of the underlying structural alterations in MS pathology.

Collectively, DTI was one of the first techniques developed to model diffusion in the brain, and it remains a valuable research method. Studies using DTI have helped establish the presence of diffuse pathology in MA, showing measurable differences in normal-appearing white matter in vivo that affect areas beyond visible lesions. Its simple yet elegant tensor model has provided insights into one of the most complex systems, the human nervous system, helping to bridge neural structure and clinical outcomes in ways that lesion load alone could not. However, DTI has limitations. Its Gaussian model can distort the underlying diffusion and cannot solve the crossing fibers problem, leading to imperfect interpretations. Despite its limitations, DTI remains a valuable tool in human neuroscience and will continue to play a key role in uncovering the neural underpinnings of functional impairment in MS.

Diffusion Kurtosis Imaging

Diffusion kurtosis imaging (DKI) expands on the capabilities of DTI by characterizing the non-Gaussian behavior of water diffusion, offering a more nuanced depiction of the complex microstructural heterogeneity within biological tissues.[166] In DKI, the b-value, an imaging parameter that quantifies the strength and timing of the diffusion weighting applied, can be implemented at increased intensity levels. Higher b-values increase the sensitivity to shorter molecule movement distances and, therefore, enhance the detection of subtle microstructural variations, which are often missed by DTI's lower b-value constraints.[161] In DKI's mathematical framework, a term accounts for kurtosis or the degree to which the diffusion profile deviates from Gaussian behavior. Higher kurtosis values indicate a greater deviation from the Gaussian

distribution, suggesting that water movement must navigate a more complex environment.[161,167] Additionally, DKI's capability to model non-Gaussian water enhances its effectiveness in regions with isotropic diffusion characteristics, such as gray matter, where water diffusion does not have a predominant direction, thereby enabling more comprehensive imaging across both white and gray matter tissues.[167]

DKI captures directional kurtosis using a fourth-order tensor that encompasses 21 combined degrees of freedom, compared to just 6 in standard DTI.[161,168] This increased complexity in modeling necessitates a corresponding increase in scanning effort, as DKI typically requires imaging at least three different b-values and 15 distinct directions.[168] From the DKI tensor, several metrics that relate to those obtained from DTI can be derived, allowing for the quantification of overall and directional microstructural complexity. The most commonly reported metrics include mean kurtosis (MK), axial kurtosis (AK), radial kurtosis (RK), and fractional anisotropy kurtosis (FAK). However, due to the high dimensionality of the kurtosis tensor, many additional quantifications are also possible. [161,169] MK, which reflects the overall diffusional heterogeneity, increases as tissue complexity increases. AK measures diffusion along the primary fiber direction, where lower values indicate more diffusion along this direction. RK provides information on diffusion perpendicular to the main fiber direction, increasing as water is more restricted in this direction. Like RD, RK values have been linked to processes such as myelination and axonal health in white matter. In a mouse model, RK and MK were better indicators of myelin content than DTI metrics.[170]

Within MS research, some studies have shown that DKI measures reveal larger differences between MS patients and controls in normal-appearing white matter compared to DTI measures. This includes regions where DKI detected differences and DTI did not.[171] Further studies

implementing DKI and DTI found that both metrics are sensitive to tissue differences between individuals with MS and controls. However, DTI performed best in regions with highly aligned fibers, such as the corpus callosum, and DKI excelled in areas with complex fiber orientations, such as the corona radiata.[172] This suggests that the two models can be used in tandem to provide complementary information. Similarly, studies in the spinal cord suggest that DKI of the white and gray matter can provide a more comprehensive characterization of neural damage.[173] In regards to clinical outcomes, RK within the corticospinal tract has been associated with EDSS at baseline and 12-month follow up.[174] Kurtosis metrics measured within the corpus callosum were also moderately associated with the EDSS.[175] Additionally, studies have reported that decreased MK in cortical gray matter is strongly associated with poor cognitive performance.[176,177]

Taken together, DKI addresses some of the limitations of DTI and may offer additional insights into neural alterations in MS that contribute to functional impairment. Although it is a less explored technique in MS, studies have highlighted the effectiveness of DKI in offering insights into neural impairment, particularly in regions with complex tissue. In addition, DKI enables the investigation of isotropic tissue, such as normal-appearing gray matter, potentially deepening our understanding of the structural changes linked to clinical outcomes.

Neurite Orientation Dispersion and Density Imaging

Neurite Orientation Dispersion and Density Imaging (NODDI), similar to DKI, expands on traditional diffusion MRI techniques by providing insights into tissue microstructural environments. To achieve this, NODDI utilizes a multi-compartment model to distinguish between three microstructural environments: intra-neurite, extra-neurite, and cerebrospinal fluid.[178] Each compartment is modeled using a different diffusion distribution: intra-neurite space is modeled using a Watson distribution, extra-neurite space with a Gaussian anisotropy distribution, and

cerebrospinal fluid with an isotropic Gaussian distribution. The intra-neurite compartment is designed to model both axons and dendrites, allowing it to be utilized to assess the structural integrity of both gray and white matter.[178] By modeling these distinct compartments, NODDI offers a more nuanced depiction of cellular architecture than the simple single Gaussian DTI model. NODDI outputs two primary parameters, orientation dispersion index (ODI) and neurite density index (NDI), which respectively quantify the directional dispersion and density of neurites.[178] By distinguishing between neuron density and orientation, both of which affect DTI measures like FA, NODDI enables a more precise interpretation of the underlying data.[179]

NODDI is a relatively new technique, and research using it for in vivo assessment of MS patients is limited in number. However, studies employing NODDI have shown promise in detecting early microstructural abnormalities in normal-appearing white matter, lesions, and cortex.[180,181] A common finding across NODDI studies in MS is a reduction in NDI in both lesions and normal-appearing white matter compared to controls, and a decrease in ODI in lesions, likely indicating axonal loss. In addition, multiple studies have noted an increase in ODI in normal-appearing white matter in MS patients compared to controls, potentially indicating pathological disruptions in the alignment and togetherness of tightly packed fibers.[180,182–184]

Given its ability to detect microstructural disruption, NODDI metrics, such as increased ODI in normal-appearing white matter, may provide a valuable approach for studying diffuse tissue damage early in the course of MS. Additionally, studies have shown that NODDI metrics identify more extensive changes in lesions and normal-appearing white matter compared to DTI.[182] Research on the clinical correlations between NODDI metrics and the EDSS is limited and has produced mixed findings.[180–183,185] Studies applying NODDI in the spinal cord have provided evidence that ODI reductions in MS lesions align with histopathological findings.[186] Further spinal

cord studies have found reduced NDI in both lesions and normal-appearing white matter in MS patients compared to controls, and lower NDI in the white matter of patients was associated with higher disability.[185,187] Altogether, given its potential to reveal microstructural features not accessible through traditional diffusion techniques, further research is warranted to fully explore and validate the utility of NODDI in MS.

Fixel-based Analysis

Fixel-Based Analysis (FBA) is another advanced neuroimaging framework option designed to address the limitations of traditional diffusion models. Specifically, FBA provides detailed information about complex fiber arrangements within each voxel, enabling the differentiation of multiple fiber bundles in close proximity.[188,189] Central to the use of FBA is a technique called constrained spherical deconvolution (CSD), which enables the identification of multiple fiber orientations within a voxel. Unlike traditional diffusion models, CSD does not assume a single dominant fiber direction per voxel, instead, it uses estimates to identify the number of fiber populations within a voxel and their orientations.[190] This approach is particularly useful for mapping complex white matter structures such as fanning, kissing, or intersecting fibers commonly found throughout the brain.[191,192]

CSD leverages high angular resolution diffusion imaging, an advanced imaging protocol that collects diffusion-weighted images across many directions, typically at high b-values. Collecting data from a large number of directions increases sensitivity to distinct fiber pathways and provides a more comprehensive diffusion imaging dataset of the brain's diverse fiber orientations.[193] In CSD, an expected signal for a single white matter fiber population, known as the response function, is used in a deconvolution process to extract a white matter fiber orientation distribution from the diffusion MRI signal measured in each voxel.[190] This results in the

identification of distinct fiber tracts within individual voxels, enabling the independent analysis of each fiber population. This capability is valuable for obtaining accurate measurements in complex regions, such as the corona radiata.

Fixel within FBA refers to an individual "fiber element within a voxel", making it possible to quantify the white matter properties of a fiber bundle even if multiple fiber populations are present within the same voxel.[191] Three metrics are derived from FBA: fiber density (FD), fiber cross-section (FC), and combined fiber density and cross-section (FDC) (Figure 1.5). FD is a measure of white matter microstructure and quantifies the intra-axonal volume of specific fiber bundles.[194] FC is a macroscopic quantification that reflects the cross-sectional area of the fiber bundles. FDC combines both metrics, offering a comprehensive measure of the microstructural and macrostructural makeup of the fiber population.[188] Together, they provide insight into pathophysiological processes in white matter, such as axonal loss and/or atrophy, enabling a nuanced evaluation of white matter differences at a subvoxel level.

FBA offers unique advantages for studying MS by estimating the complete fiber orientation distribution, allowing it to better account for confounding processes such as inflammation, edema, and gliosis that can impact standard DTI analysis.[195] FBA research in MS has found that FD is reduced in both lesions and normal-appearing white matter, demonstrating similar sensitivity to FA in detecting lesion tissue. However, unlike FA, FD remained robust in areas with crossing fibers, where FA is often unreliable.[195] Additionally, FD and FC were found to be reduced in the inferior fronto-occipital fasciculus, including the optic radiations, in MS patients with optic neuritis, suggesting that FBA can be a valuable tool for studying correlates of early axonal degeneration in MS.[195]

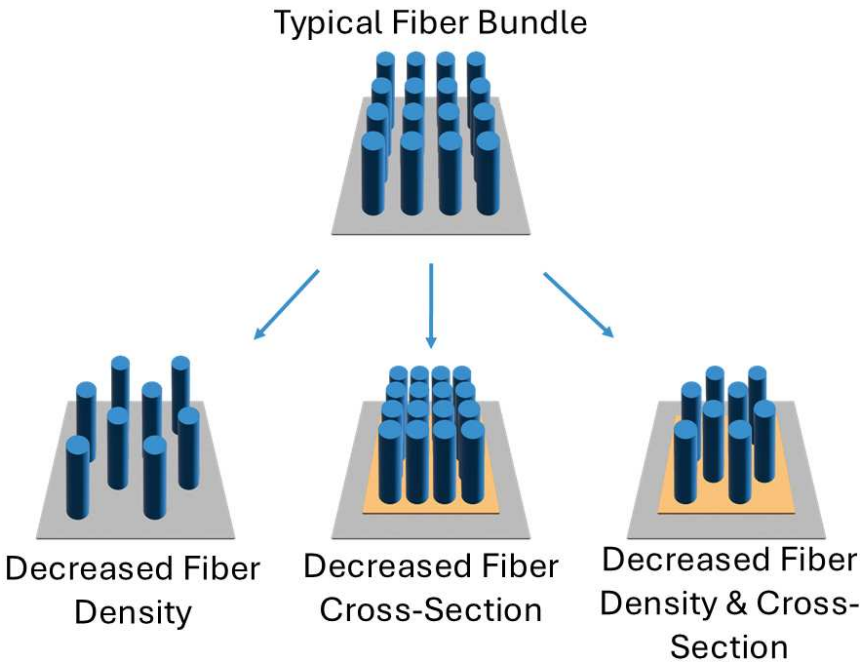

Figure 1.5. Representation of Fixel-Based Analysis Metrics. Illustration of the three metrics derived from fixel-based analysis, which quantifies white matter properties at the level of individual fiber populations within a voxel. The top panel shows a typical, healthy fiber bundle. Bottom left: *Decreased Fiber density (FD)*—reduced number of intra-axonal fibers, reflecting decreased axonal density. Bottom middle: *Decreased Fiber cross-section (FC)*—a smaller cross-sectional area of the fiber bundle, reflecting macroscopic atrophy. Bottom right: *Decreased Fiber density and cross-section (FDC)*—a reduction in both FD and FC, indicating combined micro- and macrostructural alterations.

A recent study identified that FBA metrics were associated with MS phenotype, with secondary progressive MS showing the greatest microstructural and macrostructural damage, followed by primary progressive and then relapsing-remitting MS. FBA metrics also correlated with the degree of cognitive impairment, distinguishing between cognitively preserved, mildly impaired, and significantly impaired MS patients. Moreover, baseline FBA metrics have been shown to predict cognitive decline over a five-year period, highlighting their potential utility for researchers investigating neural correlates of disease progression in MS.[196] Additional associations have been reported between FD and FC and gait impairment, as well as errors in a force-tracking

task, in MS patients with minimal disability.[197] Lastly, FDC reductions in brainstem monoaminergic tracts are associated with cognitive fatigue in MS, supporting the idea that axonal damage to these pathways leads to the dysfunction of the monoaminergic system, contributing to central fatigue.[198]

FBA is an emerging neuroimaging framework for assessing white matter properties in neurodegenerative and aging populations, offering advantages over traditional diffusion imaging methods, particularly in regions with complex fiber orientations. FBA is highly robust in areas where fibers cross, diverge, or bend, providing more accurate measurements of white matter properties in these challenging spaces. Early studies using FBA in MS have demonstrated correlations with clinical outcomes, such as cognitive impairment, physical disability, central fatigue, and disease progression. FBA captures both microstructural (FD) and macrostructural (FC) information, allowing for comprehensive characterization of white matter tracts. Taken together, FBA is a promising research tool for revealing white matter changes linked to MS outcomes.

Structural Networks

Using dMRI and subsequent modeling techniques, structural networks in the brain can be constructed by mapping connections between different regions using tractography, a process that models the pathways of white matter fibers. Tractography enables the visualization of white matter tracts across the brain, allowing researchers to examine the structural connections underlying neural communication. Tracing tracts through white matter is where advanced frameworks like FBA are especially advantageous, offering improved precision in mapping fibers through complex regions. In contrast, tractography based on DTI may be less reliable in the complex areas, and more reliable in areas where white matter fibers are tightly aligned, such as the corpus callosum

and internal capsule. This limitation is particularly relevant in MS, where multifocal lesions can disrupt tracts and prevent accurate tracing of fibers. Studies have shown that CSD and other advanced techniques, which incorporate more complex modeling, are better equipped to handle tissue complexity and are more resilient to damage-related artifacts, likely allowing for more accurate tract tracing through affected regions.[199,200] Consequently, structural networks mapped with FBA provide a more robust foundation for both whole-brain and regional analyses, enhancing our understanding of both large-scale and localized brain networks.

Studies assessing structural networks in MS patients have found notable alterations in both local and global connectivity compared to controls. For instance, research has shown pronounced network differences in sensorimotor, visual, default-mode, and language networks, with these alterations correlating with EDSS scores.[201] Another study, which used a metric sensitive to both short- and long-range connections, found altered connectivity even in early relapsing-remitting MS, suggesting that these measures may be useful for investigating early network-level changes in the disease. The same study identified increased connections through major intra- and interhemispheric tracts, the cingulum and corpus callosum, which may reflect compensatory mechanisms in early MS.[202] Additional studies highlight structural reorganization linked to deficits in attention and executive function, cerebellar connectometry differences that are strongly correlated with disability, as well as connectivity differences within the limbic system that are associated with major depression in MS.[203–205] While some studies show connectivity differences are linked to lesion load and location, others find little overlap between lesion location, network connectivity, and underlying function, arguing that injury within normal-appearing white matter is a likely contributor.[204,206,207]

While the studies presented here are informative and contribute significantly to our understanding of MS by enabling researchers to link microstructural alterations with clinical manifestations, many arrived at these conclusions using DTI tractography. Further research would benefit from reassessing global and local measures using advanced techniques. Overall, network dysfunction is evident from the early stages of MS, and structural connectivity likely evolves over time as the CNS attempts to adapt and compensate for the accumulation of neural injury.

Magnetization Transfer Imaging

Magnetization Transfer Imaging (MTI) is another powerful MRI technique that measures protons differently from conventional and dMRI by focusing on the interactions between free water protons and protons bound to macromolecules. In conventional MRI, signals are primarily derived from the spins of mobile hydrogen nuclei, with the time between the radiofrequency pulse and maximum signal intensity typically exceeding 10 milliseconds. In contrast, the spins of hydrogen protons within macromolecules, such as myelin and proteins, decay much more rapidly, often with decay times of 1 millisecond or less, making them undetectable in conventional MRI.[208]

MTI utilizes a radiofrequency pulse far from the normal resonance frequency of free water, known as an "off-resonance" pulse. This approach selectively excites the protons in macromolecules, while leaving the protons in free water largely unaffected.[209] Due to the constant motion of mobile water, there are frequent interactions and exchanges between these mobile protons and the stationary protons of macromolecules. When water molecules bind transiently to the surfaces of macromolecules, the spins of the protons can exchange. When adequate off-resonance power is applied, macromolecular spins reach a saturated state, where the numbers of parallel and antiparallel spins become equal, resulting in a net magnetization vector of zero. This saturated magnetization can then be transferred to mobile protons, causing partial saturation of

their spins.[209] As a result, the greater the amount of macromolecules present within a tissue, the greater the extent of magnetization transfer. This magnetization exchange is fundamental to MTI, enabling it to detect subtle changes in tissue composition and providing insights into the macromolecular environment that are not discernible using traditional MRI techniques.

The magnetization transfer ratio (MTR) is commonly implemented to quantify MTI and facilitate interpretation. MTR is calculated as the ratio between signal intensities from MR images acquired with and without the application of a saturating pulse.[208] This approach standardizes comparisons across different tissue types and brain regions. MTR is expressed as a percentage, where lower values indicate reduced magnetization transfer. For example, in the ventricles, where the abundance of macromolecules is low, the signals from saturated and non-saturated pulse acquisitions are nearly identical, resulting in an MTR close to zero. In contrast, regions such as the corpus callosum, which contains high levels of myelin and densely packed fibers, yield higher MTR values. Typically, white matter exhibits MTR values that are 7-8% higher than those of gray matter.[209]

Research using animal models, including a rodent model of MS, has shown that MTR correlates with histopathological features such as axonal loss, demyelination, edema, and macrophage presence.[210–213] Additionally, postmortem studies of MS patients have demonstrated associations between MTR values and axonal loss and demyelination in lesions and normal-appearing white matter.[214–216] In vivo studies have shown that MTR decreases in normal-appearing white matter up to 1–12 months before the formation of contrast-enhancing lesions. MTR is particularly low in T1 hypointense “black hole” lesions compared to isointense lesions, though it may gradually increase over time, potentially reflecting recovery from acute inflammation.[217,218] Together, this suggests that MTR serves as an indicator of lesion severity and as a predictor of

future lesion development or recovery. Several studies highlight that lower whole-brain MTR values are associated with increased disability, further building upon histological studies that link MTR to diffuse tissue damage.[219] In addition to white matter changes, MTR studies have linked lower values to gray matter demyelination, identifying cortical abnormalities that correlate with disability even in the early stages of MS.[220,221]

Collectively, MTR offers a unique structural imaging approach that provides independent and complementary information to conventional and dMRI. MTR has shown associations with clinical disability and serves as a quantitative indicator for both present and potential future tissue damage. Although MTR cannot distinguish between specific pathologies like edema, myelin loss, or demyelination, it provides insight into the extent of tissue alteration. Together, this makes MTR a valuable addition to MRI-based research and clinical studies in MS.

Myelin Water Imaging

Myelin Water Imaging (MWI) is an advanced MRI technique specifically designed to quantify the myelin content in brain tissue, providing insights into white matter health, especially in demyelinating diseases like MS. Conventional FLAIR imaging has been widely used to visualize demyelination in MRI, but signal changes in FLAIR images can reflect not only demyelination but also edema, inflammation, and axonal loss.[222] This overlap has fueled interest in myelin-specific imaging for research applications. MWI is proposed to take advantage of the unique folds in myelin structure to measure water trapped within the lipid bilayers surrounding axons. In the MTI section, we discussed the different spin decay times between free water (characterized by a long spin decay) and water in macromolecules (characterized by a short spin decay, typically less than 1 ms). In between these two typical relaxation times is an additional

quantifiable relaxation time that represents water found between the lipid bilayers of myelin, termed “myelin water”.[223]

It’s important to clarify that the molecules expressing this relaxation timing are not free water or part of macromolecules but rather the water trapped between myelin layers. Due to its close proximity to macromolecules and highly restricted environment, myelin water produces unique signal characteristics that can be detected and quantified. MWI can be generated from various MRI protocols, with T2-based MWI being the most common.[224] Regardless of the specific imaging technique, MWI relies on detecting the faster relaxation time of myelin water compared to that of extracellular and intra-axonal water. This enables the calculation of the myelin water fraction (MWF), a metric representing the proportion of myelin water to total water within a voxel, thereby quantifying myelin density.[225]

Histological studies have demonstrated a strong correlation between MWF and postmortem myelin density across white matter, gray matter, and lesions.[226,227] Animal studies similarly show that MWF is closely related to myelin density and suggest that MWF is less influenced by inflammation compared to MTI.[228,229] In vivo studies reveal that lesions exhibit roughly 50% lower MWF than contralateral white matter, while normal-appearing white matter in individuals with MS also has lower MWF compared to controls. Additionally, overall water content was elevated in all measured tissues in MS patients compared to controls, possibly indicating diffuse microedema.[230]

Longitudinal studies have shown that MWF changes in lesions over time, with increases in MWF interpreted as edema resolution and potential remyelination.[231] MWF alterations have been identified in normal-appearing brain tissue in individuals with clinically isolated syndrome, and predicted short-term conversion risk to clinically diagnosed MS.[232] Furthermore, baseline

MWF can predict MWF at follow-up, and initial lesion severity has been linked to a lesion's myelin recovery potential.[233] Regional analyses indicate clinical correlations between MWF and cognitive and sensorimotor functions in neuroanatomically relevant areas.[234,235] Specifically, MWF in motor pathways like the corticospinal tract and cerebellar peduncles have been associated with walking performance and fall risk in MS patients.[236]

Taken together, MWI is an advanced MRI technique that was developed to provide an indirect measure of myelin content in the CNS. This imaging approach offers a unique perspective on myelin density, enabling the differentiation between healthy and affected white matter in neurodegenerative diseases. While MWI and MWF have strong histological support, it's important to note that MWF is a ratio and can be influenced by changes in total water levels. For example, elevated water content from diffuse microedema, commonly suggested in MS, can make MWF appear reduced. This sensitivity to total water should be carefully considered when interpreting findings and reported clearly by studies using MWF as an outcome variable. MWI offers the potential for tracking disease progression and has also been used to evaluate the effectiveness of treatments aimed at preserving or restoring myelin, making it a valuable tool in neuroimaging research.

Ultra-High Field Magnetic Resonance Imaging

Thus far in this review, we have not discussed the hardware used to capture MRI images in detail. Most of the studies highlighted here rely on MRI scanners with magnetic field strengths of 1.5 or 3 Tesla (T), which are currently the most commonly used systems in clinical and research settings. Tesla refers to the strength of the magnetic field, where a higher Tesla rating provides a stronger magnetic field and, therefore, greater signal sensitivity. While 1.5T and 3T are widely available and sufficient for many imaging purposes, some of the studies included in this review

utilize a cutting-edge 7T MRI system. This ultra-high-field MRI technology offers substantial advantages in resolution and sensitivity, pushing the boundaries of what can be detected in the brain, particularly in conditions like MS.

The primary advantage of implementing 7T MRI over 3T MRI is the improved signal-to-noise ratio. Higher magnetic field strengths significantly increase tissue signal while reducing background noise, which enables greater spatial resolution and enhanced tissue contrast. This combination enables 7T MRI to provide an enhanced level of detail, making it possible to visualize small-scale structural changes and subtle tissue abnormalities that lower-field systems may miss. For example, in MS research, 7T MRI has proven particularly useful for assessing grey matter pathology and detecting cortical lesions, an area of research that remains challenging with lower-field MRI.

To that end, recent studies have shown that 3T MRI could only detect about ¼ of the cortical lesions identified with postmortem histopathology.[237] A comparative study between 7T and 3T MRI found that 7T MRI increased the cortical lesion detection rate by 200–225%, with particularly high identification rates for certain lesion types.[238] Further, 7T MRI is better at distinguishing lesions located at cortical and subcortical junctions, and excluding some cortical lesions identified with 3T that were actually signals from blood vessels.[239] Intra-rater lesion scoring using 7T MRI is excellent and poor using 3T MRI.[240] Although the benefits of lesion identification within the brain may be confined to the gray matter, within the spinal cord, lesion detection is 50% higher using 7T MRI compared to 3T MRI.[241,242] Lastly, 7T MRI may also improve the detection of biomarkers such as central vein sign and paramagnetic rims, which can help with the speed and accuracy of diagnoses.[243,244]

Despite these advantages, practical barriers still exist for implementing 7T MRI in all clinical settings. The cost of a 7T MRI system is estimated to be between $7–10 million in the United States. Additionally, the hardware requires more space, is heavier, and takes longer to install.[245] Scanning times with 7T MRI are also longer, and several additional safety considerations must be taken into account. These include significant acoustic noise levels (up to 110 dB) and the lack of safety testing for many implanted medical devices in 7T environments, which complicates its clinical application.[246]

The implementation of 7T MRI in MS research presents significant advantages over traditional 3T MRI, particularly in detecting subtle cortical lesions, which are key indicators of disability. Additionally, 7T MRI has the potential to aid in identifying tissue attributes that could enhance the speed and accuracy of diagnosis. Although logistical and safety concerns remain, the superior resolution offered by 7T MRI is poised to be invaluable for both clinical practice and research in MS and other neurodegenerative disorders. Overall, the transition to ultra-high-field MRI is a promising step forward, with the potential to improve our understanding and management of complex neurological conditions.

Conclusion

Over the past several decades, the field of neuroimaging has advanced significantly, providing clinicians and researchers with an expansive toolkit to investigate, diagnose, and monitor complex neurological diseases. In MS, MRI remains the backbone of clinical imaging, playing a critical role in diagnosing, monitoring, and predicting disease progression. Conventional T1- and T2-weighted imaging is essential for identifying and quantifying CNS injury. These conventional MRI techniques form the foundation of the McDonald criteria, the primary diagnostic protocol for MS. As imaging protocols and technologies advance, the goal remains to refine these criteria by

identifying robust imaging biomarkers that improve diagnostic sensitivity while minimizing the risk of misdiagnosis.

Beyond assessing macroscopic injury, a major frontier in MS imaging lies in capturing pathology outside focal lesions through advanced imaging techniques. Conventional DTI was among the first models used to study white matter in MS, providing measures such as FA and MD that were proposed to serve as an indicator of structural integrity. DTI studies have revealed diffuse abnormalities both within lesions and in normal-appearing white matter in MS patients compared to neurotypical controls, with metrics capturing damage beyond focal lesions showing stronger correlations with clinical outcomes. However, DTI has limitations, notably its low sensitivity to crossing fibers and its simplistic modeling of tissue microstructure. Newer diffusion models, such as NODDI and FBA, offer refined insights by explicitly accounting for and modeling the complex architecture of neural tissue. These techniques provide more detailed measures of underlying microstructural changes while maintaining accuracy in regions with intricate crossing fibers. By capturing diffuse injury and subtle alterations in tissue composition, these methods enable a more precise interpretation of MS-related damage that extends beyond traditional lesion tracking and simple DTI models, providing a more comprehensive view of the disease's impact on neural integrity.

The future of MS imaging holds exciting potential with the emergence of ultra-high-field MRI (7T), which offers higher resolution, increased sensitivity, and improved tissue contrast. This next-generation imaging technology holds the potential to improve the identification of important imaging markers. For instance, 7T MRI substantially improves the detection of cortical lesions, a key challenge in MS neuroimaging, providing information that is otherwise hidden at lower scanning resolution. These improvements could allow for faster, more accurate diagnoses,

enhanced disease monitoring, and deeper investigation into the structural changes underlying MS-related symptoms. However, despite these benefits, the widespread clinical adoption of 7T MRI is currently limited by economic and logistical barriers. To ensure that high-quality neuroimaging is accessible to a broad patient population and that subsequent care decisions are well-informed, the continued development of advanced imaging techniques for lower-field MRI remains essential.

In summary, neuroimaging in MS has reached a promising stage, where advanced techniques and multimodal approaches enable the accurate capture of anatomical information at both the macrostructural and microstructural levels, leading to informative interpretations. With ongoing innovations in MRI technology, the field is well-positioned to deepen our understanding of the neural underpinnings of MS-related impairments, optimize patient care, and ultimately enhance outcomes for individuals with this challenging disease.

References

1. Lassmann, H. Pathology and disease mechanisms in different stages of multiple sclerosis. *Journal of the Neurological Sciences* vol. 333 Preprint at https://doi.org/10.1016/j.jns.2013.05.010 (2013).
2. Howard, J., Trevick, S. & Younger, D. S. Epidemiology of Multiple Sclerosis. *Neurologic Clinics* vol. 34 Preprint at https://doi.org/10.1016/j.ncl.2016.06.016 (2016).
3. Trapp, B. D. *et al.* Axonal Transection in the Lesions of Multiple Sclerosis. *New England Journal of Medicine* **338**, (1998).
4. Popescu, B. F. G., Pirko, I. & Lucchinetti, C. F. Pathology of multiple sclerosis: Where do we stand? *CONTINUUM Lifelong Learning in Neurology* vol. 19 Preprint at https://doi.org/10.1212/01.CON.0000433291.23091.65 (2013).
5. Horng, S. & Fabian, M. The pathophysiology and clinical presentation of multiple sclerosis. in *Handbook of Relapsing-Remitting Multiple Sclerosis* (2017). doi:10.1007/978-3-319-40628-2_2.
6. Gelfand, J. M. Multiple sclerosis: diagnosis, differential diagnosis, and clinical presentation. *Handb Clin Neurol* **122**, 269–290 (2014).
7. Dobson, R. & Giovannoni, G. Multiple sclerosis – a review. *European Journal of Neurology* vol. 26 27–40 Preprint at https://doi.org/10.1111/ene.13819 (2019).
8. Miller, D. H., Chard, D. T. & Ciccarelli, O. Clinically isolated syndromes. *The Lancet Neurology* vol. 11 Preprint at https://doi.org/10.1016/S1474-4422(11)70274-5 (2012).
9. Brownlee, W. J., Hardy, T. A., Fazekas, F. & Miller, D. H. Diagnosis of multiple sclerosis: progress and challenges. *The Lancet* vol. 389 Preprint at https://doi.org/10.1016/S0140-6736(16)30959-X (2017).
10. Lublin, F. D. *et al.* Defining the clinical course of multiple sclerosis: The 2013 revisions. *Neurology* vol. 83 Preprint at https://doi.org/10.1212/WNL.0000000000000560 (2014).
11. Romero-Pinel, L. *et al.* The age at onset of relapsing-remitting multiple sclerosis has increased over the last five decades. *Mult Scler Relat Disord* **68**, 104103 (2022).
12. Orton, S. M. *et al.* Sex ratio of multiple sclerosis in Canada: a longitudinal study. *Lancet Neurology* **5**, (2006).
13. Kobelt, G., Thompson, A., Berg, J., Gannedahl, M. & Eriksson, J. New insights into the burden and costs of multiple sclerosis in Europe. *Multiple Sclerosis* **23**, (2017).
14. Cree, B. A. C. *et al.* Long-term evolution of multiple sclerosis disability in the treatment era. *Ann Neurol* **80**, (2016).
15. Goldenberg, M. M. *DISEASE OVERVIEW Multiple Sclerosis Review*. *P&T®* vol. 37 (2012).
16. Okuda, D. T. *et al.* Incidental MRI anomalies suggestive of multiple sclerosis: The radiologically isolated syndrome. *Neurology* **72**, (2009).
17. Granberg, T., Martola, J., Kristoffersen-Wiberg, M., Aspelin, P. & Fredrikson, S. Radiologically isolated syndrome - Incidental magnetic resonance imaging findings suggestive of multiple sclerosis, a systematic review. *Multiple Sclerosis Journal* vol. 19 Preprint at https://doi.org/10.1177/1352458512451943 (2013).
18. Lebrun-Frenay, C. *et al. Radiologically Isolated Syndrome*. (2023).

19. Thompson, A. J. *et al.* Diagnosis of multiple sclerosis: 2017 revisions of the McDonald criteria. *The Lancet Neurology* vol. 17 Preprint at https://doi.org/10.1016/S1474-4422(17)30470-2 (2018).
20. Schwenkenbecher, P. *et al.* Impact of the McDonald Criteria 2017 on Early Diagnosis of Relapsing-Remitting Multiple Sclerosis. *Frontiers in Neurology* vol. 10 Preprint at https://doi.org/10.3389/fneur.2019.00188 (2019).
21. Solomon, A. J. & Corboy, J. R. The tension between early diagnosis and misdiagnosis of multiple sclerosis. *Nature Reviews Neurology* vol. 13 Preprint at https://doi.org/10.1038/nrneurol.2017.106 (2017).
22. Ford, H. Clinical presentation and diagnosis of multiple sclerosis. *Clinical Medicine, Journal of the Royal College of Physicians of London* **20**, (2020).
23. Van Der Vuurst De Vries, R. M. *et al.* Application of the 2017 Revised McDonald Criteria for Multiple Sclerosis to Patients with a Typical Clinically Isolated Syndrome. *JAMA Neurol* **75**, (2018).
24. Rocca, M. A. *et al.* Current and future role of MRI in the diagnosis and prognosis of multiple sclerosis. *The Lancet Regional Health - Europe* vol. 44 Preprint at https://doi.org/10.1016/j.lanepe.2024.100978 (2024).
25. Chertcoff, A., Schneider, R., Azevedo, C. J., Sicotte, N. & Oh, J. Recent Advances in Diagnostic, Prognostic, and Disease-Monitoring Biomarkers in Multiple Sclerosis. *Neurologic Clinics* vol. 42 Preprint at https://doi.org/10.1016/j.ncl.2023.06.008 (2024).
26. Lublin, F. History of modern multiple sclerosis therapy. in *Journal of Neurology* vol. 252 (2005).
27. Brown, R. W., Cheng, Y. N., Haacke, E. M., Thompson, M. R. & Venkatesan, R. Classical Response of a Single Nucleus to a Magnetic Field. in *Magnetic Resonance Imaging* (2014). doi:10.1002/9781118633953.ch2.
28. Tait, M. J., Saadoun, S., Bell, B. A. & Papadopoulos, M. C. Water movements in the brain: role of aquaporins. *Trends in Neurosciences* vol. 31 Preprint at https://doi.org/10.1016/j.tins.2007.11.003 (2008).
29. Whittall, K. P. *et al.* In vivo measurement of T2 distributions and water contents in normal human brain. *Magn Reson Med* **37**, (1997).
30. Serai, S. D. Basics of magnetic resonance imaging and quantitative parameters T1, T2, T2*, T1rho and diffusion-weighted imaging. *Pediatric Radiology* vol. 52 Preprint at https://doi.org/10.1007/s00247-021-05042-7 (2022).
31. Hopkins, A. L., Yeung, H. N. & Bratton, C. B. Multiple field strength in vivo T1 and T2 for cerebrospinal fluid protons. *Magn Reson Med* **3**, (1986).
32. Wansapura, J. P., Holland, S. K., Dunn, R. S. & Ball, W. S. NMR relaxation times in the human brain at 3.0 Tesla. *Journal of Magnetic Resonance Imaging* **9**, (1999).
33. Barkovich, A. J. Concepts of myelin and myelination in neuroradiology. *American Journal of Neuroradiology* vol. 21 Preprint at (2000).
34. Poustchi-Amin, M., Mirowitz, S. A., Brown, J. J., McKinstry, R. C. & Li, T. Principles and applications of echo-planar imaging: a review for the general radiologist. *Radiographics : a review publication of the Radiological Society of North America, Inc* vol. 21 Preprint at https://doi.org/10.1148/radiographics.21.3.g01ma23767 (2001).

35. Stehling, M. K., Turner, R. & Mansfield, P. Echo-planar imaging: Magnetic resonance imaging in a fraction of a second. *Science* vol. 254 Preprint at https://doi.org/10.1126/science.1925560 (1991).
36. Wattjes, M. P. *et al.* 2021 MAGNIMS–CMSC–NAIMS consensus recommendations on the use of MRI in patients with multiple sclerosis. *The Lancet Neurology* vol. 20 Preprint at https://doi.org/10.1016/S1474-4422(21)00095-8 (2021).
37. Bojorquez, J. Z. *et al.* What are normal relaxation times of tissues at 3 T? *Magnetic Resonance Imaging* vol. 35 Preprint at https://doi.org/10.1016/j.mri.2016.08.021 (2017).
38. Koenig, S. H. Classes of hydration sites at protein-water interfaces: the source of contrast in magnetic resonance imaging. *Biophys J* **69**, (1995).
39. Barkhof, F. & Koeller, K. K. Demyelinating Diseases of the CNS (Brain and Spine). in 165–176 (2020). doi:10.1007/978-3-030-38490-6_13.
40. Matthews, P. M. *et al.* A practical review of the neuropathology and neuroimaging of multiple sclerosis. *Practical Neurology* vol. 16 Preprint at https://doi.org/10.1136/practneurol-2016-001381 (2016).
41. Bakshi, R., Ariyaratana, S., Benedict, R. H. B. & Jacobs, L. Fluid-attenuated inversion recovery magnetic resonance imaging detects cortical and juxtacortical multiple sclerosis lesions. *Arch Neurol* **58**, (2001).
42. Tewarie Prejaas and Schoonheim, M. and H. A. Structural and Functional Neuroimaging in Multiple Sclerosis: From Atrophy, Lesions to Global Network Disruption. in *The Neuroimaging of Brain Diseases: Structural and Functional Advances* (ed. Habas, C.) 171–213 (Springer International Publishing, Cham, 2018). doi:10.1007/978-3-319-78926-2_8.
43. Van Walderveen, M. A. A. *et al.* Histopathologic correlate of hypointense lesions on T1-weighted spin- echo MRI in multiple sclerosis. *Neurology* **50**, (1998).
44. Cotton, F., Weiner, H. L., Jolesz, F. A. & Guttmann, C. R. G. MRI contrast uptake in new lesions in relapsing-remitting MS followed at weekly intervals. *Neurology* **60**, (2003).
45. Gadian, D. G. *et al.* Gadolinium-dtpa as a contrast agent in mr imaging— theoretical projections and practical observations. *J Comput Assist Tomogr* **9**, (1985).
46. Miller, D. H. *et al.* Serial gadolinium enhanced magnetic resonance imaging in multiple sclerosis. *Brain* **111**, (1988).
47. Grossman, R. I., Gonzalez-Scarano, F., Atlas, S. W., Galetta, S. & Silberberg, D. H. Multiple sclerosis. Gadolinium enhancement in MR imaging. *Radiology* **161**, (1986).
48. Bagnato, F. *et al.* Imaging Mechanisms of Disease Progression in Multiple Sclerosis: Beyond Brain Atrophy. *Journal of Neuroimaging* vol. 30 Preprint at https://doi.org/10.1111/jon.12700 (2020).
49. McFarland, H. F. *et al.* Using gadolinium-enhanced magnetic resonance imaging lesions to monitor disease activity in multiple sclerosis. *Ann Neurol* **32**, (1992).
50. Kermode, A. G. *et al.* Breakdown of the blood-brain barrier precedes symptoms and other mri signs of new lesions in multiple sclerosis: Pathogenetic and clinical implications. *Brain* **113**, (1990).
51. Katz, D. *et al.* Correlation between magnetic resonance imaging findings and lesion development in chronic, active multiple sclerosis. *Ann Neurol* **34**, (1993).

52. Barkhof, F. The clinico-radiological paradox in multiple sclerosis revisited. *Current Opinion in Neurology* vol. 15 Preprint at https://doi.org/10.1097/00019052-200206000-00003 (2002).
53. Filippi, M. & Rocca, M. A. Conventional MRI in multiple sclerosis. *Journal of Neuroimaging* vol. 17 Preprint at https://doi.org/10.1111/j.1552-6569.2007.00129.x (2007).
54. Mollison, D. *et al.* The clinico-radiological paradox of cognitive function and MRI burden of white matter lesions in people with multiple sclerosis: A systematic review and meta-analysis. *PLoS ONE* vol. 12 Preprint at https://doi.org/10.1371/journal.pone.0177727 (2017).
55. Kurtzke, J. F. Rating neurologic impairment in multiple sclerosis: An expanded disability status scale (EDSS). *Neurology* **33**, (1983).
56. Zivadinov, R. & Leist, T. P. Clinical-magnetic resonance imaging correlations in multiple sclerosis. *Journal of Neuroimaging* vol. 15 Preprint at https://doi.org/10.1177/1051228405283291 (2005).
57. Sormani, M. P., Rovaris, M., Comi, G. & Filippi, M. A reassessment of the plateauing relationship between T2 lesion load and disability in MS. *Neurology* **73**, (2009).
58. Li, D. K. B. *et al.* MRI T2 lesion burden in multiple sclerosis: A plateauing relationship with clinical disability. *Neurology* **66**, (2006).
59. Rudick, R. A., Lee, J. C., Simon, J. & Fisher, E. Significance of T2 lesions in multiple sclerosis: A 13-year longitudinal study. *Ann Neurol* **60**, (2006).
60. Brex, P. A. *et al.* A Longitudinal Study of Abnormalities on MRI and Disability from Multiple Sclerosis. *New England Journal of Medicine* **346**, (2002).
61. Thompson, A. J. *et al.* Serial gadolinium-enhanced MRI in relapsing/remitting multiple sclerosis of varying disease duration. *Neurology* **42**, (1992).
62. Thompson, A. J. *et al.* Major differences in the dynamics of primary and secondary progressive multiple sclerosis. *Ann Neurol* **29**, (1991).
63. Gonzalez-Scarano, F., Grossman, R. I., Galetta, S., Atlas, S. W. & Silberberg, D. H. Multiple sclerosis disease activity correlates with gadolinium-enhanced magnetic resonance imaging. *Ann Neurol* **21**, (1987).
64. Truyen, L. *et al.* Accumulation of hypointense lesions (‘black holes’) on T1 spin-echo MRI correlates with disease progression in multiple sclerosis. *Neurology* **47**, (1996).
65. Filippi, M. *et al.* Assessment of lesions on magnetic resonance imaging in multiple sclerosis: practical guidelines. *Brain* vol. 142 Preprint at https://doi.org/10.1093/brain/awz144 (2019).
66. Charil, A. *et al.* Statistical mapping analysis of lesion location and neurological disability in multiple sclerosis: Application to 452 patient data sets. *Neuroimage* **19**, (2003).
67. Kincses, Z. T. *et al.* Lesion probability mapping to explain clinical deficits and cognitive performance in multiple sclerosis. *Multiple Sclerosis Journal* **17**, (2011).
68. Rossi, F. *et al.* Relevance of Brain Lesion Location to Cognition in Relapsing Multiple Sclerosis. *PLoS One* **7**, (2012).
69. Kidd, D. *et al.* Cortical lesions in multiple sclerosis. *Brain* **122**, (1999).

70. Filippi, M., Preziosa, P. & Rocca, M. A. Magnetic resonance outcome measures in multiple sclerosis trials: Time to rethink? *Current Opinion in Neurology* vol. 27 Preprint at https://doi.org/10.1097/WCO.0000000000000095 (2014).
71. Bo, L., Geurts, J. J. G., Mork, S. J. & Valk, P. Grey matter pathology in multiple sclerosis. *Acta Neurol Scand* **113**, 48–50 (2006).
72. Geurts, J. J. G. *et al.* Cortical lesions in multiple sclerosis: Combined postmortem MR imaging and histopathology. *American Journal of Neuroradiology* **26**, (2005).
73. Seewann, A. *et al.* Imaging the tip of the iceberg: Visualization of cortical lesions in multiple sclerosis. *Multiple Sclerosis Journal* **17**, (2011).
74. Seewann, A. *et al.* Postmortem verification of MS cortical lesion detection with 3D DIR. *Neurology* **78**, (2012).
75. Calabrese, M., Filippi, M. & Gallo, P. Cortical lesions in multiple sclerosis. *Nat Rev Neurol* **6**, 438–444 (2010).
76. Ziccardi, S. *et al.* Cortical lesions at diagnosis predict long-term cognitive impairment in multiple sclerosis: A 20-year study. *Eur J Neurol* **30**, (2023).
77. Hackmack, K. *et al.* Can we overcome the 'clinico-radiological paradox' in multiple sclerosis? *J Neurol* **259**, (2012).
78. Calabrese, M. *et al.* Cortical lesion load associates with progression of disability in multiple sclerosis. *Brain* **135**, (2012).
79. Kutzelnigg, A. *et al.* Cortical demyelination and diffuse white matter injury in multiple sclerosis. *Brain* **128**, (2005).
80. Lukas, C. *et al.* Relevance of spinal cord abnormalities to clinical disability in multiple sclerosis: MR imaging findings in a large cohort of patients. *Radiology* **269**, (2013).
81. Bot, J. C. J. *et al.* Spinal cord abnormalities in recently diagnosed MS patients: Added value of spinal MRI examination. *Neurology* **62**, (2004).
82. Zivadinov, R. & Bakshi, R. Role of MRI in multiple sclerosis I: Inflammation and lesions. *Frontiers in Bioscience* vol. 9 Preprint at https://doi.org/10.2741/1251 (2004).
83. Lycklama, G. *et al.* Spinal-cord MRI in multiple sclerosis. *Lancet Neurol* **2**, 555–562 (2003).
84. Kearney, H., Miller, D. H. & Ciccarelli, O. Spinal cord MRI in multiple sclerosis-diagnostic, prognostic and clinical value. *Nature Reviews Neurology* vol. 11 Preprint at https://doi.org/10.1038/nrneurol.2015.80 (2015).
85. Swanton, J. K. *et al.* Early MRI in optic neuritis: The risk for disability. *Neurology* **72**, (2009).
86. Okuda, D. T. *et al.* Asymptomatic spinal cord lesions predict disease progression in radiologically isolated syndrome. *Neurology* **76**, (2011).
87. Rovira, A. & Auger, C. Spinal Cord in Multiple Sclerosis: Magnetic Resonance Imaging Features and Differential Diagnosis. *Seminars in Ultrasound, CT and MRI* **37**, (2016).
88. Kreiter, D., Postma, A. A., Hupperts, R. & Gerlach, O. Hallmarks of spinal cord pathology in multiple sclerosis. *Journal of the Neurological Sciences* vol. 456 Preprint at https://doi.org/10.1016/j.jns.2023.122846 (2024).
89. De Stefano, N. *et al.* Clinical relevance of brain volume measures in multiple sclerosis. *CNS Drugs* vol. 28 Preprint at https://doi.org/10.1007/s40263-014-0140-z (2014).

90. Filippi, M. *et al.* Interferon beta-1a for brain tissue loss in patients at presentation with syndromes suggestive of multiple sclerosis: A randomised, double-blind, placebo-controlled trial. *Lancet* **364**, (2004).
91. Rudick, R. A., Fisher, E., Lee, J. C., Simon, J. & Jacobs, L. Use of the brain parenchymal fraction to measure whole brain atrophy in relapsing-remitting MS. *Neurology* **53**, (1999).
92. Pagani, E. *et al.* Regional brain atrophy evolves differently in patients with multiple sclerosis according to clinical phenotype. *American Journal of Neuroradiology* **26**, (2005).
93. De Stefano, N. *et al.* Assessing brain atrophy rates in a large population of untreated multiple sclerosis subtypes. *Neurology* **74**, (2010).
94. Zivadinov, R. *et al.* A longitudinal study of brain atrophy and cognitive disturbances in the early phase of relapsing-remitting multiple sclerosis. *J Neurol Neurosurg Psychiatry* **70**, (2001).
95. Jacobsen, C. *et al.* Brain atrophy and disability progression in multiple sclerosis patients: A 10-year follow-up study. *J Neurol Neurosurg Psychiatry* **85**, (2014).
96. Uher, T. *et al.* Early magnetic resonance imaging predictors of clinical progression after 48 months in clinically isolated syndrome patients treated with intramuscular interferon β-1a. *Eur J Neurol* **22**, (2015).
97. Calabrese, M. *et al.* Cortical atrophy is relevant in multiple sclerosis at clinical onset. *J Neurol* **254**, (2007).
98. Eikelenboom, M. J. *et al.* Multiple sclerosis: Neurofilament light chain antibodies are correlated to cerebral atrophy. *Neurology* **60**, (2003).
99. Miller, D. H., Barkhof, F., Frank, J. A., Parker, G. J. M. & Thompson, A. J. Measurement of atrophy in multiple sclerosis: Pathological basis, methodological aspects and clinical relevance. *Brain* vol. 125 Preprint at https://doi.org/10.1093/brain/awf177 (2002).
100. Rudick, R. A., Fisher, E., Lee, J.-C., Duda, J. T. & Simon, J. Brain atrophy in relapsing multiple sclerosis: relationship to relapses, EDSS, and treatment with interferon β-1a. *Multiple Sclerosis Journal* **6**, (2000).
101. Andravizou, A. *et al.* Brain atrophy in multiple sclerosis: mechanisms, clinical relevance and treatment options. *Autoimmunity Highlights* **10**, (2019).
102. Lee, J. Y. *et al.* Clinically available software for automatic brain volumetry: Comparisons of volume measurements and validation of intermethod reliability. *Korean J Radiol* **22**, (2021).
103. Chard, D. T. *et al.* Brain atrophy in clinically early relapsing-remitting multiple sclerosis. *Brain* **125**, (2002).
104. Saindane, A. M. *et al.* The effect of gadolinium-enhancing lesions on whole brain atrophy in relapsing-remitting MS. *Neurology* **55**, (2000).
105. Chard, D. T. *et al.* The longitudinal relation between brain lesion load and atrophy in multiple sclerosis: A 14 year follow up study. *J Neurol Neurosurg Psychiatry* **74**, (2003).
106. Rocca, M. A. *et al.* Brain MRI atrophy quantification in MS. *Neurology* **88**, (2017).
107. Koubiyr, I. *et al.* Longitudinal fibre-specific white matter damage predicts cognitive decline in multiple sclerosis. *Brain Commun* **6**, (2024).
108. Simon, J. H. *et al.* Corpus callosum and subcallosal-periventricular lesions in multiple sclerosis: Detection with MR. *Radiology* **160**, (1986).

109. Eshaghi, A. *et al.* Progression of regional grey matter atrophy in multiple sclerosis. *Brain* **141**, (2018).
110. Steenwijk, M. D. *et al.* Cortical atrophy patterns in multiple sclerosis are non-random and clinically relevant. *Brain* **139**, (2016).
111. Batista, S. *et al.* Basal ganglia, thalamus and neocortical atrophy predicting slowed cognitive processing in multiple sclerosis. *J Neurol* **259**, (2012).
112. Schoonheim, M. M. *et al.* Subcortical atrophy and cognition: Sex effects in multiple sclerosis. *Neurology* **79**, (2012).
113. Zivadinov, R. *et al.* Thalamic atrophy is associated with development of clinically definite multiple sclerosis. *Radiology* **268**, (2013).
114. Rocca, M. A. *et al.* Thalamic damage and long-term progression of disability in multiple sclerosis. *Radiology* **257**, (2010).
115. Houtchens, M. K. *et al.* Thalamic atrophy and cognition in multiple sclerosis. *Neurology* **69**, (2007).
116. Sandroff, B. M. *et al.* Thalamic atrophy moderates associations among aerobic fitness, cognitive processing speed, and walking endurance in persons with multiple sclerosis. *J Neurol* **269**, (2022).
117. Stevenson, V. L. *et al.* Spinal cord atrophy and disability in MS: A longitudinal study. *Neurology* **51**, (1998).
118. Lovas, G., Szilágyi, N., Majtényi, K., Palkovits, M. & Komoly, S. Axonal changes in chronic demyelinated cervical spinal cord plaques. *Brain* **123**, (2000).
119. Daams, M. *et al.* Mean upper cervical cord area (MUCCA) measurement in long-standing multiple sclerosis: Relation to brain findings and clinical disability. *Multiple Sclerosis Journal* **20**, (2014).
120. Gallego-Delgado, P. *et al.* Neuroinflammation in the normal-appearing white matter (NAWM) of the multiple sclerosis brain causes abnormalities at the nodes of Ranvier. *PLoS Biol* **18**, (2020).
121. Lassmann, H. Multiple Sclerosis Pathology. *Cold Spring Harb Perspect Med* **8**, a028936 (2018).
122. Van Der Valk, P. & Amor, S. Preactive lesions in multiple sclerosis. *Current Opinion in Neurology* vol. 22 Preprint at https://doi.org/10.1097/WCO.0b013e32832b4c76 (2009).
123. Elliott, C. *et al.* Abnormalities in normal-appearing white matter from which multiple sclerosis lesions arise. *Brain Commun* **3**, (2021).
124. Koh, D. M. & Collins, D. J. Diffusion-weighted MRI in the body: Applications and challenges in oncology. *American Journal of Roentgenology* **188**, (2007).
125. Le Bihan, D. *et al.* Separation of diffusion and perfusion in intravoxel incoherent motion MR imaging. *Radiology* **168**, (1988).
126. Barreto, M. M. *et al.* Correlation between computed tomographic and magnetic resonance imaging findings of parenchymal lung diseases. *European Journal of Radiology* vol. 82 Preprint at https://doi.org/10.1016/j.ejrad.2013.04.037 (2013).
127. Bihan, D. Le. Molecular diffusion, tissue microdynamics and microstructure. *NMR Biomed* **8**, (1995).

128. Stejskal, E. O. & Tanner, J. E. Spin diffusion measurements: Spin echoes in the presence of a time-dependent field gradient. *J Chem Phys* **42**, (1965).
129. Bammer, R. Basic principles of diffusion-weighted imaging. *Eur J Radiol* **45**, (2003).
130. Carr, H. Y. & Purcell, E. M. Effects of diffusion on free precession in nuclear magnetic resonance experiments. *Physical Review* **94**, (1954).
131. Feng, Y., Okamoto, R. J., Namani, R., Genin, G. M. & Bayly, P. V. Measurements of mechanical anisotropy in brain tissue and implications for transversely isotropic material models of white matter. *J Mech Behav Biomed Mater* **23**, (2013).
132. Huisman, T. A. G. M. Diffusion-weighted and diffusion tensor imaging of the brain, made easy. *Cancer Imaging* **10**, S163–S171 (2010).
133. Prange, M. & Meaney, D. F. Defining Brain Mechanical Properties: Effects of Region, Direction, and Species. in *SAE Technical Papers* vols 2000-November (2000).
134. Alexander, A. L., Lee, J. E., Lazar, M. & Field, A. S. Diffusion Tensor Imaging of the Brain. *Neurotherapeutics* **4**, 316–329 (2007).
135. Cercignani, M., Lannucci, G. & Filippi, M. Diffusion-weighted imaging in multiple sclerosis. *Ital J Neurol Sci* **20**, (1999).
136. Hanyu, H. *et al.* Diffusion-weighted MR imaging of the hippocampus and temporal white matter in alzheimer's disease. *J Neurol Sci* **156**, (1998).
137. Schocke, M. F. H. *et al.* Diffusion-weighted MRI differentiates the Parkinson variant of multiple system atrophy from PD. *Neurology* **58**, (2002).
138. Liu, A. Y., Maldjian, J. A., Bagley, L. J., Sinson, G. P. & Grossman, R. I. Traumatic brain injury: Diffusion-weighted MR imaging findings. *American Journal of Neuroradiology* **20**, (1999).
139. Roberts, T. P. L. & Rowley, H. A. Diffusion weighted magnetic resonance imaging in stroke. *Eur J Radiol* **45**, (2003).
140. Basser, P. J., Mattiello, J. & Lebihan, D. Estimation of the Effective Self-Diffusion Tensor from the NMR Spin Echo. *J Magn Reson B* **103**, (1994).
141. Le Bihan, D. *et al.* Diffusion tensor imaging: Concepts and applications. *Journal of Magnetic Resonance Imaging* **13**, (2001).
142. Madden, D. J. *et al.* Diffusion tensor imaging of cerebral white matter integrity in cognitive aging. *Biochimica et Biophysica Acta (BBA) - Molecular Basis of Disease* **1822**, 386–400 (2012).
143. Budde, M. D., Xie, M., Cross, A. H. & Song, S. K. Axial diffusivity is the primary correlate of axonal injury in the experimental autoimmune encephalomyelitis spinal cord: A quantitative pixelwise analysis. *Journal of Neuroscience* **29**, (2009).
144. Tu, T. W. *et al.* Radiological-pathological correlation of diffusion tensor and magnetization transfer imaging in a closed head traumatic brain injury model. *Ann Neurol* **79**, (2016).
145. Song, S. K. *et al.* Demyelination increases radial diffusivity in corpus callosum of mouse brain. *Neuroimage* **26**, (2005).
146. Budde, M. D. *et al.* Toward accurate diagnosis of white matter pathology using diffusion tensor imaging. *Magn Reson Med* **57**, (2007).

147. Song, S. K. *et al.* Dysmyelination revealed through MRI as increased radial (but unchanged axial) diffusion of water. *Neuroimage* **17**, (2002).
148. Pierpaoli, C. *et al.* Water diffusion changes in wallerian degeneration and their dependence on white matter architecture. *Neuroimage* **13**, (2001).
149. Sun, S. W., Liang, H. F., Cross, A. H. & Song, S. K. Evolving Wallerian degeneration after transient retinal ischemia in mice characterized by diffusion tensor imaging. *Neuroimage* **40**, (2008).
150. Tournier, J. D., Mori, S. & Leemans, A. Diffusion tensor imaging and beyond. *Magnetic Resonance in Medicine* vol. 65 Preprint at https://doi.org/10.1002/mrm.22924 (2011).
151. Cercignani, M. & Gandini Wheeler-Kingshott, C. From micro- to macro-structures in multiple sclerosis: what is the added value of diffusion imaging. *NMR in Biomedicine* vol. 32 Preprint at https://doi.org/10.1002/nbm.3888 (2019).
152. Werring, D. J., Clark, C. A., Barker, G. J., Thompson, A. J. & Miller, D. H. Diffusion tensor imaging of lesions and normal-appearing white matter in multiple sclerosis. *Neurology* **52**, (1999).
153. Filippi, M. *et al.* A quantitative study of water diffusion in multiple sclerosis lesions and normal-appearing white matter using echo- planar imaging. *Arch Neurol* **57**, (2000).
154. Goldberg-Zimring, D., Mewes, A. U. J., Maddah, M. & Warfield, S. K. Diffusion tensor magnetic resonance imaging in multiple sclerosis. *Journal of Neuroimaging* vol. 15 Preprint at https://doi.org/10.1177/1051228405283363 (2005).
155. Van Hecke, W. *et al.* Correlation of cognitive dysfunction and diffusion tensor MRI measures in patients with mild and moderate multiple sclerosis. *Journal of Magnetic Resonance Imaging* **31**, (2010).
156. Lin, X., Tench, C. R., Morgan, P. S., Niepel, G. & Constantinescu, C. S. 'Importance sampling' in MS: Use of diffusion tensor tractography to quantify pathology related to specific impairment. *J Neurol Sci* **237**, (2005).
157. Sigal, T., Shmuel, M., Mark, D., Gil, H. & Anat, A. Diffusion Tensor Imaging of Corpus Callosum Integrity in Multiple Sclerosis: Correlation with Disease Variables. *Journal of Neuroimaging* **22**, (2012).
158. Ciccarelli, O. *et al.* Investigation of MS normal-appearing brain using diffusion tensor MRI with clinical correlations. *Neurology* **56**, (2001).
159. Oh, J. *et al.* Spinal cord quantitative MRI discriminates between disability levels in multiple sclerosis. *Neurology* **80**, (2013).
160. Oh, J. *et al.* Multiparametric MRI correlates of sensorimotor function in the spinal cord in multiple sclerosis. *Multiple Sclerosis Journal* **19**, (2013).
161. Zhuo, J. & Gullapalli, R. P. Diffusion Kurtosis Imaging. in *Neuroimaging Techniques in Clinical Practice* 215–228 (Springer International Publishing, Cham, 2020). doi:10.1007/978-3-030-48419-4_15.
162. Liu, C., Bammer, R. & Moseley, M. E. Limitations of apparent diffusion coefficient-based models in characterizing non-Gaussian diffusion. *Magn Reson Med* **54**, (2005).
163. Tournier, J., Mori, S. & Leemans, A. Diffusion tensor imaging and beyond. *Magn Reson Med* **65**, 1532–1556 (2011).

164. Jeurissen, B., Leemans, A., Tournier, J. D., Jones, D. K. & Sijbers, J. Investigating the prevalence of complex fiber configurations in white matter tissue with diffusion magnetic resonance imaging. *Hum Brain Mapp* **34**, (2013).
165. Sepehrband, F. *et al.* Perivascular space fluid contributes to diffusion tensor imaging changes in white matter. *Neuroimage* **197**, (2019).
166. Jensen, J. H., Helpern, J. A., Ramani, A., Lu, H. & Kaczynski, K. Diffusional kurtosis imaging: The quantification of non-Gaussian water diffusion by means of magnetic resonance imaging. *Magn Reson Med* **53**, (2005).
167. Steven, A. J., Zhuo, J. & Melhem, E. R. Diffusion kurtosis imaging: An emerging technique for evaluating the microstructural environment of the brain. *American Journal of Roentgenology* **202**, (2014).
168. Jensen, J. H. & Helpern, J. A. MRI quantification of non-Gaussian water diffusion by kurtosis analysis. *NMR in Biomedicine* vol. 23 Preprint at https://doi.org/10.1002/nbm.1518 (2010).
169. Neto Henriques, R., Correia, M. M., Nunes, R. G. & Ferreira, H. A. Exploring the 3D geometry of the diffusion kurtosis tensor-Impact on the development of robust tractography procedures and novel biomarkers. *Neuroimage* **111**, (2015).
170. Kelm, N. D. *et al.* Evaluation of diffusion kurtosis imaging in ex vivo hypomyelinated mouse brains. *Neuroimage* **124**, (2016).
171. Yoshida, M. *et al.* Diffusional kurtosis imaging of normal-appearing white matter in multiple sclerosis: Preliminary clinical experience. *Jpn J Radiol* **31**, (2013).
172. Li, H. Q. *et al.* Evaluation of patients with relapsing-remitting multiple sclerosis using tract-based spatial statistics analysis: Diffusion kurtosis imaging. *BMC Neurol* **18**, (2018).
173. Raz, E. *et al.* A better characterization of spinal cord damage in multiple sclerosis: A diffusional kurtosis imaging study. in *American Journal of Neuroradiology* vol. 34 (2013).
174. Spampinato, M. V. *et al.* Diffusional Kurtosis Imaging of the Corticospinal Tract in Multiple Sclerosis: Association with Neurologic Disability. *American Journal of Neuroradiology* **38**, 1494–1500 (2017).
175. de Kouchkovsky, I. *et al.* Quantification of normal-appearing white matter tract integrity in multiple sclerosis: a diffusion kurtosis imaging study. *J Neurol* **263**, (2016).
176. Zhu, Q. *et al.* Increased cortical lesion load contributed to pathological changes beyond focal lesion in cortical gray matter of multiple sclerosis: A diffusion kurtosis imaging analysis. *Cerebral Cortex* **33**, (2023).
177. Bester, M. *et al.* Non-Gaussian diffusion MRI of gray matter is associated with cognitive impairment in multiple sclerosis. *Multiple Sclerosis* **21**, (2015).
178. Zhang, H., Schneider, T., Wheeler-Kingshott, C. A. & Alexander, D. C. NODDI: Practical in vivo neurite orientation dispersion and density imaging of the human brain. *Neuroimage* **61**, (2012).
179. Caranova, M., Soares, J. F., Batista, S., Castelo-Branco, M. & Duarte, J. V. A systematic review of microstructural abnormalities in multiple sclerosis detected with NODDI and DTI models of diffusion-weighted magnetic resonance imaging. *Magnetic Resonance Imaging* vol. 104 Preprint at https://doi.org/10.1016/j.mri.2023.09.010 (2023).

180. Granberg, T. *et al.* In vivo characterization of cortical and white matter neuroaxonal pathology in early multiple sclerosis. *Brain* **140**, (2017).
181. Sacco, S. *et al.* Neurite orientation dispersion and density imaging for assessing acute inflammation and lesion evolution in MS. *American Journal of Neuroradiology* **41**, (2020).
182. Margoni, M. *et al.* Quantification of normal-appearing white matter damage in early relapse-onset multiple sclerosis through neurite orientation dispersion and density imaging. *Mult Scler Relat Disord* **58**, (2022).
183. Hagiwara, A. *et al.* White matter abnormalities in multiple sclerosis evaluated by quantitative synthetic MRI, diffusion tensor imaging, and neurite orientation dispersion and density imaging. *American Journal of Neuroradiology* **40**, (2019).
184. Spano, B. *et al.* Disruption of neurite morphology parallels MS progression. *Neurol Neuroimmunol Neuroinflamm* **5**, (2018).
185. Collorone, S. *et al.* Reduced neurite density in the brain and cervical spinal cord in relapsing–remitting multiple sclerosis: A NODDI study. *Multiple Sclerosis Journal* **26**, (2020).
186. Grussu, F. *et al.* Neurite dispersion: a new marker of multiple sclerosis spinal cord pathology? *Ann Clin Transl Neurol* **4**, (2017).
187. By, S., Xu, J., Box, B. A., Bagnato, F. R. & Smith, S. A. Application and evaluation of NODDI in the cervical spinal cord of multiple sclerosis patients. *Neuroimage Clin* **15**, (2017).
188. Raffelt, D. A. *et al.* Investigating white matter fibre density and morphology using fixel-based analysis. *Neuroimage* **144**, (2017).
189. Raffelt, D. A. *et al.* Connectivity-based fixel enhancement: Whole-brain statistical analysis of diffusion MRI measures in the presence of crossing fibres. *Neuroimage* **117**, (2015).
190. Tournier, J. D., Calamante, F. & Connelly, A. Robust determination of the fibre orientation distribution in diffusion MRI: Non-negativity constrained super-resolved spherical deconvolution. *Neuroimage* **35**, (2007).
191. Dhollander, T. *et al.* Fixel-based Analysis of Diffusion MRI: Methods, Applications, Challenges and Opportunities. *NeuroImage* vol. 241 Preprint at https://doi.org/10.1016/j.neuroimage.2021.118417 (2021).
192. Jeurissen, B., Leemans, A., Jones, D. K., Tournier, J. D. & Sijbers, J. Estimating the number of fiber orientations in diffusion MRI voxels: a constrained spherical deconvolution study. in *Proceedings of the International Society for Magnetic Resonance in Medicine* vol. 18 (2010).
193. Tuch, D. S. *et al.* High angular resolution diffusion imaging reveals intravoxel white matter fiber heterogeneity. *Magn Reson Med* **48**, (2002).
194. Raffelt, D. *et al.* Apparent Fibre Density: A novel measure for the analysis of diffusion-weighted magnetic resonance images. *Neuroimage* **59**, (2012).
195. Gajamange, S. *et al.* Fibre-specific white matter changes in multiple sclerosis patients with optic neuritis. *Neuroimage Clin* **17**, (2018).

196. Koubiyr, I. *et al.* Longitudinal fibre-specific white matter damage predicts cognitive decline in multiple sclerosis. *Brain Commun* **6**, (2023).
197. Strik, M. *et al.* Axonal loss in major sensorimotor tracts is associated with impaired motor performance in minimally disabled multiple sclerosis patients. *Brain Commun* **3**, (2021).
198. Carandini, T. *et al.* Disruption of brainstem monoaminergic fibre tracts in multiple sclerosis as a putative mechanism for cognitive fatigue: a fixel-based analysis. *Neuroimage Clin* **30**, (2021).
199. Farquharson, S. *et al.* White matter fiber tractography: Why we need to move beyond DTI. *J Neurosurg* **118**, (2013).
200. Hernandez-Gutierrez, E. *et al.* Multi-tensor fixel-based metrics in tractometry: application to multiple sclerosis. *Front Neurosci* **18**, (2024).
201. Shu, N. *et al.* Diffusion tensor tractography reveals disrupted topological efficiency in white matter structural networks in multiple sclerosis. *Cerebral Cortex* vol. 21 Preprint at https://doi.org/10.1093/cercor/bhr039 (2011).
202. Li, Y. *et al.* Diffusion tensor imaging based network analysis detects alterations of neuroconnectivity in patients with clinically early relapsing-remitting multiple sclerosis. *Hum Brain Mapp* **34**, (2013).
203. Nigro, S. *et al.* Structural connectomic alterations in the limbic system of multiple sclerosis patients with major depression. *Multiple Sclerosis* **21**, (2015).
204. Romascano, D. *et al.* Multicontrast connectometry: A new tool to assess cerebellum alterations in early relapsing-remitting multiple sclerosis. *Hum Brain Mapp* **36**, (2015).
205. Llufriu, S. *et al.* Structural networks involved in attention and executive functions in multiple sclerosis. *Neuroimage Clin* **13**, (2017).
206. Dineen, R. A. *et al.* Disconnection as a mechanism for cognitive dysfunction in multiple sclerosis. *Brain* **132**, (2009).
207. He, Y. *et al.* Impaired small-world efficiency in structural cortical networks in multiple sclerosis associated with white matter lesion load. *Brain* **132**, (2009).
208. Henkelman, R. M., Stanisz, G. J. & Graham, S. J. Magnetization transfer in MRI: A review. *NMR in Biomedicine* vol. 14 Preprint at https://doi.org/10.1002/nbm.683 (2001).
209. Horsfield, M. A. Magnetization transfer imaging in multiple sclerosis. *Journal of Neuroimaging* vol. 15 Preprint at https://doi.org/10.1177/1051228405282242 (2005).
210. Rausch, M., Hiestand, P., Baumann, D., Cannet, C. & Rudin, M. MRI-based monitoring of inflammation and tissue damage in acute and chronic relapsing EAE. *Magn Reson Med* **50**, (2003).
211. Deloire-Grassin, M. S. A. *et al.* In vivo evaluation of remyelination in rat brain by magnetization transfer imaging. *J Neurol Sci* **178**, (2000).
212. Dousset, V. *et al.* Lysolecithin-induced demyelination in primates: Preliminary in vivo study with MR and magnetization transfer. *American Journal of Neuroradiology* **16**, (1995).
213. Dousset, V. *et al.* Experimental allergic encephalomyelitis and multiple sclerosis: Lesion characterization with magnetization transfer imaging. *Radiology* **182**, (1992).

214. Bot, J. C. J. *et al.* The spinal cord in multiple sclerosis: Relationship of high-spatial-resolution quantitative MR imaging findings to histopathologic results. *Radiology* **233**, (2004).
215. Mottershead, J. P. *et al.* High field MRI correlates of myelin content and axonal density in multiple sclerosis: A post-mortem study of the spinal cord. *J Neurol* **250**, (2003).
216. Van Waesberghe, J. H. T. M. *et al.* Axonal loss in multiple sclerosis lesions: Magnetic resonance imaging insights into substrates of disability. *Ann Neurol* **46**, (1999).
217. Hiehle, J. F., Grossman, R. I., Ramer, K. N., Gonzalez-Scarano, F. & Cohen, J. A. Magnetization transfer effects in MR-detected multiple sclerosis lesions: Comparison with gadolinium-enhanced spin-echo images and nonenhanced T1- weighted images. *American Journal of Neuroradiology* **16**, (1995).
218. Goodkin, D. E. *et al.* A serial study of new MS lesions and the white matter from which they arise. *Neurology* **51**, (1998).
219. Traboulsee, A. *et al.* Disability in multiple sclerosis is related to normal appearing brain tissue MTR histogram abnormalities. *Multiple Sclerosis* **9**, (2003).
220. Chen, J. T. H. *et al.* Clinically feasible MTR is sensitive to cortical demyelination in MS. *Neurology* **80**, (2013).
221. Davies, G. R. *et al.* Evidence for grey matter MTR abnormality in minimally disabled patients with early relapsing-remitting multiple sclerosis. *J Neurol Neurosurg Psychiatry* **75**, (2004).
222. Alonso-Ortiz, E., Levesque, I. R. & Pike, G. B. MRI-based myelin water imaging: A technical review. *Magn Reson Med* **73**, (2015).
223. Whittall, K. P. *et al.* In vivo measurement of T2 distributions and water contents in normal human brain. *Magn Reson Med* **37**, 34–43 (1997).
224. Lee, J. *et al.* So You Want to Image Myelin Using MRI: An Overview and Practical Guide for Myelin Water Imaging. *Journal of Magnetic Resonance Imaging* vol. 53 Preprint at https://doi.org/10.1002/jmri.27059 (2021).
225. MacKay, A. L. & Laule, C. Magnetic Resonance of Myelin Water: An in vivo Marker for Myelin. *Brain Plasticity* **2**, (2016).
226. Laule, C. *et al.* Myelin water imaging of multiple sclerosis at 7 T: Correlations with histopathology. *Neuroimage* **40**, (2008).
227. Laule, C. *et al.* Myelin water imaging in multiple sclerosis: Quantitative correlations with histopathology. *Multiple Sclerosis* **12**, (2006).
228. Kozlowski, P., Liu, J., Yung, A. C. & Tetzlaff, W. High-resolution myelin water measurements in rat spinal cord. *Magn Reson Med* **59**, (2008).
229. Stanisz, G. J., Webb, S., Munro, C. A., Pun, T. & Midha, R. MR Properties of Excised Neural Tissue Following Experimentally Induced Inflammation. *Magn Reson Med* **51**, (2004).
230. Laule, C. *et al.* Water content and myelin water fraction in multiple sclerosis: A T 2 relaxation study. *J Neurol* **251**, (2004).
231. Vavasour, I. M. *et al.* Longitudinal changes in myelin water fraction in two MS patients with active disease. *J Neurol Sci* **276**, (2009).

232. Kitzler, H. H. *et al.* Multi-component relaxation in clinically isolated syndrome: Lesion myelination may predict multiple sclerosis conversion. *Neuroimage Clin* **20**, (2018).
233. Vargas, W. S. *et al.* Measuring longitudinal myelin water fraction in new multiple sclerosis lesions. *Neuroimage Clin* **9**, (2015).
234. Kolind, S. *et al.* Brain and cord myelin water imaging: A progressive multiple sclerosis biomarker. *Neuroimage Clin* **9**, (2015).
235. Kolind, S. *et al.* Myelin water imaging reflects clinical variability in multiple sclerosis. *Neuroimage* **60**, (2012).
236. Edwards, E. M. *et al.* Associations between myelin water imaging and measures of fall risk and functional mobility in multiple sclerosis. *Journal of Neuroimaging* **33**, (2023).
237. Bouman, P. M. *et al.* Histopathology-validated recommendations for cortical lesion imaging in multiple sclerosis. *Brain* **143**, (2020).
238. Kilsdonk, I. D. *et al.* Increased cortical grey matter lesion detection in multiple sclerosis with 7 T MRI: A post-mortem verification study. *Brain* **139**, (2016).
239. Tallantyre, E. C. *et al.* 3 Tesla and 7 Tesla MRI of multiple sclerosis cortical lesions. *J Magn Reson Imaging* **32**, (2010).
240. Nielsen, A. S. *et al.* Focal cortical lesion detection in multiple sclerosis: 3 tesla DIR versus 7 tesla FLASH-T2. *Journal of Magnetic Resonance Imaging* **35**, (2012).
241. Dula, A. N. *et al.* Magnetic resonance imaging of the cervical spinal cord in multiple sclerosis at 7T. *Multiple Sclerosis* **22**, (2016).
242. De Graaf, W. L. *et al.* Clinical application of multi-contrast 7-T MR imaging in multiple sclerosis: Increased lesion detection compared to 3 T confined to grey matter. *Eur Radiol* **23**, (2013).
243. Absinta, M. *et al.* Identification of chronic active multiple sclerosis lesions on 3T MRI. *American Journal of Neuroradiology* **39**, (2018).
244. Tallantyre, E. C. *et al.* A comparison of 3T and 7T in the detection of small parenchymal veins within MS lesions. *Invest Radiol* **44**, (2009).
245. Ineichen, B. V., Beck, E. S., Piccirelli, M. & Reich, D. S. New Prospects for Ultra-High-Field Magnetic Resonance Imaging in Multiple Sclerosis. *Investigative Radiology* vol. 56 Preprint at https://doi.org/10.1097/RLI.0000000000000804 (2021).
246. Kraff, O. & Quick, H. H. 7T: Physics, safety, and potential clinical applications. *Journal of Magnetic Resonance Imaging* vol. 46 Preprint at https://doi.org/10.1002/jmri.25723 (2017).

CHAPTER 2 – POWER PRODUCTION DURING THE FIVE TIMES SIT TO STAND TEST IN PEOPLE WITH MULTIPLE SCLEROSIS[1]

Introduction

Multiple sclerosis (MS) is a chronic neurological condition affecting an estimated 2.8 million people worldwide and is a leading cause of long-term disability in young adults.[1,2] In MS pathology, damage to myelinated axons disrupts neural communication within the brain and spinal cord, leading to a variety of symptoms.[3,4] Among the most impactful of these symptoms is a progressive decline in motor and sensory function.[5,6] These physical limitations can significantly interfere with daily life, as many people with MS face increasing challenges with movement and balance over time.[7,8]

One of the most detrimental consequences of MS-related physical impairments is an increased risk of falls.[9] Falls begin early in the disease course, sometimes preceding a clinical MS diagnosis, and increase in frequency as the disease advances.[10] Falls pose a heightened risk of physical injury (e.g., fractures, head injuries), and they precipitate a cascade of psychological and social effects.[11,12] Falls and the fear of falling impede individual independence by reducing physical activity, limiting comfort and confidence in movement, and decreasing social engagement, ultimately leading to diminished quality of life.[11,13–161]

Many falls occur during transfer movements when an individual changes body positions, such as when rising and lowering from a chair.[17] As such, clinical assessments of sit-to-stand

[1] This chapter is published as: Patrick CM, Bast IE, Scarsbrook MW, Swanson CW, Fling BW, Johnson KA. Power Production During the Five Times Sit to Stand Test in People with Multiple Sclerosis. *Multiple Sclerosis and Related Disorders.* 2025; 106582.

transfer ability are particularly relevant. The Five Times Sit-to-Stand Test (5XSST) is a reliable measure of transfer ability and functional strength in aging and neurological populations.[18–21] Moreover, according to clinical practice guidelines for neurorehabilitation, the 5XSST is the best practice for assessing sit-to-stand transfer ability in people with MS.[22]

Beyond evaluating functional mobility, metrics derived from force plates during a sit-to-stand transfer, such as peak lower-body power, differentiate fallers from non-fallers in older adults.[23] While measuring lower-body power during transfers may help identify fall risk in people with MS, the equipment and time required to measure power is largely inaccessible to clinicians. Accordingly, equations that use readily available metrics such as patient height, weight, and time to complete the transfer assessment have been developed to estimate lower-body power during sit-to-stand transfers.[24] Currently, it is unknown whether these equations accurately estimate lower-body power during transfers in individuals with MS. Given the high rate of falls among people with MS and the harmful impact falls have on health and well-being, assessing transfer ability and lower-body power with clinically feasible tests like the 5XSST can provide valuable insights for enhancing health monitoring and outcomes within neurological conditions such as MS.

Therefore, the aims of this study were to 1) examine differences in 5XSST vertical ground reaction force (vGRF) profiles and associated kinetic metrics between people with MS and matched controls, 2) establish the relationship between force plate-derived lower-body power with estimated lower-body power during the 5XSST, and 3) compare force plate derived power and estimated power during the 5XSST between fallers and non-fallers with MS. Together, this work aids in developing accessible methods for fall risk monitoring, prevention, and neurorehabilitation for people with MS.

Materials and Methods

The data for this study was collected as part of a larger investigation into the neural underpinnings of motor control in people with MS. The study was reviewed and approved by the Colorado State University Institutional Review Board (IRB#18-7738H), and all participants provided written informed consent prior to participation.

Participants

A total of 56 participants from northern Colorado were enrolled in this study, including 29 individuals with a neurologist confirmed diagnosis of relapsing-remitting MS and 27 sex- and age-matched neurotypical (NT) controls. Only individuals with mild to moderate disability (0–6.5, self-reported Expanded Disability Status Scale (EDSS)) were eligible to participate. Participants were excluded if they reported a musculoskeletal injury, joint replacement, vestibular disorder, or any neurological conditions other than MS known to impact mobility.

Five Times Sit-to-Stand Test (5XSST)

Participants completed five repetitions of a sit-to-stand movement using a standard chair with a straight back, no armrests, and a seat height of 17 inches (43.2 cm), consistent with recommended height ranges.[25] Prior to the 5XSST, participants' feet were positioned shoulder width apart with each foot situated on independent force plates. During the movement, participants were instructed to maintain a forward gaze and perform five sit-to-stand and stand-to-sit movements as quickly and safely as possible, with arms and hands placed across their chest.

Force Parameters

Throughout the 5XSST, only participants' feet were situated on the force plates, with each foot positioned on a separate force plate (Model 4060-10, Bertec Corp., Columbus, OH, USA). The chair was positioned off platform and did not contribute to the force signal. vGRF was

collected bilaterally at 1000 Hz and subsequently added together for a complete vGRF measure. Force measurements were processed using a 20 Hz lowpass filter in MATLAB (v.9.14.0, MathWorks Inc., Natick, MA, USA). Following filtering, several outcome metrics were extracted from the force profile using a custom MATLAB script and visualized in Figure 2.1.

The completion time for the 5XSST was measured from the onset of trunk flexion during the first stand action, defined as a ≥2.5% decrease in foot weight,[26] to the completion of the fifth sit, identified as a local minimum in the vGRF profile using a first-derivative approach. Incline, a measure of the rate of force development (RFD), is the slope of the vGRF profile between 20% and 90% of maximum vGRF,[26] expressed as percent body weight per second (%BW/s; Figure 2.1A and 1B). Maximum vGRF was calculated as the maximal vGRF generated by participants during the rising phase of the movement and normalized to participant body weight (Figure 2.1C). Peak-to-Trough is the difference in force between the max vGRF and the following local minimum (trough) prior to full standing position (Figure 2.1C and D). Instrumented power was calculated as the center-of-mass (COM) vertical velocity multiplied by vGRF. Participant body mass and vGRF were used to calculate COM vertical acceleration, then integrated to calculate COM vertical velocity. All force metrics were calculated for each individual sit-to-stand movement and then averaged across the five repetitions.

Estimated Power

Estimated power was calculated using an equation that strongly correlates to instrumented power from force plate and video analysis of the 5XSST and a leg press power assessment in older adults (Equation 2.1).[24,27] This equation estimates leg length as half of the participant's height (Equation 2.1). Therefore, a second power estimate was calculated using measured leg length, defined as the distance between the medial malleolus and the greater trochanter, to more accurately

capture body displacement and consequently better approximate instrumented power (Equation 2.2).

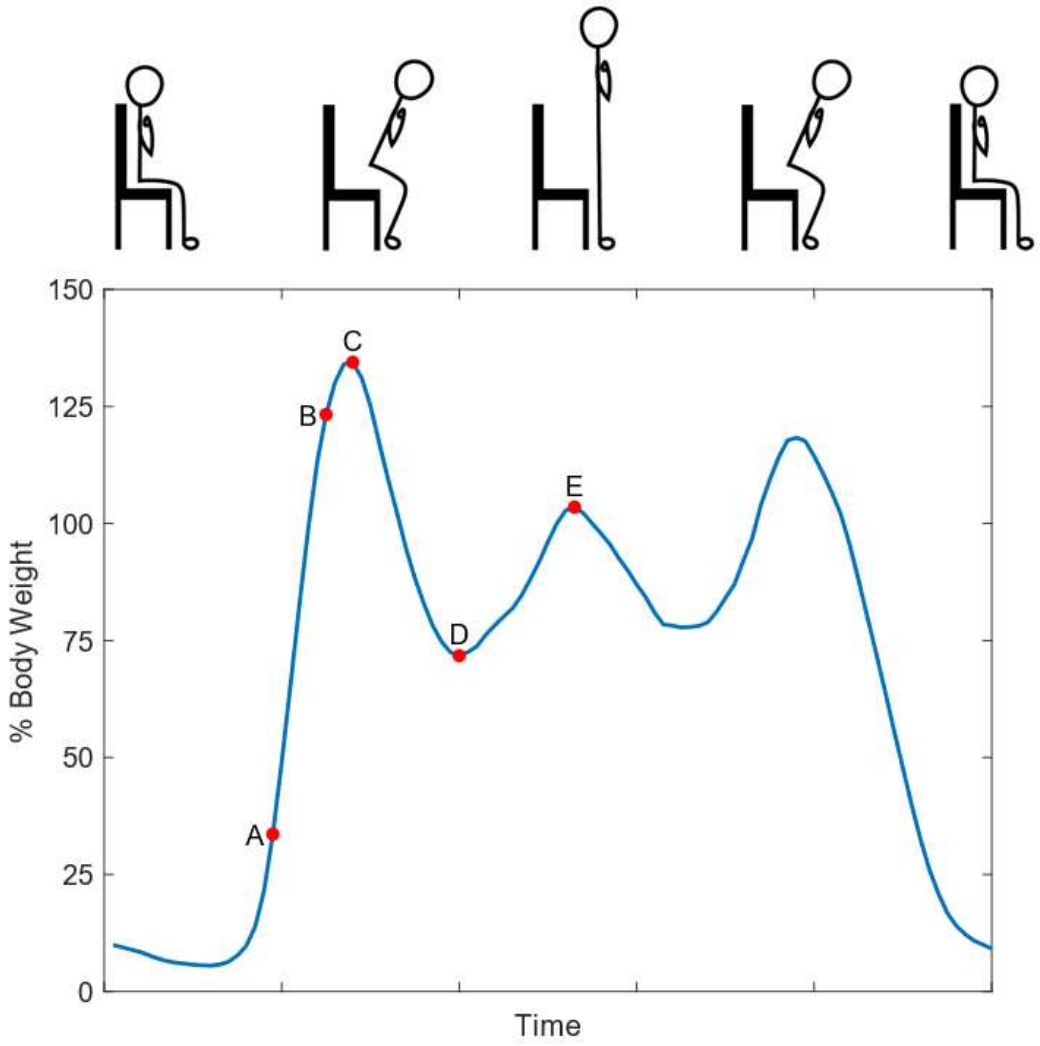

Figure 2.1. Representative vGRF profile during a single sit-to-stand-to-sit transition. (Top) Relative body position across one repetition of the sit-to-stand task. (Bottom) Corresponding vGRF profile normalized to body weight. (A) 20% of maximum vGRF; (B) 90% of maximum vGRF; (C) maximum vGRF, peak; (D) local minimum following max vGRF, trough; (E) Stand, ~100% body weight.

Equation 2.1:

$$Mean\ SST\ power\ (W)\ =\ \frac{Body\ mass\ \times\ 0.9\ \times\ [Height\ \times\ 0.5 - Chair\ Height]}{\left(\frac{5XSST\ time}{n\ of\ SST\ repetitions}\right)\ \times\ 0.5}$$

Equation 2.2:

$$Mean\ SST\ power\ (W)\ =\ \frac{Body\ mass\ \times\ 0.9\ \times\ [\boldsymbol{Leg\ Length} - Chair\ Height]}{\left(\frac{5XSST\ time}{n\ of\ SST\ repetitions}\right)\ \times\ 0.5}$$

Disability and Functional Impairment

The Expanded Disability Status Scale (EDSS) is a widely used scale to assess neurological function and disease progression in people with MS.[28] Participants with MS reported their EDSS score using a self-administered questionnaire. Self-reported EDSS scoring is strongly associated with physician-assessed EDSS scoring.[29]

Fall History

Participants reported all falls that occurred in the six months prior to study enrollment. Those having at least one fall were classified as fallers.[30]

Secondary Assessments

Participants also completed the Timed Up and Go (TUG) test and mini Balance Evaluation Systems Test (miniBEST), clinical assessments of mobility and balance validated in the MS population.[31,32] Briefly, the TUG test measures functional mobility by recording the time taken to rise from a chair, walk seven meters, turn, and return to the chair.[33] The miniBEST assesses dynamic balance across four domains: anticipatory postural adjustments, reactive postural control, sensory orientation, and balance during gait.[34] Individuals with MS also completed the 12-item Multiple Sclerosis Walking Scale (MSWS12) questionnaire, which assesses the impact of MS on walking ability in daily life and is predictive of faller status in people with MS.[30,35]

Statistical Analysis

One-dimensional statistical parametric mapping (SPM) was used to identify which parts of the vGRF profile differed between individuals with MS and NT controls.[36,37] This analysis focused on differences in body control within the rising and lowering phases of the sit-to-stand movement. To center the analysis on the core portion of the movement, vGRF data points were isolated from 25% body weight during rising to 25% body weight during lowering. These data points were registered to 101 nodes to time-normalize the movement from 0–100%. A two-sample SPM t-test was then applied to compare force profiles between groups at each node.

Additional 5XSST metrics were imported to R Statistical Software (v4.4.2; R Core Team, Vienna, Austria, 2024) for statistical analysis. Two sample t-tests were used for group comparisons between people with MS and NT controls for maximum vGRF, incline, peak-to-trough, instrumented lower-body power, and estimated lower-body power. For each variable in each group, quantile-quantile plots and Shapiro-Wilks Tests were used to confirm normality. Levene's Test was used to confirm equal variance for each variable. A Welch two sample t-test was used to compare 5XSST completion time, as it failed the assumption of equal variance. For comparisons between fallers and non-fallers with MS, the same normality and variance testing was conducted. Two-sample t-tests were used for instrumented power, estimated power, incline, and peak-to-trough, Welch's t-test was used for maximum vGRF, and Mann-Whitney U tests were used for 5XSST completion time, TUG, miniBEST, and MSWS-12. All group comparisons were conducted as one-tailed tests. Cohen's d was used to calculate effect sizes (*d*). Correlations between instrumented and estimated lower-body power were calculated using Pearson's product-moment correlation coefficient (r). The alpha level was set to 0.05 for all statistical tests, with Bonferroni correction applied for multiple comparisons of force plate-derived metrics.

Results

Group Characteristics

The MS group presented with mild to moderate disability, with an average score of 3.2 ± 1.7 (median: 4, range: 0 - 6.5) on the EDSS (Table 2.1). The MS and NT groups were similar in age ($p = 0.908$), height ($p = 0.161$), and body mass index (BMI, $p = 0.994$). Compared to the NTs, people with MS took longer to complete the TUG test ($p = 0.002$) and performed worse on the miniBEST ($p < 0.001$). People with MS also reported more falls, averaging 1.7 ± 2.9 falls in the past six months, whereas no falls were reported by the NT group (Table 2.1).

Table 2.1. Group Characteristics. Average demographic and clinical characteristics of participant groups. Fallers were people with MS who reported 1 or more falls within the past 6 months. Non-fallers were people with MS who reported 0 falls within the past 6 months. BMI = Body Mass Index; EDSS = Expanded Disability Status Scale; MSWS12 = Twelve Item MS Walking Scale; TUG = Timed-Up and Go Test; miniBEST = Mini-Balance Evaluation Systems Test.

Characteristic	Multiple Sclerosis		Neurotypical		*p-value*
	Mean	*SD*	*Mean*	*SD*	
n	29	-	27	-	-
Sex (male:female)	9:20	-	8:19	-	
Age *(years)*	47.5	12.2	47.1	15.2	0.908
BMI (kg/m²)	24.9	3.7	24.9	3.3	0.994
Height (cm)	166.4	7.6	169.3	7.9	0.161
EDSS	3.2	1.7	-	-	-
MSWS12 Total	27.5	14.4	-	-	-

MSWS12 Percentage (%)	32.3	30.0	-	-	-
TUG (s)	18.7	4.8	15.5	1.8	0.002
miniBEST Total	24.0	5.6	29.2	2.5	<0.001
Falls Past 6 months			-	-	-
- Fallers (n = 10)	1.7	2.9			
- Non-fallers (n = 19)	0	0			

5XSST Performance and Force Profile Comparison

Force profile differences between groups are presented in Table 2.2. People with MS took longer to complete the 5XSST compared to the NTs, showed lower maximal vGRF, lower incline, lower peak-to-trough, and lower mean and maximal power.

Table 2.2. Comparison of 5XSST performance time, force production, and power outputs between the MS and NT groups. Bonferroni correction for multiple comparisons was applied and available in the corrected *p-value* column.

Variable	Multiple Sclerosis		Neurotypical		*Uncorrected*	*Corrected*	Cohen's *d*
	Mean	*SD*	*Mean*	*SD*	*p-value*	*p-value*	
Completion Time (s)	13.4	3.6	11.0	2.2	0.002	0.011	0.82
Max vGRF (%BW)	129.9	11.1	138.7	10.5	0.002	0.011	-0.81
Incline (%BW/s)	723.1	267.3	972.8	213.5	<0.001	<0.001	-1.03
Peak-to-Trough (%BW)	65.3	23.8	83.3	21.6	0.002	0.013	-0.80
Mean Power (W)	202.1	67.5	258.9	81.1	0.003	0.020	-0.76
Max Power (W)	378.0	140.2	492.5	154.3	0.003	0.016	-0.78

SPM analysis (Figure 2.2A) revealed differences in the vGRF between MS and NT groups during the sit-to-stand-to-sit movement. Corresponding force profiles for both groups are shown in Figure 2.2B. During the rising phase of the movement, the NT group generated higher vGRF from 2-18% of the task cycle ($p < 0.001$). This was followed by a lower trough in the NT group compared to the MS group, between 32–38% of the task cycle ($p < 0.001$). The lowering phase of the movement was nearly a mirror of the rising phase with the NT group exhibiting lower vGRF at a local minimum following the standing phase (58–72%, $p < 0.001$) and higher vGRF at the local maximum during the lowering phase (78–95%, $p < 0.001$). Overall, the MS group demonstrated a flatter vGRF profile, characterized by lower values at both peaks and higher values at both troughs, while the NT group displayed a more dynamic profile with more pronounced peaks and troughs.

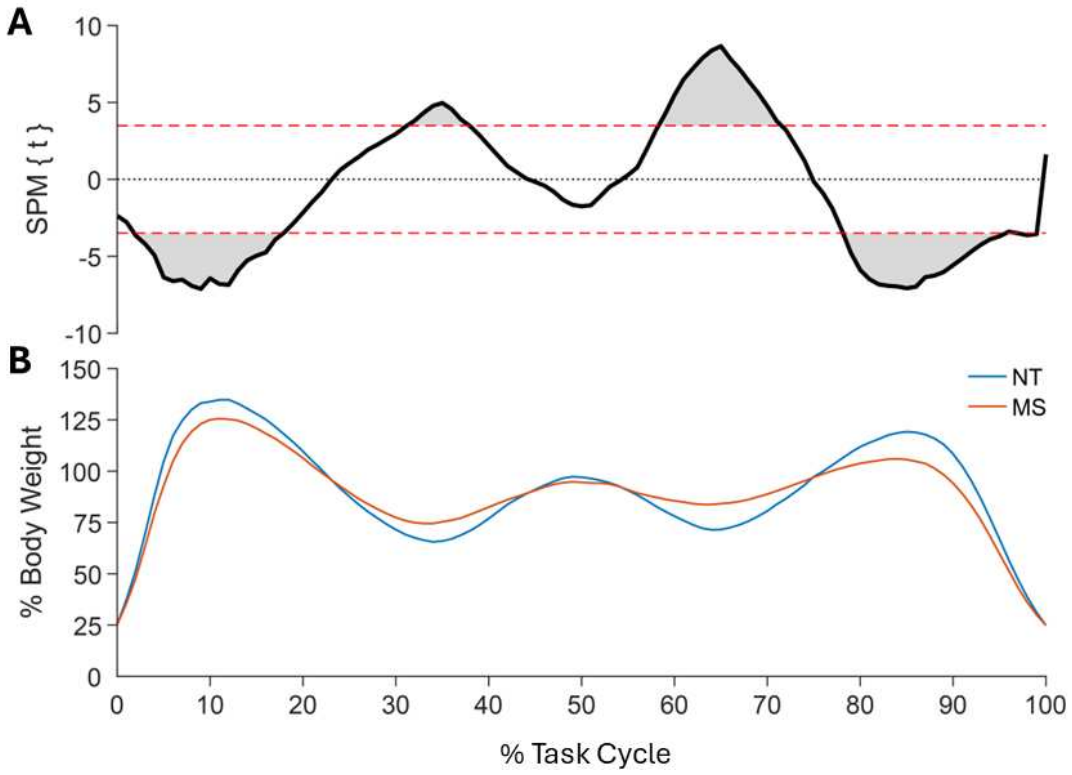

Figure 2.2. Group differences in vGRF during the sit-to-stand-to-sit task. (A) Statistical parametric mapping (SPM) results comparing vGRF profiles between the MS and NT groups. Shaded regions above and below the red dotted lines indicate significant (alpha = 0.05) differences along the task cycle. (B) Mean vGRF profiles expressed as %BW for people with MS (orange line) and NT controls (blue line).

Instrumented and Estimated Power

A moderate positive relationship was found between instrumented power and estimated power using Equation 2.1 ($r = 0.525$, $p = 0.003$) (Figure 2.3A). When leg length was used in place of 0.5 × height (Equation 2.2), a slightly stronger correlation was observed ($r = 0.594$, $p < 0.001$) (Figure 2.3B). Both relationships exhibit low r² values, indicating that the models explain a limited proportion of the variance in instrumented power (Equation 2.1: $r^2 = 0.275$; Equation 2.2: $r^2 = 0.352$).

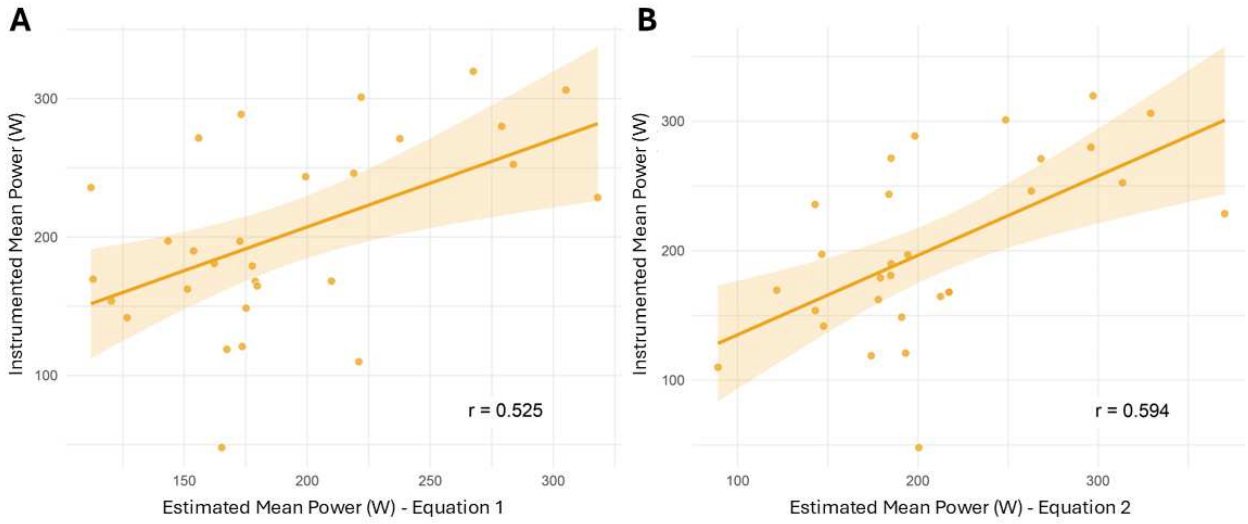

Figure 2.3. Correlations between instrumented power and estimated power in people with MS. (A) Equation 2.1 ($r = 0.525$, $p = 0.003$), (B) Equation 2.2 ($r = 0.594$, $p < 0.001$).

Kinetic and Clinical Comparisons – MS Fallers and Non-Fallers

In the MS group, differences in instrumented and estimated power were observed between fallers (n = 10) and non-fallers (n = 19). Non-fallers demonstrated higher mean values for instrumented power ($p = 0.026$, $d = 0.82$) and estimated power ($p = 0.028$, $d = 0.72$) compared to fallers (Figure 2.4). Given that Equation 2.2 yielded the strongest correlation in the MS group (Figure 2.3B), it was selected for this comparison. In addition to power, incline was the only other 5XSST metric that differed between groups (fallers: 602.4 ± 151.2 %BW/s vs. non-fallers: 786.6

± 295.6 %BW/s, p = 0.018). No differences were observed in 5XSST completion time (fallers: 14.3 ± 3.3 seconds vs. non-fallers: 12.9 ± 3.7 seconds, p = 0.097), max vGRF (fallers: 128.1 ± 5.4 %BW vs. non-fallers: 130.9 ± 13.2 %BW, p = 0.212), or peak-to-trough (fallers: 60.9 ± 16.1 %BW vs. non-fallers: 67.5 ± 27.2 %BW, p = 0.209). Across other clinical assessments, fallers took longer to complete the TUG test (fallers: 21.2 ± 3.7 seconds vs. non-fallers: 17.4 ± 4.9 seconds, p = 0.004), scored lower on the miniBEST (fallers: 20.0 ± 5.6 vs. non-fallers: 26.2 ± 4.3, p = 0.002), and reported higher scores on the MSWS-12 (fallers: 60.2 ± 23.0% vs. non-fallers: 17.7 ± 21.9%, p < 0.001), compared to non-fallers.

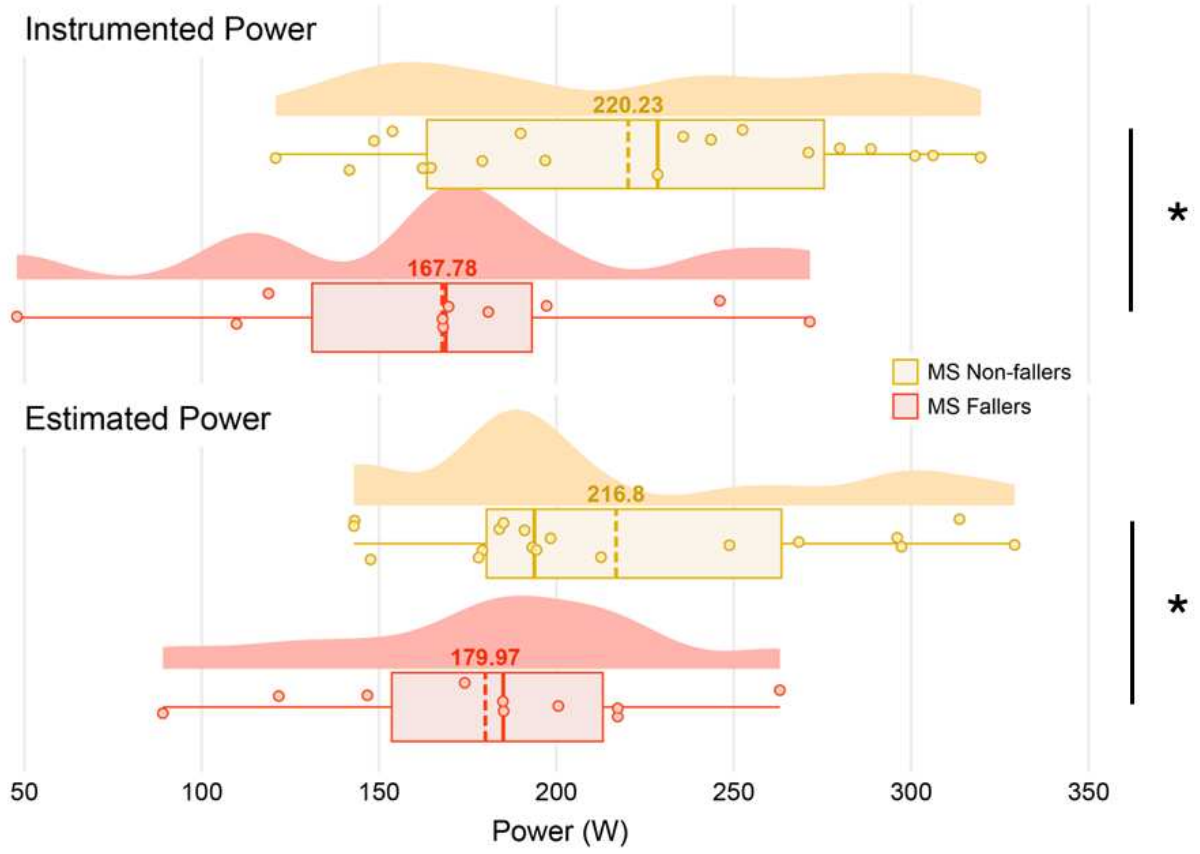

Figure 2.4. Comparison of instrumented and estimated power between Fallers and Non-Fallers with MS. (Top) Instrumented Power (p = 0.026, d = 0.82). (Bottom) Estimated Power calculated by Equation 2.2 (p = 0.028, d = 0.72). Dotted Line = Mean; Solid Line = Median. * Indicates significance (p < 0.05).

Discussion

The aims of this study were to compare vGRF profiles and associated kinetics during the 5XSST between people with MS and NT controls, assess the relationship between instrumented power and estimated power in people with MS, and compare 5XSST outcomes and performance of common clinical mobility assessments between fallers and non-fallers with MS. The findings indicate 1) People with MS control body weight differently during transfers compared to NT controls, 2) Existing equations developed to estimate lower-body power in elderly populations correlate moderately but may under- or overestimate actual power production in people with MS, and 3) Reduced lower body power during sit-to-stand transfers coincides with higher fall risk in people with MS.

5XSST Performance Differences Between People with MS and NT Controls

Compared to matched NT controls, people with MS took longer to complete the 5XSST task taking an average of 13.4 ± 3.6 seconds. This time is consistent with times measured by stopwatch in other studies in people with MS of similar age and disability level.[38–40]

Differences in force profile shape reflect distinct strategies for body weight control during the transfer movement between the two groups. Specifically, during the rising (concentric) phase, the NT group exhibited greater peak force (max vGRF) and greater RFD (incline) (Table 2.2 & Figure 2.2), reflecting a superior ability to generate force during the initial push-off from a seated position. This larger and quicker force generation allowed the NT group to build greater vertical momentum, resulting in a pronounced deceleration phase prior to standing, quantified as the peak-to-trough metric (Table 2.2). In contrast, people with MS produced smaller force at a slower RFD, resulting in reduced momentum, a shallower trough, a significantly lower peak-to-trough value, and ultimately, a flatter overall vGRF curve shape (Table 2.2 & Figure 2.2). A similar pattern was

observed during the lowering (eccentric) phase, where people with MS exhibited a shallower trough and smaller maximum vGRF compared to NT controls. Taken together, individuals with MS were less dynamic and slower when transferring to and from a standing position.

These findings may indicate deficits in explosive strength and dynamic weight transfer in people with MS. It is well established that lower-body strength, specifically knee extension strength, is related to 5XSST time in people with MS.[39–42] While knee extension strength was not measured in this study, the differences observed between groups during the rising and lowering phases suggest that people with MS had weaker lower-body strength compared to NT peers, which likely contributed to a longer time to complete the 5XSST. Furthermore, the flatter force profile in people with MS may indicate a compensatory strategy to prioritize balance and stability over speed, potentially due to challenges with reduced proprioception, impaired motor control, and diminished muscle strength, common impairments in people with MS.[4,43] Taken together, these findings emphasize the need for targeted interventions, such as strength training and neuromuscular rehabilitation, to improve ballistic force generation and transfer ability in people with MS.

Equations for Estimating Power

Lower-body power is a valuable indicator of fall risk in aging populations.[23] However, measuring power by force plates or machines may not be practical in some clinical settings. Estimating lower-body power through equations that use readily available patient metrics offers a feasible alternative. The findings from this study indicate that estimated lower-body power is moderately correlated to instrumented power in people with MS, and substituting measured leg length slightly improves the strength of the correlation (Figure 2.3). While half height serves as a

reasonable approximation for the displacement occurring during the movement, using leg length may offer modest yet valuable improvements in power estimation.

Although the two equations were moderately correlated with instrumented power, both had large variability and low r^2 values, suggesting that the agreement between the estimates and instrumented power was low. Equation 2.1 underestimated lower-body power (-10.3 ± 61.1 W (estimated – instrumented power)), whereas Equation 2.2 overestimated (+7.3 ± 60.0 W (estimated – instrumented power)). Given that the equations were developed in a different population (NT older adults) they still show promise for estimating lower-body power in people with MS, potentially due to similarities in mobility impairment between middle-aged adults with MS and NT older adults.[44] Regression models have estimated peak and average lower-body power in the 5XSST for healthy and older adults,[45,46] but applying this approach to MS would require a large, diverse sample, which is beyond the scope of this analysis.

Comparison of Fallers vs. Non-fallers with MS

Consistent with previous findings,[30,47,48] fallers with MS in our study performed worse on clinical assessments of dynamic mobility and postural stability as compared to non-fallers with MS. However, these groups did not differ in the time to complete the 5XSST. While clinicians typically observe and subjectively evaluate movement quality during the 5XSST, the time it takes to complete the task is the primary quantitative outcome. These findings indicate that the 5XSST time may not be a good indicator of fall risk in people with MS with mild to moderate disability. Although the lack of a significant difference may be influenced by the sample size, the differences in other clinical assessments (TUG, miniBEST, and MSWS-12) provide additional support that time to complete 5XSST may not be sensitive enough to detect differences in fall risk among people with MS. A novel finding from this study is that fallers and non-fallers with MS exhibited

distinct characteristics during the 5XSST task. Specifically, fallers with MS demonstrated lower instrumented and estimated power (Figure 2.4) and lower RFD (incline) compared to non-fallers. These differences were accompanied by moderate to large effect sizes, underscoring the potential value of power and RFD metrics in identifying fall risk in people with MS.

Overall, these findings emphasize the importance of rapidly generating lower-body force to reduce fall risk in people with MS. This is consistent with findings that showed knee extension RFD discriminates fallers and non-fallers with MS.[49] Resistance training that emphasizes "a fast concentric phase and a slow eccentric phase" improves 5XSST performance in people with MS.[42] Together, these studies, along with our findings, underscore the critical role of rapid force generation in mitigating fall risk. However, the accessibility and portability of equipment such as knee extension machines and other lower-body strength assessment tools can be a limitation in some clinical settings. Thus, there is a need for practical and accurate clinical assessments to aid decision-making in the absence of specialized machinery. Notably, our findings suggest that estimated power, calculated with the leg length modification, can effectively differentiate fallers with MS from non-fallers with MS, offering a viable alternative to instrumented power measurements.

Limitations

Several factors should be considered when interpreting these findings. This study relies solely on force plate data to assess the 5XSST without tracking body position. While body tracking could provide additional insight, ground reaction force data alone is a well-established method for evaluating functional lower limb performance.

Although age, height, and BMI did not differ between groups, the small, uneven sample of MS fallers (n = 10) and non-fallers (n = 19) may limit the power to detect differences. Additionally,

fall status was based on self-reported falls over six months, introducing potential recall bias. Fall frequencies also varied widely, with some participants reporting only one or two falls and others more than ten.

All people with MS in this study had relapsing-remitting MS, limiting generalizability to other subtypes. Additionally, the narrow range of self-reported EDSS scores reflects a population with mild disability, restricting applicability to those with more severe impairment.

Conclusion

This study highlights that people with MS control their bodies differently during the 5XSST movement compared to NT peers, generating less vGRF, lower rates of force development, and reduced power, resulting in longer time to complete the task. While estimated lower-body power equations provided a moderate approximation of instrumented power, large variability in estimation accuracy underscores the need for improvement. Notably, substituting leg length, a clinically accessible metric, for 0.5 x height, strengthened the correlation between estimated and instrumented power. Future studies should explore factors that increase estimation accuracy in the MS population, enabling clinicians to better assess fall risk. Finally, there is a need for future research to determine whether interventions like high-velocity resistance training improve lower body power during sit-to-stand transfers and subsequently reduce fall risk in people with MS.

References

1. Walton, C. *et al.* Rising prevalence of multiple sclerosis worldwide: Insights from the Atlas of MS, third edition. *Multiple Sclerosis Journal* **26**, (2020).
2. Brownlee, W. J., Hardy, T. A., Fazekas, F. & Miller, D. H. Diagnosis of multiple sclerosis: progress and challenges. *The Lancet* vol. 389 Preprint at https://doi.org/10.1016/S0140-6736(16)30959-X (2017).
3. Dobson, R. & Giovannoni, G. Multiple sclerosis – a review. *European Journal of Neurology* vol. 26 27–40 Preprint at https://doi.org/10.1111/ene.13819 (2019).
4. Horng, S. & Fabian, M. The pathophysiology and clinical presentation of multiple sclerosis. in *Handbook of Relapsing-Remitting Multiple Sclerosis* (2017). doi:10.1007/978-3-319-40628-2_2.
5. Ghasemi, N., Razavi, S. & Nikzad, E. Multiple sclerosis: Pathogenesis, symptoms, diagnoses and cell-based therapy. *Cell Journal* vol. 19 Preprint at (2017).
6. Green, R., Cutter, G., Friendly, M. & Kister, I. Which symptoms contribute the most to patients' perception of health in multiple sclerosis? *Mult Scler J Exp Transl Clin* **3**, (2017).
7. Lublin, F. D. *et al.* How patients with multiple sclerosis acquire disability. *Brain* **145**, (2022).
8. Cameron, M. H. & Nilsagard, Y. Balance, gait, and falls in multiple sclerosis. in *Handbook of Clinical Neurology* vol. 159 (2018).
9. Mazumder, R., Murchison, C., Bourdette, D. & Cameron, M. Falls in people with multiple sclerosis compared with falls in healthy controls. *PLoS One* **9**, (2014).
10. Moen, S. M., Celius, E. G., Nordsletten, L. & Holmøy, T. Fractures and falls in patients with newly diagnosed clinically isolated syndrome and multiple sclerosis. *Acta Neurol Scand* **124**, (2011).
11. Peterson, E. W., Cho, C. C. & Finlayson, M. L. Fear of falling and associated activity curtailment among middle aged and older adults with multiple sclerosis. *Multiple Sclerosis* **13**, (2007).
12. Tinetti, M. E., Doucette, J., Claus, E. & Marottoli, R. Risk Factors for Serious Injury During Falls by Older Persons in the Community. *J Am Geriatr Soc* **43**, (1995).
13. Peterson, E. W., Cho, C. C., von Koch, L. & Finlayson, M. L. Injurious Falls Among Middle Aged and Older Adults With Multiple Sclerosis. *Arch Phys Med Rehabil* **89**, (2008).
14. Coleman, C. I., Sidovar, M. F., Roberts, M. S. & Kohn, C. Impact of Mobility Impairment on Indirect Costs and Health-Related Quality of Life in Multiple Sclerosis. *PLoS One* **8**, (2013).
15. Sutliff, M. H. Contribution of impaired mobility to patient burden in multiple sclerosis. *Current Medical Research and Opinion* vol. 26 Preprint at https://doi.org/10.1185/03007990903433528 (2010).
16. Zwibel, H. L. Contribution of impaired mobility and general symptoms to the burden of multiple sclerosis. *Advances in Therapy* vol. 26 Preprint at https://doi.org/10.1007/s12325-009-0082-x (2009).
17. Robinovitch, S. N. *et al.* Video capture of the circumstances of falls in elderly people residing in long-term care: An observational study. *The Lancet* **381**, (2013).

18. Mong, Y., Teo, T. W. & Ng, S. S. 5-Repetition Sit-to-Stand Test in Subjects With Chronic Stroke: Reliability and Validity. *Arch Phys Med Rehabil* **91**, (2010).
19. Paul, S. S., Canning, C. G., Sherrington, C. & Fung, V. S. C. Reproducibility of measures of leg muscle power, leg muscle strength, postural sway and mobility in people with Parkinson's disease. *Gait Posture* **36**, (2012).
20. Wang, T. H., Liao, H. F. & Peng, Y. C. Reliability and validity of the five-repetition sit-to-stand test for children with cerebral palsy. *Clin Rehabil* **26**, (2012).
21. Lord, S. R., Murray, S. M., Chapman, K., Munro, B. & Tiedemann, A. Sit-to-stand performance depends on sensation, speed, balance, and psychological status in addition to strength in older people. *Journals of Gerontology - Series A Biological Sciences and Medical Sciences* **57**, (2002).
22. Moore, J. L. *et al.* A core set of outcome measures for adults with neurologic conditions undergoing rehabilitation. *Journal of Neurologic Physical Therapy* vol. 42 Preprint at https://doi.org/10.1097/NPT.0000000000000229 (2018).
23. Cheng, Y. Y. *et al.* Can sit-to-stand lower limb muscle power predict fall status? *Gait Posture* **40**, (2014).
24. Alcazar, J. *et al.* The sit-to-stand muscle power test: An easy, inexpensive and portable procedure to assess muscle power in older people. *Exp Gerontol* **112**, 38–43 (2018).
25. Bohannon, R. W. Reference values for the five-repetition sit-to-stand test: A Descriptive meta-analysis of data from elders. *Percept Mot Skills* **103**, (2006).
26. Lindemann, U. *et al.* Measuring power during the sit-to-stand transfer. *Eur J Appl Physiol* **89**, (2003).
27. Baltasar-Fernandez, I. *et al.* Comparison of available equations to estimate sit-to-stand muscle power and their association with gait speed and frailty in older people: Practical applications for the 5-rep sit-to-stand test. *Exp Gerontol* **156**, (2021).
28. Kurtzke, J. F. Rating neurologic impairment in multiple sclerosis: An expanded disability status scale (EDSS). *Neurology* **33**, (1983).
29. Bowen, J., Gibbons, L., Gianas, A. & Kraft, G. H. Self-administered expanded disability status scale with functional system scores correlates well with a physician-administered test. *Multiple Sclerosis* **7**, (2001).
30. Abate, C., Gromisch, E. S., Campo, M., Ruiz, J. A. & DelMastro, H. M. Predicting faller status in persons with multiple sclerosis using the Multiple Sclerosis Walking Scale-12. *Mult Scler Relat Disord* **92**, 105924 (2024).
31. Sebastião, E., Sandroff, B. M., Learmonth, Y. C. & Motl, R. W. Validity of the Timed Up and Go Test as a Measure of Functional Mobility in Persons with Multiple Sclerosis. *Arch Phys Med Rehabil* **97**, (2016).
32. Potter, K. *et al.* Reliability, validity, and responsiveness of the mini-balance evaluation systems test in ambulatory individuals with multiple sclerosis. *Physiotherapy Canada* **71**, (2019).
33. Ramari, C., Hvid, L. G., David, A. C. de & Dalgas, U. The importance of lower-extremity muscle strength for lower-limb functional capacity in multiple sclerosis: Systematic review. *Annals of Physical and Rehabilitation Medicine* vol. 63 Preprint at https://doi.org/10.1016/j.rehab.2019.11.005 (2020).
34. Franchignoni, F., Horak, F., Godi, M., Nardone, A. & Giordano, A. Using psychometric techniques to improve the Balance Evaluation Systems Test: the mini-BESTest. *J Rehabil Med* **42**, 323–331 (2010).

35. Hobart, J. C., Riazi, A., Lamping, D. L., Fitzpatrick, R. & Thompson, A. J. Measuring the impact of MS on walking ability: The 12-item MS Walking Scale (MSWS-12). *Neurology* **60**, (2003).
36. Pataky, T. C. One-dimensional statistical parametric mapping in Python. *Comput Methods Biomech Biomed Engin* **15**, (2012).
37. Pataky, T. C. Generalized n-dimensional biomechanical field analysis using statistical parametric mapping. *J Biomech* **43**, (2010).
38. Özüdoğru, A., Canlı, M., Gürses, Ö. A., Alkan, H. & Yetiş, A. Determination of five times-sit-to-stand test performance in patients with multiple sclerosis: validity and reliability. *Somatosens Mot Res* **40**, 72–77 (2023).
39. Kjølhede, T. *et al.* Relationship between muscle strength parameters and functional capacity in persons with mild to moderate degree multiple sclerosis. *Mult Scler Relat Disord* **4**, 151–158 (2015).
40. Jensen, H. B. *et al.* Effect of slow release-Fampridine on muscle strength, rate of force development, functional capacity and cognitive function in an enriched population of MS patients. A randomized, double blind, placebo controlled study. *Mult Scler Relat Disord* **10**, 137–144 (2016).
41. Møller, A. B. *et al.* Validity and variability of the 5-repetition sit-to-stand test in patients with multiple sclerosis. *Disabil Rehabil* **34**, 2251–2258 (2012).
42. Dalgas, U. *et al.* Resistance training improves muscle strength and functional capacity in multiple sclerosis. *Neurology* **73**, 1478–1484 (2009).
43. Gelfand, J. M. Multiple sclerosis: diagnosis, differential diagnosis, and clinical presentation. *Handb Clin Neurol* **122**, 269–290 (2014).
44. Swanson, C. W., Richmond, S. B., Sharp, B. E. & Fling, B. W. Middle-age people with multiple sclerosis demonstrate similar mobility characteristics to neurotypical older adults. *Mult Scler Relat Disord* **51**, 102924 (2021).
45. Smith, W. N. *et al.* Simple equations to predict concentric lower-body muscle power in older adults using the 30-second chair-rise test: a pilot study. *Clin Interv Aging* **5**, (2010).
46. Ruiz-Cárdenas, J. D., Rodríguez-Juan, J. J., Smart, R. R., Jakobi, J. M. & Jones, G. R. Validity and reliability of an iPhone App to assess time, velocity and leg power during a sit-to-stand functional performance test. *Gait Posture* **59**, 261–266 (2018).
47. Ross, E. *et al.* Cohort study comparing the berg balance scale and the Mini-BESTest in people who have multiple sclerosis and are ambulatory. *Phys Ther* **96**, (2016).
48. Kalron, A. Association between gait variability, falls and mobility in people with multiple sclerosis: A specific observation on the EDSS 4.0-4.5 level. *NeuroRehabilitation* **40**, (2017).
49. Kristensen, N. M. *et al.* Neuromuscular rate of force development discriminates fallers in ambulatory persons with multiple sclerosis - an exploratory study. *Mult Scler Relat Disord* **75**, (2023).

CHAPTER 3 – ASSOCIATIONS BETWEEN CORTICOSPINAL TRACT NEUROPHYSIOLOGY AND LOWER-LIMB MOTOR FUNCTION IN PEOPLE WITH MULTIPLE SCLEROSIS

Introduction

Multiple sclerosis (MS) is a chronic disease of the central nervous system and the most common non-traumatic neurodegenerative disease among young adults.[1,2] With disease onset typically between the ages of 20 – 40, and a life expectancy that often approaches that of the general population, individuals commonly live with MS for several decades.[3–6] This prolonged disease course imposes a substantial long-term burden, often requiring continuous medical care, rehabilitation, and lifestyle modifications, contributing to significant socioeconomic costs over the lifespan.[7,8]

The clinical presentation of MS is highly variable, with individuals experiencing a diverse range of symptoms such as muscle weakness, fatigue, spasticity, sensory disturbances, and cognitive dysfunction.[9–11] Symptoms arise from neural injury caused by an aberrant immune response that damages myelin and axons, triggering inflammatory and neurodegenerative processes throughout the central nervous system.[12,13] Resulting neuronal damage disrupts neural signal transmission, leading to delayed conduction and reduced signal amplitude, compromising communication across functional neural networks.[14–17] Over time, the accumulation of structural damage and disrupted neural communication gives rise to functional impairments that interfere with daily activities.[2,18]

Among the most prevalent and impactful symptoms of MS are mobility and balance impairments, affecting more than 90% of patients.[19,20] These challenges often begin early in the

disease course and progress to interfere with personal, occupational, and social functioning.[7,21] One of the most serious consequences of impaired mobility and balance in MS is an elevated risk of falls.[22] As MS progresses, fall frequency increases, elevating the risk of serious injury such as fractures and head trauma.[21,23,24] In addition to physical harm, falls can contribute to fear of falling, reduced self-efficacy, and avoidance of physical activity. Together, these effects can contribute to social withdrawal and diminished quality of life.[8,20,23,25–28]

One of the most prominent contributors to fall risk in individuals with MS is lower-extremity weakness.[29,30] The lower-limbs are disproportionately affected in MS, as they are innervated by some of the longest axons in the central nervous system, making them more vulnerable to demyelination and axonal damage.[31–33] Consequently, impairments in lower-limb strength and motor control are common, with evidence showing reduced motor unit recruitment, reduced capacity for maximal force generation, and slower rates of force development (RFD).[33–40] The combination of reduced strength and rate of force development limits the ability to safely perform dynamic tasks such as standing up, recovering from perturbations, or changing direction while walking.[41–43]

Impairments in motor output among individuals with MS are closely tied to disruptions in central motor pathways, particularly the corticospinal tract (CST), which plays a central role in voluntary motor control.[36,44–47] Transcranial magnetic stimulation (TMS) is a frequently used technique to non-invasively probe CST function in clinical populations such as MS.[48] TMS-derived metrics such as motor-evoked potential (MEP), MEP onset latency, and cortical silent period (CSP) offer insight into excitability, conduction efficiency, and intracortical inhibition within the CST.[49] These metrics reflect the integrity of the CST and offer insight into the state and responsiveness of the motor system in individuals with MS. Associating TMS measures with

assessments of muscle function, such as maximum voluntary isometric contractions (MVIC), reflects how central motor system alterations in individuals with MS contribute to deficits in maximal voluntary force production.

While isolated assessments of CST function and muscular strength via MVIC are informative, it is equally important to understand how these impairments affect dynamic real-world motor tasks. The sit-to-stand movement is a fundamental component of daily mobility, performed approximately 60 times per day by healthy adults.[50] Falls often occur during transfer movements, such as the sit-to-stand, as they require strength, balance, and coordination.[51] Together, sit-to-stand performance serves as a clinically relevant indicator of fall risk and functional capacity. The Five Times Sit-to-Stand Test (5XSST) is a widely used and validated assessment that captures lower-limb strength and is recommended by neurorehabilitation guidelines as a best-practice tool for evaluating transfer ability in people with MS.[52–57] Additionally, metrics derived from the sit-to-stand movement, such as mean and max power production, have been shown to differentiate fallers from non-fallers in MS and other clinical populations (Chapter 2).[58] However, it remains unknown how TMS-derived neurophysiological measures relate to performance during functional transfer movements such as the 5XSST. Exploring these relationships may inform more targeted and effective rehabilitation strategies to enhance CST excitability or task-specific training aimed at improving force generation.

The present study aimed to evaluate CST function, tibialis anterior (TA) maximal motor output, and functional mobility via the 5XSST in individuals with MS compared to age- and sex-matched neurotypical (NT) controls, and to examine the associations between neurophysiologic measures and motor performance. The following hypotheses were tested: 1. Individuals with MS will exhibit reduced MEP area, increased normalized MEP onset latency, and increased CSP area

compared to NT controls. 2. Individuals with MS will demonstrate impaired muscular and functional performance, characterized by lower MVIC maximal force production and reduced muscle activation during MVIC, and diminished 5XSST force generation, and slower 5XSST task completion. 3. MEP area will correlate positively with MVIC force and electromyography (EMG) amplitude, and normalized MEP latency will correlate with MVIC RFD measures in participants with MS. 4. MEP area will correlate with 5XSST concentric and eccentric force production metrics, normalized MEP latency will correlate with concentric and eccentric 5XSST force modulation measures in participants with MS, and CSP Area will correlate with eccentric 5XSST force production metrics.

Materials and Methods

The present study is a secondary analysis of data collected as part of a broader investigation into the neural correlates of motor impairment in individuals with MS. Ethical review and approval was granted from the Colorado State University Institutional Review Board (IRB#18-7738H), and informed written consent was provided by all participants in accordance with the Declaration of Helsinki prior to participation.

Participants

Of the 59 individuals enrolled in the original study (30 with relapsing-remitting MS and 29 NT controls), only 50 participants completed the TMS protocol, the primary outcome measure in this investigation, and were therefore included in the present analysis. The final sample consisted of 26 individuals with a neurologist-confirmed diagnosis of relapsing-remitting MS and 24 age- and sex-matched NT controls. Inclusion criteria for individuals with MS required participants to have mild to moderate disability, defined as a self-reported Expanded Disability Status Scale (EDSS) score ranging from 0 to 6.5. Exclusion criteria for all participants included

musculoskeletal injury, joint replacement, pregnancy, or vestibular dysfunction. Additionally, participants with contraindications to TMS, such as a history of seizures, epilepsy, or metal implants, were excluded. Participants with MS were excluded if they had any neurological conditions besides MS, and NT controls were required to have no history of neurological conditions.

Transcranial Magnetic Stimulation Acquisition

TMS was used to assess the functional integrity of the CST by probing three neurophysiological processes, excitability, inhibition, and conduction latency. Single-pulse TMS was delivered using a 2 × 95 mm angled butterfly coil (120-degree, Cool D-B80, MagVenture), positioned approximately 45–65° from the mid-sagittal plane,[59] to elicit MEPs from the TA muscle of each leg. Muscle activity was recorded using surface EMG with bipolar Ag-AgCl electrodes placed over the TA muscle belly.

The optimal cortical stimulation site for eliciting responses from each TA muscle was identified by systematically delivering pulses starting 1 cm lateral and 1 cm posterior to the vertex of the cranium (defined by the intersection of the lines projecting from nasion-inion and left-right pre-auricular points) and adjusting the coil to evoke the largest and most consistent MEPs.[60] Once the motor "hot spot" was identified in each hemisphere, resting motor threshold (RMT) was determined as the lowest TMS intensity required to produce MEP peak-to-peak amplitudes of at least 0.05 mV in 5 out of 10 consecutive trials.[61] During data acquisition, participants performed unilateral dorsiflexion at 15% of their MVIC, using visual feedback to maintain the target force level. TMS pulses were delivered at 120% of the RMT for the corresponding hemisphere, targeting the previously identified motor "hotspot". Stimulations were delivered every 7 to 10 seconds over a 3-minute period, resulting in a median of 21 stimulations per side per participant.

Transcranial Magnetic Stimulation Analysis

EMG signals from the TA were acquired using a BIOPAC system (BIOPAC Systems, Inc., Santa Barbara, CA, USA) at a sampling frequency of 2000 Hz and with a 60 Hz notch filter applied during acquisition to suppress power line noise. Following data acquisition, EMG signals were preprocessed using a two-step filtering approach implemented with custom MATLAB scripts (v9.14.0, MathWorks, Natick, MA, USA). This included a 20–500 Hz bandpass filter to isolate relevant EMG frequencies,[62] followed by a wavelet packet harmonic filter to reduce electrical interference observed in several recordings.[63,64] After preprocessing, all EMG traces and their power spectrum frequency plots were visually inspected to ensure signal quality (Figure B1-6, Appendix B). MEPs were subsequently isolated from the filtered data within a time window spanning 100 ms before to 500 ms after TMS pulse onset. Trials were excluded if no clear response was observed, if the rectified EMG signal failed to exceed two standard deviations above the pre-stimulus baseline, or if the response duration was shorter than 5 ms.[65,66]

For each leg, rectified MEP traces from valid trials were averaged for each participant, and three metrics were derived, average MEP onset latency, average MEP area, and average CSP area. MEP onset latency was defined as the time interval (ms) between the TMS pulse and the onset of the MEP response in the TA. MEP latencies are reported in milliseconds per centimeter (ms/cm) to account for individual differences in height, which can influence raw conduction time measurements, particularly in the lower-extremities.[49,67,68] MEP onset was identified using a threshold-based method, defined as the first data point exceeding 125% of the average rectified EMG (calculated over the 100 ms preceding TMS stimulation) and sustained above this threshold for at least 5 ms. MEP offset and CSP onset were defined as the same data point, marked by a sustained drop below the 125% pre-stimulus threshold for a minimum of 5 ms. CSP offset was

identified as the return of voluntary EMG activity, defined as the first point surpassing 125% of the pre-stimulus average (Figure 3.1).[65]

Using these temporal markers, MEP area was calculated as the area under the rectified EMG curve between MEP onset and offset, with baseline activity area subtracted. Baseline correction involved multiplying the mean rectified EMG during the pre-stimulus period by the MEP duration and subtracting this value from the total rectified area (Figure 3.1).[66] MEP area was selected as the primary measure of CST excitability, rather than peak-to-peak amplitude, due to the presence of polyphasic MEP waveforms in individuals with MS,[69,70] which can compromise the reliability of amplitude-based metrics by failing to capture the full extent of CST excitability.[71] Similarly, CSP area was selected as the primary measure of cortical inhibition, as it captures the overall inhibitory effect more comprehensively than duration alone.[72] It was calculated as the area between the rectified EMG signal and the pre-stimulus baseline from MEP offset to CSP offset (Figure 3.1).

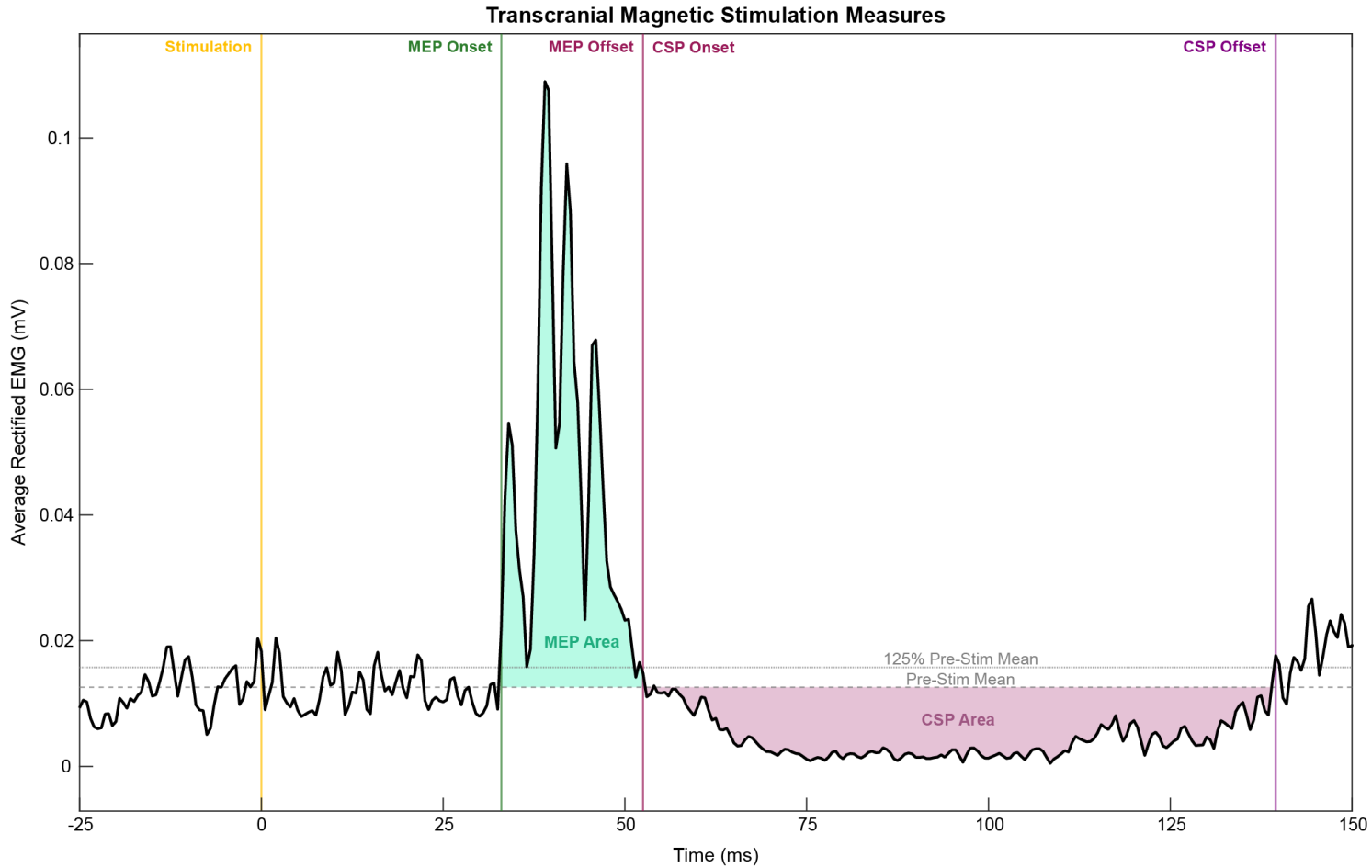

Figure 3.1. Neurophysiological Outcome Measurements. Averaged rectified MEP waveform from an example participant. MEP onset latency was identified as the first datapoint that exceeded 125% of the pre-stimulus rectified EMG and was sustained for at least 5 ms. MEP offset was identified as the first datapoint below the 125% pre-stimulus rectified EMG and was sustained for at least 5 ms. MEP area was calculated as the area under the rectified EMG curve between MEP onset and offset, with pre-stimulus EMG activity subtracted (shaded green). CSP onset was defined as the same point as MEP offset. CSP offset was identified as the return of voluntary EMG activity, defined as the first point surpassing 125% of the pre-stimulus average. CSP area was calculated as the area between the rectified EMG signal and the pre-stimulus baseline from CSP onset to CSP offset (shaded pink).

Tibialis Anterior Maximum Voluntary Isometric Contraction Acquisition

Before TMS data collection, participants performed a series of MVICs to determine peak force capability for each TA muscle. Participants' feet were secured using a strap positioned over the dorsum of the foot just posterior to the metatarsals. To ensure consistent positioning, a stabilizing strap was placed around the heel to prevent posterior slippage, and the ankle joint maintained a neutral position (0° dorsiflexion). The foot was stabilized to prevent any movement that could lead to shortening of the TA muscle, while ensuring participant comfort. The dorsal strap was fastened to a high-capacity carabiner, which was connected to a force transducer (TSD121C, BIOPAC Systems, Inc.) mounted directly beneath the platform. This setup was designed so that force would be transmitted axially with minimal angular deviation, thereby enabling accurate measurement of dorsiflexion vertical force.[73]

For MVIC trials, participants were instructed to generate dorsiflexion force as rapidly and forcefully as possible, sustaining the effort until the force output plateaued and was no longer increasing, with no contraction exceeding 4 seconds. Participants received visual feedback on force production, along with verbal encouragement, throughout testing.[74] Participants completed between three and five MVIC trials for each TA muscle, continuing until maximal force output stabilized, indicated by no further increase across attempts and the two highest force values falling within 10% of each other. A minimum of 30 seconds of rest was provided between trials to minimize fatigue.

Tibialis Anterior Maximum Voluntary Isometric Contraction Acquisition

Outcome metrics derived from the MVIC trials included measures of strength, rate of force development, and muscle activation. Average maximum force was defined as the highest 100 ms mean force within the MVIC waveform for each leg. These values were then averaged across both

legs and normalized to body weight to account for individual differences. Peak rate of force development during the MVIC (MVIC-RFD) was defined as the maximum value of the first derivative of the force signal, representing the highest RFD during the contraction.[75] MVIC-Incline, an additional RFD measure, was calculated as the slope of the force curve between 20% and 90% of the maximum force value. Surface EMG data recorded from the TA during each MVIC were used to determine peak raw EMG amplitude and peak root-mean-square (RMS) EMG amplitude, providing estimates of muscle activation during maximal effort.[76–78]

Five Times Sit-to-Stand Test Acquisition

Participants performed five consecutive sit-to-stand-to-sit transfer movements using a chair of standard height (43.2 cm; 17 inches) with a straight back and no armrests, consistent with established guidelines.[79] Participants were positioned so that each foot was placed on a separate force plate (Model 4060-10, Bertec Corp., Columbus, OH, USA), approximately shoulder-width apart, in a stance that was comfortable for performing repeated sit-to-stand movements. During the task, participants were instructed to cross their arms over their chest, maintain a forward gaze, and complete the five rise-and-sit cycles as quickly and safely as possible.

Vertical ground reaction force (vGRF) data were collected simultaneously from both force plates at a sampling rate of 1000 Hz and summed to generate a total vGRF signal. The chair used during the 5XSST was positioned off the force platforms and did not contribute to the recorded force measurements. Raw force signals were subsequently low-pass filtered at 20 Hz in MATLAB, and a custom script was used to extract relevant performance metrics from the resulting vGRF waveform (Figure 3.2).

Five Times Sit-to-Stand Test Analysis

Total task duration time was quantified from the start of the first standing movement to the final seated position on the fifth repetition. Movement onset was determined by a ≥ 2.5% reduction in foot weight, reflecting the initiation of forward trunk movement.[80] The endpoint was defined using a first-derivative analysis to identify the local minimum in vGRF corresponding to re-seating on the final repetition.

Additional vGRF metrics were extracted for each sit-to-stand-to-sit cycle and averaged across the five repetitions. All force values were normalized to body weight (%BW) to account for individual differences. SST-Incline was calculated as the slope of the vGRF curve between 20% and 90% of the peak force generated during the rising or concentric phase (Figure 3.2A–B).[80] Peak concentric rate of force development (SST-cRFD) was also computed as the maximum of the first derivative of the vGRF curve during the rising phase.[75] Max concentric vGRF (SST-cMax vGRF) was defined as the peak vGRF achieved during the rising action (Figure 3.2C). The moment of full standing (stand) was identified as the point at which the vertical velocity of the center of mass (COM) returned to zero following the concentric phase, indicating the end of upward movement (Figure 3.2D). Instrumented power (SST-Mean power) was estimated by multiplying the COM vertical velocity by the vGRF. COM vertical acceleration was first derived from vGRF and participant body mass, then integrated to yield vertical velocity.

During the lowering or eccentric phase, maximum eccentric vGRF (SST-eMax vGRF) was defined as the peak vGRF generated while descending into the chair (Figure 3.2E). SST-Decline, a measure of the negative RFD, was calculated as the slope of the vGRF curve between 90% and 20% of SST-eMax vGRF (Figure 3.2F–G). Peak eccentric rate of force development (SST-eRFD) was defined as the minimum of the first derivative of the vGRF signal during the lowering phase.[81]

Sit-to-stand time was measured from movement initiation to the stand event, and stand-to-sit time was measured from stand to seat contact.

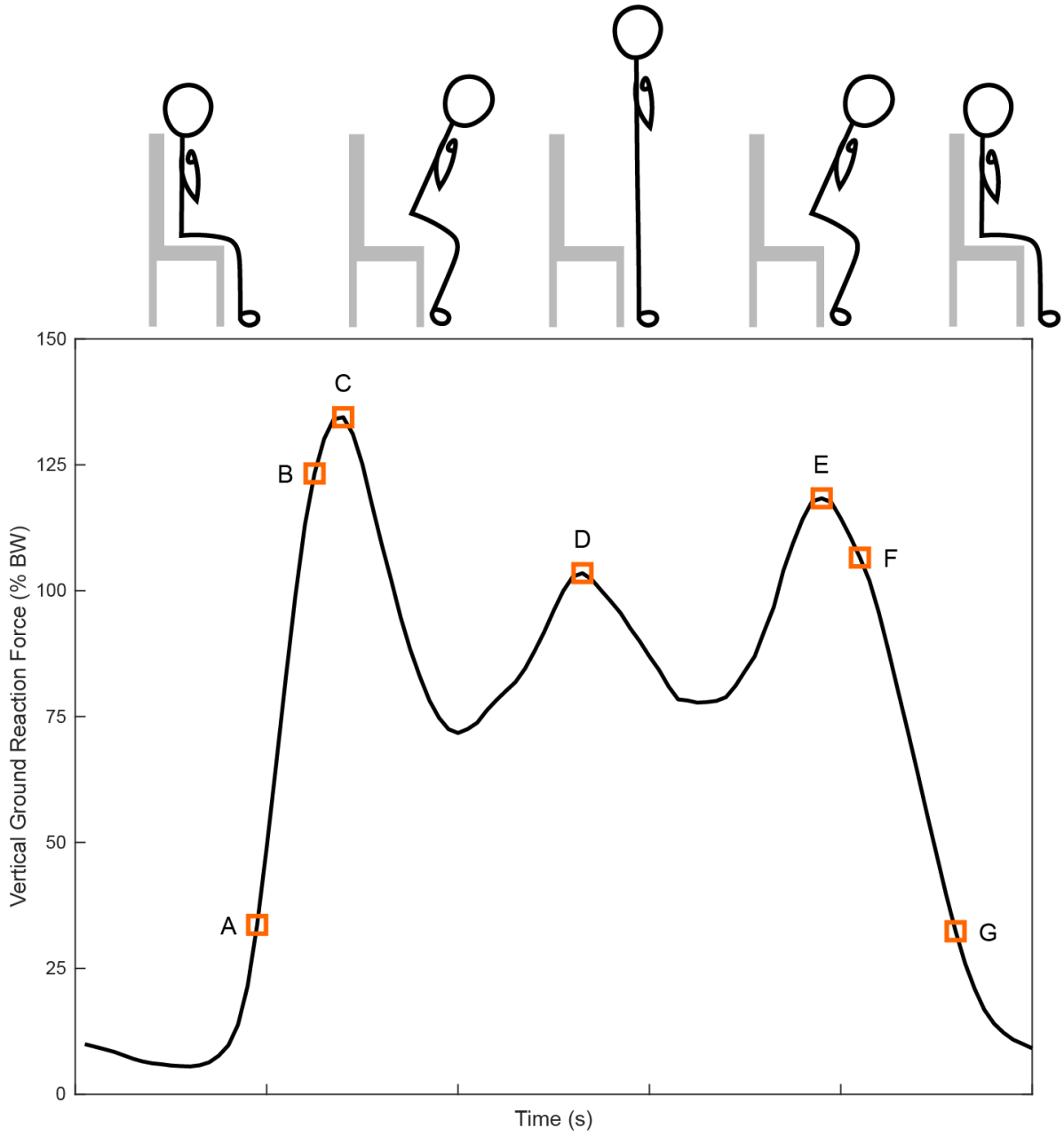

Figure 3.2. Representative Vertical Ground Reaction Force Profile During a Single Sit-To-Stand-to-Sit Transition. (Top) Body position across a single repetition of the 5XSST, representing a sit-to-stand-to-sit movement. (Bottom) Corresponding vGRF profile normalized to body weight. (A) 20% of maximum concentric vGRF; (B) 90% of maximum concentric vGRF; (C) maximum concentric vGRF; (D) Stand, ~100% body weight; (E) maximum eccentric vGRF; (F) 90% of maximum eccentric vGRF; (G) 20% of maximum eccentric vGRF.

Expanded Disability Status Scale (EDSS)

The EDSS is a standardized assessment tool used to evaluate neurological function and track disease progression in individuals with MS.[82] Participants with MS provided their EDSS scores using a validated self-report questionnaire, which strongly correlates with physician-administered assessments.[83]

Statistical Analysis

All statistical analyses were performed using R (version 4.4.2; R Core Team, 2024). Data distributions for each variable for each group were evaluated for normality using the Shapiro-Wilk test and visually inspected with Q–Q plots. Homogeneity of variances was assessed with Levene's test. Between-group comparisons were made using independent-samples t-tests when assumptions of normality and equal variance were met. If variance equality was violated, Welch's t-test was administered, and for non-normally distributed data, the Mann–Whitney U test was used. Cohen's d was used to calculate effect sizes (*d*). Group differences in sex distribution were assessed using a chi-squared test. Associations between TMS outcomes and functional performance metrics were examined using Pearson correlation coefficients when both variables were continuous and normally distributed. When at least one variable was ordinal or non-normally distributed, Spearman's rank-order correlation was used. Correlation strength was interpreted using the following thresholds: very weak (0.00 – 0.19), weak (0.20 – 0.39), moderate (0.40 – 0.59), strong (0.60 – 0.79), and very strong (0.80 – 1.00).[84]

Results

Participant Characteristics

Participant demographics are summarized in Table 3.1. Participants with MS displayed no statistically significant differences in age ($p = 0.775$), height ($p = 0.060$), weight ($p = 0.503$), or

body mass index (BMI; $p = 0.844$) compared to NT participants. Participants with MS reported mild to moderate disability levels, with a median EDSS score of 3.5 (range: 0-4) and an average time since diagnosis of 11.81 ± 10.71 years.

Table 3.1. Participant Characteristics. Statistical comparisons were performed using independent t-tests[a], χ^2 tests[b], or Mann–Whitney U tests[c]. [†] Indicates data presented as median and interquartile range. **Bolded** values indicate statistical significance (*p-value* < 0.05). BMI = Body Mass Index; EDSS = Expanded Disability Status Scale

	MS		Control		
	M	*SD*	*M*	*SD*	*p-value*
Characteristic					
n	26	-	24	-	-
Sex (female/male)	19-7	-	18-8	-	0.853[b]
Age (years)	48.19	11.95	47.07	15.65	0.775[a]
Height (cm)	165.74	7.32	169.76	7.44	0.060[a]
Weight (kg)	68.39	9.35	71.82	12.91	0.503[c]
BMI (kg/m^2)	25	3.85	24.8	3.28	0.844[a]
EDSS[†]	3.5	0.88	-	-	-
Time Since Diagnosis (years)	11.81	10.71	-	-	-

Group Comparisons of Corticospinal Excitability, Inhibition, and Latency

No statistically significant differences in RMT were found between participants with MS and NT controls (MS: 67.13 ± 6.84% MSO vs. NT: 69.21 ± 7.73% MSO, $p = 0.196$, $pFDR = 0.196$, $d = -0.28$). Participants with MS demonstrated significant delays in normalized MEP onset latencies (MS: 0.197 ± 0.027 ms/cm vs. NT: 0.184 ± 0.011 ms/cm, $p = 0.031$, $pFDR = 0.041$, $d =$

0.62) and significant reductions in MEP area (MS: 0.79 ± 0.36 mV*ms vs. NT: 1.12 ± 0.50 mV*ms, $p = 0.011$, $pFDR = 0.040$, $d = -0.75$) and CSP area (MS: 0.70 ± 0.41 mV*ms vs. NT: 1.01 ± 50 mV*ms, $p = 0.020$, $pFDR = 0.040$, $d = -0.68$) compared to NT controls (Figure 3.3a-c).

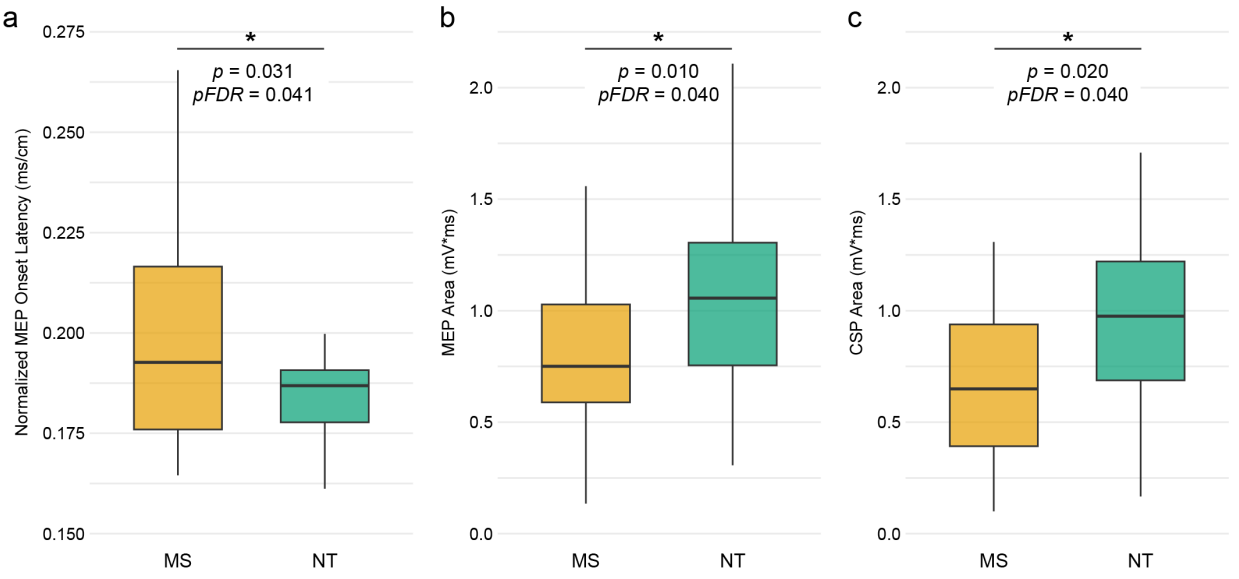

Figure 3.3. Group Comparisons of Transcranial Magnetic Stimulation Neurophysiology Measures. Neurophysiological differences between participants with MS and NT controls. a) Group comparison of normalized MEP onset latency. b) Group comparison of MEP area. c) Group comparison of CSP area. *p* = uncorrected p-value; *pBON* = Bonferroni adjusted p-value; * indicates *pBON* < 0.05.

Group Comparisons of Tibialis Anterior Strength and Muscle Activation

TA MVIC outcome measures are presented in Table 3.2. Compared to NT participants, individuals with MS demonstrated significantly reduced maximal force production during MVICs (*pFDR* = 0.027). Additionally, the MS group exhibited a significantly lower rate of force development, as reflected by both MVIC-Incline (*pFDR* = 0.002) and peak MVIC-RFD (*pFDR* = 0.046). Muscle activation during MVICs was also significantly reduced in the MS group, with lower raw EMG amplitude (*pFDR* = 0.037) and RMS EMG values (*pFDR* = 0.037) compared to controls.

Table 3.2. Group Comparisons of Tibialis Anterior Maximum Voluntary Isometric Contraction Measures. MVIC performance metrics for the TA muscle comparing participants with MS and NT controls. Statistical comparisons were performed using independent t-tests[a] or Mann–Whitney U tests[b]. *p* = uncorrected p-value; *pFDR* = False Discovery Rate-adjusted p-value.

Variable (unit)	MS		Control				
	M	*SD*	*M*	*SD*	*p-value*	*pFDR-value*	*Effect size*
Max Force (%BW)	33.45	11.23	41.89	11.44	**0.011** [a]	**0.027** [a]	-0.75
Peak MVIC-RFD (%BW/s)	58.13	30.36	87.41	30.85	**<0.001** [b]	**0.002** [b]	-0.96
MVIC-Incline (%BW/s)	25.46	12.01	32.59	12.59	**0.046** [a]	**0.046** [a]	-0.58
Peak Rectified EMG (mV)	0.19	0.09	0.25	0.01	**0.026** [a]	**0.037** [a]	-0.65
Peak RMS EMG (mV)	0.05	0.03	0.07	0.03	**0.030** [a]	**0.037** [a]	-0.64

Group Comparisons of 5XSST Performance

Performance outcomes from the 5XSST are summarized in Table 3.3. Participants with MS completed the 5XSST significantly more slowly than NT participants (*pFDR* = 0.040). During the concentric phase, no significant group differences were observed in movement (sit-to-stand) time, though the MS group demonstrated a trend toward slower performance (*pFDR* = 0.086). Compared to controls, participants with MS exhibited significantly lower SST-cMax vGRF (*pFDR* = 0.004), reduced peak SST-cRFD (*pFDR* = 0.019), lower SST-Incline (*pFDR* = 0.004), and lower SST-Mean power output (*pFDR* = 0.014).

During the eccentric phase, participants with MS were significantly slower to return to the seated position (stand-to-sit) (*pFDR* = 0.017). Additionally, they demonstrated significantly lower

SST-eMax vGRF (*pFDR* = 0.001), reduced peak SST-eRFD (*pFDR* = 0.014), and lower SST-Decline (*pFDR* = 0.016) compared to NT participants.

Table 3.3. Group Comparisons of Five Times Sit-to-Stand Measures. Comparison of 5XSST measures between participants with MS and NT controls. Statistical comparisons were conducted using independent *t*-tests[a], Mann–Whitney *U* tests[b], or Welch's *t*-tests[c]. *p* = uncorrected p-value; *pFDR* = False Discovery Rate-adjusted p-value.

Variable (unit)	MS		Control		*p-value*	*pFDR-value*	*Effect size*
	M	*SD*	*M*	*SD*			
Total Time (s)	13.06	3.47	10.79	2.17	**0.036** [b]	**0.040**	0.78
Concentric							
Sit-to-Stand Time (s)	1.30	0.32	1.12	0.28	0.086 [b]	0.086	0.60
SST-cMax vGRF (%BW)	129.89	11.78	140.41	9.75	**0.001** [a]	**0.004**	-0.97
Peak SST-cRFD (%BW/s)	1273.33	459.69	1610.40	547.02	**0.016** [b]	**0.019**	-0.63
SST-Incline (%BW/s)	751.06	264.47	993.07	217.92	**<0.001** [a]	**0.004**	-0.93
SST-Mean Power (W)	201.61	69.66	263.77	80.28	**0.005** [a]	**0.014**	-0.83
Eccentric							
Stand-to-Sit Time (s)	1.31	0.46	1.04	0.21	**0.010** [c]	**0.017**	0.75
SST-eMax vGRF (%BW)	116.15	8.15	125.26	9.28	**<0.001** [b]	**0.001**	-1.05
Peak SST-cRFD	-791.60	396.83	-912.40	164.92	**0.007** [b]	**0.014**	0.39

(%BW/s)							
SST-Decline (%BW/s)	-469.64	225.69	-607.35	129.75	**0.011** [c]	**0.016**	0.74

Associations Between Corticospinal Metrics and Tibialis Anterior Measures

In participants with MS, MEP area was significantly associated with TA strength and muscle activation outcomes derived from MVIC trials (Figure 3.4). Specifically, MEP area demonstrated moderate correlations with maximal force output (r = 0.44, p = 0.024, *pFDR* = 0.033), MVIC-Incline (r = 0.56, p = 0.003, *pFDR* = 0.006), and peak MVIC-RFD (*rho* = 0.43, p = 0.028, *pFDR* = 0.033) (Figure 3.4a-c). Additionally, strong correlations were observed between MEP area and raw EMG amplitude (r = 0.76, p < 0.001, *pFDR* < 0.001) and RMS EMG (r = 0.72, p < 0.001, *pFDR* < 0.001) (Figure 3.4d) produced during MVIC. Normalized MEP onset latency was moderately correlated with peak MVIC-RFD (*rho* = -0.43, p = 0.028, *pFDR* = 0.033), but was not significantly associated with MVIC-Incline (r = -0.34, p = 0.087, *pFDR* = 0.087).

Associations Between Corticospinal Metrics and 5XSST Force Production and Modulation

In participants with MS, MEP area was significantly correlated with SST-cMax vGRF (r = 0.55, p = 0.004, *pFDR* = 0.019) and SST-eMax vGRF (*rho* = 0.47, p = 0.016, *pFDR* = 0.039) (Figure 3.5a-b). MEP area was also significantly correlated with SST-Incline (r = 0.44, p = 0.023, *pFDR* = 0.039). MEP area did not survive multiple comparison testing for correlation with SST-Mean power (r = 0.40, p = 0.042, *pFDR* = 0.052). No significant correlation was observed between MEP area and SST-Decline (r = -0.16, p = 0.425, *pFDR* = 0.425).

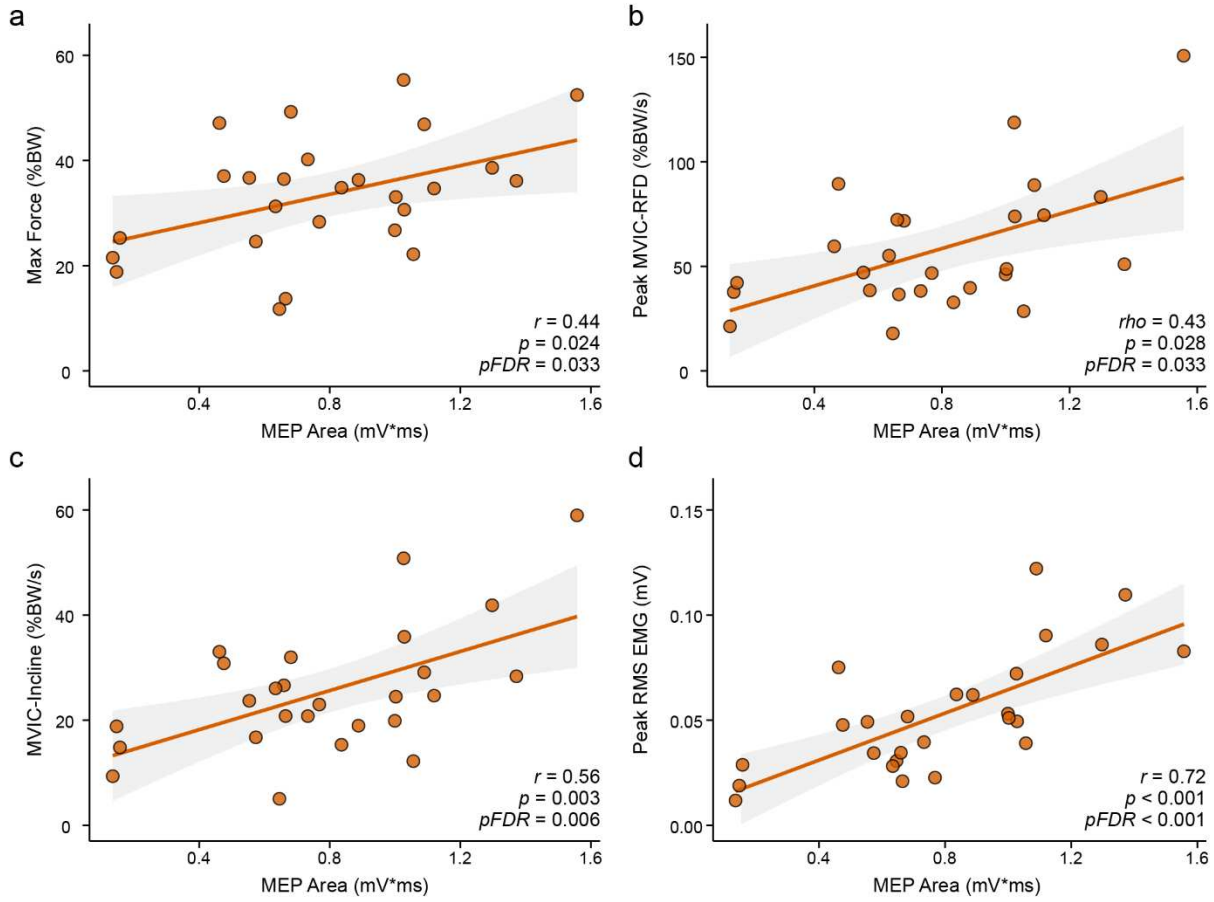

Figure 3.4. Associations Between Corticospinal Excitability and Tibialis Anterior Maximum Voluntary Contraction Measures in People with Multiple Sclerosis. Correlations between MEP area and TA MVIC measures in participants with MS. a) Moderate association between MEP area and maximum dorsiflexion force. b) Moderate association between MEP area and peak MVIC-RFD. c) Moderate association between MEP area and MVIC-Incline. d) Strong association between MEP area and RMS EMG amplitude. *p* = uncorrected p-value; *pFDR* = False Discovery Rate-adjusted p-value.

Normalized MEP onset latency was significantly correlated with peak SST-cRFD (r = -0.42, p = 0.033, *pFDR* = 0.042), SST-Incline (r = -0.51, p = 0.008, *pFDR* = 0.020) (Figure 3.5c), peak SST-eRFD (*rho* = 0.62, $p < 0.001$, *pFDR* = 0.005), and SST-Decline (r = 0.49, p = 0.012, *pFDR* = 0.020) (Figure 3.5d). No significant association was observed between normalized MEP latency and SST-Mean power (r = -0.31, p = 0.118, *pFDR* = 0.118).

CSP area was significantly correlated with SST-cMax vGRF (r = 0.48, p = 0.012, *pFDR* = 0.030) and SST-eMax vGRF (*rho* = 0.48, p = 0.015, *pFDR* = 0.030). No significant correlations

were found between CSP area and SST-Incline ($r = 0.21$, $p = 0.303$, $pFDR = 0.405$) or SST-Decline ($r = -0.08$, $p = 0.710$, $pFDR = 0.710$).

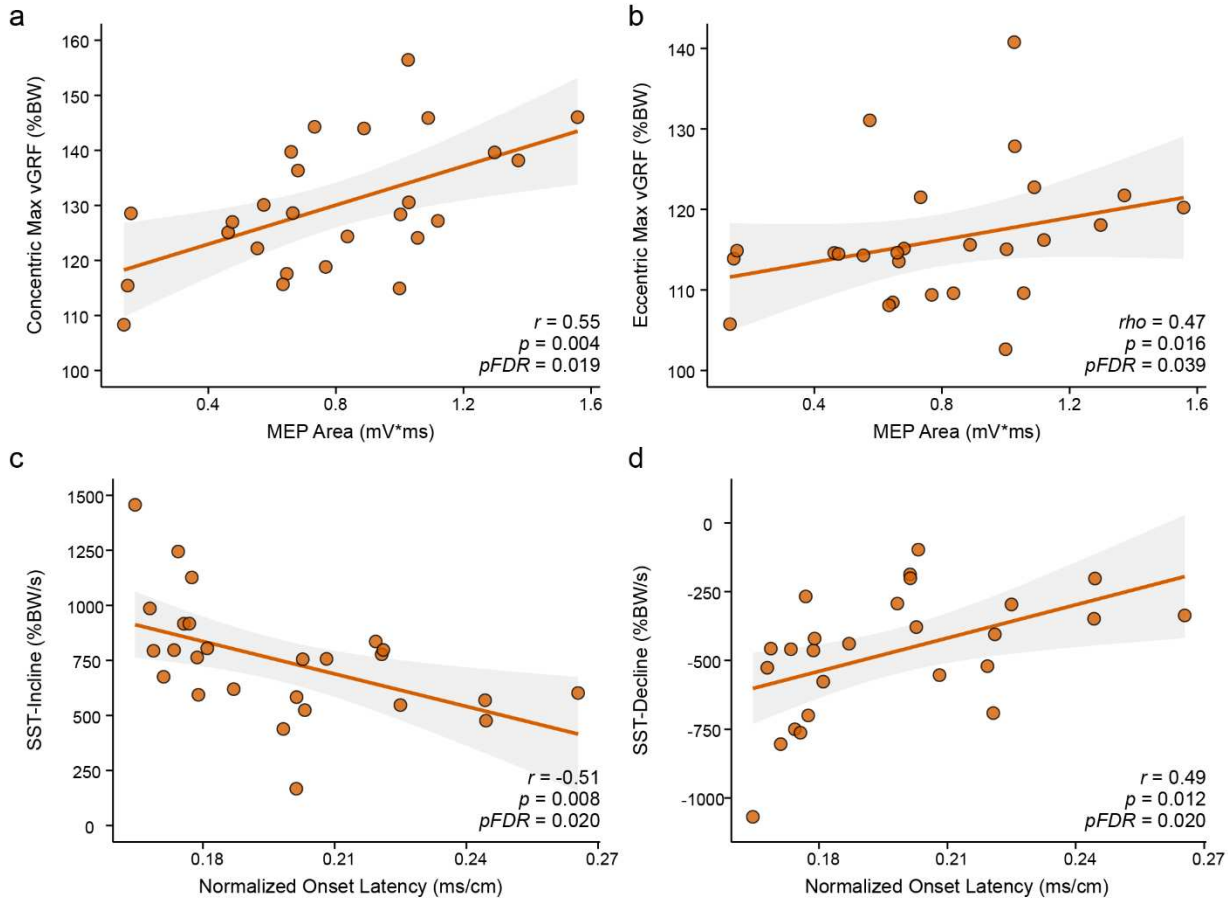

Figure 3.5. Associations Between Corticospinal Excitability and Latency and Five Times Sit-to-Stand Measures in People with Multiple Sclerosis. Correlations between TMS neurophysiology measures and force-related metrics during the 5XSST in participants with MS. a) Moderate association between MEP area and SST-cMax vGRF. b) Moderate association between MEP area and SST-eMax vGRF. c) Moderate association between normalized MEP onset latency and SST-Incline. d) Moderate association between normalized MEP onset latency and SST-Decline. *p* = uncorrected p-value; *pFDR* = False Discovery Rate-adjusted p-value.

Discussion

This study investigated CST function, maximal voluntary output of the TA, and 5XSST performance in individuals with MS compared to NT controls. Individuals with MS exhibited impaired CST integrity, reduced muscle strength and activation during MVIC, and slower, less

forceful performance during the 5XSST. In participants with MS, neurophysiological measures such as MEP area and latency were significantly associated with isolated and functional lower-extremity motor performance, highlighting the contribution of CST integrity to neuromuscular output.

Group Differences in Corticospinal Excitability, Latency, and Inhibition

Group comparisons of neurophysiological measures revealed no significant difference in RMT, indicating that the threshold for eliciting a motor response is largely preserved in individuals with MS with mild to moderate disability, reflecting relatively intact resting CST excitability.[49] This observation is consistent with existing literature, which reports comparable RMT values between MS and NT controls, however, some studies have noted elevated RMT.[17] MEP onset latency was normalized to participant height to account for individual differences in body size, as greater height increases the distance the neural signal must travel and can influence latency measures.[49,67,68] After normalization, individuals with MS demonstrated significantly prolonged MEP latency (Figure 3.3a), indicating impaired conduction along the CST. These findings are consistent with prior evidence showing delayed MEP latency in MS, even among participants with minimal clinical disability.[17,85–87]

Group comparisons of CST excitability showed that MEP area was significantly reduced in individuals with MS (Figure 3.3b), indicating lower CST excitability.[49] This observation is consistent with prior research demonstrating reduced MEP area or amplitude in people with MS compared to controls.[17,85–88] In addition, intracortical inhibition was also reduced in participants with MS, as evidenced by significantly reduced CSP area compared to NT controls (Figure 3.3c), suggesting lower inhibitory activity within the motor cortex. Observations of reduced CSP area in participants with MS may be linked to the decrease in CST excitability, as reflected by a

diminished MEP area. Previous studies have reported mixed findings regarding CSP differences between individuals with MS and neurotypical controls, with several noting prolonged CSP duration.[17,88–90] However, most of this literature focuses exclusively on duration, which may not fully characterize inhibitory processes. Prior work has shown that measures such as silent period depth and area may provide more sensitive and reliable indices of cortical inhibition, with silent period area demonstrating the strongest consistency[72,91,92] MEP area and CSP area are thought to reflect the functional status of glutamatergic and $GABA_B$-mediated activity within the CST, respectively.[49] Given the role of these neurotransmitters in shaping motor output, the observed differences likely reflect that both excitatory and inhibitory processes within the CST are disrupted in MS.

Group Differences in Tibialis Anterior Strength and Muscle Activation

Comparison of maximal isometric dorsiflexion strength revealed that individuals with MS generated significantly less force relative to their body weight compared to NT controls (Table 3.2). In addition to reduced peak force output, participants with MS demonstrated slower force generation across the central portion of the force-time curve, as evidenced by a significantly lower MVIC-Incline (20–90% of MVIC) and reduced peak MVIC-RFD compared to NT participants, which showed the largest effect size among the MVIC metrics evaluated (Table 3.2). MVIC-Incline and peak MVIC-RFD capture distinct yet complementary aspects of volitional force generation, where MVIC-Incline represents sustained force generation rate, while peak RFD reflects the maximal capacity for rapid activation.[75,80] Together, this indicates that individuals with MS exhibit reductions in both maximal and sustained TA force generation. These findings align with prior research demonstrating that individuals with MS exhibit reduced isometric force output and slower RFD compared to neurotypical controls.[33,35,37,43]

In addition to reduced force output, participants with MS demonstrated significantly lower peak EMG amplitude, both raw and RMS, during MVIC, reflecting reduced muscle activation in the TA during maximal effort contractions (Table 3.2). These findings are consistent with previous research, which has shown reduced EMG amplitude during MVIC in individuals with MS.[37]

Together, these findings are consistent with prior research indicating that the TA is one of the lower-limb muscles most affected by MS-related impairments[93–95] Weakness in the TA contributes to balance impairment and foot drop, a common symptom in MS characterized by difficulty dorsiflexing the ankle during the swing phase of gait.[93,94,96–98] Collectively, these findings indicate impaired neuromuscular output in the TA among individuals with MS, characterized by reduced force-generating capacity, slower force development, and diminished muscle activation.

Group Differences in 5XSST Performance

Previous research has consistently shown that individuals with MS complete the 5XSST more slowly than NT controls, reflecting impairments in lower-body strength.[57,99–101] Consistent with these findings, participants with MS in the present study took significantly longer to complete the 5XSST compared to matched NT controls. Although total task duration was prolonged, group differences in the time to complete the concentric (sit-to-stand) phase did not reach statistical significance. Concentric and particularly eccentric phase durations are not frequently reported in the literature due to the difficulty of precisely identifying phase transitions without equipment such as force plates or inertial sensors. However, one previous study reported that individuals with MS took approximately 25% longer to rise from a seated position, with extended duration primarily driven by a 32% increase in the time following seat-off. These delays were attributed to lower-limb weakness and a reduced ability to generate force and power.[56]

Despite no significant group differences in concentric phase duration, individuals with MS exhibited significantly reduced concentric force-related metrics, including lower SST-cMax vGRF, SST-Incline, SST-cRFD, and SST-Mean power (Table 3.3). This is consistent with previous literature demonstrating reduced lower-extremity strength and power in people with MS.[35,39,40] The present study's findings indicate a decreased ability to generate force and power during the sit-to-stand action in people with MS, despite similar concentric phase durations. These results indicate that impairments in force production may exist even in the absence of detectable timing differences, underscoring the importance of kinetic assessments in identifying functional impairments that may not be captured by time-based performance measures alone. For example, previous research has shown that lower-limb power output derived from sit-to-stand movements can differentiate between fallers and non-fallers, suggesting that force- and power-based metrics may reveal meaningful functional deficits (Study 1).[58]

In contrast to the sit-to-stand time, individuals with MS took significantly longer to complete the eccentric (stand-to-sit) phase, with a larger between-group effect size observed for eccentric time compared to concentric time (Table 3.3). Force-related metrics during the eccentric phase similarly revealed significant differences, including lower SST-eMax vGRF and increased SST-eRFD and SST-Decline in participants with MS (Table 3.3). Notably, the effect size for SST-eMax vGRF exceeded that of SST-cMax vGRF, indicating a greater magnitude of difference in eccentric compared to concentric force production between participants with MS and NT controls. This pattern contrasts with previous findings, which demonstrate greater impairments in concentric strength compared to eccentric strength in individuals with MS compared to controls, in the quadriceps and hamstrings.[102] However, the present study's results align with previous literature showing that eccentric training improved sit-to-stand performance more than concentric training,

suggesting that eccentric strength may be a greater area of impairment and opportunity for improvement in people with MS in rising and lowering tasks.[103]

Functionally, the stand-to-sit phase requires controlled deceleration of body mass toward a visually obscured target (the chair), placing increased demands on eccentric muscle control and proprioceptive accuracy. Prior research has documented proprioceptive deficits in MS,[104–106] which may contribute to prolonged stand-to-sit durations, as a slower descent may reflect a compensatory strategy to ensure a safe return to a seated position in the context of impaired eccentric control and position sense. Taken together, these findings suggest that eccentric tasks requiring full-body dynamic control, such as the stand-to-sit movement, may be particularly informative for assessing impairment in MS. The combined demands of eccentric strength and accurate proprioceptive feedback may reveal functional limitations not captured in more traditional assessments.

Collectively, these findings indicate that individuals with MS experience deficits in both concentric and eccentric force production, as well as impaired modulation of dynamic weight transfer during a functional, full-body task. Although knee extensor strength was not directly assessed, the performance differences observed across both movement phases align with previous literature linking lower-limb strength to 5XSST outcomes in MS.[40,56,57,99,101,107] These results help highlight the potential value of incorporating eccentric-focused and power-based assessments into clinical evaluations and support the use of targeted interventions to improve ballistic force generation, transfer ability, and eccentric control in individuals with MS.

Corticospinal Excitability and Conduction Relate to Tibialis Anterior Strength and Muscle Activation

In participants with MS, MEP area was significantly correlated with TA MVIC maximum force output (Figure 3.4a), indicating that greater CST excitability is associated with higher maximal dorsiflexion force. MEP area was also significantly associated with both peak MVIC-RFD and MVIC-Incline (Figure 3.4b–c), suggesting that CST excitability contributes not only to the magnitude but also the rate of force generation during MVICs. These findings support the interpretation that impaired excitatory drive from the motor cortex may limit both the capacity and speed of force production in individuals with MS. This interpretation aligns with prior work demonstrating associations between MEP amplitude and muscle strength, RFD, and contraction intensity.[108–114]

MEP area was also strongly correlated with peak raw and RMS EMG amplitude (Figure 3.4d). This relationship suggests that reduced CST excitability is associated with diminished muscle activation during MVIC, supporting the hypothesis that impaired CST function contributes to decreased motor output. The strength of these correlations highlights a tight coupling between neural and muscular performance, consistent with the neurophysiological basis of MS as a central nervous system disorder.[2,13,115,116] Such findings underscore the role of descending CST integrity in shaping peripheral motor function.

Normalized MEP onset latency was significantly correlated with MVIC-RFD and showed a trend toward significance with MVIC-Incline. MEP latency reflects the conduction efficiency of the CST. When latency is prolonged, the transmission of neural signals from the motor cortex to the muscle is delayed.[49] This delay may hinder the timely recruitment of motor units and also may disrupt the temporal synchronization of their activation, thereby reducing the ability to rapidly

initiate muscle contractions and impair explosive force generation.[117–119] The weaker relationship between MEP latency and MVIC-Incline may be explained by the nature of the incline metric, which is measured over a longer time window. This extended duration may allow for compensation for delayed neural transmission, reducing the apparent impact of conduction inefficiencies.

Corticospinal Excitability, Inhibition, and Conduction Latency Relate to 5XSST Force Production and Modulation

While the TA is not the primary mover during the 5XSST, previous studies have shown that it exhibits the highest muscle activation among other lower-limb muscles during the sit-to-stand movement from chair heights similar to that used in the present study.[120,121] The TA is the first lower body muscle to activate during a sit-to-stand movement and is important for stabilizing the foot during the task.[121–123] Furthermore, TMS-derived measures from the TA provide informative estimates of overall CST integrity. This is especially true in lower-extremity assessments, where TMS signals traverse the entire CST,[124] including lumbar spinal segments shared by nerves innervating both the TA and other key muscle contributors to the 5XSST, such as the quadriceps.[125,126] Although differences such as CST innervation density and fiber recruitment patterns may exist,[127] TA-based TMS metrics in the present study are still reflective of broader CST function.

In individuals with MS, MEP area was significantly correlated with maximal vGRF during both the concentric and eccentric phases of the 5XSST, with a slightly stronger association observed for SST-cMax vGRF (Figure 3.5a-b). These findings suggest that CST excitability level contributes to peak force generation during dynamic transitions that require rapid and controlled lower-limb output. The slightly stronger relationship observed during the concentric phase may reflect a greater reliance on excitatory CST drive to sustain upward movement during sit-to-stand

transitions. This finding aligns with previous studies, which have shown increased CST excitability during concentric contractions compared to eccentric ones.[128–130] Additionally, CST excitability is higher during the preparation phase for concentric contractions compared to eccentric contractions, as well as during imagined concentric movements compared to eccentric movements, highlighting differences in the neural control of these actions.[131,132]

A moderate positive correlation was also observed between MEP area and SST-Mean power output, however, this relationship did not survive correction for multiple comparisons. Given the significant associations between the MEP area and force-based measures, it is plausible, although preliminary, that reduced CST excitability likely contributes to impaired power generation in individuals with MS. This interpretation is consistent with the broader literature linking CST function to lower-limb strength and dynamic movement capacity.[36,44–47] Future investigations with larger samples may more clearly characterize the nature of the relationship between CST excitability and lower-limb power. Collectively, these results support the interpretation that reduced excitability of the corticospinal system in MS may underlie deficits in peak force and mean power production during functionally relevant, full-body movements. These impairments likely reflect a diminished ability to effectively recruit motor units, impacting the performance of everyday tasks such as rising from and returning to a seated position.

Interestingly, while MEP area correlated with SST-Incline, no association was observed with SST-Decline. This pattern suggests that CST excitability may play a more prominent role in peak force generation (e.g., cMax and SST-eMax vGRF) than in deceleration during eccentric movement. These findings highlight the complexity of neuromuscular control during functional tasks such as the 5XSST, which require coordinated activation across multiple muscle groups.

Additionally, prior research indicates that eccentric movements engage broader and distinct cortical areas compared to concentric movements.[133–135]

In line with this, eccentric control during the 5XSST places high demands on motor planning and proprioceptive feedback, as individuals must decelerate their body mass toward an unseen target. In this context, the absence of an association between CST excitability and SST-Decline may reflect a greater reliance on proprioceptive feedback and motor planning processes, rather than excitability of the CST. Given the prevalence of proprioceptive impairments in MS,[104–106] individuals may adopt compensatory motor strategies that prioritize stability and safety over speed during eccentric transitions. Additionally, full-body movements that demand rapid force development and stabilization, especially those involving the lower-extremities, have been linked to descending pathways beyond the CST, such as the reticulospinal tract.[136–138] These alternative pathways may support both rapid force initiation and the controlled eccentric movement, particularly in individuals with compromised CST integrity, as is often seen in individuals with MS.

Normalized MEP latency was significantly correlated with measures of force production during both the concentric (SST-Incline and SST-cRFD) and eccentric (SST-Decline and SST-eRFD) phases of the 5XSST (Figure 3.5c-d), suggesting that delayed CST conduction impairs the nervous system's ability to rapidly scale force during dynamic tasks. Longer latencies reflect slower signal transmission from the motor cortex to the muscle, which can compromise the precise timing of muscle recruitment required for quick and controlled force generation.[139–141] These effects are relevant in the 5XSST, which demands coordinated activation across multiple lower-limb muscles. For example, during the concentric phase, the TA, quadriceps, and gluteal muscles must activate in succession to initiate movement and generate vertical impulse.[123,142] Delays in

neural conduction may disrupt the temporal coordination of muscle activity, leading to inefficient or slowed force responses.

Previous literature has demonstrated that CST inhibition, as measured by CSP duration, is reduced during eccentric contractions compared to concentric contractions, suggesting differential inhibitory control across movement types.[130,143,144] In the present study, CSP area was significantly correlated with both SST-eMax vGRF and SST-cMax vGRF in participants with MS, linking inhibitory activity to peak force output during both phases of the 5XSST. However, the relationship between CSP area and SST-cMax vGRF was noticeably weaker than that observed for MEP area, pointing to a relatively greater contribution of CST excitability to concentric peak force production. In contrast, SST-eMax vGRF showed nearly identical correlation strengths with both MEP and CSP area, suggesting that both excitatory and inhibitory processes may similarly influence eccentric peak force. This pattern may cautiously suggest that while both excitatory and inhibitory activity shape neuromuscular output, excitatory drive may be more critical during the execution of concentric movements like the 5XSST.[110,129,131,132]

CSP area was not significantly correlated with SST-Incline or SST-Decline in participants with MS. The lack of association suggests that in individuals with MS with mild to moderate disability, CST inhibition, as measured by TMS, may have a limited role in regulating rapid force modulation during dynamic multi-muscle tasks like the 5XSST. Instead, inhibitory processes may be more relevant to the control of overall force magnitude rather than the rate at which force is generated.

Overall, TMS-derived measures of CST excitability and conduction were meaningfully associated with lower-limb force production during both concentric and eccentric phases of the 5XSST. These findings suggest that reduced excitability and slower conduction along the CST

may impair both peak force output and the rapid modulation of force during full-body functional movements in individuals with MS. Together, the results highlight CST drive in supporting dynamic lower-limb performance and offer insight into the neural contributions to underlying movement impairments in individuals with MS.

Potential for Modulating Corticospinal Excitability Through Rehabilitation

Rehabilitative interventions, specifically strength training, have shown potential for modifying CST neurophysiological function, representing a promising approach for developing targeted rehabilitation strategies in MS. A substantial body of evidence indicates that resistance training can induce neurophysiological adaptations within the corticospinal system. One of the most consistently reported findings is a reduction in intracortical inhibition following strength training, particularly in untrained healthy individuals, suggesting enhanced CST responsiveness.[145–148] In addition to changes in inhibition, some studies report increased CST excitability following resistance training, as measured by MEP amplitude.[148–154] However, findings are not universal, and the underlying mechanisms remain an active area of investigation.[145,155,156]

Importantly, evidence suggests that changes in CST excitability may be time-dependent. In the acute phase, increases in excitability are commonly observed. These short-term changes likely reflect temporary adjustments in cortical and spinal excitability.[149,150,153] In contrast, long-term training has been linked to improved neural efficiency, as demonstrated by reduced MEP recruitment slopes, indicating that the CST can produce motor output with less cortical input.[157] Exercise intensity also appears to be a critical factor. Higher-intensity resistance training was shown to elicit greater increases in CST excitability compared to lower-intensity training, suggesting that a sufficient stimulus is necessary to drive central adaptations.[158] Training type may

further influence neurophysiological outcomes. Both hypertrophy-focused and traditional strength training protocols have been associated with excitability increases, indicating that different approaches to resistance training can produce similar central effects.[152]

Strength training has also been shown to increase motor unit discharge rates and lower the recruitment threshold of motor units, indicating that motor units are activated more readily and fire at higher frequencies during voluntary contractions.[159] Additionally, increased motor unit conduction velocity has been reported following training, reflecting improved signal transmission along motor axons.[160] These motor unit adaptations contribute to enhanced force production, supporting the broader improvements in neuromuscular performance seen with strength training. Collectively, these findings highlight the multifaceted nature of neuromuscular adaptations to strength training, encompassing both central and peripheral mechanisms.

In individuals with MS, resistance training has likewise been shown to induce neurophysiological changes. Studies report increased neural drive following training, suggesting that even in the presence of demyelination and axonal injury, the corticospinal system retains a degree of plasticity.[161] Moreover, task-specific training, such as walking interventions, has been shown to enhance CST excitability in people with progressive MS.[162] These findings underscore the potential for targeted rehabilitation strategies to promote central nervous system adaptations and support improvements in motor function in populations with neurological impairment.

Beyond physical training, neuromodulatory techniques such as transcranial direct current stimulation (tDCS) may offer additional promise. tDCS, particularly anodal tDCS, has been shown to increase CST excitability.[163–165] By delivering low-amplitude electrical current over the motor cortex, anodal tDCS is thought to decrease the threshold for neuronal membrane excitability and subsequently modulate cortical plasticity[166] Although current evidence is limited, pairing tDCS

with training may further enhance neurophysiological responses and support improvements in motor function.[167,168]

Together, these findings illustrate the potential for both physical and neuromodulatory interventions to modulate CST physiology at multiple levels of the motor pathway. This underscores the promise of targeted strategies to improve lower-limb motor output and mobility in people with MS. Future research is needed to better define the short- and long-term effects of these interventions, clarify the underlying mechanisms, and optimize protocols to support meaningful and sustained functional improvements.

Limitations

This study has several limitations that should be considered when interpreting the results. First, CST function was assessed using single-pulse MEPs, which reflect neural responsiveness at a single stimulus intensity. While this approach provides a practical estimate of CST excitability, it does not capture the full input–output relationship or synaptic recruitment dynamics that could be obtained from motor recruitment curves. The inclusion of recruitment curve measures in future work may provide a more comprehensive understanding of CST integrity and responsiveness.

Second, TMS was administered separately from the study motor tasks. Although this method allows for standardized assessment, it limits insight into how CST function is modulated during task execution. Applying TMS during movement may yield a more ecologically valid view of task-specific neural control and more directly link neurophysiological measures to functional performance.

Third, EMG recordings were not collected during the 5XSST, preventing analysis of muscle activation patterns and timing across groups. Surface EMG data could have provided

insight into neuromuscular strategies differences between groups, especially during the eccentric and concentric transitions of the 5XSST.

Fourth, the study collected only force plate-derived kinetic variables to evaluate 5XSST performance without concurrent kinematic data. Although ground reaction forces from force plates are a validated proxy for lower-limb function, additional information such as joint angles, trunk movement, and segmental timing could offer deeper insights into movement strategy differences between groups.

Fifth, the study sample included only individuals with relapsing-remitting MS and mild to moderate disability (EDSS ≤ 4), limiting the generalizability of the findings to those with more advanced disability or other MS subtypes, such as secondary or primary progressive MS. Given the known heterogeneity in disease symptoms and progression, future studies should examine whether these findings extend to individuals with more severe impairments and other MS phenotypes.

Finally, both the MS and NT groups had an uneven sex distribution, with a greater proportion of female participants. While this reflects the known sex distribution in MS prevalence, potential sex-related differences in neuromuscular performance and neurophysiologic responses may provide some influence on outcome measures.

Conclusion

This study provides evidence linking corticospinal system function to lower-limb motor performance in individuals with MS. Compared to NT controls, individuals with MS demonstrated reduced CST excitability and prolonged conduction times, reflecting disruptions to CST transmission. Alongside these neural differences, individuals with MS exhibited altered neuromuscular control, characterized by reduced force output and impaired force modulation

during MVIC and 5XSST. Significant correlations between MEP area and latency, as well as measures of force production, suggest that these neurophysiological alterations are linked to impairments in movement performance. These findings underscore the relevance of CST integrity for functional lower-limb performance in individuals with MS with mild to moderate disability. Future work should continue to investigate the neurophysiological mechanisms contributing to movement dysfunction, with particular emphasis on identifying distinct neural factors that influence concentric versus eccentric control during full-body tasks. Additionally, future research is needed to determine whether interventions such as high-velocity resistance training, eccentric strength training, or neuromodulation approaches, like transcranial direct current stimulation, can enhance CST function and improve muscle output and transfer performance in people with MS.

References

1. Dilokthornsakul, P. *et al.* Multiple sclerosis prevalence in the United States commercially insured population. *Neurology* **86**, 1014–1021 (2016).
2. Compston, A. & Coles, A. Multiple sclerosis. *The Lancet* **372**, 1502–1517 (2008).
3. Huang, W. J., Chen, W. W. & Zhang, X. Multiple sclerosis: Pathology, diagnosis and treatments (review). *Experimental and Therapeutic Medicine* vol. 13 Preprint at https://doi.org/10.3892/etm.2017.4410 (2017).
4. Leray, E., Moreau, T., Fromont, A. & Edan, G. Epidemiology of multiple sclerosis. *Rev Neurol (Paris)* **172**, 3–13 (2016).
5. Lunde, H. M. B., Assmus, J., Myhr, K. M., Bø, L. & Grytten, N. Survival and cause of death in multiple sclerosis: A 60-year longitudinal population study. *J Neurol Neurosurg Psychiatry* **88**, (2017).
6. Mésidor, M., Sylvestre, M. P., Marrie, R. A. & Rousseau, M. C. Does age at diagnosis influence the use of health services for multiple sclerosis? *Mult Scler Relat Disord* **46**, (2020).
7. Dunn, J. Impact of mobility impairment on the burden of caregiving in individuals with multiple sclerosis. *Expert Review of Pharmacoeconomics and Outcomes Research* vol. 10 Preprint at https://doi.org/10.1586/erp.10.34 (2010).
8. Sutliff, M. H. Contribution of impaired mobility to patient burden in multiple sclerosis. *Current Medical Research and Opinion* vol. 26 Preprint at https://doi.org/10.1185/03007990903433528 (2010).
9. Joy, J. E. & Johnston Jr, R. B. Characteristics and management of major symptoms. in *Multiple Sclerosis: Current Status and Strategies for the Future* 115–75 (National Academies Press, 2001).
10. Hoang, P. D., Gandevia, S. C. & Herbert, R. D. Prevalence of joint contractures and muscle weakness in people with multiple sclerosis. *Disability and Rehabilitation* vol. 36 Preprint at https://doi.org/10.3109/09638288.2013.854841 (2014).
11. Kister, I. *et al.* Natural History of Multiple Sclerosis Symptoms. *Int J MS Care* **15**, 146–156 (2013).
12. Weissert, R. The immune pathogenesis of multiple sclerosis. *Journal of Neuroimmune Pharmacology* vol. 8 Preprint at https://doi.org/10.1007/s11481-013-9467-3 (2013).
13. Lassmann, H. Multiple Sclerosis Pathology. *Cold Spring Harb Perspect Med* **8**, a028936 (2018).
14. Diem, R., Tschirne, A. & Bähr, M. Decreased amplitudes in multiple sclerosis patients with normal visual acuity: A VEP study. *Journal of Clinical Neuroscience* **10**, (2003).
15. Rocca, M. A. *et al.* Abnormal adaptation over time of motor network recruitment in multiple sclerosis patients with fatigue. *Multiple Sclerosis* **22**, (2016).
16. Waxman, S. G. Axonal conduction and injury in multiple sclerosis: The role of sodium channels. *Nature Reviews Neuroscience* vol. 7 Preprint at https://doi.org/10.1038/nrn2023 (2006).
17. Snow, N. J., Wadden, K. P., Chaves, A. R. & Ploughman, M. Transcranial Magnetic Stimulation as a Potential Biomarker in Multiple Sclerosis: A Systematic Review with

Recommendations for Future Research. *Neural Plasticity* vol. 2019 Preprint at https://doi.org/10.1155/2019/6430596 (2019).
18. Di Filippo, M., Portaccio, E., Mancini, A. & Calabresi, P. Multiple sclerosis and cognition: synaptic failure and network dysfunction. *Nature Reviews Neuroscience* vol. 19 Preprint at https://doi.org/10.1038/s41583-018-0053-9 (2018).
19. Green, R., Cutter, G., Friendly, M. & Kister, I. Which symptoms contribute the most to patients' perception of health in multiple sclerosis? *Mult Scler J Exp Transl Clin* **3**, (2017).
20. Peterson, E. W., Cho, C. C., von Koch, L. & Finlayson, M. L. Injurious Falls Among Middle Aged and Older Adults With Multiple Sclerosis. *Arch Phys Med Rehabil* **89**, (2008).
21. Moen, S. M., Celius, E. G., Nordsletten, L. & Holmøy, T. Fractures and falls in patients with newly diagnosed clinically isolated syndrome and multiple sclerosis. *Acta Neurol Scand* **124**, (2011).
22. Mazumder, R., Murchison, C., Bourdette, D. & Cameron, M. Falls in people with multiple sclerosis compared with falls in healthy controls. *PLoS One* **9**, (2014).
23. Peterson, E. W., Cho, C. C. & Finlayson, M. L. Fear of falling and associated activity curtailment among middle aged and older adults with multiple sclerosis. *Multiple Sclerosis* **13**, (2007).
24. Tinetti, M. E., Doucette, J., Claus, E. & Marottoli, R. Risk Factors for Serious Injury During Falls by Older Persons in the Community. *J Am Geriatr Soc* **43**, (1995).
25. Coleman, C. I., Sidovar, M. F., Roberts, M. S. & Kohn, C. Impact of Mobility Impairment on Indirect Costs and Health-Related Quality of Life in Multiple Sclerosis. *PLoS One* **8**, (2013).
26. Zwibel, H. L. Contribution of impaired mobility and general symptoms to the burden of multiple sclerosis. *Advances in Therapy* vol. 26 Preprint at https://doi.org/10.1007/s12325-009-0082-x (2009).
27. Scholz, M., Haase, R., Trentzsch, K., Weidemann, M. L. & Ziemssen, T. Fear of falling and falls in people with multiple sclerosis: A literature review. *Multiple Sclerosis and Related Disorders* vol. 47 Preprint at https://doi.org/10.1016/j.msard.2020.102609 (2021).
28. Kalron, A., Aloni, R., Givon, U. & Menascu, S. Fear of falling, not falls, impacts leisure-time physical activity in people with multiple sclerosis. *Gait Posture* **65**, (2018).
29. Cattaneo, D. *et al.* Risks of falls in subjects with multiple sclerosis. *Arch Phys Med Rehabil* **83**, (2002).
30. Matsuda, P. N. *et al.* Falls in Multiple Sclerosis. *PM&R* **3**, 624–632 (2011).
31. Giovannoni, G. *et al.* Is multiple sclerosis a length-dependent central axonopathy? The case for therapeutic lag and the asynchronous progressive MS hypotheses. *Multiple Sclerosis and Related Disorders* vol. 12 Preprint at https://doi.org/10.1016/j.msard.2017.01.007 (2017).
32. Kurtzke, J. F. On the origin of EDSS. *Multiple Sclerosis and Related Disorders* vol. 4 Preprint at https://doi.org/10.1016/j.msard.2015.02.003 (2015).
33. Taul-Madsen, L., Riemenschneider, M., Jørgensen, M. L. K., Dalgas, U. & Hvid, L. G. Identification of disability status in persons with multiple sclerosis by lower limb

neuromuscular function – Emphasis on rate of force development. *Mult Scler Relat Disord* **67**, (2022).
34. Sieljacks, P. S., Søberg, C. A., Michelsen, A. S., Dalgas, U. & Hvid, L. G. Lower extremity muscle strength across the adult lifespan in multiple sclerosis: Implications for walking and stair climbing capacity. *Exp Gerontol* **139**, (2020).
35. Jørgensen, M. L. K., Dalgas, U., Wens, I. & Hvid, L. G. Muscle strength and power in persons with multiple sclerosis – A systematic review and meta-analysis. *Journal of the Neurological Sciences* vol. 376 Preprint at https://doi.org/10.1016/j.jns.2017.03.022 (2017).
36. Fritz, N. E., Keller, J., Calabresi, P. A. & Zackowski, K. M. Quantitative measures of walking and strength provide insight into brain corticospinal tract pathology in multiple sclerosis. *Neuroimage Clin* **14**, 490–498 (2017).
37. Scott, S. M., Hughes, A. R., Galloway, S. D. R. & Hunter, A. M. Surface EMG characteristics of people with multiple sclerosis during static contractions of the knee extensors. *Clin Physiol Funct Imaging* **31**, (2011).
38. Schwid, S. R. *et al.* Quantitative assessment of motor fatigue and strength in MS. *Neurology* **53**, (1999).
39. Ramari, C., Hvid, L. G., David, A. C. de & Dalgas, U. The importance of lower-extremity muscle strength for lower-limb functional capacity in multiple sclerosis: Systematic review. *Annals of Physical and Rehabilitation Medicine* vol. 63 Preprint at https://doi.org/10.1016/j.rehab.2019.11.005 (2020).
40. Stagsted, R. A. W. *et al.* Lower extremity muscle power – A critical determinant of physical function in aging and multiple sclerosis. *Exp Gerontol* **150**, (2021).
41. Ramari, C. *et al.* Implications of lower extremity muscle power and force for walking and fatigability in multiple sclerosis – An exploratory pilot-study. *Clinical Biomechanics* **96**, (2022).
42. Kasser, S. L. & Jacobs, J. V. Understanding and treating balance impairment in multiple sclerosis. *Journal of Clinical Outcomes Management* **21**, (2014).
43. Kristensen, N. M. *et al.* Neuromuscular rate of force development discriminates fallers in ambulatory persons with multiple sclerosis - an exploratory study. *Mult Scler Relat Disord* **75**, (2023).
44. Reich, D. S. *et al.* Corticospinal tract abnormalities are associated with weakness in multiple sclerosis. *American Journal of Neuroradiology* **29**, (2008).
45. Kerbrat, A. *et al.* Multiple sclerosis lesions in motor tracts from brain to cervical cord: Spatial distribution and correlation with disability. *Brain* **143**, (2020).
46. Baird, J. F., Hubbard, E. A., Sutton, B. P. & Motl, R. W. The relationship between corticospinal tract integrity and lower-extremity strength is attenuated when controlling for age and sex in multiple sclerosis. *Brain Res* **1701**, (2018).
47. Hubbard, E. A., Wetter, N. C., Sutton, B. P., Pilutti, L. A. & Motl, R. W. Diffusion tensor imaging of the corticospinal tract and walking performance in multiple sclerosis. *J Neurol Sci* **363**, 225–231 (2016).
48. Sahota, P. *et al.* Transcranial magnetic stimulation: Role in the evaluation of disability in multiple sclerosis. *Neurol India* **53**, (2005).

49. Farzan, F. Single-pulse transcranial magnetic stimulation (TMS) protocols and outcome measures. *Neuromethods* **89**, (2014).
50. Dall, P. M. & Kerr, A. Frequency of the sit to stand task: An observational study of free-living adults. *Appl Ergon* **41**, (2010).
51. Robinovitch, S. N. *et al.* Video capture of the circumstances of falls in elderly people residing in long-term care: An observational study. *The Lancet* **381**, (2013).
52. Lord, S. R., Murray, S. M., Chapman, K., Munro, B. & Tiedemann, A. Sit-to-stand performance depends on sensation, speed, balance, and psychological status in addition to strength in older people. *Journals of Gerontology - Series A Biological Sciences and Medical Sciences* **57**, (2002).
53. Mong, Y., Teo, T. W. & Ng, S. S. 5-Repetition Sit-to-Stand Test in Subjects With Chronic Stroke: Reliability and Validity. *Arch Phys Med Rehabil* **91**, (2010).
54. Moore, J. L. *et al.* A core set of outcome measures for adults with neurologic conditions undergoing rehabilitation. *Journal of Neurologic Physical Therapy* vol. 42 Preprint at https://doi.org/10.1097/NPT.0000000000000229 (2018).
55. Wang, T. H., Liao, H. F. & Peng, Y. C. Reliability and validity of the five-repetition sit-to-stand test for children with cerebral palsy. *Clin Rehabil* **26**, (2012).
56. Bowser, B., O'Rourke, S., Brown, C. N., White, L. & Simpson, K. J. Sit-to-stand biomechanics of individuals with multiple sclerosis. *Clinical Biomechanics* **30**, (2015).
57. Møller, A. B. *et al.* Validity and variability of the 5-repetition sit-to-stand test in patients with multiple sclerosis. *Disabil Rehabil* **34**, 2251–2258 (2012).
58. Cheng, Y. Y. *et al.* Can sit-to-stand lower limb muscle power predict fall status? *Gait Posture* **40**, (2014).
59. Groppa, S. *et al.* A practical guide to diagnostic transcranial magnetic stimulation: Report of an IFCN committee. *Clinical Neurophysiology* vol. 123 Preprint at https://doi.org/10.1016/j.clinph.2012.01.010 (2012).
60. Sivaramakrishnan, A., Tahara-Eckl, L. & Madhavan, S. Spatial localization and distribution of the TMS-related 'hotspot' of the tibialis anterior muscle representation in the healthy and post-stroke motor cortex. *Neurosci Lett* **627**, (2016).
61. Rossini, P. M. *et al.* Non-invasive electrical and magnetic stimulation of the brain, spinal cord and roots: basic principles and procedures for routine clinical application. Report of an IFCN committee. *Electroencephalogr Clin Neurophysiol* **91**, (1994).
62. Muceli, S. & Merletti, R. Tutorial. Frequency analysis of the surface EMG signal: Best practices. *Journal of Electromyography and Kinesiology* **79**, 102937 (2024).
63. Goldberger, A. L. *et al.* PhysioBank, PhysioToolkit, and PhysioNet: components of a new research resource for complex physiologic signals. *Circulation* **101**, (2000).
64. Xu, L. Cancellation of harmonic interference by baseline shifting of wavelet packet decomposition coefficients. *IEEE Transactions on Signal Processing* **53**, (2005).
65. Sivaramakrishnan, A. & Madhavan, S. Stimulus intensity affects variability of motor evoked responses of the non-paretic, but not paretic tibialis anterior muscle in stroke. *Brain Sci* **10**, (2020).
66. Taga, M. *et al.* Corticoreticulospinal tract neurophysiology in an arm and hand muscle in healthy and stroke subjects. *Journal of Physiology* **599**, (2021).

67. Udupa, K. & Chen, R. Central motor conduction time. in *Handbook of Clinical Neurology* vol. 116 (2013).
68. Furby, A., Bourriez, J. L., Jacquesson, J. M., Mounier-Vehier, F. & Guieu, J. D. Motor evoked potentials to magnetic stimulation: technical considerations and normative data from 50 subjects. *J Neurol* **239**, (1992).
69. Hess, C. W., Mills, K. R., Murray, N. M. F. & Schriefer, T. N. Magnetic brain stimulation: Central motor conduction studies in multiple sclerosis. *Ann Neurol* **22**, (1987).
70. Kukowski, B. Duration, configuration and amplitude of the motor response evoked by magnetic brain stimulation in patients with multiple sclerosis. *Electromyogr Clin Neurophysiol* **33**, (1993).
71. Spampinato, D. A., Ibanez, J., Rocchi, L. & Rothwell, J. Motor potentials evoked by transcranial magnetic stimulation: interpreting a simple measure of a complex system. *Journal of Physiology* vol. 601 Preprint at https://doi.org/10.1113/JP281885 (2023).
72. Hupfeld, K. E., Swanson, C. W., Fling, B. W. & Seidler, R. D. TMS-induced silent periods: A review of methods and call for consistency. *Journal of Neuroscience Methods* vol. 346 Preprint at https://doi.org/10.1016/j.jneumeth.2020.108950 (2020).
73. He, J. & Fu, Z.-F. Frequency response function measurement. in *Modal Analysis* 140–158 (Elsevier, 2001). doi:10.1016/B978-075065079-3/50007-3.
74. Amagliani, R., Petrella, J. & Jung, A. Type of Encouragement Influences Peak Muscle Force in College-Age Women. *Int J Exerc Sci* **3**, 165–173 (2010).
75. Mclellan, C. P., Lovell, D. I. & Gass, G. C. The role of rate of force development on vertical jump performance. *J Strength Cond Res* **25**, (2011).
76. Mark Burden, A., Lewis, S. E. & Willcox, E. The effect of manipulating root mean square window length and overlap on reliability, inter-individual variability, statistical significance and clinical relevance of electromyograms. *Man Ther* **19**, (2014).
77. Bilodeau, M., Schindler-Ivens, S., Williams, D. M., Chandran, R. & Sharma, S. S. EMG frequency content changes with increasing force and during fatigue in the quadriceps femoris muscle of men and women. *Journal of Electromyography and Kinesiology* **13**, (2003).
78. Farina, D., Madeleine, P., Graven-Nielsen, T., Merletti, R. & Arendt-Nielsen, L. Standardising surface electromyogram recordings for assessment of activity and fatigue in the human upper trapezius muscle. *Eur J Appl Physiol* **86**, (2002).
79. Bohannon, R. W. Reference values for the five-repetition sit-to-stand test: A Descriptive meta-analysis of data from elders. *Percept Mot Skills* **103**, (2006).
80. Lindemann, U. *et al.* Measuring power during the sit-to-stand transfer. *Eur J Appl Physiol* **89**, (2003).
81. Uygur, M., de Freitas, P. B. & Barone, D. A. Rate of force development and relaxation scaling factors are highly sensitive to detect upper extremity motor impairments in multiple sclerosis. *J Neurol Sci* **408**, (2020).
82. Kurtzke, J. F. Rating neurologic impairment in multiple sclerosis: An expanded disability status scale (EDSS). *Neurology* **33**, (1983).

83. Bowen, J., Gibbons, L., Gianas, A. & Kraft, G. H. Self-administered expanded disability status scale with functional system scores correlates well with a physician-administered test. *Multiple Sclerosis* **7**, (2001).
84. Wuensch, K. L. & Evans, J. D. Straightforward Statistics for the Behavioral Sciences. *J Am Stat Assoc* **91**, (1996).
85. Gagliardo, A. *et al.* Motor evoked potentials in multiple sclerosis patients without walking limitation: Amplitude vs. conduction time abnormalities. *J Neurol* **254**, (2007).
86. Kale, N., Agaoglu, J., Onder, G. & Tanik, O. Correlation between disability and transcranial magnetic stimulation abnormalities in patients with multiple sclerosis. *Journal of Clinical Neuroscience* **16**, (2009).
87. Neva, J. L. *et al.* Multiple measures of corticospinal excitability are associated with clinical features of multiple sclerosis. *Behavioural Brain Research* **297**, (2016).
88. Tataroglu, C., Genc, A., Idiman, E., Cakmur, R. & Idiman, F. Cortical silent period and motor evoked potentials in patients with multiple sclerosis. *Clin Neurol Neurosurg* **105**, (2003).
89. Nantes, J. C. *et al.* Cortical Damage and Disability in Multiple Sclerosis: Relation to Intracortical Inhibition and Facilitation. *Brain Stimul* **9**, (2016).
90. Strauss, S., Herr, T., Nafz, C., Seusing, N. & Grothe, M. The Cortical Silent Period and Its Association with Fatigue in Multiple Sclerosis: The Need for Standardized Data Collection. *Brain Sci* **14**, (2024).
91. Kuo, Y. L., Dubuc, T., Boufadel, D. F. & Fisher, B. E. Measuring ipsilateral silent period: Effects of muscle contraction levels and quantification methods. *Brain Res* **1674**, (2017).
92. Fling, B. W. & Seidler, R. D. Fundamental differences in callosal structure, neurophysiologic function, and bimanual control in young and older adults. *Cerebral Cortex* **22**, (2012).
93. Martin, C. L. *et al.* Gait and balance impairment in early multiple sclerosis in the absence of clinical disability. *Multiple Sclerosis* **12**, (2006).
94. Benedetti, M. G. *et al.* Gait abnormalities in minimally impaired multiple sclerosis patients. *Multiple Sclerosis* **5**, (1999).
95. Kirmaci, Z. İ. K. *et al.* Muscle architecture and its relationship with lower extremity muscle strength in multiple sclerosis. *Acta Neurol Belg* **122**, (2022).
96. Gunn, H., Creanor, S., Haas, B., Marsden, J. & Freeman, J. Frequency, characteristics, and consequences of falls in multiple sclerosis: Findings from a cohort study. *Arch Phys Med Rehabil* **95**, (2014).
97. Hobart, J., Blight, A. R., Goodman, A., Lynn, F. & Putzki, N. Timed 25-Foot Walk: Direct evidence that improving 20% or greater is clinically meaningful in MS. *Neurology* **80**, (2013).
98. Citaker, S. *et al.* Relationship between lower extremity isometric muscle strength and standing balance in patients with multiple sclerosis. *NeuroRehabilitation* **33**, (2013).
99. Kjølhede, T. *et al.* Relationship between muscle strength parameters and functional capacity in persons with mild to moderate degree multiple sclerosis. *Mult Scler Relat Disord* **4**, 151–158 (2015).

100. Özüdoğru, A., Canlı, M., Gürses, Ö. A., Alkan, H. & Yetiş, A. Determination of five times-sit-to-stand test performance in patients with multiple sclerosis: validity and reliability. *Somatosens Mot Res* **40**, 72–77 (2023).
101. Jensen, H. B. *et al.* Effect of slow release-Fampridine on muscle strength, rate of force development, functional capacity and cognitive function in an enriched population of MS patients. A randomized, double blind, placebo controlled study. *Mult Scler Relat Disord* **10**, 137–144 (2016).
102. Ponichtera, J. A., Rodgers, M. M., Glaser, R. M., Mathews, T. A. & Camaione, D. N. Concentric and eccentric isokinetic lower extremity strength in persons with multiple sclerosis. *Journal of Orthopaedic and Sports Physical Therapy* **16**, (1992).
103. Patrocinio de Oliveira, C. E., Moreira, O. C., Carrión-Yagual, Z. M., Medina-Pérez, C. & de Paz, J. A. Effects of Classic Progressive Resistance Training Versus Eccentric-Enhanced Resistance Training in People With Multiple Sclerosis. *Arch Phys Med Rehabil* **99**, (2018).
104. Fling, B. W., Dutta, G. G., Schlueter, H., Cameron, M. H. & Horak, F. B. Associations between proprioceptive neural pathway structural connectivity and balance in people with multiple sclerosis. *Front Hum Neurosci* **8**, (2014).
105. Yang, F. & Liu, X. Relative importance of vision and proprioception in maintaining standing balance in people with multiple sclerosis. *Mult Scler Relat Disord* **39**, (2020).
106. Ozkan, T. *et al.* Investigation of parameters related to lower extremity muscle strength and proprioception in Patients with Multiple Sclerosis: a cross-sectional study. *Mult Scler Relat Disord* **79**, (2023).
107. Dalgas, U. *et al.* Resistance training improves muscle strength and functional capacity in multiple sclerosis. *Neurology* **73**, 1478–1484 (2009).
108. Plow, E. B. *et al.* Neurophysiological correlates of aging-related muscle weakness. *J Neurophysiol* **110**, (2013).
109. Wilson, M. T. *et al.* Enhanced skeletal muscle contractile function and corticospinal excitability precede strength and architectural adaptations during lower-limb resistance training. *Eur J Appl Physiol* **123**, (2023).
110. Clos, P., Garnier, Y., Martin, A. & Lepers, R. Corticospinal excitability is altered similarly following concentric and eccentric maximal contractions. *Eur J Appl Physiol* **120**, (2020).
111. Weavil, J. C., Sidhu, S. K., Mangum, T. S., Richardson, R. S. & Amann, M. Intensity-dependent alterations in the excitability of cortical and spinal projections to the knee extensors during isometric and locomotor exercise. *Am J Physiol Regul Integr Comp Physiol* **308**, (2015).
112. Goodall, S., Romer, L. M. & Ross, E. Z. Voluntary activation of human knee extensors measured using transcranial magnetic stimulation. *Exp Physiol* **94**, (2009).
113. Todd, G., Taylor, J. L. & Gandevia, S. C. Measurement of voluntary activation of fresh and fatigued human muscles using transcranial magnetic stimulation. *Journal of Physiology* **551**, (2003).
114. Castelli, F. *et al.* Rate of force development is correlated with corticospinal excitability during explosive voluntary contractions. Preprint at https://doi.org/10.1101/2024.08.27.607589 (2024).

115. Ghasemi, N., Razavi, S. & Nikzad, E. Multiple sclerosis: Pathogenesis, symptoms, diagnoses and cell-based therapy. *Cell Journal* vol. 19 Preprint at (2017).
116. Filippi, M. & Rocca, M. A. MRI evidence for multiple sclerosis as a diffuse disease of the central nervous system. in *Journal of Neurology* vol. 252 (2005).
117. Maffiuletti, N. A. *et al.* Rate of force development: physiological and methodological considerations. *European Journal of Applied Physiology* vol. 116 Preprint at https://doi.org/10.1007/s00421-016-3346-6 (2016).
118. Semmler, J. G. Motor unit synchronization and neuromuscular performance. *Exerc Sport Sci Rev* **30**, (2002).
119. Del Vecchio, A. Neuromechanics of the Rate of Force Development. *Exerc Sport Sci Rev* **51**, (2023).
120. Cuesta-Vargas, A. I. & González-Sánchez, M. Differences in muscle activation patterns during sit to stand task among subjects with and without intellectual disability. *Biomed Res Int* **2013**, (2013).
121. Kim, S. H. & Ju, S. K. Comparison of muscle activity during sit-to-stand movement at different chair heights between obese and normal-weight subjects. *J Exerc Rehabil* **17**, (2021).
122. Kasai, T. & Kawai, K. Quantitative EMG analysis of analysis of anticipatory postural adjustments of voluntary contraction of leg muscles in standing man. *Electroencephalography and Clinical Neurophysiology/ Evoked Potentials* **93**, (1994).
123. Rodrigues-De-Paula Goulart, F. & Valls-Solé, J. Patterned electromyographic activity in the sit-to-stand movement. *Clinical Neurophysiology* **110**, (1999).
124. Tavy, D. L. J. *et al.* Transcranial magnetic stimulation in patients with cervical spondylotic myelopathy: Clinical and radiological correlations. *Muscle Nerve* **17**, (1994).
125. Singh, O. & Al Khalili, Y. *Anatomy, Back, Lumbar Plexus*. *StatPearls* (2019).
126. Granger, C. J. & Cohen-Levy, W. B. *Anatomy, Bony Pelvis and Lower Limb, Posterior Tibial Nerve*. *StatPearls* (2019).
127. Duchateau, J. & Enoka, R. M. Distribution of motor unit properties across human muscles. *Journal of Applied Physiology* vol. 132 Preprint at https://doi.org/10.1152/japplphysiol.00290.2021 (2022).
128. Clos, P. *et al.* Corticospinal Excitability Is Lower During Eccentric Than Concentric Cycling in Men. *Front Physiol* **13**, (2022).
129. Doguet, V. *et al.* Muscle length effect on corticospinal excitability during maximal concentric, isometric and eccentric contractions of the knee extensors. *Exp Physiol* **102**, (2017).
130. Duchateau, J. & Baudry, S. Insights into the neural control of eccentric contractions. *Journal of Applied Physiology* vol. 116 Preprint at https://doi.org/10.1152/japplphysiol.00002.2013 (2014).
131. Grosprêtre, S., Papaxanthis, C. & Martin, A. Corticospinal Modulations during Motor Imagery of Concentric, Eccentric, and Isometric Actions. *Med Sci Sports Exerc* **52**, (2020).
132. Canepa, P. *et al.* Motor Cortical Excitability Changes in Preparation to Concentric and Eccentric Movements. *Neuroscience* **475**, (2021).

133. Kwon, Y. H. & Park, J. W. Different cortical activation patterns during voluntary eccentric and concentric muscle contractions: An fMRI study. *NeuroRehabilitation* **29**, (2011).
134. Perrey, S. Brain activation associated with eccentric movement: A narrative review of the literature. *European Journal of Sport Science* vol. 18 Preprint at https://doi.org/10.1080/17461391.2017.1391334 (2018).
135. Fang, Y., Siemionow, V., Sahgal, V., Xiong, F. & Yue, G. H. Distinct brain activation patterns for human maximal voluntary eccentric and concentric muscle actions. *Brain Res* **1023**, (2004).
136. Glover, I. S. & Baker, S. N. Cortical, corticospinal, and reticulospinal contributions to strength training. *Journal of Neuroscience* **40**, (2020).
137. Glover, I. S. & Baker, S. N. Both Corticospinal and Reticulospinal Tracts Control Force of Contraction. *Journal of Neuroscience* **42**, (2022).
138. Škarabot, J., Folland, J. P., Holobar, A., Baker, S. N. & Del Vecchio, A. Startling stimuli increase maximal motor unit discharge rate and rate of force development in humans. *J Neurophysiol* **128**, (2022).
139. Nardone, R. *et al.* Central motor conduction studies in patients with spinal cord disorders: A review. *Spinal Cord* vol. 52 Preprint at https://doi.org/10.1038/sc.2014.48 (2014).
140. Phu, S., Lord, S. R., Sturnieks, D. L. & Okubo, Y. Impact of pathological conditions on postural reflex latency and adaptability following unpredictable perturbations: A systematic review and meta-analysis. *Gait and Posture* vol. 95 Preprint at https://doi.org/10.1016/j.gaitpost.2022.04.014 (2022).
141. Horak, F. B., Shupert, C. L. & Mirka, A. Components of postural dyscontrol in the elderly: A review. *Neurobiology of Aging* vol. 10 Preprint at https://doi.org/10.1016/0197-4580(89)90010-9 (1989).
142. Cheng, P. T., Chen, C. L., Wang, C. M. & Hong, W. H. Leg Muscle Activation Patterns of Sit-to-Stand Movement in Stroke Patients. *Am J Phys Med Rehabil* **83**, (2004).
143. Howatson, G. *et al.* Ipsilateral motor cortical responses to TMS during lengthening and shortening of the contralateral wrist flexors. *European Journal of Neuroscience* **33**, (2011).
144. Inghilleri, M., Berardelli, A., Cruccu, G. & Manfredi, M. Silent period evoked by transcranial stimulation of the human cortex and cervicomedullary junction. *J Physiol* **466**, (1993).
145. Kidgell, D. J., Bonanno, D. R., Frazer, A. K., Howatson, G. & Pearce, A. J. Corticospinal responses following strength training: a systematic review and meta-analysis. *European Journal of Neuroscience* vol. 46 Preprint at https://doi.org/10.1111/ejn.13710 (2017).
146. Latella, C., Kidgell, D. J. & Pearce, A. J. Reduction in corticospinal inhibition in the trained and untrained limb following unilateral leg strength training. *Eur J Appl Physiol* **112**, (2012).
147. Christie, A. & Kamen, G. Cortical inhibition is reduced following short-term training in young and older adults. *Age (Omaha)* **36**, (2014).
148. Weier, A. T., Pearce, A. J. & Kidgell, D. J. Strength training reduces intracortical inhibition. *Acta Physiologica* **206**, (2012).

149. Mason, J. *et al.* Determining the early corticospinal-motoneuronal responses to strength training: A systematic review and meta-analysis. *Rev Neurosci* **30**, (2019).
150. Mason, J. *et al.* Determining the Corticospinal Responses to Single Bouts of Skill and Strength Training. *J Strength Cond Res* **33**, (2019).
151. Griffin, L. & Cafarelli, E. Transcranial magnetic stimulation during resistance training of the tibialis anterior muscle. *Journal of Electromyography and Kinesiology* **17**, (2007).
152. Latella, C. *et al.* Effects of acute resistance training modality on corticospinal excitability, intra-cortical and neuromuscular responses. *Eur J Appl Physiol* **117**, (2017).
153. Nuzzo, J. L., Barry, B. K., Gandevia, S. C. & Taylor, J. L. Acute strength training increases responses to stimulation of corticospinal axons. *Med Sci Sports Exerc* **48**, (2016).
154. Tallent, J., Goodall, S., Gibbon, K. C., Hortobágyi, T. & Howatson, G. Enhanced corticospinal excitability and volitional drive in response to shortening and lengthening strength training and changes following detraining. *Front Physiol* **8**, (2017).
155. Selvanayagam, V. S., Riek, S. & Carroll, T. J. Early neural responses to strength training. *J Appl Physiol* **111**, (2011).
156. Latella, C., Hendy, A. M., Pearce, A. J., VanderWesthuizen, D. & Teo, W. P. The time-course of acute changes in corticospinal excitability, intra-cortical inhibition and facilitation following a single-session heavy strength training of the biceps brachii. *Front Hum Neurosci* **10**, (2016).
157. Maeo, S., Balshaw, T. G., Lanza, M. B., Hannah, R. & Folland, J. P. Corticospinal excitability and motor representation after long-term resistance training. *European Journal of Neuroscience* **53**, (2021).
158. Colomer-Poveda, D., Hortobágyi, T., Keller, M., Romero-Arenas, S. & Márquez, G. Training intensity-dependent increases in corticospinal but not intracortical excitability after acute strength training. *Scand J Med Sci Sports* **30**, (2020).
159. Del Vecchio, A. *et al.* The increase in muscle force after 4 weeks of strength training is mediated by adaptations in motor unit recruitment and rate coding. *Journal of Physiology* **597**, (2019).
160. Casolo, A. *et al.* Strength Training Increases Conduction Velocity of High-Threshold Motor Units. *Med Sci Sports Exerc* **52**, (2020).
161. Dalgas, U. *et al.* Neural drive increases following resistance training in patients with multiple sclerosis. *J Neurol* **260**, (2013).
162. Chaves, A. R., Devasahayam, A. J., Riemenschneider, M., Pretty, R. W. & Ploughman, M. Walking Training Enhances Corticospinal Excitability in Progressive Multiple Sclerosis—A Pilot Study. *Front Neurol* **11**, (2020).
163. Nitsche, M. A. & Paulus, W. Excitability changes induced in the human motor cortex by weak transcranial direct current stimulation. *Journal of Physiology* **527**, (2000).
164. Nitsche, M. A. & Paulus, W. Sustained excitability elevations induced by transcranial DC motor cortex stimulation in humans. *Neurology* **57**, (2001).
165. Dissanayaka, T., Zoghi, M., Farrell, M., Egan, G. F. & Jaberzadeh, S. Does transcranial electrical stimulation enhance corticospinal excitability of the motor cortex in healthy

individuals? A systematic review and meta-analysis. *European Journal of Neuroscience* **46**, (2017).
166. Roche, N., Geiger, M. & Bussel, B. Mechanisms underlying transcranial direct current stimulation in rehabilitation. *Annals of Physical and Rehabilitation Medicine* vol. 58 Preprint at https://doi.org/10.1016/j.rehab.2015.04.009 (2015).
167. Hendy, A. M. & Kidgell, D. J. Anodal-tDCS applied during unilateral strength training increases strength and corticospinal excitability in the untrained homologous muscle. *Exp Brain Res* **232**, (2014).
168. Mitsutake, T., Imura, T., Hori, T., Sakamoto, M. & Tanaka, R. Effects of Combining Online Anodal Transcranial Direct Current Stimulation and Gait Training in Stroke Patients: A Systematic Review and Meta-Analysis. *Frontiers in Human Neuroscience* vol. 15 Preprint at https://doi.org/10.3389/fnhum.2021.782305 (2021).

CHAPTER 4 – ASSOCIATIONS BETWEEN CLINICAL AND NEUROPHYSIOLOGICAL FUNCTION AND MULTIPLE DIFFUSION MAGNETIC RESONANCE IMAGING MODELS IN PEOPLE WITH MULTIPLE SCLEROSIS

Introduction

Multiple sclerosis (MS) is a chronic immune-mediated neurological disease characterized by demyelination and axonal damage, resulting in a diverse array of motor, sensory, and cognitive impairments.[1] Among its most debilitating symptoms are mobility-related deficits, contributing to reduced quality of life and loss of long-term independence.[2–4] These physical limitations are often associated with underlying structural or functional neural changes,[5] yet the specific contributors to these impairments remain incompletely understood. Uncovering the neurobiological underpinnings of balance and mobility impairments remains a critical objective in MS research and highlights the need for tools capable of detecting clinically relevant changes.

In MS, inflammatory white matter lesions in the central nervous system are a hallmark feature of the disease and serve as the basis for diagnosis using conventional MRI.[6–8] While lesion load has traditionally been used as a marker of disease burden, its relationship with clinical function is inconsistent.[9,10] Diffusion magnetic resonance imaging (dMRI) is a non-invasive imaging technique sensitive to the micro- and macrostructural properties of white matter (WM) in vivo.[11–13] dMRI is widely used in clinical research to compare WM structural integrity across populations, monitor longitudinal changes, and explore relationships with functional outcomes.[14] In neurological disorders such as MS, where WM damage is prevalent, dMRI is particularly valuable for detecting microstructural abnormalities.[15] Various diffusion models have been developed to quantify tissue characteristics and assess their associations with behavioral and

neurological measures. Among these models, diffusion tensor imaging (DTI) is the most commonly used.[16] It models diffusion in brain tissue using an ellipsoid tensor to estimate the direction and magnitude of water molecule movement.[17]

In MS, alterations in DTI-derived metrics are consistently observed within WM lesions, reflecting focal structural damage. Additionally, alterations are found in normal-appearing WM, suggesting the presence of more diffuse WM structural abnormalities that are not detectable with conventional MRI.[18] Regional DTI metrics extracted from the corticospinal tract (CST) have been associated with motor disability in MS,[19,20] supporting the utility of DTI in identifying neural correlates of disability. Despite its widespread application, DTI is limited by its underlying assumption of Gaussian diffusion. Given the complex microenvironment of neural tissue, which comprises cell membranes, organelles, and other barriers that water must encounter, diffusion in the brain is rarely uniformly Gaussian.[21,22] Additionally, DTI assumes a single diffusion direction and is therefore inherently limited in regions where fibers cross, as the tensor model cannot resolve multiple fiber orientations within a single voxel.[23,24] This poses a sizable issue, as estimates suggest that 60-90% of all WM contains multidirectional fiber configurations.[25] Even within predominantly coherent tracts like the CST, axons must traverse complex regions like the corona radiata, where crossing fibers are abundant. In such areas, DTI tensor models may misrepresent underlying WM structural properties.

Diffusion kurtosis imaging (DKI) addresses these limitations using a higher-order tensor model that captures non-Gaussian diffusion. DKI quantifies diffusion kurtosis, a statistical measure of the deviation from a Gaussian distribution, enabling more accurate measures of tissue complexity and microstructural heterogeneity.[22,26,27] Within the context of MS, studies have demonstrated that DKI metrics may detect greater differences between MS patients and controls

in normal-appearing WM compared to DTI.[28] However, other literature suggests that DTI performs optimally in regions with aligned fibers, such as the corpus callosum, whereas DKI performs optimally in areas with more complex fiber configurations.[29] These findings suggest that DTI and DKI may offer complementary insights into WM pathology.

Another dMRI approach developed to overcome the constraints of traditional tensor-based models is Fixel-Based Analysis (FBA).[30,31] FBA can resolve multiple fiber populations within a single voxel, allowing for the isolation of individual fiber pathways or fiber elements (fixel) and more precise quantification of WM properties in regions with crossing fibers.[32] In addition, FBA provides distinct quantitative metrics that reflect both microstructural and macrostructural properties of WM, enabling the characterization of axonal damage and tract atrophy.[32,33] These measures provide a more nuanced depiction of WM pathology than conventional tensor-derived scalar metrics, thereby supporting improved interpretation of disease-related WM alterations in MS. Although FBA has been less commonly used in MS, recent research has shown that FBA reveals more widespread WM integrity differences between individuals with MS and healthy controls compared to DTI.[34] Examining FBA alongside DTI and DKI within the same study cohort may provide insight into the added value of advanced diffusion models for characterizing MS-related WM pathology in relation to key outcome metrics.

While the described dMRI techniques are well-suited for imaging and quantifying WM structural integrity, they do not capture functional aspects of neural pathways. Transcranial magnetic stimulation (TMS) offers a separate non-invasive approach to probe neurophysiological function, particularly excitability and conduction properties of the CST.[35] In MS, where demyelination and axonal damage frequently affect motor pathway function, TMS measures have been associated with disease progression and clinical disability measures.[36,37] To date, few studies

have directly connected dMRI WM integrity measures to TMS functional neurophysiology measures.[38–41] Moreover, to our knowledge, none have focused on the lower-limbs, despite lower-limb dysfunction being a primary driver of disability in MS. Bridging the gap between dMRI measures and TMS-derived neurophysiological outcomes in MS allows for better interpretations of how structural disruptions relate to impaired neural function, offering a means to assess the functional relevance of WM damage.

The present study compared dMRI metrics from multiple models, including DTI, DKI, and FBA, within the CST between individuals with relapsing-remitting MS and age- and sex-matched neurotypical (NT) controls. To examine the functional relevance of structural group differences, we performed correlation analyses between fixel- and tensor-derived metrics and neurophysiological markers of CST conduction and excitability, as well as clinical measures of impairment. Through this approach, the study aimed to investigate whether FBA metrics capture a greater extent of WM alterations in the CST in individuals with MS compared to NT controls relative to tensor-based methods and whether such differences are associated with corticomotor output and functional mobility performance measures.

Materials and Methods

Study Overview

Participants completed two days of in-person assessments. On Day 1, participants underwent MRI scanning followed by clinical balance and mobility assessments. On Day 2, participants underwent TMS assessment and additional specialized mobility testing. The study was reviewed and approved by the Colorado State University Institutional Review Board (IRB#18-7738H), and all participants provided written informed consent prior to participation in accordance

with the Declaration of Helsinki. For reference, a list of outcome metrics and their interpretations is provided in Table 4.1.

Table 4.1. Outcome Metrics Across Imaging, Clinical, and Neurophysiological Domains. List of the primary outcome metrics for the present study. Each metric is listed with its full name, abbreviation, and a brief description.

Domain	Full Name	Abbreviation	Description
Diffusion Tensor Imaging (DTI) Metrics	Mean Diffusivity	MD	Average rate of diffusion
	Axial Diffusivity	AD	Diffusion along the principal axis of the tensor
	Radial Diffusivity	RD	Diffusion perpendicular to the principal axis of the tensor
	Fractional Anisotropy	FA	Degree of directionality (anisotropy)
Diffusion Kurtosis Imaging (DKI) Metrics	Mean Kurtosis	MK	Overall diffusion kurtosis (deviation from Gaussian diffusion) across directions
	Axial Kurtosis	AK	Kurtosis along the principal diffusion direction
	Radial Kurtosis	RK	Kurtosis perpendicular to the principal direction
Fixel-Based Analysis (FBA) Metrics	Fiber Density and Cross-section	FDC	Combined measure of fiber density and cross-sectional area
	Fiber Density	FD	Estimate of intra-axonal volume
	Log Fiber Cross-section	LogFC	Log-transformed measure of fiber bundle cross-section area
miniBEST Subscores	Anticipatory Postural Adjustments	APA	Anticipatory balance control (e.g., rise to toes)
	Reactive Postural Control	RPC	Automatic responses to external perturbations (e.g., compensatory stepping)
	Sensory Orientation	SO	Balance in altered sensory conditions (e.g., standing on a foam pad with eyes-closed)
	Dynamic Gait	DG	Dynamic walking patterns (e.g., stepping over obstacles)

Clinical Disability	Expanded Disability Status Scale	EDSS	MS-related disability score
TMS Neurophysiology	Motor-Evoked Potential Area	MEP Area	Measure of corticospinal excitability
	MEP Onset Latency	MEP Latency	Measure of neural conduction integrity

Participants

A total of 49 participants were included in this study, comprising 25 individuals with a neurologist-confirmed diagnosis of relapsing-remitting MS and 24 age- and sex-matched NT controls. Inclusion criteria for MS participants required mild to moderate disability, defined as a self-reported Expanded Disability Status Scale (EDSS) score between 0 and 4. Participants were excluded if they were unable to walk 500 meters or stand for 10 minutes unassisted safely or if they reported a musculoskeletal injury, joint replacement, vestibular disorder, or any neurological condition other than MS. NT participants were required to be free of any neurological condition and meet the same physical ability criteria as those in the MS group.

Expanded Disability Status Scale (EDSS)

The EDSS is a commonly used measure to evaluate neurological impairment and monitor disease progression in individuals with MS. The EDSS incorporates ratings from the Functional Systems Score, which assesses key neurological domains, including vision, sensory, and motor function.[42] Participants with MS provided their EDSS scores using a validated self-report questionnaire. Previous research has demonstrated a strong association between self-reported EDSS scores and those obtained through clinician assessment.[43]

Mini-Balance Evaluation Systems Test (miniBEST)

Balance and mobility impairment were assessed using the miniBEST, a standardized clinical assessment designed to evaluate dynamic balance across four domains: anticipatory postural adjustments, reactive postural control, sensory orientation, and dynamic gait.[44] The test consists of 14 items, each scored on a 3-point ordinal scale (0 = severe impairment, 1 = moderate impairment, 2 = normal performance), with higher scores indicating better balance function. In the present study, scores from both limbs were included for items involving single-leg assessments, such as single-leg stance. Scores from each domain were summed to generate a composite score, yielding a maximum possible score of 32 points. All assessments were conducted by a trained evaluator following standardized clinical administration protocols.

TMS Acquisition

To assess CST functional integrity, motor evoked potentials (MEPs) were elicited using TMS and recorded from the tibialis anterior (TA) muscle of each leg. Bipolar Ag-AgCl surface electrodes were placed over the belly of the TA muscle to record muscle activity via electromyography (EMG). Single TMS pulses were delivered to the primary motor cortex contralateral to the target muscle using a 2 × 95 mm angled butterfly coil (120-degree, Cool D-B80, MagVenture) positioned at approximately 45–65° from the mid-sagittal line.[45] The motor "hot spot" for each TA muscle was identified by starting 1 cm lateral and 1 cm posterior to the vertex of the cranium (determined from the intersection of the nasion-inion and left-right pre-auricular points) and systematically adjusting the coil position until the most consistent and largest MEP was observed.[46]

Resting motor threshold (RMT) was determined for each hemisphere and defined as the lowest stimulation intensity required to evoke a peak-to-peak MEP amplitude of at least 0.05 mV

in 5 out of 10 consecutive trials.[47] Prior to data collection, participants performed three to five unilateral maximum voluntary contractions (MVCs) of the TA muscle on each leg. Maximum force was defined as the highest value within ±10% of trials. During the TMS session, participants were instructed to unilaterally dorsiflex the ankle at 15% of their MVC, using visual feedback for guidance. TMS pulses at 120% of RMT were delivered to the identified "hot spot" of the corresponding motor cortex. Each testing session lasted approximately 3 minutes per leg, with stimuli delivered every 7–10 seconds, resulting in a median of 21 total stimulations per hemisphere.

TMS Analysis

EMG data were collected at a sampling rate of 2000 Hz using a BIOPAC system (BIOPAC Systems, Inc., Santa Barbara, CA, USA), with a 60 Hz notch filter applied to mitigate power line noise. Following the acquisition, all participant EMG signals were processed using a bandpass filter (20–500 Hz)[48] in combination with a wavelet packet harmonic filter[49,50] to remove electrical interference observed in several recordings. Filtering was performed using custom scripts in MATLAB (v.9.14.0, MathWorks Inc., Natick, MA, USA). All EMG traces and corresponding power spectrum-frequency plots were manually inspected to ensure data quality and filtering effectiveness. MEPs were extracted using a time window extending from 100 ms before to 250 ms after the delivery of the TMS pulse. Trials were excluded if they lacked a discernible stimulation response or failed to meet inclusion criteria, defined as a rectified waveform that failed to exceed two standard deviations above the pre-stimulation rectified EMG signal or a response duration of less than 5 ms.[51,52]

For each participant, valid trials were averaged together, and two key metrics were derived: average MEP onset latency and average MEP area. MEP onset latency was defined as the time

(ms) from the TMS pulse to the onset of the MEP. MEP onset was identified using a threshold-based approach, defined as the first datapoint that exceeded 125% of the average pre-stimulus rectified EMG (100 ms) and was sustained for at least 5 ms. MEP offset was defined as the first data point below the 125% pre-stimulus rectified EMG and was sustained for at least 5 ms (Figure 4.1).[52] The MEP area was calculated as the area under the rectified EMG curve between MEP onset and offset, with pre-stimulus EMG activity subtracted. Baseline correction was performed by multiplying the mean pre-stimulus rectified EMG by the MEP duration and subtracting this value from the total area (Figure 4.1).[51] MEP area served as the primary outcome measure for CST excitability due to the presence of polyphasic MEP waveforms commonly observed in individuals with MS.[53–55]

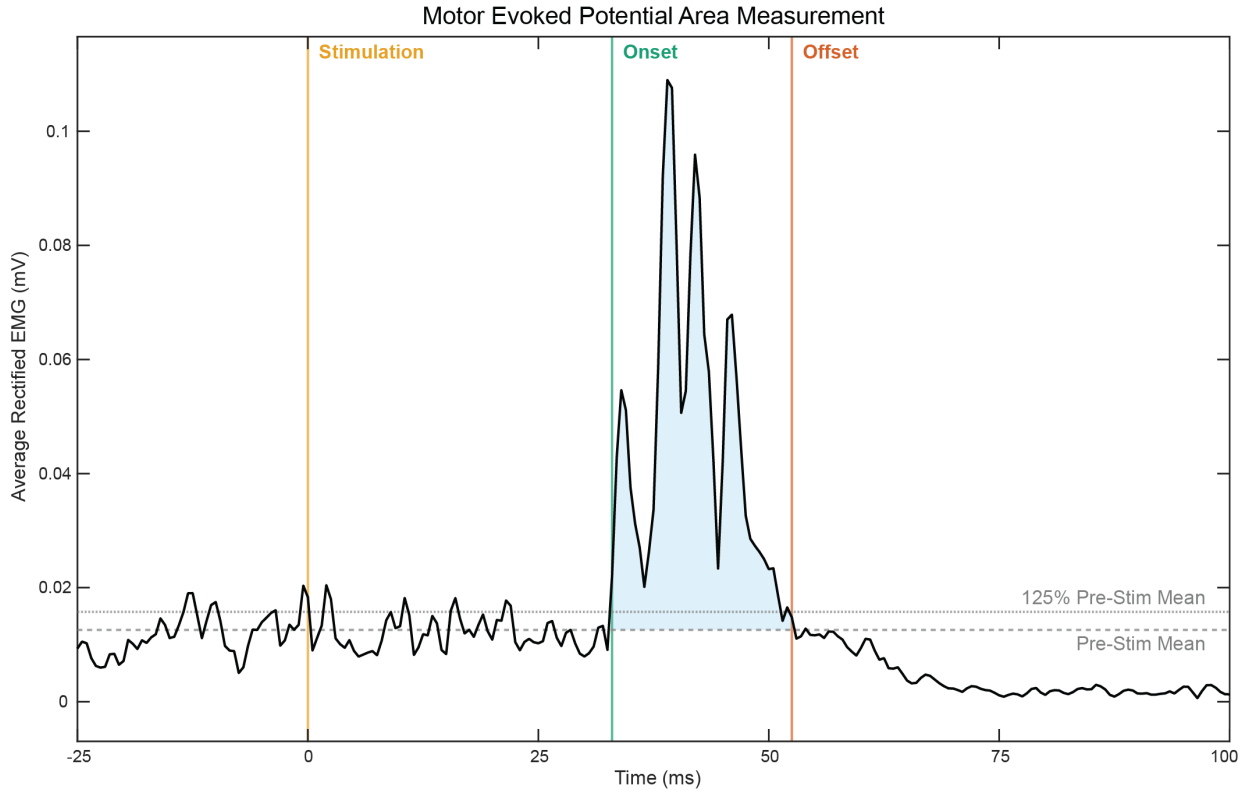

Figure 4.1. Neurophysiological Outcome Measurements. Averaged rectified MEP waveform from an example participant. MEP onset latency was identified as the first datapoint that exceeded 125% of the pre-stimulus rectified EMG and was sustained for at least 5 ms. MEP offset was identified as the first datapoint below the 125% pre-stimulus rectified EMG and was sustained for

at least 5 ms. MEP area was calculated as the area under the rectified EMG curve between MEP onset and offset, with pre-stimulus EMG activity subtracted (shaded blue).

MRI Acquisition

dMRI data were acquired on a 3.0 T Siemens MAGNETOM Prismafit (Siemens Medical Solutions USA, Inc., Malvern, PA) with the following parameters: repetition time (TR) = 4000 ms, echo time (TE) = 77 ms, flip angle = 84°, voxel size = 2.0 × 2.0 × 2.0 mm^3, slice thickness = 2.0 mm, slices = 72, and field of view (FoV) = 224 mm (224 mm right-left (RL), 216 mm anterior-posterior (AP), 144 mm foot-head (FH)), using a 32-channel head coil and parallel imaging. A multi-shell diffusion scheme was employed, comprising 177 directions distributed across four b-value shells: 12 b = 0 s/mm^2 (interspersed), 55 b = 800 s/mm^2, 55 b = 1600 s/mm^2, 55 b = 2400 s/mm^2. To correct for susceptibility-induced distortions, 88 volumes were acquired with an anterior-to-posterior (AP) phase-encoding direction, and 89 volumes were acquired with a posterior-to-anterior (PA) phase-encoding direction.

Additional structural scans were collected for post-processing dMRI registration, volumetric measurements, and lesion identification. Specifically, a high-resolution T1-weighted magnetization-prepared rapid gradient-echo (MP-RAGE): TR = 2400 ms, TE = 2.07 ms, inversion time (TI) = 1000ms, flip angle = 8°, voxel size = 0.8 × 0.8 × 0.8 mm^3, FoV = 256 mm (180 mm (RL), 256 mm (AP), 256 mm (FH)), slices = 224, slice thickness = 0.8 mm, and a T2-weighted fluid-attenuated inversion recovery scan (FLAIR) scan with the following parameters: TR = 6000 ms, TE = 428 ms, TI = 2000 ms, flip angle = 120°, voxel size = 1.0 × 1.0 × 1.0 mm^3, FoV = 256 mm (176 mm (RL), 256 mm (AP), 256 mm (FH)), slices = 176, slice thickness = 1 mm.

MRI Analysis

dMRI Preprocessing

All preprocessing, tractography, and analyses of dMRI data were conducted using MRtrix3 (Tournier et al. 2019,[56] https://www.mrtrix.org/), an open-source software package for advanced dMRI analysis. dMRI data were preprocessed using the recommended MRtrix3 pipeline,[30] which included denoising,[57,58] Gibbs ringing removal,[59] motion and eddy-current distortion correction,[60] and bias field correction.[61]

Tensor Derived Metrics

Two standard tensor models, DTI and DKI, were applied to the diffusion-weighted images using MRtrix3 commands. For DTI analysis, only the b = 800 s/mm² images were used to align with the model's assumption of Gaussian diffusion. Higher b-values introduce non-Gaussian effects, which can bias tensor estimates and reduce the reliability of the resulting metrics. In contrast, the DKI model requires multiple shells and explicitly accounts for non-Gaussian diffusion.[26,27,62] Data from all three b-values (b = 800, 1600, and 2400 s/mm²) were concatenated[56] and included to estimate kurtosis metrics. DTI and DKI images were preprocessed using the same pipeline as the FBA images.

Tensor estimation was performed in two stages. First, an initial weighted least-squares fit was applied to the diffusion signal. This was followed by two iterations of improved fitting using iteratively reweighted least-squares.[63,64] Constrained optimization was incorporated to prevent the generation of physically implausible values, such as negative diffusivity or kurtosis.[65] The final DTI and DKI maps were then registered to the population template space using the identical warps generated during participant-to-template registration for FBA.

From the DTI model, the following metrics were derived: mean diffusivity (MD), axial diffusivity (AD), radial diffusivity (RD), and fractional anisotropy (FA). MD represents the average diffusivity of water molecules in all directions within a voxel, AD reflects the diffusivity along the principal diffusion direction, and RD indicates the diffusivity perpendicular to the principal direction. FA quantifies the degree of directional preference of diffusion, with values closer to 1 indicating highly anisotropic diffusion and values closer to 0 indicating more isotropic diffusion.[66]

The following metrics were obtained from the DKI model: mean kurtosis (MK), axial kurtosis (AK), and radial kurtosis (RK). MK provides an overall kurtosis measure of the deviation from Gaussian diffusion across all directions. AK reflects kurtosis along the primary diffusion direction, and RK measures kurtosis perpendicular to the principal diffusion direction.[67]

Fixel-Based Analysis (FBA)

Per best practices for FBA, which recommends using high b-value data to reduce contamination from extracellular signals,[30] images acquired at b = 800s/mm² were excluded from this portion of the analysis. Following preprocessing, an automated, unsupervised method was used to estimate tissue-specific response functions for single-fiber WM, gray matter, and cerebrospinal fluid.[68] These individual response functions were then averaged to generate group-level response functions.[30] Participant images were then up-sampled to 1.5 mm isotropic voxel size to improve anatomical contrast and facilitate more accurate registration and tractography. Using multi-shell 3-tissue constrained spherical deconvolution, WM fiber orientation distributions (FODs) were estimated for each participant.[69] Joint bias field correction and global intensity normalization were also applied.[33,70,71]

A study-specific FOD template was constructed to enable group-wise comparison using non-linear data registration from 15 individuals with MS and 15 NT controls.[56] The NT participants were randomly selected, while MS participants were chosen with consideration for lesion burden and anatomical integrity to minimize the impact of extreme pathology on template quality. There were no significant group differences in age or sex among the participants selected for template construction. All participant FODs were then registered to this template using non-linear transformation.[72]

From FODs, the following fixel-based metrics were derived: Fiber density (FD), fiber cross-section (FC), and fiber density and cross-section (FDC). FD is a microstructural metric representing the intra-axonal volume of a specific fiber population or fixel. FC is a macrostructural measure that quantifies the cross-sectional area of a fiber bundle.[30,32] Because FC values are typically non-normally distributed, a log transformation (LogFC) was applied before statistical analyses to center the data around zero. FDC is a combined metric integrating FD and FC to measure micro- and macrostructure comprehensively.[30,32]

Tractography and Regions of Interest

This study employed a tract-of-interest approach focused on the CST. Streamline tractography was seeded in the precentral and postcentral gyri using cortical masks derived from the study-specific T1 template image. Streamlines were generated unidirectionally, projecting from the cortex toward the brainstem, and were constrained to pass through two CST waypoint masks located in the pons and medulla. CST waypoint masks were sourced from Boyne et al. (2022)[73] and transformed from MNI into the study template space. To improve anatomical specificity, manually drawn exclusion masks were applied to eliminate streamlines originating from the corticobulbar region and any that entered the corpus callosum, cerebellum, or thalamus.

Five thousand streamlines were generated from each hemisphere to standardize streamline counts bilaterally. After generation, the left and right hemisphere tracts were combined into a single file for statistical analysis. To improve the biological accuracy of streamline densities, the Spherical-deconvolution Informed Filtering of Tractograms 2 algorithm was applied, assigning weight to each streamline based on the underlying fiber orientation distributions.[74] This ensures that the streamline counts accurately reflect the underlying WM architecture. The final rendering of the streamlines is shown in Figure 4.2. For voxel-based analyses, the combined streamline file was converted into a track density image and thresholded to produce a binary mask representing voxels traversed by CST streamlines.[75] This binary mask was then applied to the DTI and DKI maps to restrict the analysis to voxels within the CST.

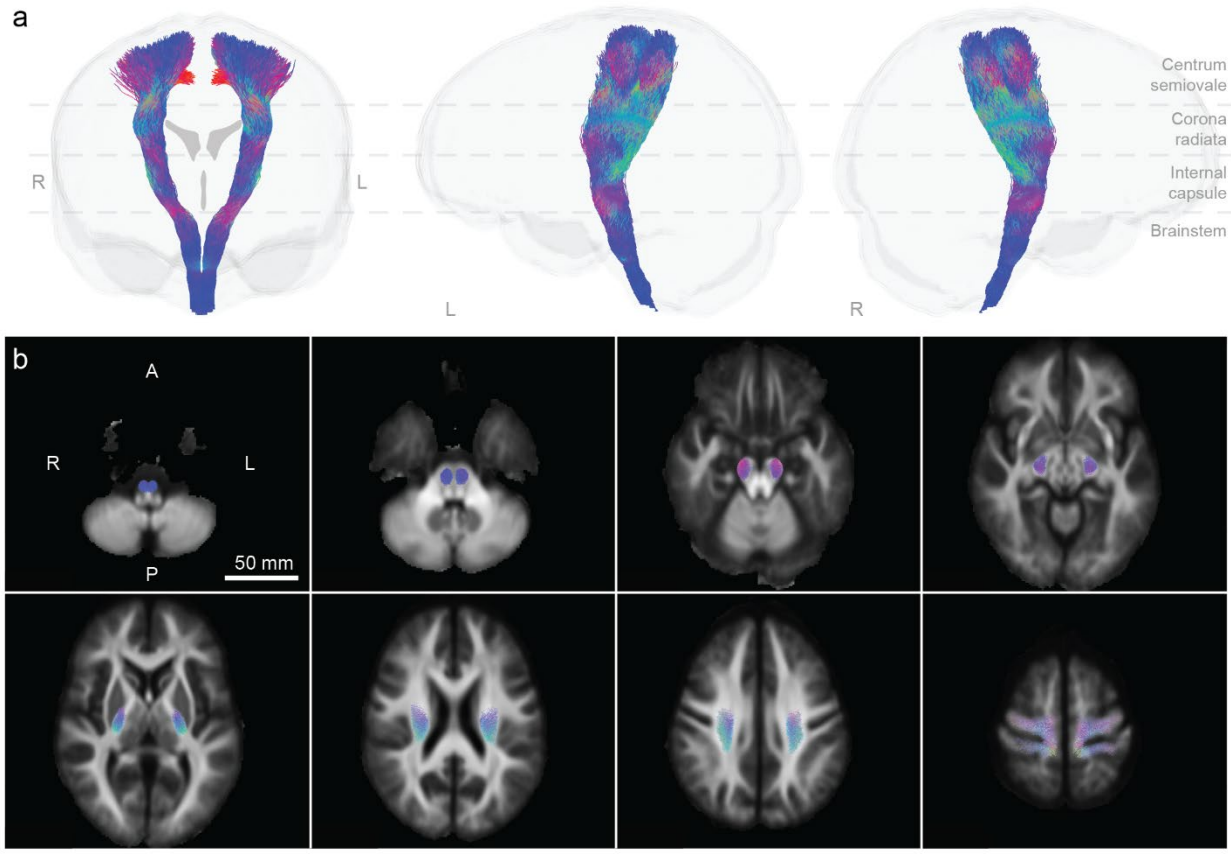

Figure 4.2. Corticospinal Tract Streamlines. a) Volume rendering of bilateral CST streamlines viewed from anterior, left, and right perspectives. Streamlines are color-coded by orientation: red = medial-lateral, blue = superior-inferior, and green = anterior-posterior. b) CST streamlines

overlaid on axial slices of the template brain. Slices progress from inferior to superior, starting in the medulla (top left) and ascending from the brainstem to the cerebrum, ending with streamlines in the precentral and postcentral gyri (bottom right).

Brain Volumetrics

The recon-all pipeline from FreeSurfer (version 7.4.0, Fischl (2012)[76], http://surfer.nmr.mgh.harvard.edu/fswiki) was run using each participant's high-resolution T1-weighted anatomical image to obtain estimated total intracranial volume (eTIV).[77] eTIV was included as a nuisance variable in statistical analyses to control for individual differences in head size. A study-specific T1-weighted anatomical template was created using the same participants selected for the study-specific FOD template, employing non-rigid registration.[56] This T1 template was also processed with the recon-all pipeline to define study-specific cortical regions of interest, specifically the bilateral precentral and postcentral gyri.

Lesion Segmentation

WM lesions were segmented using the deep learning–enhanced version of the Lesion Segmentation Toolbox.[78] Both T1-weighted and T2-FLAIR images were provided as inputs for automated lesion detection. Total lesion volume (mL) and lesion volume within the CST mask (mL) were calculated for each participant to quantify the overall lesion burden and tract-specific involvement. A lesion probability map for the participants with MS in this study is presented in Figure C1 (Appendix C).

Statistical Analysis

Group Comparisons

All statistical analyses were conducted using R Statistical Software (v4.4.2; R Core Team, Vienna, Austria, 2024). The normality of participant characteristics, brain volume, dynamic balance, and neurophysiological variables was assessed using the Shapiro-Wilk test and quantile-

quantile plots, while Levene's test was used to evaluate the equality of variances. Student's t-tests were used for group comparisons when assumptions of normality and equal variance were met. If the assumptions of normality or equal variance were violated, Mann-Whitney U tests or Welch's t-tests were used, respectively. Group differences in sex distribution were assessed using a chi-squared test. A general linear model was used to compare MEP onset latency between groups while controlling for participant height.

Statistical Analysis of Tensor-Derived Metrics

Voxel-wise group comparisons of DTI and DKI metrics were conducted using threshold-free cluster enhancement.[79] Covariates included age, sex, and eTIV, given the influence of head size on tensor measures.[80] All analyses were corrected for multiple comparisons using FWE, with significance defined as $pFWE < 0.05$. For visualization, voxel-wise significance values were mapped onto the corresponding streamlines that traversed them, and streamlines were color-coded to reflect significance.

Statistical Analysis of Fixel-Based Metrics

Group differences in FDC, FD, and LogFC within the CST were assessed using threshold-free connectivity-based fixel enhancement, a statistical framework designed for FBA.[31] A general linear model was used to estimate group effects, with age and sex included as covariates for all metrics. Additionally, for FDC and LogFC analyses, the logarithm of eTIV was also included to account for differences in head size, which can influence macrostructural measures.[81] All comparisons were corrected for multiple comparisons using familywise error correction (FWE), with significant fixels defined as those with a corrected *p-value* less than 0.05 ($pFWE < 0.05$).

Post-hoc Group Comparisons

To quantitatively summarize group differences and illustrate within-group variability, mean values for each diffusion metric were extracted from fixels or voxels that showed significant group differences ($pFWE < 0.05$) for each specific metric. For example, mean FD values were calculated exclusively from fixels where FD was significantly different between groups. Bonferroni correction was applied to control for multiple comparisons across metrics with alpha equal to 0.05.

Post-hoc Correlation Analyses in Participants with MS

To explore the associations between diffusion metrics and functional outcomes in people with MS, correlation analyses were performed using mean diffusion metric values extracted from fixels or voxels that demonstrated significant group differences ($pFWE < 0.05$).[82] These average values were then correlated with clinical impairment measures, miniBEST total score and EDSS, and neurophysiologic outcomes, MEP onset latency and MEP Area. False Discovery Rate (FDR) correction was applied to control for multiple comparisons, and significance was defined as $pFDR < 0.05$. Correlation strengths were interpreted using the following scale: very weak ($rho = 0.00 – 0.19$), weak ($rho = 0.20 – 0.39$), moderate ($rho = 0.40 – 0.59$), strong ($rho = 0.60 – 0.79$), and very strong ($rho = 0.80 – 1.00$).[83]

For completeness, additional correlation analyses are provided in the supplementary materials. Associations between diffusion metrics and CST lesion volume in participants with MS are reported in Table C1 (Appendix C). Associations between TMS outcome measures and clinical impairment measures in participants with MS are reported in Table C2 (Appendix C). Associations between diffusion metrics averaged across the whole CST and outcome measures in participants with MS are reported in Table C3 (Appendix C).

Results

Participant Characteristics, Brain Volumetrics, Clinical Disability, and Neurophysiological Comparison

Table 4.2 summarizes participant characteristics, brain volumetrics, clinical impairment scores, and neurophysiologic outcome measures. There were no significant differences between participants with MS and NT controls for age, sex, height, weight, or body mass index. MS participants did not have significant differences in eTIV compared to NT controls. Segmentation of lesions in MS participants revealed an average total lesion burden of 7.39 ± 9.3 mL, with segmented lesions overlapping an average of 1.53 ± 2.24% of the CST, corresponding to 0.50 ± 0.74 mL.

In terms of clinical disability, MS participants presented with mild to moderate disability, with self-reported EDSS scores ranging from 0 to 4 and a median score of 3.5. Additionally, participants with MS produced significantly lower scores on the miniBEST total score ($p < 0.001$), reactive postural control subscore ($p < 0.001$), and dynamic gait subscore ($p < 0.001$) compared to NT participants (Table 4.2).

For neurophysiologic measures, RMT was comparable between MS participants and controls ($p = 0.226$). In contrast, the MEP area was significantly reduced in individuals with MS compared to NT controls ($p = 0.012$). The groups had no significant differences in MEP onset latency (Table 4.2). However, a significant group effect was observed when MEP onset latency was examined while controlling for participant height using a linear model ($t(46) = 2.34$, $p = 0.024$).

Table 4.2. Participant Characteristics, Brain Volumetrics, Clinical Disability, and Neurophysiologic Measures. Data in each subsection are presented as mean and standard deviation † or median and interquartile range‡. Statistical comparisons were performed using independent t-tests[a], χ^2 tests[b], Mann–Whitney U tests[c], or Welch's t-tests[d]. **Bolded** values indicate statistical significance ($p < 0.05$).

Abbreviations: SD – Standard Deviation; IQR – Interquartile Range; BMI – Body Mass Index; eTIV – Estimated Total Intracranial Volume; CST – Corticospinal Tract; EDSS – Expanded Disability Status Scale; FSS – Functional System Score; APC – Anticipatory Postural Adjustments; RPC – Reactive Postural Control; SO – Sensory Orientation; DG – Dynamic Gait; TMS – Transcranial Magnetic Stimulation; MEP – Motor Evoked Potential; %MSO – Percent Maximal Stimulation Output.

	Multiple Sclerosis		Neurotypical		
Variable (unit)	*Mean/Median*	*SD/IQR*	*Mean/Median*	*SD/IQR*	*p-value*
Characteristics†					
n	25	-	24	-	-
Age (years)	48.30	12.18	47.07	15.65	0.758 [a]
Sex (female/male)	18/7	-	16/8	-	0.924 [b]
Height (cm)	165.76	7.47	169.76	7.44	0.067 [a]
Weight (kg)	70.31	13.61	68.72	21.66	0.653 [c]
BMI (kg/m^2)	25.31	3.57	24.80	3.28	0.620 [a]
Disease Duration (years)	12.24	10.69	-	-	-
Brain Volume†					
eTIV (mL)	1534.67	162.43	1476.72	225.58	0.306 [a]
Total Lesion Volume (mL)	7.39	9.23	-	-	-
CST Lesion Volume (mL)	0.50	0.73	-	-	-
Disability Scores‡					
EDSS	3.5	1	-	-	-
Pyramidal FSS	3	3	-	-	-
Cerebellar FSS	2	2	-	-	-
Sensation FSS	3	3	-	-	-
Bladder FSS	1	2	-	-	-

Vision FSS	2	2	-	-	-
Brainstem FSS	0	2	-	-	-
Cerebral FSS	2	3	-	-	-
Mini-Balance Evaluation Systems Test†					
Total Score	25.32	4.51	29.46	2.21	**<0.001** [c]
APA	6.28	1.81	7.29	1.00	0.065 [c]
RPC	5.92	1.50	7.46	0.78	**<0.001** [c]
SO	5.60	0.71	5.92	0.28	0.068 [c]
DG	7.52	1.26	8.79	0.98	**<0.001** [c]
TMS Measures†					
MEP Area (mV x ms)	0.78	0.37	1.12	0.50	**0.012** [a]
MEP Onset Latency (ms)	32.84	4.85	31.31	2.56	0.174 [d]
RMT (% MSO)	67.26	6.95	69.21	7.73	0.226 [c]

DTI Group Comparison

DTI revealed significant increases in MD, AD, and RD, and a significant decrease in FA in participants with MS compared to NT controls in dispersed voxel clusters throughout the CST. Streamline segments corresponding to significant voxels ($pFWE < 0.05$) are shown in Figure 4.3, where orange indicates the locations of significant differences.

MD displayed the greatest extent of group differences among the DTI metrics, with 10.37% of CST voxels identified as significantly increased in participants with MS compared to NT controls. Significant voxel clusters were located in the periventricular and corona radiata regions of both hemispheres, with more extensive differences observed in the left CST, extending superiorly into the centrum semiovale and inferiorly to the posterior limb of the internal capsule (PLIC) and the superior portions of the midbrain. The right CST largely had consolidated

differences around the periventricular space and corona radiata, in addition to a small cluster of significant voxels in the right PLIC (Figure 4.3a).

AD displayed the least extensive group differences among the DTI metrics, with significant increases in participants with MS compared to NT controls observed in only 0.12% of CST voxels. AD differences were mostly limited to a small cluster of voxels in the left corona radiata region. (Figure 4.3b).

RD was significantly increased in participants with MS compared to NT controls in 5.64% of CST voxels, with clusters primarily located in the periventricular and corona radiata regions of both hemispheres, and with more extensive differences in the left CST extending superior to the centrum semiovale. A cluster of significant RD voxels was also observed within the PLIC in the left CST (Figure 4.3c).

FA was significantly reduced in participants with MS compared to NT controls in 1.58% of CST voxels, with clusters located in the periventricular region of both hemispheres. The left CST also showed a cluster of significant FA reductions within the PLIC (Figure 4.3d).

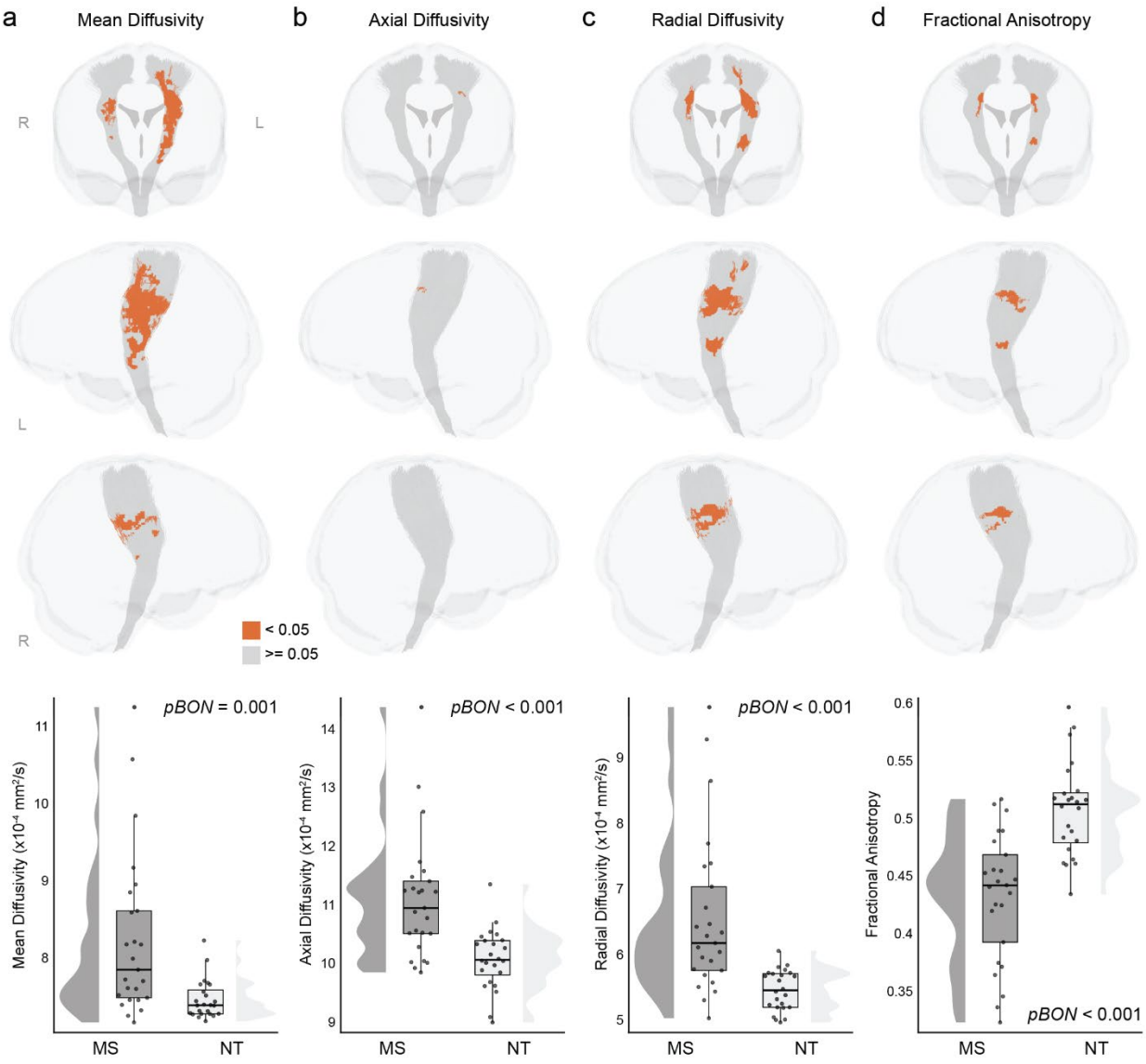

Figure 4.3. Diffusion Tensor Imaging Group Comparison. Regions within the CST showing significant differences in DTI metrics between participants with MS and NT controls. Streamline segments corresponding to significant voxels (*pFWE* < 0.05) *are shown in orange*. Boxplots display within-group variability across the significant voxels for each metric. Comparisons are Bonferroni corrected (*pBON*). a) Increased mean diffusivity in MS compared to NT controls. b) Increased axial diffusivity in MS compared to NT controls. c) Increased radial diffusivity in MS compared to NT controls. d) Decreased fractional anisotropy in MS compared to NT controls**.**

DKI Group Comparison

DKI revealed significant decreases in MK, AK, and RK in participants with MS compared to NT controls in voxel clusters throughout the CST. Streamline segments corresponding to significant voxels ($pFWE < 0.05$) are shown in Figure 4.4, where green indicates the locations of significant differences.

MK showed the most widespread significant group differences among the DKI metrics, with 20.71% of CST voxels identified as significantly reduced in participants with MS compared to NT controls. Significant voxel clusters were primarily located in the periventricular and corona radiata regions and extended inferiorly through the PLIC and midbrain in both hemispheres, with additional significant voxels scattered throughout the brainstem (Figure 4.4a).

AK exhibited the least coverage of group differences among the DKI metrics, with significant decreases in participants with MS compared to NT controls observed in only 0.29% of CST voxels. AK differences were localized primarily to a small cluster in the periventricular region of the right CST. (Figure 4.4b).

RK was significantly reduced in participants with MS compared to NT controls in 12.19% of CST voxels, with clusters primarily located around the periventricular regions and the corona radiata of both hemispheres. Additionally, both CSTs showed RK differences in the PLIC, although differences were more extensive in the left CST (Figure 4.4c).

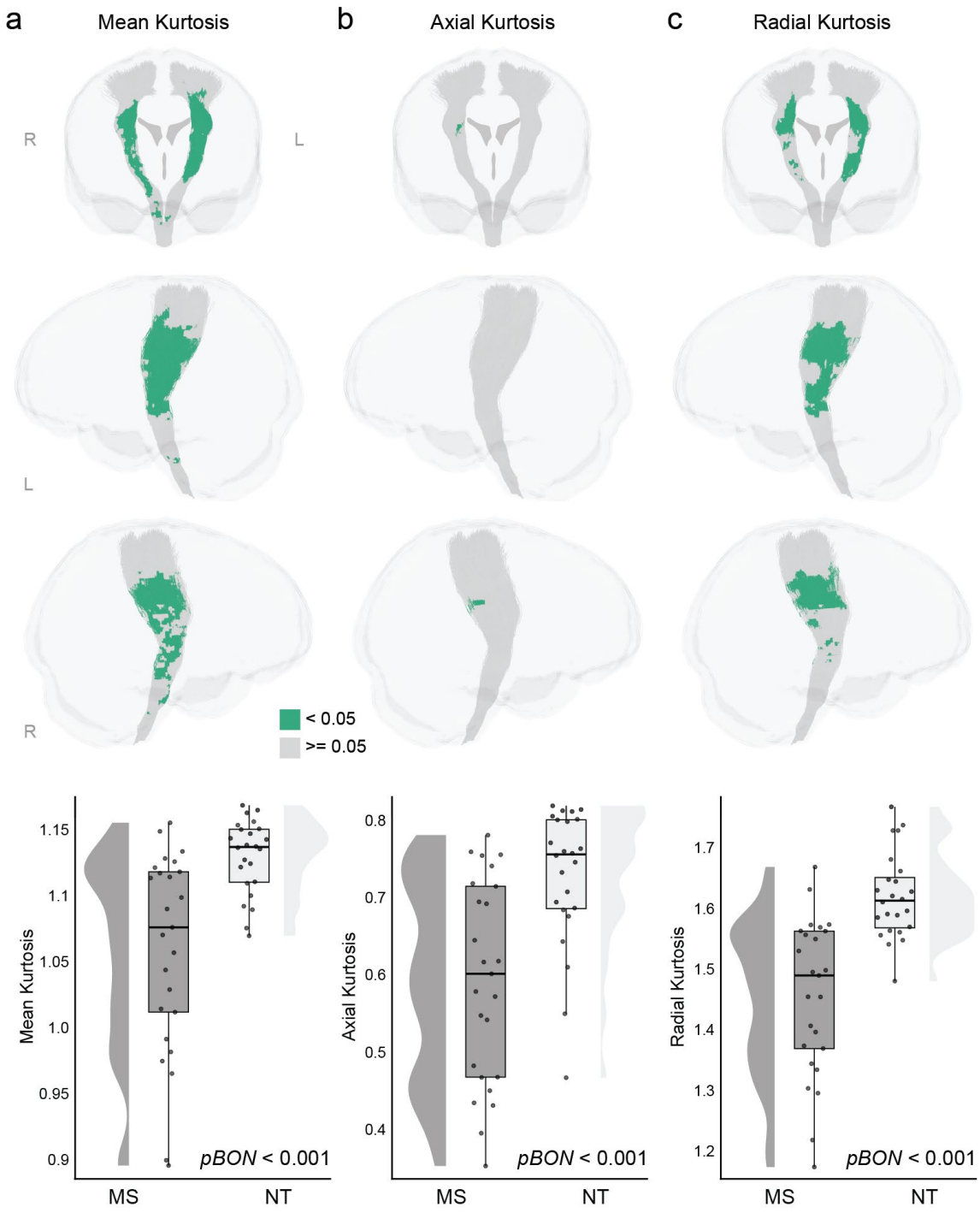

Figure 4.4. Diffusion Kurtosis Imaging Group Comparison. Regions within the CST showing significant differences in DKI metrics between participants with MS and NT controls. Streamline segments corresponding to significant voxels (*pFWE* < 0.05) *are shown in green*. Boxplots display within-group variability across the significant voxels for each metric. Comparisons are Bonferroni corrected (*pBON*). a) Decreased mean kurtosis in MS compared to NT controls. b) Decreased axial kurtosis in MS compared to NT controls. c) Decreased radial kurtosis in MS compared to NT controls.

FBA Group Comparison

FBA revealed significant decreases in FDC, FD, and LogFC throughout the CST in participants with MS compared to NT controls. Streamline segments corresponding to significant fixels ($pFWE < 0.05$) are shown in Figure 4.5, where blue indicates the locations of significant differences.

FDC demonstrated widespread differences, with 51.53% of fixels within the CST showing significant group effects. In participants with MS, significant FDC reductions extended from the centrum semiovale through the corona radiata and the PLIC and tapered off in the pons and medulla in both hemispheres (Figure 4.5a).

FD exhibited less extensive differences compared to FDC. Significantly reduced FD fixels in participants with MS compared to NT controls were observed in 7.27% of CST fixels. FD differences in the left CST are primarily located in the middle of the CST, spanning from the centrum semiovale to the brainstem. FD differences in the right CST are similarly located in the middle of the tract around the centrum semiovale and corona radiata but shift more posteriorly around the PLIC, extending to the brainstem (Figure 4.5b).

LogFC showed the greatest extent of group differences among all diffusion-derived metrics. Significant reductions in LogFC in participants with MS compared to NT controls were observed in 64.88% of CST fixels. Significant LogFC fixels were distributed extensively, spanning from parts of superior centrum semiovale regions through the entirety of the brainstem in both hemispheres (Figure 4.5c).

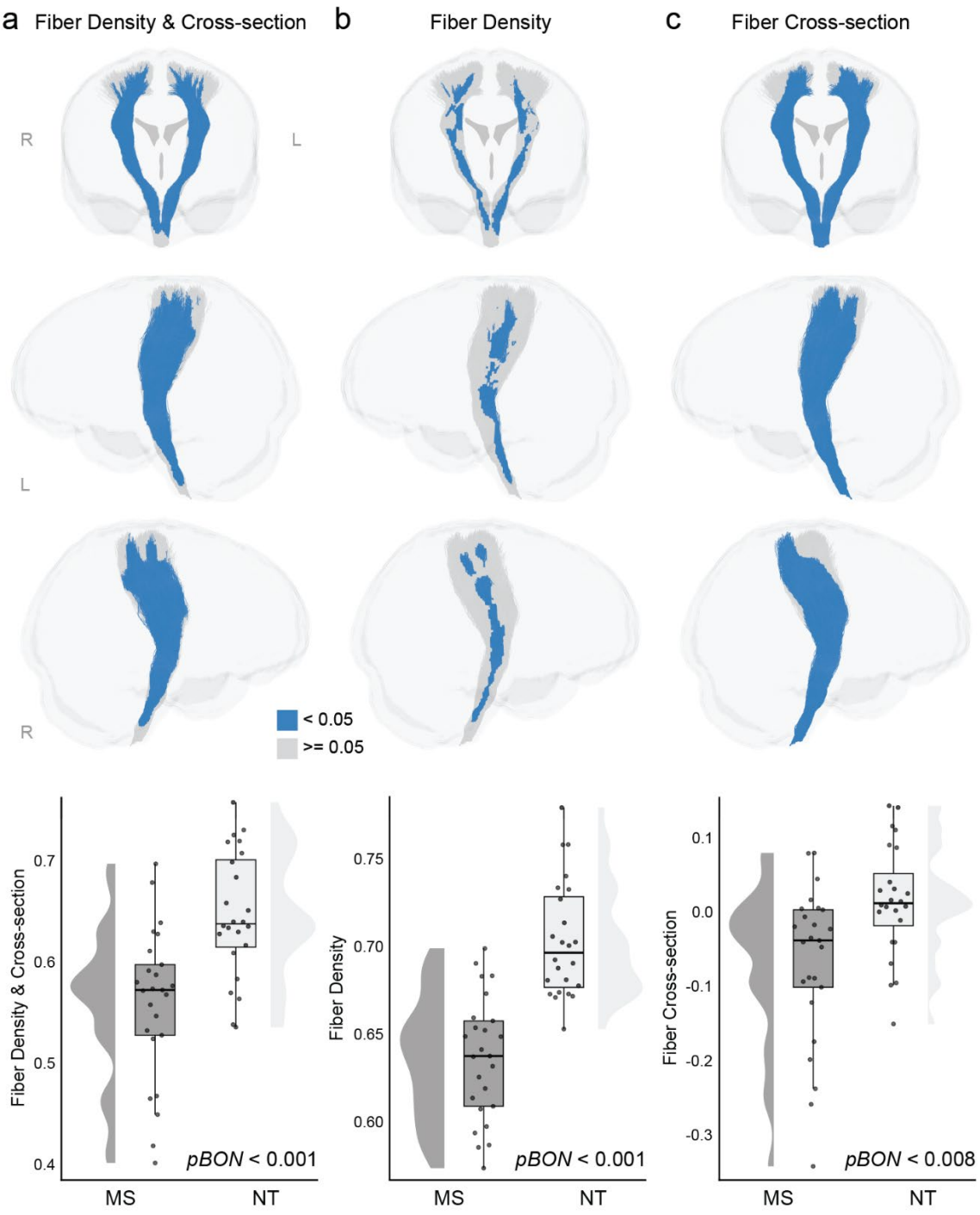

Figure 4.5. Fixel-Based Analysis Group Comparison. Regions within the CST showing significant differences in FBA metrics between participants with MS and NT controls. Streamline segments corresponding to significant fixels (*pFWE* < 0.05) *are shown in blue*. Boxplots display within-group variability across the significant fixels for each metric. Comparisons are Bonferroni corrected (*pBON*). a) Decreased fiber density and cross-section in MS compared to NT controls. b) Decreased fiber density in MS compared to NT controls. c) Decreased fiber cross-section in MS compared to NT controls. Fiber cross-section is displayed on a logarithmic scale.

Associations Between Diffusion Metrics and Clinical Impairment Scores in MS

Associations between diffusion metrics and clinical impairment scores in participants with MS are summarized in Table 4.3. Significant associations were observed between miniBEST total score and FA (*rho* = 0.52, *pFDR* = 0.031), RD (*rho* = -0.49, *pFDR* = 0.041), RK (*rho* = 0.56, *pFDR* = 0.014), FDC (*rho* = 0.52, *pFDR* = 0.014), and FD (*rho* = 0.53, *pFDR* = 0.014), all demonstrating a moderate correlation. MD (*rho* = -0.41, *pFDR* = 0.080), MK (*rho* = 0.43, *pFDR* = 0.075), and CST lesion volume (*rho* = -0.44, *pFDR* = 0.065) also exhibited moderate correlations with miniBEST total score, however, these associations did not survive correction for multiple comparisons. Significant associations were observed between EDSS and only FDC (*rho* = -0.65, *pFDR* = 0.002) and LogFC (*rho* = -0.65, *pFDR* = 0.002), with strong negative correlation coefficients.

Associations Between Diffusion Metrics and Neurophysiological Measures in MS

Associations between diffusion metrics and neurophysiological outcomes are also presented in Table 4.3. MEP onset latency showed significant correlations with nearly all diffusion metrics and lesion metrics, with the strongest correlation coefficients observed for FD (*rho* = -0.75, *pFDR* < 0.001), FA (*rho* = -0.75, *pFDR* < 0.001), and RK (*rho* = -0.71, *pFDR* = 0.001). Significant associations were observed between MEP area and only FBA metrics, FDC (*rho* = 0.52, *pFDR* = 0.014), FD (*rho* = 0.49, *pFDR* = 0.021), and LogFC (*rho* = 0.46, *pFDR* = 0.031), with moderate positive correlations. FA (*rho* = 0.44, *pFDR* = 0.064), RK (*rho* = 0.40, *pFDR* = 0.096), and CST lesion volume (*rho* = -0.40, *pFDR* = 0.065) also demonstrated moderate correlations with MEP area. However, these associations did not survive correction for multiple comparisons.

Table 4.3. Associations Between Diffusion Metrics and Clinical and Neurophysiologic Measures in Participants with Multiple Sclerosis. Spearman's rank correlation coefficients (*rho*) are presented for associations between CST dMRI metrics and clinical and neurophysiological measures in participants with MS. Both uncorrected *p-values* and false discovery rate-corrected values are shown (*pFDR*). Statistically significant associations after FDR correction (*pFDR* < 0.05) are indicated in **bold**.

Abbreviations:
DTI – Diffusion Tensor Imaging; MD – Mean Diffusivity; AD – Axial Diffusivity; RD – Radial Diffusivity; FA – Fractional Anisotropy; DKI – Diffusion Kurtosis Imaging; MK – Mean Kurtosis; AK – Axial Kurtosis; RK – Radial Kurtosis; FBA – Fixel-Based Analysis; FDC – Fiber Density and Cross-section; FD – Fiber Density; LFC – Log of Fiber Cross-section; CST – Corticospinal Tract; miniBEST – Mini-Balance Evaluation Systems Test; EDSS – Expanded Disability Status Scale; MEP – Motor Evoked Potential.

	DTI				DKI			FBA			*CST Lesion*
Variable	*MD*	*AD*	*RD*	*FA*	*MK*	*AK*	*RK*	*FDC*	*FD*	*LFC*	*Volume*
miniBEST Total Score											
rho	-0.41	-0.10	-0.49	0.52	0.43	0.31	0.56	0.52	0.53	0.37	-0.44
p-value	0.040	0.647	0.013	0.008	0.031	0.132	0.003	0.007	0.006	0.066	0.028
pFDR-value	0.080	0.690	**0.041**	**0.031**	0.075	0.176	**0.014**	**0.014**	**0.014**	0.079	0.065
EDSS											
rho	0.33	0.01	0.35	-0.24	-0.32	-0.26	-0.36	-0.65	-0.34	-0.65	0.37
p-value	0.110	0.981	0.086	0.240	0.121	0.208	0.074	<0.001	0.093	<0.001	0.065
pFDR-value	0.165	0.981	0.154	0.320	0.176	0.227	0.128	**0.002**	0.101	**0.002**	0.075
MEP Onset Latency											
rho	0.59	0.47	0.68	-0.75	-0.60	-0.45	-0.71	-0.57	-0.75	-0.33	0.54
p-value	0.002	0.019	<0.001	<0.001	0.001	0.023	<0.001	0.003	<0.001	0.106	0.006
pFDR-value	**0.009**	0.050	**0.002**	**<0.001**	**0.009**	0.068	**0.001**	**0.009**	**<0.001**	0.106	**0.027**
MEP Area											
rho	-0.22	0.12	-0.33	0.44	0.29	0.19	0.40	0.52	0.49	0.46	-0.40
p-value	0.282	0.569	0.114	0.028	0.165	0.355	0.048	0.008	0.014	0.023	0.049
pFDR-value	0.348	0.650	0.165	0.064	0.198	0.355	0.096	**0.014**	**0.021**	**0.031**	0.065

Discussion

In this cross-sectional study, the structural integrity of the CST was examined in individuals with MS compared to age- and sex-matched NT controls using three diffusion imaging

frameworks, DTI, DKI, and FBA. The study findings demonstrate that diffusion-derived metrics from each framework identified clusters of significant structural differences within the CST between participants with MS and NT controls. Among the three approaches, FBA revealed the most extensive WM alterations, identifying a greater proportion of the CST with significant group differences compared to DTI and DKI. Additionally, FBA metrics consistently showed moderate to strong correlations with measures of clinical impairment and neurophysiological function, suggesting that FBA may be particularly useful for detecting disease-related damage relevant to mobility and neural function in individuals with MS with mild to moderate disability. Together, these findings link WM micro- and macrostructure to functional outcomes, providing insights into how structural damage translates to motor dysfunction in MS and highlighting the utility of advanced diffusion imaging methods in detecting subtle WM alterations not captured by conventional measures.

Clinical and Neurophysiological Impairments in MS Participants

Group comparisons of age, sex, and physical characteristics revealed no significant differences between participants with MS and NT participants, although height approached significance (Table 4.2). As expected based on inclusion criteria, MS participants presented with mild to moderate disability, reflected by EDSS scores ranging from 0 to 4. An EDSS score above 4 typically marks the onset of gait impairments requiring a walking aid past distances of 500 meters,[42] indicating that participants in this study largely retained functional ambulatory ability. Concurrently, pyramidal and sensory FSS were the highest among functional domains, suggesting motor and sensory dysfunction within the cohort (Table 4.2).

Assessment of balance using the miniBEST revealed significantly poorer performance in MS participants compared to NT controls, with significant group differences observed for total

score, reactive postural control, and dynamic gait. In contrast, anticipatory postural control and sensory orientation were not significant (Table 4.2). Together, these findings indicate that individuals with MS with mild to moderate disability exhibit impairments in balance, particularly in reactive postural responses and functional mobility. This aligns with previous literature showing that balance impairments can emerge in MS patients with low disability and may even precede formal MS diagnosis.[84–86] These observed balance deficits likely stem from WM damage, Which disrupts the sensory feedback and motor output required for maintaining posture and responding to perturbations.[87,88]

Comparison of neurophysiological measures showed that RMT was comparable between groups (Table 4.2), suggesting that CST excitability or the threshold required to elicit a motor response was preserved among these participants with MS.[89] This finding contributes to a mixed body of literature, with some studies reporting no differences in RMT between individuals with MS and NT controls, while others have found a significant increase in people with MS.[36] In contrast, MEP area was significantly reduced in MS participants, reflecting diminished CST excitability.[89] These results are consistent with previous findings, which show that the MEP area or amplitude is reduced in people with MS.[90–92] In an initial comparison, MEP onset latency did not differ significantly between groups (Table 4.2). However, on average, participants in the NT group were taller, and greater height is known to influence MEP latency times by increasing the distance neural signals must travel, particularly for lower-extremity TMS protocols.[89,93,94] A significant group difference in onset latency was identified when height was included as a covariate in a linear model, indicating delayed CST conduction in the MS group after adjusting for body size. Delayed MEP latency is consistent with prior studies, which have shown that MEP latency is increased even in minimally disabled MS cohorts.[90,92]

These findings indicate that despite similar demographic profiles, individuals with MS demonstrate clear clinical and neurophysiological impairments characterized by poorer mobility function, diminished CST excitability, and delayed neural conduction.

Structural Differences in the CST Identified by DTI, DKI, and FBA

dMRI analysis is continually evolving, with increasingly sophisticated models enhancing the ability to characterize WM structural integrity more thoroughly. However, determining the clinical utility of these models and understanding when the adoption of advanced approaches is warranted remains an important topic of investigation. Only one other study has evaluated DTI, DKI, and FBA within a single MS study.[95] Examining all three methods within the same investigation provides an opportunity to assess whether the models yield complementary findings and gauge the relative effectiveness of advanced diffusion approaches in detecting MS-related structural abnormalities, thereby informing both clinical research applications and future methodological choices.

DTI

Among the DTI measures, MD exhibited the most widespread group differences and was elevated relative to matched controls, consistent with previous findings.[13] MD reflects the average diffusivity within a voxel and is sensitive to increases in extracellular water content, often associated with pathophysiological processes such as edema or inflammation.[96,97] In line with this, a large number of significant MD voxel differences were located in and around periventricular regions (Figure 4.3a), corresponding to areas of highest lesion burden in this study cohort (Figure C1, Appendix C), and consistent with common lesion locations in MS.[98] However, significantly increased MD voxel clusters were also located in the bilateral PLIC and right centrum semiovale despite a relatively low frequency of lesions in these areas among MS participants. This finding

suggests that MD may also capture more subtle inflammation or microedema that are not directly attributable to visible lesion presence.

AD, commonly regarded as a marker of axonal integrity,[99] showed limited group differences. While reductions in AD are often associated with axonal loss, AD values within lesions are elevated relative to normal-appearing WM, and lesion pathology may artificially displace the principal diffusion axis from biologically meaningful directions.[100–102] Many DTI studies in MS omit AD values, likely due to these interpretational challenges and the observation that MD, RD, and FA may better capture WM structural changes relevant to MS pathology.[103] Given that AD is most reliable in lesion-free, tightly packed, coherently oriented fibers,[104] and most group differences in the present study occurred in regions of high fiber dispersion (Figure 4.3b), AD may have limited ability for detecting early structural damage in mild to moderate MS.

Patterns for RD and FA largely mirrored those observed for MD, with clusters of significant voxels in the periventricular regions, corona radiata, and left PLIC. However, these were less extensive than MD for both metrics (Figures 4.3c and 4.3d). RD increases are commonly associated with demyelination.[105,106] At the same time, FA reductions are interpreted as a loss of overall axonal integrity and can be attributed to various pathophysiologic processes, such as demyelination, inflammation, gliosis, or axonal loss.[107] These DTI findings suggest that CST structural abnormalities in MS are characterized by increased MD and RD, coupled with reductions in FA. These differences were particularly pronounced in regions with high lesion burden, likely reflecting the combined effects of demyelination, axonal loss, inflammation, and increased extracellular water content within and surrounding lesions. Differences detected in the PLIC may indicate more subtle pathological changes.

While DTI metrics are sensitive to structural alterations, caution is warranted when interpreting these findings. In regions such as the corona radiata, where crossing and dispersing fibers are common, DTI is unable to resolve complex fiber architecture.[11] Thus, detected group differences may reflect a combination of actual pathological changes and confounding effects of fiber geometry. Additionally, although specific metrics such as RD are frequently interpreted as a proxy for myelination and have been associated with myelin content, it is essential to recognize that all DTI metrics are influenced by various pathological processes.[107] For instance, increases in RD may reflect demyelination, but could also reflect other processes, such as axonal loss or gliosis.[108] Consequently, while DTI provides insights into WM integrity, its metrics are inherently nonspecific and should be interpreted cautiously in isolation.

DKI

Consistent with previous literature, MK, AK, and RK values were lower in MS participants compared to NT participants, indicating decreased heterogeneity in WM tissue.[29,109] Compared to DTI metrics, DKI metrics revealed a greater number of significant voxels in the CST in group comparisons. Among the DKI measures, MK exhibited the greatest number of significant voxel differences, spanning from periventricular and corona radiata regions through the PLIC and midbrain, with additional scattered clusters in the pons and medulla (Figure 4.4a). These reductions suggest that MK can identify WM alterations in regions of high and low lesion burden.

In contrast, AK showed limited group differences, with significant voxels confined to a small cluster in the right periventricular region (Figure 4.4b). Although reduced AK can indicate decreased intracellular diffusion complexity and is associated with axonal loss,[26] its restriction to only a small significant cluster, despite occurring in a region of high lesion burden, suggests that AK may have a limited ability to detect pathological changes in people with MS with mild to

moderately disability. Other studies using DKI have also found that AK reveals fewer group differences compared to MK and RK in people with MS compared to controls. However, those findings involved whole-brain analyses and reported a much larger percentage of significant voxels relative to the present study.[29]

RK, which has been associated with myelin integrity,[110] showed significant reductions in the periventricular and corona radiata regions and within the PLIC, suggesting decreased myelin content in both lesion sites and normal-appearing WM (Figure 4.4c). Notably, MK and RK revealed bilateral abnormalities in the PLIC, whereas DTI metrics primarily detected differences in the left CST. These findings suggest that DKI metrics, particularly MK and RK, may detect additional microstructural abnormalities in MS that are not captured by DTI measures.

Overall, DKI and DTI showed overlapping group differences in the periventricular and corona radiata regions, with DKI detecting more extensive abnormalities than DTI. Prior studies suggest that DKI may perform better in regions with complex fiber geometry,[29] so the convergence of findings in these areas further corroborates the DTI results. In contrast, DKI identified fewer significant voxels in the centrum semiovale, a region of higher fiber dispersion, where MD and RD detected differences, highlighting a discrepancy in an area where DKI is expected to be more accurate. Altogether, DKI revealed a broader extent of group differences than its DTI metric counterparts, suggesting that non-Gaussian diffusion modeling may provide complementary insights into microstructural assessments of WM in MS.

FBA

Consistent with previous literature, all FBA metrics were reduced in MS participants compared to NT controls,[34,111,112] although some studies in low-disability MS populations report limited or no FD differences.[113] Compared to DTI and DKI, FBA revealed the most extensive

group differences. LogFC showed the largest number of reductions in participants with MS compared to NT participants, identifying significant fixels in nearly two-thirds of the CST (Figure 4.5c). As a measure of fiber cross-sectional area, LogFC reflects macrostructural WM differences,[30,32] and its widespread reduction suggests substantial CST atrophy in MS, likely resulting from cumulative damage over time,[32] even in individuals with mild to moderate disability. LogFC differences were observed in regions with high, low, and no visible lesion burden, indicating that tract atrophy is not limited to areas of overt lesion damage.

FD, quantifying intra-axonal volume,[33] also showed significant reductions in MS participants relative to NT controls, though more spatially contained, spanning from the centrum semiovale through the brainstem bilaterally (Figure 4.5b). Significant FD reductions overlapped with higher lesion probability regions in the periventricular space, possibly reflecting axonal loss from lesion-related damage. Additional reductions superior and inferior to these areas suggest FD may capture axonal loss stemming from lesion site damage and diffuse microstructural differences within normal-appearing white matter.

FDC, a composite metric that combines FD and FC,[30,32] was also reduced in MS participants compared to NT participants and identified numerous significant fixels throughout the CST (Figure 4.5a). As it incorporates both microstructural and macrostructural information, reduced FDC suggests that CST differences reflect both axonal degeneration and tract atrophy, consistent with post-mortem studies reporting reduced tract area and axonal density in the CST of people with MS compared to controls.[87]

Compared to DTI and DKI, FBA identified more spatially extensive structural differences in the CST, including regions within the brainstem and substantial portions of the centrum semiovale that were not highlighted by the other methods. While differences in the spatial extent

of abnormalities were observed across methods, it is important to recognize that each approach models diffusion using distinct frameworks and quantifies microstructure with different metrics. Without a definitive ground truth, direct comparisons of sensitivity or specificity remain speculative. For example, LogFC, the FBA metric associated with the largest number of significant fixels, indexes macroscopic changes in fiber bundle cross-sectional area, a property not directly captured by DTI or DKI.

While the presence of different metrics makes direct comparison across methods challenging, it also offers the opportunity to capture distinct and complementary aspects of white matter structure. Because FBA provides both microstructural and macrostructural information, it supports more nuanced interpretations of underlying pathology. For instance, prior work has associated specific fixel patterns, such as concurrent reductions in FDC and LogFC without changes in FD, with Wallerian degeneration,[95] a process involving secondary axonal degeneration distal to the site of injury.[114] A similar pattern was observed in this study, particularly in the corona radiata regions, potentially reflecting a pathological process that conventional diffusion models can detect but may not be able to fully characterize.

In this study, DTI and DKI metrics, except for AD, were strongly correlated with lesion volume and exhibited numerous significant voxels in areas of high lesion burden. In contrast, FBA metrics showed only moderate correlations with lesion volume, suggesting that FBA may capture additional aspects of WM integrity (Table C1, Appendix C).

Clinical and Neurophysiological Associations with DTI, DKI, and FBA Metrics

This study offers new evidence on how dMRI metrics relate to clinical impairment and neurophysiological function in individuals with MS. By examining these relationships cross-sectionally, this analysis aimed to characterize the WM structural alterations underlying functional

deficits. While DTI metrics have been linked to disability, mobility, and balance,[115–117] few studies have explored whether more advanced diffusion models, such as DKI and FBA, offer added value in identifying associations with functional outcomes.[113,118]

EDSS

Only FDC and LogFC showed significant associations with EDSS (Table 4.3). These findings suggest that atrophy of the corticospinal tract, likely resulting from long-term white matter damage, is associated with overall disability as measured by EDSS. This relationship is likely driven in part by the strong influence of mobility impairments on EDSS scoring. Alternatively, these findings may suggest that atrophy within the CST is consistent with more widespread white matter degeneration in individuals with MS, potentially contributing to disability across multiple functional domains. This interpretation is supported by prior whole-brain FBA studies, which have reported global reductions in LogFC in MS participants compared to controls, even in studies with a low EDSS median score.[34]

While the correlation coefficients reported here between DTI and DKI metrics and EDSS were not significant and slightly lower than those reported by Spampinato et al. (2017),[118] they were of comparable magnitude. The modest sample size and relatively low number of participants with EDSS scores of 1 or 2 may have limited this study's ability to detect additional significant associations. Moreover, EDSS scores in this study were obtained via a self-report instrument rather than direct clinician assessment, which, although validated,[43] may introduce some measurement variability compared to traditional EDSS administration.

miniBEST

Multiple dMRI metrics were significantly correlated with miniBEST scores, indicating that WM structural integrity of the CST is associated with mobility function in individuals with MS

(Table 4.3). The strongest relationships were observed for metrics linked to demyelination, increased RD and decreased RK, as well as axonal loss, reduced FA, FD, and FDC, suggesting that both pathological processes contribute to balance impairments. Axonal loss may disrupt descending motor commands, while demyelination slows conduction velocity, impairing timely motor responses to perturbations. This is further supported by strong correlations between miniBEST total scores and MEP onset latency and MEP area (Table C2, Appendix C), suggesting that delayed and diminished corticospinal excitability contributes to balance deficits.

An important consideration is that key neural circuits supporting postural control and balance are located within the cerebellum, brainstem, and spinal cord.[119] WM alterations in these regions were not assessed in the present study. However, evidence suggests that diminished proprioceptive input from muscle spindles may increase reliance on supraspinal CST input for maintaining balance in aging populations.[120] This supports assessing CST structural integrity superior to the brainstem and its relationship to balance deficits in MS.

The current study is among the first to demonstrate that DKI and FBA metrics relate to clinical balance and mobility scores. The present findings further expand upon those of Strik et al. (2021),[113] who showed that FDC reductions were associated with impaired walking and upper extremity force tracking in minimally disabled individuals with MS. The present results show that FDC and FD significantly correlate with balance performance, collectively indicating that CST structural alterations impact locomotion, arm function, and dynamic balance even at low disability levels in MS. These results highlight the potential of advanced diffusion models to detect subtle motor pathway abnormalities associated with balance and mobility.

Neurophysiology

This study provides the first comprehensive examination of the relationships between dMRI metrics and TMS-derived outcomes in the lower-extremities in MS, and is the first to incorporate FBA metrics. Neural conduction delays, as reflected by MEP onset latency, are a hallmark feature of MS pathology and are primarily attributed to demyelination.[121] Nearly every dMRI metric demonstrated a significant association with MEP onset latency, except for AD, AK, and LogFC (Table 4.3). Metrics associated with myelin integrity, such as RD and RK, axonal density, FD, and overall integrity, FA, were most strongly associated with MEP onset latency (Table 4.3). These observed relationships indicate that disrupted myelin sheaths and reduced axonal density, which often follow or co-occur with demyelination,[122] impair the speed and efficiency of neural conduction, leading to slower onset latencies.

It should be emphasized that none of these dMRI methods directly measure myelin content as myelin-associated water contributes very little to the dMRI signal; instead, they provide indirect markers of tissue properties influenced by myelin and axonal structure.[33,123] While CST lesion volume was also associated with delayed MEPs, diffusion metrics appear to correlate more strongly with MEP onset latency, suggesting that these measures capture additional WM damage in the CST that visible lesions alone do not account for. These findings emphasize that while CST lesion volume contributes to impaired neural conduction, relying solely on lesion quantification may underestimate the extent of diffuse microstructural damage, which dMRI can detect.

In this study, significant associations were observed between MEP area and FDC, FD, and LogFC (Table 4.3). Reductions in FD likely reflect loss of axonal content, which decreases the number of fibers available to contribute to excitatory output. Additionally, decreases in LogFC, which indicate tract atrophy, could further impair transmission efficiency by reducing the cross-

sectional area of the tract available for signal propagation. Although FA and RK showed moderate correlations with MEP area, these correlations did not survive correction for multiple comparisons, suggesting that larger sample sizes are necessary to explore these relationships further.

Another study linking excitatory TMS measures in MS patients has demonstrated that microstructural damage in the motor cortex grey matter, as measured by neurite orientation dispersion and density imaging, predicts higher TMS RMT thresholds.[40] Thus, although this study found no differences in RMT between MS and NT participants, it is critical to acknowledge that WM structural integrity differences alone do not fully explain TMS-derived neurophysiologic measures and neural function. The dMRI metrics examined here were restricted to the CST between the precentral and postcentral gyri and the brainstem and, therefore, they do not capture cortical pathology or spinal cord lesions, both of which are common in MS and likely influence MEP outcomes.[124–126] Future studies incorporating comprehensive brain and spinal cord imaging will be necessary to elucidate the complex contributors to neurophysiological dysfunction fully.

An important methodological consideration for these associations is that dMRI measures for each framework were derived from voxels or fixels that showed significant group differences between participants with MS and NT participants, connecting WM structural alterations with functional outcomes. When dMRI metrics were averaged across the entire CST, many associations, particularly for metrics like FA, where fewer than 2% of CST voxels are significant between groups, were obscured (Table C3, Appendix C). In contrast, FBA-derived measures, particularly FDC, largely retained significant associations even when assessed across the entire tract, likely due to the widespread differences detected by FBA.

Overall, while all dMRI frameworks yielded metrics associated with clinical outcomes, FBA-derived measures demonstrated the most consistent associations with both clinical

impairment scores and neurophysiological outcome measures in people with MS. This may be driven by FBA's ability to isolate only fiber orientations specific to the CST and separately quantify microstructural and macrostructural differences, providing a more comprehensive assessment of WM pathology.

Limitations

Several important methodological considerations must be acknowledged when interpreting these findings. First, it is critical to recognize that DTI and DKI metrics were calculated from all voxels containing at least one CST streamline. This means that even voxels with minimal fiber presence contributed to the voxel-wise diffusion measures. Tensor-based metrics represent an average of diffusion properties within a voxel, which may encompass multiple fiber populations or partial volume effects, in contrast to FBA metrics that isolate diffusion information specific to individual fiber orientations. Additionally, significance testing for DTI and DKI metrics was performed across the full CST without the use of techniques such as Tract-Based Spatial Statistics (TBSS), which restricts analysis to a skeletonized tract core and may reduce susceptibility to misalignment and peripheral voxel artifacts caused by registration.[127] As a result, tensor-based analyses may be more vulnerable to partial volume contamination, particularly at tract edges, potentially influencing the spatial distribution and extent of detected group differences.

Regarding FBA, it is important to note that the diffusion-weighted images were acquired at b-values lower than those typically recommended for optimal fixel-based modeling. Current guidelines suggest b-values around 3000 s/mm² to maximize sensitivity to intra-axonal water diffusion.[33,128] In contrast, the acquisition parameters in this study were more optimized for multi-shell DKI and DTI modeling.[129,130] Notably, previous studies have shown that methods employed in FBA outperform tensor-based models in characterizing white matter architecture, even when

using lower b-values.[131] While robust group differences were still detected, it is possible that higher b-value acquisitions would have further enhanced the specificity and sensitivity of the FBA measures. Additionally, while FBA identified more extensive group differences than DKI and DTI, and DKI more than DTI, it is important to note that, without post-mortem validation, these in vivo diffusion findings, though biologically plausible and consistent with expected patterns of CST pathology in MS, remain inferential rather than definitive.

Streamlines used for tractography were seeded from the precentral and postcentral gyri, as the primary motor cortex was the main target for TMS stimulations. However, the CST descends from multiple motor-related regions, including premotor and supplementary motor cortices.[132,133] Consequently, potential contributions from damage in these ancillary motor regions to clinical and neurophysiological impairments may have been underrepresented. Future studies incorporating a broader definition of the CST might capture additional lesion burden and microstructural abnormalities relevant to mobility, balance, and motor output.

This study utilized single-pulse MEP recordings without including TMS recruitment curves. Recruitment curves provide a richer characterization of CST excitability and output by examining the relationship between stimulus intensity and MEP amplitude.[89] Incorporating recruitment curves could have allowed for a more nuanced understanding of the integrity and responsiveness of the CST and may have strengthened associations with dMRI findings.

The study sample consisted of individuals with mild to moderate disability (EDSS ≤ 4) and relapsing-remitting MS, consistent with testing the lower bounds of dMRI metric sensitivity. However, this focus limits the generalizability of the findings to more severely disabled individuals or those with progressive forms of MS, where greater neurodegeneration and different pathological mechanisms may predominate. Future studies including more diverse clinical phenotypes are

needed to determine whether the same diffusion metrics remain effective in capturing white matter changes across the full MS disease spectrum. Finally, the MS and NT groups had an uneven sex distribution, with a higher proportion of female participants. Although this reflects the known epidemiology of MS, where diagnoses are more prevalent in females than males,[134] sex differences in brain structure and function could influence diffusion measures or clinical outcomes. Thus, while unlikely to fully account for the observed differences, this imbalance represents a potential source of bias that should be considered when interpreting the results.

Conclusion

This study incorporated multiple dMRI frameworks and demonstrated that each could identify significant structural differences in the CST between MS participants with mild to moderate disability and NT controls. Among the frameworks examined, FBA revealed a greater extent of CST WM alterations than DKI and DTI, with DKI identifying more widespread differences than DTI. Among all metrics examined, FDC from FBA demonstrated significant associations with all outcome measures, showing moderate to strong correlations with clinical balance performance, disability scores, neural conduction measures, and excitatory motor output in individuals with MS. These findings suggest that FBA metrics capture both microstructural and macrostructural aspects of CST degeneration that underlie functional impairments in MS. Establishing links between advanced diffusion imaging metrics and clinical and neurophysiological outcomes are critical for understanding how structural abnormalities translate to function outcomes. Future work should validate these findings in larger, more diverse MS cohorts and examine how FBA metrics reflect white matter changes over time in individuals with MS.

References

1. Goldenberg, M. M. *DISEASE OVERVIEW Multiple Sclerosis Review*. *P&T®* vol. 37 (2012).
2. Green, R., Cutter, G., Friendly, M. & Kister, I. Which symptoms contribute the most to patients' perception of health in multiple sclerosis? *Mult Scler J Exp Transl Clin* **3**, (2017).
3. Cameron, M. H. & Nilsagard, Y. Balance, gait, and falls in multiple sclerosis. in *Handbook of Clinical Neurology* vol. 159 (2018).
4. Lublin, F. D. *et al.* How patients with multiple sclerosis acquire disability. *Brain* **145**, (2022).
5. Dutta, R. & Trapp, B. D. Mechanisms of neuronal dysfunction and degeneration in multiple sclerosis. *Progress in Neurobiology* vol. 93 Preprint at https://doi.org/10.1016/j.pneurobio.2010.09.005 (2011).
6. Lassmann, H. Pathology and disease mechanisms in different stages of multiple sclerosis. *Journal of the Neurological Sciences* vol. 333 Preprint at https://doi.org/10.1016/j.jns.2013.05.010 (2013).
7. Thompson, A. J. *et al.* Diagnosis of multiple sclerosis: 2017 revisions of the McDonald criteria. *The Lancet Neurology* vol. 17 Preprint at https://doi.org/10.1016/S1474-4422(17)30470-2 (2018).
8. Howard, J., Trevick, S. & Younger, D. S. Epidemiology of Multiple Sclerosis. *Neurologic Clinics* vol. 34 Preprint at https://doi.org/10.1016/j.ncl.2016.06.016 (2016).
9. Zivadinov, R. & Leist, T. P. Clinical-magnetic resonance imaging correlations in multiple sclerosis. *Journal of Neuroimaging* vol. 15 Preprint at https://doi.org/10.1177/1051228405283291 (2005).
10. Mollison, D. *et al.* The clinico-radiological paradox of cognitive function and MRI burden of white matter lesions in people with multiple sclerosis: A systematic review and meta-analysis. *PLoS ONE* vol. 12 Preprint at https://doi.org/10.1371/journal.pone.0177727 (2017).
11. Tournier, J., Mori, S. & Leemans, A. Diffusion tensor imaging and beyond. *Magn Reson Med* **65**, 1532–1556 (2011).
12. Alexander, D. C., Dyrby, T. B., Nilsson, M. & Zhang, H. Imaging brain microstructure with diffusion MRI: practicality and applications. *NMR in Biomedicine* vol. 32 Preprint at https://doi.org/10.1002/nbm.3841 (2019).
13. Werring, D. J., Clark, C. A., Barker, G. J., Thompson, A. J. & Miller, D. H. Diffusion tensor imaging of lesions and normal-appearing white matter in multiple sclerosis. *Neurology* **52**, (1999).
14. Goveas, J. *et al.* Diffusion-MRI in neurodegenerative disorders. *Magnetic Resonance Imaging* vol. 33 Preprint at https://doi.org/10.1016/j.mri.2015.04.006 (2015).
15. Inglese, M. & Bester, M. Diffusion imaging in multiple sclerosis: Research and clinical implications. *NMR in Biomedicine* vol. 23 Preprint at https://doi.org/10.1002/nbm.1515 (2010).

16. Caranova, M., Soares, J. F., Batista, S., Castelo-Branco, M. & Duarte, J. V. A systematic review of microstructural abnormalities in multiple sclerosis detected with NODDI and DTI models of diffusion-weighted magnetic resonance imaging. *Magnetic Resonance Imaging* vol. 104 Preprint at https://doi.org/10.1016/j.mri.2023.09.010 (2023).
17. Basser, P. J., Mattiello, J. & LeBihan, D. MR diffusion tensor spectroscopy and imaging. *Biophys J* **66**, (1994).
18. Cercignani, M., Lannucci, G. & Filippi, M. Diffusion-weighted imaging in multiple sclerosis. *Ital J Neurol Sci* **20**, (1999).
19. Lin, X., Tench, C. R., Morgan, P. S., Niepel, G. & Constantinescu, C. S. 'Importance sampling' in MS: Use of diffusion tensor tractography to quantify pathology related to specific impairment. *J Neurol Sci* **237**, (2005).
20. Hubbard, E. A., Wetter, N. C., Sutton, B. P., Pilutti, L. A. & Motl, R. W. Diffusion tensor imaging of the corticospinal tract and walking performance in multiple sclerosis. *J Neurol Sci* **363**, 225–231 (2016).
21. Liu, C., Bammer, R. & Moseley, M. E. Limitations of apparent diffusion coefficient-based models in characterizing non-Gaussian diffusion. *Magn Reson Med* **54**, (2005).
22. Zhuo, J. & Gullapalli, R. P. Diffusion Kurtosis Imaging. in *Neuroimaging Techniques in Clinical Practice* 215–228 (Springer International Publishing, Cham, 2020). doi:10.1007/978-3-030-48419-4_15.
23. Tuch, D. S. *et al.* High angular resolution diffusion imaging reveals intravoxel white matter fiber heterogeneity. *Magn Reson Med* **48**, (2002).
24. De Luca, A., Froeling, M. & Leemans, A. Models: Signal Representation vs. Microstructural Models. in *A Practical Guide to Advanced Diffusion MRI* 83–110 (Springer Nature Switzerland, Cham, 2024). doi:10.1007/978-3-031-70337-9_4.
25. Jeurissen, B., Leemans, A., Tournier, J. D., Jones, D. K. & Sijbers, J. Investigating the prevalence of complex fiber configurations in white matter tissue with diffusion magnetic resonance imaging. *Hum Brain Mapp* **34**, (2013).
26. Steven, A. J., Zhuo, J. & Melhem, E. R. Diffusion kurtosis imaging: An emerging technique for evaluating the microstructural environment of the brain. *American Journal of Roentgenology* **202**, (2014).
27. Jensen, J. H. & Helpern, J. A. MRI quantification of non-Gaussian water diffusion by kurtosis analysis. *NMR in Biomedicine* vol. 23 Preprint at https://doi.org/10.1002/nbm.1518 (2010).
28. Yoshida, M. *et al.* Diffusional kurtosis imaging of normal-appearing white matter in multiple sclerosis: Preliminary clinical experience. *Jpn J Radiol* **31**, (2013).
29. Li, H. Q. *et al.* Evaluation of patients with relapsing-remitting multiple sclerosis using tract-based spatial statistics analysis: Diffusion kurtosis imaging. *BMC Neurol* **18**, (2018).
30. Dhollander, T. *et al.* Fixel-based Analysis of Diffusion MRI: Methods, Applications, Challenges and Opportunities. *NeuroImage* vol. 241 Preprint at https://doi.org/10.1016/j.neuroimage.2021.118417 (2021).
31. Raffelt, D. A. *et al.* Connectivity-based fixel enhancement: Whole-brain statistical analysis of diffusion MRI measures in the presence of crossing fibres. *Neuroimage* **117**, (2015).

32. Raffelt, D. A. *et al.* Investigating white matter fibre density and morphology using fixel-based analysis. *Neuroimage* **144**, (2017).
33. Raffelt, D. *et al.* Apparent Fibre Density: A novel measure for the analysis of diffusion-weighted magnetic resonance images. *Neuroimage* **59**, (2012).
34. Storelli, L., Pagani, E., Preziosa, P., Filippi, M. & Rocca, M. A. Measurement of white matter fiber-bundle cross-section in multiple sclerosis using diffusion-weighted imaging. *Multiple Sclerosis Journal* **27**, (2021).
35. Sahota, P. *et al.* Transcranial magnetic stimulation: Role in the evaluation of disability in multiple sclerosis. *Neurol India* **53**, (2005).
36. Snow, N. J., Wadden, K. P., Chaves, A. R. & Ploughman, M. Transcranial Magnetic Stimulation as a Potential Biomarker in Multiple Sclerosis: A Systematic Review with Recommendations for Future Research. *Neural Plasticity* vol. 2019 Preprint at https://doi.org/10.1155/2019/6430596 (2019).
37. Hupfeld, K. E., Swanson, C. W., Fling, B. W. & Seidler, R. D. TMS-induced silent periods: A review of methods and call for consistency. *Journal of Neuroscience Methods* vol. 346 Preprint at https://doi.org/10.1016/j.jneumeth.2020.108950 (2020).
38. Kauv, P. *et al.* The corticospinal tract in multiple sclerosis: correlation between cortical excitability and magnetic resonance imaging measures. *J Neural Transm* **132**, 265–273 (2025).
39. Lenzi, D. *et al.* Effect of corpus callosum damage on ipsilateral motor activation in patients with multiple sclerosis: A functional and anatomical study. *Hum Brain Mapp* **28**, (2007).
40. Radetz, A. *et al.* Linking Microstructural Integrity and Motor Cortex Excitability in Multiple Sclerosis. *Front Immunol* **12**, (2021).
41. Von Meyenburg, J. *et al.* Spinal cord diffusion-tensor imaging and motor-evoked potentials in multiple sclerosis patients: Microstructural and functional asymmetry. *Radiology* **267**, (2013).
42. Kurtzke, J. F. Rating neurologic impairment in multiple sclerosis: An expanded disability status scale (EDSS). *Neurology* **33**, (1983).
43. Bowen, J., Gibbons, L., Gianas, A. & Kraft, G. H. Self-administered expanded disability status scale with functional system scores correlates well with a physician-administered test. *Multiple Sclerosis* **7**, (2001).
44. Franchignoni, F., Horak, F., Godi, M., Nardone, A. & Giordano, A. Using psychometric techniques to improve the Balance Evaluation Systems Test: the mini-BESTest. *J Rehabil Med* **42**, 323–331 (2010).
45. Groppa, S. *et al.* A practical guide to diagnostic transcranial magnetic stimulation: Report of an IFCN committee. *Clinical Neurophysiology* vol. 123 Preprint at https://doi.org/10.1016/j.clinph.2012.01.010 (2012).
46. Sivaramakrishnan, A., Tahara-Eckl, L. & Madhavan, S. Spatial localization and distribution of the TMS-related 'hotspot' of the tibialis anterior muscle representation in the healthy and post-stroke motor cortex. *Neurosci Lett* **627**, (2016).

47. Rossini, P. M. *et al.* Non-invasive electrical and magnetic stimulation of the brain, spinal cord and roots: basic principles and procedures for routine clinical application. Report of an IFCN committee. *Electroencephalogr Clin Neurophysiol* **91**, (1994).
48. Muceli, S. & Merletti, R. Tutorial. Frequency analysis of the surface EMG signal: Best practices. *Journal of Electromyography and Kinesiology* **79**, 102937 (2024).
49. Goldberger, A. L. *et al.* PhysioBank, PhysioToolkit, and PhysioNet: components of a new research resource for complex physiologic signals. *Circulation* **101**, (2000).
50. Xu, L. Cancellation of harmonic interference by baseline shifting of wavelet packet decomposition coefficients. *IEEE Transactions on Signal Processing* **53**, (2005).
51. Taga, M. *et al.* Corticoreticulospinal tract neurophysiology in an arm and hand muscle in healthy and stroke subjects. *Journal of Physiology* **599**, (2021).
52. Sivaramakrishnan, A. & Madhavan, S. Stimulus intensity affects variability of motor evoked responses of the non-paretic, but not paretic tibialis anterior muscle in stroke. *Brain Sci* **10**, (2020).
53. Hess, C. W., Mills, K. R., Murray, N. M. F. & Schriefer, T. N. Magnetic brain stimulation: Central motor conduction studies in multiple sclerosis. *Ann Neurol* **22**, (1987).
54. Kukowski, B. Duration, configuration and amplitude of the motor response evoked by magnetic brain stimulation in patients with multiple sclerosis. *Electromyogr Clin Neurophysiol* **33**, (1993).
55. Spampinato, D. A., Ibanez, J., Rocchi, L. & Rothwell, J. Motor potentials evoked by transcranial magnetic stimulation: interpreting a simple measure of a complex system. *Journal of Physiology* vol. 601 Preprint at https://doi.org/10.1113/JP281885 (2023).
56. Tournier, J. D. *et al.* MRtrix3: A fast, flexible and open software framework for medical image processing and visualisation. *NeuroImage* vol. 202 Preprint at https://doi.org/10.1016/j.neuroimage.2019.116137 (2019).
57. Veraart, J., Fieremans, E. & Novikov, D. S. Diffusion MRI noise mapping using random matrix theory. *Magn Reson Med* **76**, (2016).
58. Veraart, J. *et al.* Denoising of diffusion MRI using random matrix theory. *Neuroimage* **142**, (2016).
59. Kellner, E., Dhital, B., Kiselev, V. G. & Reisert, M. Gibbs-ringing artifact removal based on local subvoxel-shifts. *Magn Reson Med* **76**, (2016).
60. Andersson, J. L. R. & Sotiropoulos, S. N. An integrated approach to correction for off-resonance effects and subject movement in diffusion MR imaging. *Neuroimage* **125**, (2016).
61. Tustison, N. J. *et al.* N4ITK: Improved N3 bias correction. *IEEE Trans Med Imaging* **29**, (2010).
62. Farquhar, M. E., Yang, Q. & Vegh, V. Robust, fast and accurate mapping of diffusional mean kurtosis. *Elife* **12**, (2024).
63. Veraart, J., Sijbers, J., Sunaert, S., Leemans, A. & Jeurissen, B. Weighted linear least squares estimation of diffusion MRI parameters: Strengths, limitations, and pitfalls. *Neuroimage* **81**, (2013).
64. Basser, P. J., Mattiello, J. & Lebihan, D. Estimation of the Effective Self-Diffusion Tensor from the NMR Spin Echo. *J Magn Reson B* **103**, (1994).

65. Morez, J. *et al.* Optimal experimental design and estimation for q-space trajectory imaging. *Hum Brain Mapp* **44**, (2023).
66. Alexander, A. L., Lee, J. E., Lazar, M. & Field, A. S. Diffusion Tensor Imaging of the Brain. *Neurotherapeutics* **4**, 316–329 (2007).
67. Stevens, J. A. & Lee, R. The Potential to Reduce Falls and Avert Costs by Clinically Managing Fall Risk. *Am J Prev Med* **55**, (2018).
68. Dhollander, T., Mito, R., Raffelt, D. & Connelly, A. Improved white matter response function estimation for 3-tissue constrained spherical deconvolution. *Proc. Intl. Soc. Mag. Reson. Med* (2019).
69. Jeurissen, B., Tournier, J. D., Dhollander, T., Connelly, A. & Sijbers, J. Multi-tissue constrained spherical deconvolution for improved analysis of multi-shell diffusion MRI data. *Neuroimage* **103**, (2014).
70. Dhollander, T. *et al.* Multi-tissue log-domain intensity and inhomogeneity normalization for quantitative apparent fibre density. *29th Proceedings of International Society of Magnetic Resonance in Medicine* 2472 (2021).
71. Raffelt, D. *et al.* Bias field correction and intensity normalisation for quantitative analysis of apparent fibre density. *Proceedings of International Society of Magnetic Resonance in Medicine* **Vol. 25**, 3541 (2017).
72. Raffelt, D. *et al.* Symmetric diffeomorphic registration of fibre orientation distributions. *Neuroimage* **56**, (2011).
73. Boyne, P., DiFrancesco, M., Awosika, O. O., Williamson, B. & Vannest, J. Mapping the human corticoreticular pathway with multimodal delineation of the gigantocellular reticular nucleus and high-resolution diffusion tractography. *J Neurol Sci* **434**, (2022).
74. Smith, R. E., Tournier, J. D., Calamante, F. & Connelly, A. SIFT2: Enabling dense quantitative assessment of brain white matter connectivity using streamlines tractography. *Neuroimage* **119**, (2015).
75. Calamante, F., Tournier, J. D., Jackson, G. D. & Connelly, A. Track-density imaging (TDI): Super-resolution white matter imaging using whole-brain track-density mapping. *Neuroimage* **53**, (2010).
76. Fischl, B. FreeSurfer. *NeuroImage* vol. 62 Preprint at https://doi.org/10.1016/j.neuroimage.2012.01.021 (2012).
77. Dale, A. M., Fischl, B. & Sereno, M. I. Cortical surface-based analysis: I. Segmentation and surface reconstruction. *Neuroimage* **9**, (1999).
78. Wiltgen, T. *et al.* LST-AI: A deep learning ensemble for accurate MS lesion segmentation. *Neuroimage Clin* **42**, (2024).
79. Smith, S. M. & Nichols, T. E. Threshold-free cluster enhancement: Addressing problems of smoothing, threshold dependence and localisation in cluster inference. *Neuroimage* **44**, (2009).
80. Takao, H., Hayashi, N., Inano, S. & Ohtomo, K. Effect of head size on diffusion tensor imaging. *Neuroimage* **57**, (2011).
81. Smith, R. E., Dhollander, T. & Connelly, A. On the regression of intracranial volume in Fixel-Based Analysis. in *International Society of Magnetic Resonance in Medicine* (2019).

82. Kirkovski, M. *et al.* An Investigation of Age-related Neuropathophysiology in Autism Spectrum Disorder Using Fixel-based Analysis of Corpus Callosum White Matter Micro- and Macrostructure. *J Autism Dev Disord* **54**, (2024).
83. Wuensch, K. L. & Evans, J. D. Straightforward Statistics for the Behavioral Sciences. *J Am Stat Assoc* **91**, (1996).
84. Moen, S. M., Celius, E. G., Nordsletten, L. & Holmøy, T. Fractures and falls in patients with newly diagnosed clinically isolated syndrome and multiple sclerosis. *Acta Neurol Scand* **124**, (2011).
85. Fjeldstad, C., Pardo, G., Bemben, D. & Bemben, M. Decreased postural balance in multiple sclerosis patients with low disability. *International Journal of Rehabilitation Research* **34**, (2011).
86. Galea, M. P., Cofré Lizama, L. E., Butzkueven, H. & Kilpatrick, T. J. Gait and balance deterioration over a 12-month period in multiple sclerosis patients with EDSS scores ≤ 3.0. *NeuroRehabilitation* **40**, (2017).
87. DeLuca, G. C., Ebers, G. C. & Esiri, M. M. Axonal loss in multiple sclerosis: A pathological survey of the corticospinal and sensory tracts. *Brain* vol. 127 Preprint at https://doi.org/10.1093/brain/awh118 (2004).
88. Fling, B. W., Dutta, G. G., Schlueter, H., Cameron, M. H. & Horak, F. B. Associations between proprioceptive neural pathway structural connectivity and balance in people with multiple sclerosis. *Front Hum Neurosci* **8**, (2014).
89. Farzan, F. Single-pulse transcranial magnetic stimulation (TMS) protocols and outcome measures. *Neuromethods* **89**, (2014).
90. Gagliardo, A. *et al.* Motor evoked potentials in multiple sclerosis patients without walking limitation: Amplitude vs. conduction time abnormalities. *J Neurol* **254**, (2007).
91. Tataroglu, C., Genc, A., Idiman, E., Cakmur, R. & Idiman, F. Cortical silent period and motor evoked potentials in patients with multiple sclerosis. *Clin Neurol Neurosurg* **105**, (2003).
92. Kale, N., Agaoglu, J., Onder, G. & Tanik, O. Correlation between disability and transcranial magnetic stimulation abnormalities in patients with multiple sclerosis. *Journal of Clinical Neuroscience* **16**, (2009).
93. Udupa, K. & Chen, R. Central motor conduction time. in *Handbook of Clinical Neurology* vol. 116 (2013).
94. Furby, A., Bourriez, J. L., Jacquesson, J. M., Mounier-Vehier, F. & Guieu, J. D. Motor evoked potentials to magnetic stimulation: technical considerations and normative data from 50 subjects. *J Neurol* **239**, (1992).
95. van der Weijden, C. W. J. *et al.* Diffusion-derived parameters in lesions, peri-lesion and normal-appearing white matter in multiple sclerosis using tensor, kurtosis and fixel-based analysis. *Journal of Cerebral Blood Flow and Metabolism* **42**, (2022).
96. Sotak, C. H. Nuclear magnetic resonance (NMR) measurement of the apparent diffusion coefficient (ADC) of tissue water and its relationship to cell volume changes in pathological states. *Neurochem Int* **45**, (2004).
97. Filippi, M. *et al.* A quantitative study of water diffusion in multiple sclerosis lesions and normal-appearing white matter using echo- planar imaging. *Arch Neurol* **57**, (2000).

98. Filippi, M. *et al.* Assessment of lesions on magnetic resonance imaging in multiple sclerosis: practical guidelines. *Brain* vol. 142 Preprint at https://doi.org/10.1093/brain/awz144 (2019).
99. Song, S. K. *et al.* Diffusion tensor imaging detects and differentiates axon and myelin degeneration in mouse optic nerve after retinal ischemia. *Neuroimage* **20**, (2003).
100. Wheeler-Kingshott, C. A. M., Ciccarelli, O., Schneider, T., Alexander, D. C. & Cercignani, M. A new approach to structural integrity assessment based on axial and radial diffusivities. *Funct Neurol* **27**, (2012).
101. Rovaris, M., Agosta, F., Pagani, E. & Filippi, M. Diffusion Tensor MR Imaging. *Neuroimaging Clin N Am* **19**, 37–43 (2009).
102. Wheeler-Kingshott, C. A. M. & Cercignani, M. About 'axial' and 'radial' diffusivities. *Magn Reson Med* **61**, (2009).
103. De Santis, S. *et al.* Evidence of early microstructural white matter abnormalities in multiple sclerosis from multi-shell diffusion MRI. *Neuroimage Clin* **22**, (2019).
104. Naismith, R. T. *et al.* Increased diffusivity in acute multiple sclerosis lesions predicts risk of black hole. *Neurology* **74**, (2010).
105. Song, S. K. *et al.* Dysmyelination revealed through MRI as increased radial (but unchanged axial) diffusion of water. *Neuroimage* **17**, (2002).
106. Song, S. K. *et al.* Demyelination increases radial diffusivity in corpus callosum of mouse brain. *Neuroimage* **26**, (2005).
107. Chang, E. H. *et al.* The role of myelination in measures of white matter integrity: Combination of diffusion tensor imaging and two-photon microscopy of CLARITY intact brains. *Neuroimage* **147**, (2017).
108. Madden, D. J. *et al.* Diffusion tensor imaging of cerebral white matter integrity in cognitive aging. *Biochimica et Biophysica Acta - Molecular Basis of Disease* vol. 1822 Preprint at https://doi.org/10.1016/j.bbadis.2011.08.003 (2012).
109. Zhu, Q. *et al.* The Application of Diffusion Kurtosis Imaging on the Heterogeneous White Matter in Relapsing-Remitting Multiple Sclerosis. *Front Neurosci* **16**, (2022).
110. Kelm, N. D. *et al.* Evaluation of diffusion kurtosis imaging in ex vivo hypomyelinated mouse brains. *Neuroimage* **124**, (2016).
111. Gajamange, S. *et al.* Fibre-specific white matter changes in multiple sclerosis patients with optic neuritis. *Neuroimage Clin* **17**, (2018).
112. Carandini, T. *et al.* Disruption of brainstem monoaminergic fibre tracts in multiple sclerosis as a putative mechanism for cognitive fatigue: a fixel-based analysis. *Neuroimage Clin* **30**, (2021).
113. Strik, M. *et al.* Axonal loss in major sensorimotor tracts is associated with impaired motor performance in minimally disabled multiple sclerosis patients. *Brain Commun* **3**, (2021).
114. Dziedzic, T. *et al.* Wallerian degeneration: A major component of early axonal pathology in multiple sclerosis. *Brain Pathology* **20**, (2010).
115. Liu, Y. *et al.* Whole brain white matter changes revealed by multiple diffusion metrics in multiple sclerosis: A TBSS study. *Eur J Radiol* **81**, (2012).
116. Tavazzi, E. *et al.* Effects of motor rehabilitation on mobility and brain plasticity in multiple sclerosis: a structural and functional MRI study. *J Neurol* **265**, (2018).

117. Pokryszko-Dragan, A. *et al.* Diffusion tensor imaging findings in the multiple sclerosis patients and their relationships to various aspects of disability. *J Neurol Sci* **391**, (2018).
118. Spampinato, M. V. *et al.* Diffusional Kurtosis Imaging of the Corticospinal Tract in Multiple Sclerosis: Association with Neurologic Disability. *American Journal of Neuroradiology* **38**, 1494–1500 (2017).
119. Takakusaki, K. Functional Neuroanatomy for Posture and Gait Control. *J Mov Disord* **10**, (2017).
120. Baudry, S. Aging changes the contribution of spinal and corticospinal pathways to control balance. *Exerc Sport Sci Rev* **44**, (2016).
121. Šoda, J., Pavelin, S., Vujović, I. & Rogić Vidaković, M. Assessment of Motor Evoked Potentials in Multiple Sclerosis. *Sensors* vol. 23 Preprint at https://doi.org/10.3390/s23010497 (2023).
122. Criste, G., Trapp, B. & Dutta, R. Axonal loss in multiple sclerosis. Causes and mechanisms. in *Handbook of Clinical Neurology* vol. 122 (2014).
123. Beaulieu, C. The basis of anisotropic water diffusion in the nervous system - A technical review. *NMR in Biomedicine* vol. 15 Preprint at https://doi.org/10.1002/nbm.782 (2002).
124. Calabrese, M., Filippi, M. & Gallo, P. Cortical lesions in multiple sclerosis. *Nat Rev Neurol* **6**, 438–444 (2010).
125. Lukas, C. *et al.* Relevance of spinal cord abnormalities to clinical disability in multiple sclerosis: MR imaging findings in a large cohort of patients. *Radiology* **269**, (2013).
126. Bot, J. C. J. *et al.* Spinal cord abnormalities in recently diagnosed MS patients: Added value of spinal MRI examination. *Neurology* **62**, (2004).
127. Smith, S. M. *et al.* Tract-based spatial statistics: Voxelwise analysis of multi-subject diffusion data. *Neuroimage* **31**, (2006).
128. Genc, S. *et al.* Impact of b-value on estimates of apparent fibre density. *Hum Brain Mapp* **41**, (2020).
129. Mohd Taib, N. H., Wan Abdullah, W. A. K., Shuaib, I. L., Magosso, E. & Mat Isa, S. Determination of optimum combination of voxel size and b-value for brain diffusion tensor imaging. *Sains Malays* **46**, (2017).
130. Sprenger, T. *et al.* Bias and precision analysis of diffusional kurtosis imaging for different acquisition schemes. *Magn Reson Med* **76**, (2016).
131. Calamuneri, A. *et al.* White matter tissue quantification at Low b-values within constrained spherical deconvolution framework. *Front Neurol* **9**, (2018).
132. Galea, M. P. & Darian-Smith, I. Multiple corticospinal neuron populations in the macaque monkey are specified by their unique cortical origins, spinal terminations, and connections. *Cerebral Cortex* **4**, (1994).
133. Dum, R. P. & Strick, P. L. The origin of corticospinal projections from the premotor areas in the frontal lobe. *Journal of Neuroscience* **11**, (1991).
134. Marrie, R. A. *et al.* Sex differences in comorbidity at diagnosis of multiple sclerosis. *Neurology* **86**, 1279–1286 (2016).

CHAPTER 5 – MICROSTRUCTURE OF THE CORTICORETICULOSPINAL TRACT IS ASSOCIATED WITH BALANCE AND MOBILITY IN PEOPLE WITH MULTIPLE SCLEROSIS

Introduction

Multiple Sclerosis (MS) is a chronic disease of the central nervous system, with an estimated global prevalence of 2.8 million individuals.[1] MS manifests through an immune-mediated inflammatory response, which results in the formation of sclerotic lesions and neural injury in the brain and spinal cord.[2,3] The pathological hallmark of MS involves damage to myelin, the lipid-rich sheath formed by oligodendrocytes that insulates axons and facilitates rapid neural conduction.[4] The loss of myelin disrupts and delays signal transmission, and over time, results in axonal damage and neurodegeneration, leading to a variety of clinical symptoms.[4,5]

Among the most common and functionally disabling symptoms of MS are impairments in balance and mobility.[6] More than 90 percent of individuals with MS experience mobility and balance difficulties, contributing to an elevated risk of falling.[7,8] Falls are a major source of physical injury and are often accompanied by psychological and social consequences, including fear of falling, reduced physical activity, and social withdrawal.[7,9–11] These effects collectively contribute to a loss of independence and reduced quality of life.[12,13]

Damage to white matter pathways involved in the transportation and integration of sensory and motor information is a major contributor to mobility impairments in MS.[14] Injury to ascending sensory tracts can reduce or delay the delivery of sensory information such as proprioception to processing centers of the brain and brainstem, while injury to descending motor pathways interferes with the magnitude and timely transmission of motor commands (Chapter 3).[14–17] This

breakdown in bidirectional communication compromises the coordination and responsiveness required for unimpaired postural control and movement execution. Identifying the white matter pathways involved in these processes and quantifying the extent of their injury may help clarify the neuroanatomical basis of motor dysfunction in MS and guide future research and clinical applications.

Previous research on motor impairment in MS has primarily focused on the corticospinal tract (CST), given its role as the principal pathway for voluntary movement. Numerous studies employing structural imaging or neurophysiological methods have demonstrated that CST damage in MS is associated with reduced muscle strength, slower walking speed, impaired balance, and greater overall disability.[16,18–25] Collectively, these studies reinforce the CST as a central contributor to motor impairment in MS. While the CST has been a major focus of MS motor research, it represents only one component of the broader motor system involved in posture and locomotion, highlighting the need to investigate other motor pathways.

The reticulospinal tract (ReST) is another major descending motor pathway that contributes to postural control, gross motor function, locomotion, and force modulation.[26–34] Originating from the pontomedullary reticular formation, a complex network of nuclei located in the posterior brainstem, the ReST descends bilaterally through the spinal cord, where it synapses with spinal interneurons and alpha motor neurons.[26,35,36] Evolutionarily, the ReST is among the oldest neural motor pathways. In species lacking highly developed cortical motor areas, it serves as the primary neural pathway for executing movement.[26,37] As the central nervous system evolved to include more developed motor cortices, the ReST expanded in neuronal number to continue supporting and modulating motor functions in higher-order species.[26,37]

Seminal work by Lawrence and Kuypers helped establish the contributions of the ReST's in supporting posture and locomotion in higher vertebrates. In their studies with non-human primates, bilateral lesions of the CST severely impacted fine motor control of the fingers, but gross motor and postural stability were preserved.[38] These functions were disrupted only when areas that give rise to the ReST were subsequently lesioned.[39] Since this original finding, many studies have further supported and expanded on the ReST's involvement in initiating and maintaining locomotor activity, regulating muscle tone, generating anticipatory postural adjustments, and corrective responses to balance disturbances.[26,31–34,40]

In stroke literature, the ReST has gained growing attention due to its potential to compensate for damage to the CST and support motor recovery.[27,41] Studies have shown that when the CST sustains an injury, the ReST system is upregulated, and gross motor movements can be partially recovered, suggesting that the ReST may serve as an alternative route for motor output in stroke patients.[27,41–43] This compensatory mechanism may be particularly relevant in cases where cortical projections to the ReST, collectively known as the corticoreticulospinal tract (CReST), remain structurally and functionally intact.[43–45] Several studies have demonstrated that greater preservation of the CReST is associated with better walking ability and gait recovery in individuals post-stroke.[46–50]

Despite its contributions to movement and its potential as a compensatory motor pathway, the CReST has been relatively underexplored in human neuroimaging studies compared to the CST. When investigated, it is often defined by projections from premotor and supplementary motor areas.[47,51,52] However, a recent anatomical tracer study in an animal model indicated a broader cortical origin, including anterior frontal regions.[53] These anterior regions have also been associated with walking performance in healthy aging and individuals with stroke and Parkinson's

disease.[54–56] Based on this evidence, a recent probabilistic tractography study provided the first comprehensive mapping of the human CReST, identifying projections from both frontal and motor cortices.[57]

However, mapping the CReST in vivo presents neuroimaging challenges, as its widespread anatomical projections traverse regions of dense white matter with complex architecture and crossing fibers, particularly within the corona radiata and brainstem.[57] These characteristics make it difficult to accurately assess using conventional diffusion imaging techniques.[58] Fixel-based analysis (FBA), an advanced diffusion magnetic resonance imaging (dMRI) method, addresses this limitation by resolving multiple fiber populations within a single voxel, making it a robust approach for examining anatomically complex tracts, such as the CReST.[59,60] Recent research using FBA has linked white matter microstructure, as measured by FBA's fiber density (FD) metric, to mobility and cognitive outcomes in other neurological and aging populations, supporting its utility in identifying structural contributors to functional impairment.[61,62] Assessing CReST FD in individuals with MS may therefore offer insights into the structural correlates of mobility impairment.

Given the CReST's extensive cortical projections, bilateral spinal influence, and role in mediating posture and locomotion, it may also contribute to residual motor function and help sustain balance and gait in the presence of neural injury in MS. The present study evaluates the structural integrity of the CReST in individuals with relapsing-remitting MS compared to age- and sex-matched neurotypical (NT) controls. Using FBA, FD, log-transformed fiber cross-section (LogFC), and fiber density and cross-section (FDC) will be evaluated to locate regions of micro- and macrostructural differences along the CReST between participants with MS and NT participants. Associations between CReST FD and clinical measures of balance and mobility

function will also be examined, including the Mini-Balance Evaluation Systems Test (miniBEST), static postural control, walking speed, the Timed Up and Go (TUG) test, and the 12-item MS Walking Scale (MSWS-12). This study aims to elucidate the relationship between CReST white matter integrity and motor impairment in individuals with MS.

Materials and Methods

Study Overview

The data used in this study originated from a broader research project investigating the neural contributions to motor impairment in individuals with MS. This study was reviewed and approved by the Colorado State University Institutional Review Board (IRB#18-7738H), and all participants provided written informed consent prior to participation in accordance with the Declaration of Helsinki.

Participants

This study consisted of 56 total participants, including 27 individuals with a neurologist-confirmed diagnosis of relapsing-remitting MS and 29 age- and sex-matched NT controls. MS participants were eligible if they reported mild to moderate disability, defined by a self-reported expanded disability status scale (EDSS) score between 0 and 4.5. Exclusion criteria for participants included the inability to walk 300 meters or stand unassisted for 10 minutes, as well as the presence of a musculoskeletal injury, vestibular disorder, joint replacement, or any neurological condition other than MS. Of the 30 individuals with MS initially assessed, three were excluded, two due to EDSS scores outside the inclusion range, and one due to MRI brain registration difficulties caused by extensive pathological tissue. NT controls were required to have no history of any neurological conditions and to meet the same physical ability criteria as the MS group.

Expanded Disability Status Scale (EDSS)

Clinical disability level was assessed using the EDSS in individuals with MS. The EDSS integrates ratings from the Functional Systems Score (FSS), which captures neurological function across multiple domains of the central nervous system.[63] In this study, participants with MS self-reported their EDSS scores using a validated questionnaire, which has shown strong associations with clinician-administered EDSS scores.[64]

Mini-Balance Evaluation Systems Test (miniBEST)

Balance performance was evaluated using the miniBEST, a standardized clinical tool designed to assess multiple domains of postural control. The miniBEST targets four distinct balance systems: anticipatory postural adjustments (APA), reactive postural control (RPC), sensory orientation (SO), and dynamic gait (DG).[65] The assessment consists of 14 items, each rated on a 3-point ordinal scale (0 = severe impairment, 1 = moderate impairment, 2 = normal performance). For items requiring unilateral performance, such as single-leg stance, scores from both limbs were recorded and included in the total. Item scores were summed to generate a composite score ranging from 0 to 32, with higher scores indicating better balance function.

Static Balance Assessment

To complement the miniBEST balance assessment, static balance was measured using the modified Clinical Test of Sensory Interaction on Balance.[66,67] During trials, participants were instructed to stand as still as possible for 30 seconds per trial, with their feet together, hands on their hips, and their gaze directed at a fixed visual target at eye level. All trials were completed without shoes to standardize sensory input from the feet. The four testing conditions included: (1) eyes-open on a firm surface, (2) eyes-closed on a firm surface, (3) eyes-open on a compliant surface, and (4) eyes-closed on a compliant surface, with the compliant surface provided by a 7-

cm thick Airex Elite Balance Pad (Airex, Sins, Switzerland). Postural sway was quantified by calculating the center of pressure (CoP) path length, representing the total distance (cm) traveled by the CoP over the duration of each trial, with greater path lengths indicating poorer postural stability.[68] CoP data were collected at 25 Hz using the BTrackS Balance Plate and processed with Balance Tracking Systems software (Balance Tracking Systems Inc., San Diego, CA).

Several participants with MS (n = 8) were unable to complete the eyes-closed conditions due to loss of balance, resulting in stepping off the platform or requiring spotter assistance before the full trial duration. These interruptions confound CoP pathlength data by artificially reducing sway measures, despite reflecting poorer balance performance. Therefore, only data from the eyes-open firm and eyes-open compliant conditions are reported and analyzed here, allowing for the evaluation of postural control under standard and proprioceptively challenging conditions. Additionally, two participants with MS were unable to complete the eyes-open compliant surface condition, and two control participants were excluded due to instrumentation error. These participants were excluded from group comparisons and association analyses for the respective trials.

Walking Speed

Participants completed two separate 2-minute walking trials to assess both habitual and fast walking speeds. For the preferred speed condition, participants were instructed to walk at a comfortable, natural pace while maintaining a forward gaze. For the fast-walking condition, participants walked at a self-selected fast pace that could be safely maintained for the full duration of the task. A rest period was provided between trials to minimize fatigue. Gait speed in both conditions was acquired using Opal wireless inertial sensors and analyzed with Mobility Lab software (Version 2; APDM Inc., Portland, OR, USA).[69,70]

Timed-Up and Go (TUG)

Functional mobility was assessed using the TUG test, which was administered as part of the miniBEST assessment battery. The TUG is a widely used and validated clinical measure for evaluating mobility in individuals with MS.[71,72] During the test, participants were instructed to rise from a seated position, walk a distance of 7 meters, turn around, return to the chair, and sit down. The total duration required to complete the task was recorded, with faster times interpreted as greater functional mobility.[73,74]

12-Item Multiple Sclerosis Walking Scale (MSWS-12)

Participants with MS completed the MSWS-12, a self-report questionnaire designed to assess the perceived impact of MS on walking ability in everyday life, and has demonstrated predictive utility for fall risk among individuals with MS. [75,76]

MRI Acquisition

dMRI data were acquired using a 3.0 Tesla Siemens MAGNETOM Prismafit scanner (Siemens Medical Solutions USA, Inc., Malvern, PA) equipped with a 32-channel head coil and parallel imaging capabilities. dMRI was performed using a multi-shell acquisition protocol which included 122 diffusion-weighted volumes distributed across three b-value shells: 12 non-diffusion-weighted ($b = 0$ s/mm^2) images interspersed throughout the scan, 55 directions at $b = 1600$ s/mm^2, and 55 directions at $b = 2400$ s/mm^2. To support susceptibility distortion correction, an equal number of volumes ($n = 61$) were collected with anterior-to-posterior and posterior-to-anterior phase-encoding directions. Additional imaging parameters were as follows: repetition time (TR) = 4000 ms, echo time (TE) = 77 ms, flip angle = 84°, isotropic voxel size = 2.0 mm^3, slice thickness = 2.0 mm, number of slices = 72, and a field of view (FoV) of 224 mm (RL: 224 mm, AP: 216 mm, FH: 144 mm).

Structural imaging included a high-resolution T1-weighted anatomical scan and a T2-weighted fluid-attenuated inversion recovery (FLAIR) sequence. The T1-weighted scan was collected with the following parameters: TR = 2400 ms, TE = 2.07 ms, inversion time (TI) = 1000 ms, flip angle = 8°, isotropic voxel size = 0.8 mm^3, slice thickness = 0.8 mm, number of slices = 224, and a FoV of 256 mm (RL: 180 mm, AP: 256 mm, FH: 256 mm). The FLAIR sequence was acquired with the following parameters: TR = 6000 ms, TE = 428 ms, TI = 2000 ms, flip angle = 120°, isotropic voxel size = 1.0 mm^3, slice thickness = 1 mm, number of slices = 176, and FoV = 256 mm (RL: 176 mm, AP: 256 mm, FH: 256 mm). These structural images were used to support post-processing steps, including registration of diffusion data, volumetric brain analyses, and lesion segmentation.

MRI Analysis

Fixel-Based Analysis (FBA)

Preprocessing, tractography, and analyses of dMRI data were conducted using MRtrix3 (Tournier et al. 2019,[77] https://www.mrtrix.org/), an open-source software package for FBA. The preprocessing pipeline followed current best practices,[60] beginning with denoising using Marchenko-Pastur principal component analysis,[78,79] then Gibbs ringing artifact removal,[80] correction for eddy currents and participant motion using Functional Magnetic Resonance Imaging of the Brain Software Library's (FSL) eddy tool,[81] and bias field correction to address intensity inhomogeneities.[82]

After preprocessing, tissue-specific response functions for WM, gray matter, and cerebrospinal fluid were estimated using an unsupervised algorithm,[83] and averaged across participants to generate group-level response functions for use in subsequent modeling.[60] Prior to fiber orientation estimation, diffusion data were resampled to 1.5 mm isotropic resolution to

enhance anatomical contrast and improve registration accuracy. Fiber orientation distributions (FODs) were then computed using multi-shell, three-tissue constrained spherical deconvolution,[84] enabling the differentiation of multiple fiber populations within a voxel. This was followed by global intensity normalization and joint bias field correction to ensure consistency across participants.[85–87]

To facilitate group-wise analysis, a population FOD template was created using data from a subset of 30 participants: 15 individuals with MS and 15 NT controls.[77] MS participants were selected to represent a range of lesion loads while minimizing severe anatomical distortions to preserve template integrity. NT participants were randomly sampled. No significant differences in age or sex were found between the groups included in the template. All individual FOD images were subsequently registered to the study template using a non-linear transformation.[88]

Fixel-wise metrics were derived from the FODs for each participant, including FD, fiber cross-section (FC), and the combined metric of FDC. FD represents the intra-axonal volume of a specific fiber population within a voxel, reflecting microstructural integrity.[85] FC quantifies the cross-sectional area of a fiber bundle and reflects macrostructural architecture such as tract expansion or compression.[89] To account for the typical skew in FC values observed across individuals, a log transformation was applied. FDC, calculated as the product of FD and FC, offers a composite index that integrates both microstructural and macrostructural characteristics of a fiber population.[60,89]

Tractography and Regions of Interest

This study employed a tract-of-interest approach to isolate and analyze the CReST, utilizing region-of-interest (ROI) masks developed by Boyne et al. 2022,[57] who generated the first human-average CReST template in MRI space. All ROI masks were originally defined in MNI

space and were nonlinearly transformed into the study-specific template space for streamline generation. The ROIs in template space are shown in (Figure D1, Appendix D). Streamline tractography was initiated from seeds randomly distributed within the cortical ROI, which spanned the entire frontal lobe to the primary somatosensory cortex. Streamlines were generated unidirectionally, projecting from the cortex to the brainstem, and were constrained to pass through the gigantocellular reticular nucleus, located at the medial pontomedullary junction, the primary nucleus giving rise to the ReST.[26,57,90] To increase anatomical specificity and reduce inclusion of non-target fibers, manually drawn exclusion masks were applied to eliminate streamlines originating in the corticobulbar region or entering the corpus callosum, thalamus, or cerebellum.

Tractography was conducted separately for each hemisphere, with 5,000 streamlines generated per side to ensure consistent sampling across hemispheres. Hemispheric tractograms were then combined into a single file for subsequent analysis. To improve the biological accuracy of streamline weights, the Spherical-Deconvolution Informed Filtering of Tractograms 2 (SIFT2)[91] algorithm was applied to combined tractogram file. This method adjusts streamline contributions based on the underlying fiber orientation distributions, yielding a fiber pathway model that more accurately reflects white matter architecture. The final rendering of the CReST streamlines is shown in Figure 5.1.

Brain Volumetrics

To account for individual differences in head size during FBA statistical analyses, estimated total intracranial volume (eTIV) was calculated for each participant. eTIV values were derived from high-resolution T1-weighted anatomical images using the recon-all pipeline in FreeSurfer (version 7.4.0; Fischl 2012).[92]

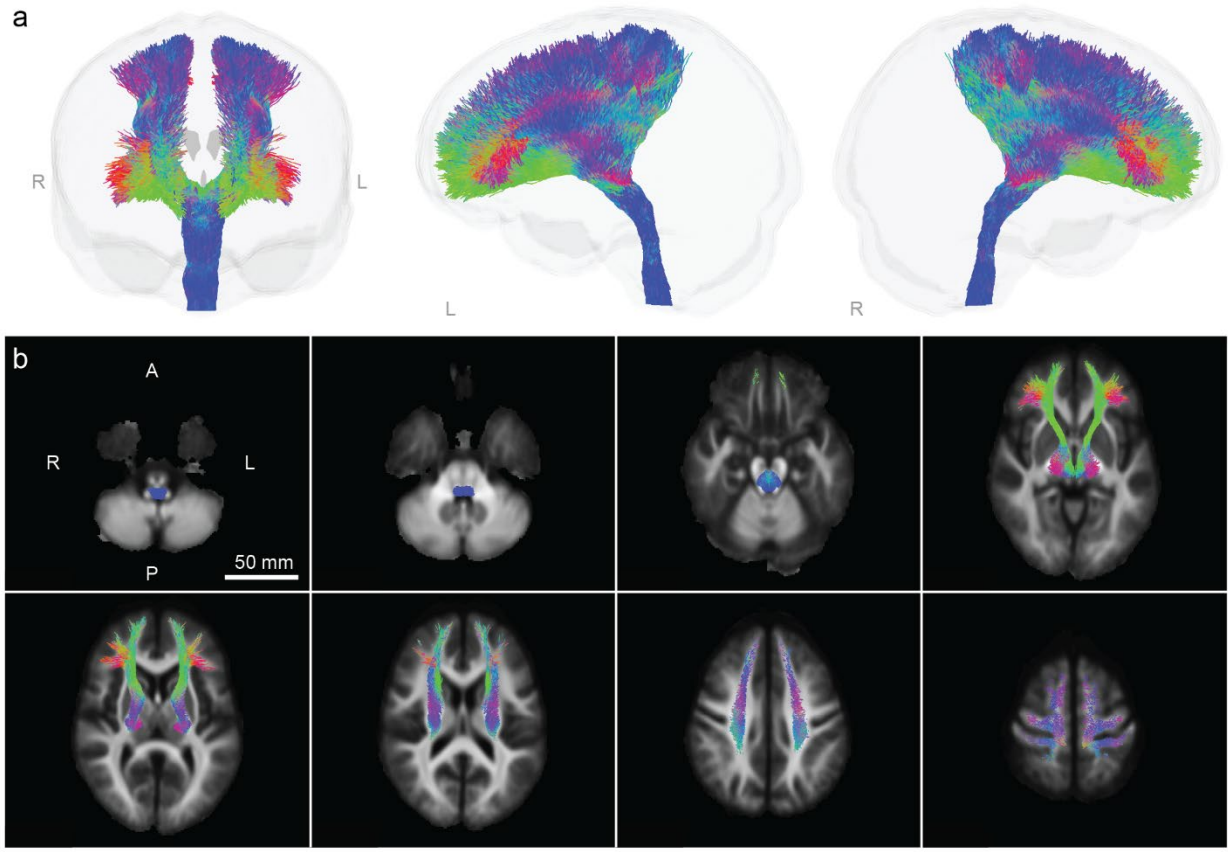

Figure 5.1. Corticoreticulospinal Tract Streamlines. a) Volume rendering of bilateral CReST streamlines viewed from anterior, left, and right perspectives. Streamlines are color-coded by orientation: red = medial-lateral, blue = superior-inferior, and green = anterior-posterior. b) CReST streamlines overlaid on axial slices of the template brain. Slices progress from inferior to superior, starting in the medulla (top left) and ascending from the brainstem to the cerebrum, ending with streamlines entering the cortex (bottom right).

Lesion Segmentation

WM lesions were identified using the deep learning–enhanced version of the Lesion Segmentation Toolbox.[93] T1-weighted and T2-FLAIR images were provided as inputs to enhance the accuracy of automated lesion detection. For each participant with MS, total lesion volume (mL) and lesion volume within the CReST were computed to quantify global and tract-specific lesion burden. A group-level lesion probability map for participants with MS is displayed in (Figure D2, Appendix D).

Statistical Analysis

Statistical Analysis of Fixel-Based Metrics

Group differences in FDC, FD, and LogFC within the CReST were assessed using threshold-free connectivity-based fixel enhancement, a statistical framework designed for FBA that accounts for spatial connectivity across fixels.[94] Group comparisons were modeled using a general linear framework, incorporating age and sex as covariates across all fixel-based metrics. For analyses involving LogFC and FDC, the logarithm of eTIV was additionally included as a covariate to adjust for inter-individual variability in head size, given its potential impact on macrostructural measures.[95] Multiple comparisons were controlled using family-wise error (FWE) correction, and significance was defined as $pFWE < 0.05$.

Post-hoc Group Comparisons

To investigate both overall and localized group differences, two sets of summary metrics were analyzed. Whole-tract average values for FD, LogFC, and FDC were extracted across the entire CReST to summarize broader patterns of micro- and macrostructural properties across the tract. Additionally, post-hoc averages were calculated from fixels that showed significant group differences ($pFWE < 0.05$) for each FBA metric to illustrate magnitude and within-group variability across the significant voxels capturing localized effects.

Associations Between Fiber Density and Balance and Mobility

To examine the relationship between CReST FD and functional outcomes, average FD values across the whole tract were correlated with balance and mobility measures, including performance on the miniBEST, CoP path length during static balance testing, gait speed, and TUG test. In participants with MS, additional exploratory correlations were conducted using FD values from fixels that showed significant group differences and lesion volume within the CReST and

functional outcomes (Table D1, Appendix D). All correlation analyses were corrected for multiple comparisons using the false discovery rate (FDR), with statistical significance defined as $pFDR < 0.05$.

Statistical Approach

All statistical analyses were conducted in R Statistical Software (version 4.4.2; R Core Team, Vienna, Austria, 2024). Normality of distributions was assessed with the Shapiro-Wilk test and visualized using quantile-quantile plots. Levene's test was used to evaluate the equality of variance. Group comparisons were conducted using Student's t-tests when the data met the assumptions of normality and equal variances. For data with unequal variances, Welch's t-tests were applied, and for non-normally distributed data, Mann-Whitney U tests were used. Group differences in sex distribution were assessed using a chi-squared test. Correlations between tract-based measures and functional outcomes were assessed using Spearman's rank correlation for variables that were ordinal or did not follow a normal distribution, such as miniBEST scores, MSWS-12, and static balance metrics. Pearson's correlation was used for outcomes that were continuous and normally distributed, such as gait speeds. Correlation strengths were interpreted using standard thresholds: very weak (0.00 – 0.19), weak (0.20 – 0.39), moderate (0.40 – 0.59), strong (0.60 – 0.79), and very strong (0.80 – 1.00).[96]

Results

Participant Characteristics, Brain Volumetrics, and Disability Scores

A summary of participant characteristics, brain volumetrics, and disability scores is presented in Table 5.1. No significant differences were observed between participants with MS and NT controls for age, sex, height, weight, or body mass index. While MS participants exhibited larger eTIV on average compared to NT controls, this difference did not reach statistical

significance. Lesion segmentation in the MS cohort revealed a mean total lesion burden of 9.54 ± 12.18 mL, with lesions overlapping an average of 2.21 ± 1.41 mL of the CReST. Participants with MS reported mild to moderate disability, with EDSS scores ranging from 0 to 4.5, and a median score of 4. Among the FSS subcomponents, pyramidal (median = 3, IQR = 2.5) and sensation (median = 3, IQR = 3) had the highest reported scores.

Table 5.1. Participant Characteristics, Brain Volumetrics, Clinical Disability, Balance, and Mobility Measures. Data in each subsection are presented as mean and standard deviation, unless indicated by ‡, in which case data are presented as median and interquartile range. Statistical comparisons were performed using independent t-tests[a], χ^2 tests[b], Mann–Whitney U tests[c], or Welch's t-tests[d]. Multiple comparisons were corrected using the false discovery rate (*pFDR*). **Bolded** values indicate statistical significance (*pFDR* < 0.05).

Abbreviations: M – Mean; SD – Standard Deviation; BMI – Body Mass Index; eTIV – Estimated Total Intracranial Volume; CReST – Corticoreticulospinal Tract; EDSS – Expanded Disability Status Scale; FSS – Functional System Score; APC – Anticipatory Postural Adjustments; RPC – Reactive Postural Control; SO – Sensory Orientation; DG – Dynamic Gait; CoP – Center of Pressure; TUG – Timed-Up and Go; MSWS-12 – Twelve Item Multiple Sclerosis Walking Scale.

Variable (unit)	Multiple Sclerosis		Neurotypical		*p-value*	*pFDR-value*
	M	*SD*	*M*	*SD*		
Characteristics						
Age (years)	49.01	11.98	46.95	15.2	0.577 [a]	-
Sex (female/male)	18/9	-	21/8	-	0.860 [b]	-
Height (cm)	166.18	7.54	168.78	8.11	0.221 [a]	-
Weight (kg)	69.60	8.18	72.37	14.24	0.780 [c]	-
BMI (kg/m^2)	25.31	3.48	25.3	4.05	0.724 [c]	-
Disease Duration (years)	13.07	10.71	-	-	-	-
Brain Volume						
eTIV (mL)	1549.63	165.13	1447.34	216.23	0.066 [c]	-

Total Lesion Volume (mL)	9.54	12.18	-	-	-	-
CReST Lesion Volume (mL)	1.41	2.21	-	-	-	-
Disability Scores[‡]						
EDSS	4	0.75	-	-	-	-
Pyramidal FSS	3	2.5	-	-	-	-
Cerebellar FSS	2	1.75	-	-	-	-
Sensation FSS	3	3	-	-	-	-
Bladder FSS	1	1.75	-	-	-	-
Vision FSS	1	2	-	-	-	-
Brainstem FSS	0	2	-	-	-	-
Cerebral FSS	2	3	-	-	-	-
Mini-Balance Evaluation Systems Test						
Total Score	24.63	5.00	28.97	2.47	**0.001** [c]	**0.001**
APA	6.11	1.85	7.17	1.14	**0.040** [c]	**0.040**
RPC	5.81	1.55	7.31	0.89	**<0.001** [c]	**0.001**
SO	5.52	0.75	5.93	0.26	**0.011** [c]	**0.014**
DG	7.19	1.71	8.55	1.09	**0.001** [c]	**0.002**
Static Balance (CoP Path Length (cm))						
Eyes-open Firm	70.50	36.19	51.85	14.64	0.101 [c]	0.144
Eyes-open Compliant	137.24	64.36	106.17	30.53	0.144 [c]	0.144
Mobility						
Preferred Walk Speed (m/s)	1.12	0.20	1.25	0.11	**0.005** [d]	**0.005**

Fast Walk Speed (m/s)	1.42	0.29	1.67	0.18	**<0.001** [d]	**0.001**
TUG (s)	17.98	4.06	15.63	3.11	**0.005** [c]	**0.005**
MSWS-12	28.13	41.15	-	-	-	-

Balance and Mobility Group Comparison

Participants with MS produced significantly lower scores on the miniBEST total score (*pFDR* = 0.001) and all subcomponents compared to controls, APA (*pFDR* = 0.04), RPC (*pFDR* = 0.001), SO (*pFDR* = 0.014), DG (*pFDR* = 0.002) (Table 5.1).

No significant differences were observed for CoP path length between participants with MS and NT controls for eyes-open firm condition (*pFDR* = 0.144) and eyes-open compliant condition (*pFDR* = 0.144) (Table 5.1).

Participants with MS had slower walking speeds in both self-selected preferred (*pFDR* = 0.005) and fast walking (*pFDR* = 0.001) conditions, as well as slower TUG times (*pFDR* = 0.005) compared with NT controls (Table 5.1). Participants with MS reported a median MSWS-12 of 28.13 (Table 5.1).

FBA Group Comparison

Group comparisons revealed localized micro- and macrostructural reductions within the CReST in participants with MS relative to NT controls, with statistically significant differences (*pFWE* < 0.05) observed in all three FBA metrics, FDC, FD, and LogFC. Streamline segments corresponding to significant fixels for each metric are visualized in Figure 5.2, where blue indicates fixels exhibiting significant group differences.

Significant FDC reductions in participants with MS compared to NT controls were identified in 16.52% of CReST fixels. These fixels were primarily located along fibers projecting

from the primary sensorimotor cortices in both hemispheres, extending from the centrum semiovale through the corona radiata and posterior limb of the internal capsule to the pons varolii of the brainstem (Figure 5.2a).

Significant reductions in FD were more spatially limited, present in only 0.60% of fixels. These differences were confined to the right hemisphere, predominantly involving fibers in the frontal lobe, anterior corona radiata, and anterior limb of the internal capsule. (Figure 5.2b).

LogFC showed the most extensive group differences, with 23.70% of fixels demonstrating significantly reduced values in participants with MS compared to NT participants. These reductions were primarily observed in bilateral centrum semiovale beneath the primary motor and somatosensory cortices, extending through the corona radiata, posterior limb of the internal capsule, and through the brainstem. Additional differences were located anterior to the primary sensorimotor projections in the corona radiata, in regions corresponding to premotor pathways (Figure 5.2c).

Tract-averaged comparisons, calculated by averaging fixel values for each metric across the entire CReST, did not reveal statistically significant group differences for FDC (MS: 0.45 ± 0.04, NT: 0.47 ± 0.04, $p = 0.063$, $pBON = 0.189$) (Figure 5.3a). While mean FD (MS: 0.46 ± 0.01, NT: 0.47 ± 0.02, $p = 0.030$, $pBON = 0.090$) was lower in the MS group compared to controls, this difference did not remain significant after correction for multiple comparisons (Figure 5.3b). There were no significant group differences observed for LogFC (MS: -0.03 ± 0.09, NT: -0.01 ± 0.08, $p = 0.547$, $pBON = 1$) (Figure 5.3c).

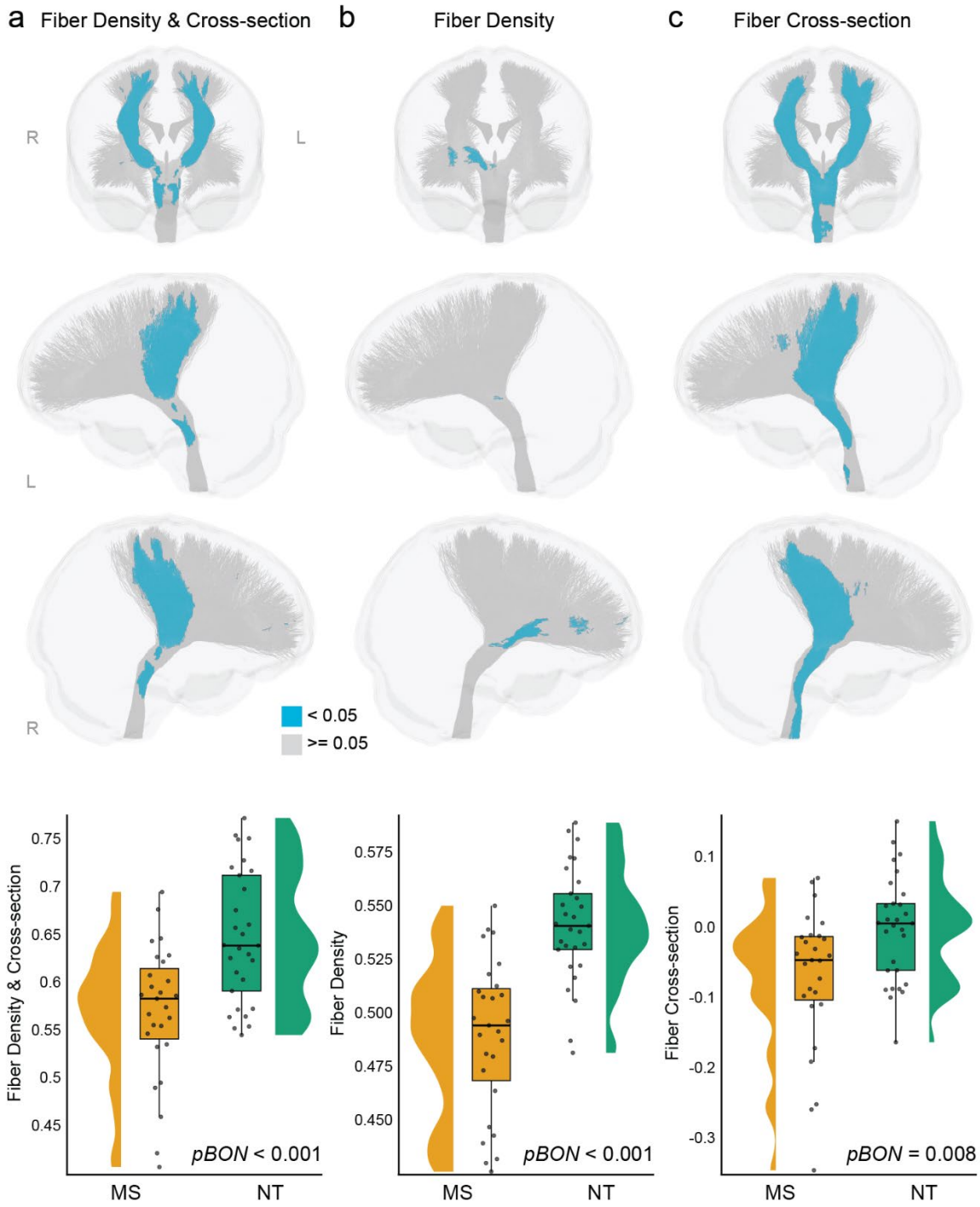

Figure 5.2. Fixel-Based Analysis Group Comparison. Regions within the CReST showing significant differences in FBA metrics between participants with MS and NT controls. Streamline segments corresponding to significant fixels (*pFWE* < 0.05) *are shown in blue*. Boxplots display within-group variability across the significant fixels for each metric. Comparisons are Bonferroni corrected (*pBON*). a) Decreased fiber density and cross-section in MS compared to NT controls. b) Decreased fiber density in MS compared to NT controls. c) Decreased fiber cross-section in MS compared to NT controls. Fiber cross-section is displayed on a logarithmic scale.

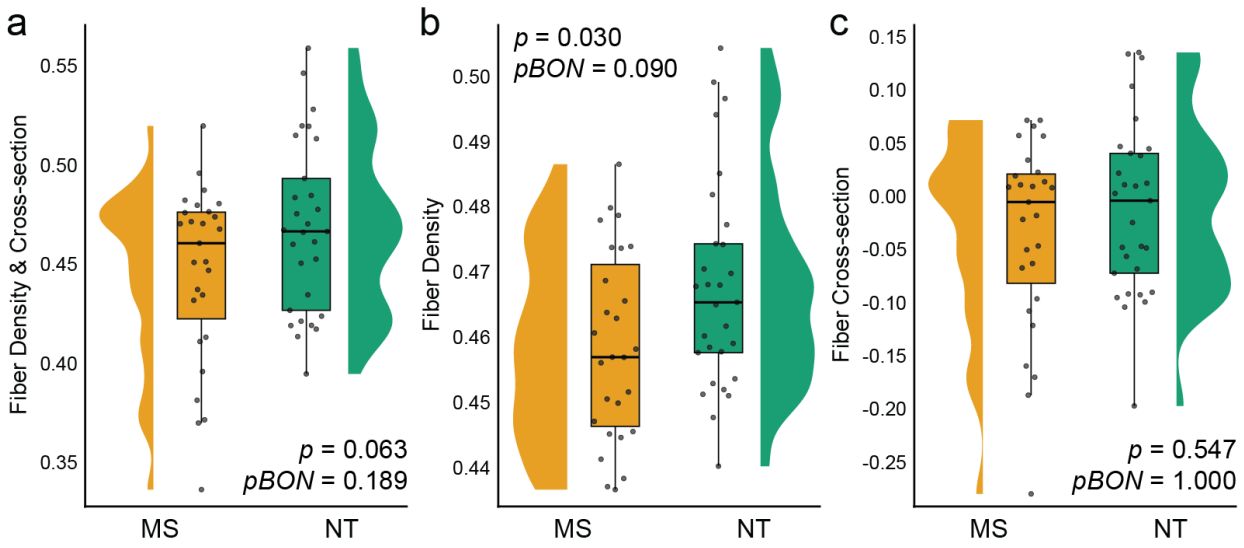

Figure 5.3. Whole-Tract Averaged Fixel-Based Analysis Group Comparison. Comparison of fixel-based metrics averaged across the entire CReST between participants with MS and NT controls. Uncorrected *p-values* and Bonferroni corrected *p-values* (*pBON*) are provided. a) No statistically significant difference in average fiber density and cross-section between MS and NT groups. b) No statistically significant difference in average fiber density between MS and NT groups. c) No statistically significant difference in average fiber cross-section between MS and NT groups. Fiber cross-section values are displayed on a logarithmic scale.

Associations Between Corticoreticulospinal Tract Fiber Density and Balance and Mobility

In participants with MS, average FD in the CReST had significant moderate correlations with the miniBEST total score (*rho* = 0.51, *pFDR* = 0.023), as well as APA (*rho* = 0.41, *pFDR* = 0.049) and RPC (*rho* = 0.49, *pFDR* = 0.023) subcomponents. Weak correlations were observed between FD and SO (*rho* = 0.37, *pFDR* = 0.061) and DG (*rho* = 0.37, *pFDR* = 0.061), which approached but did not meet statistical significance (Table 5.2). A similar associative pattern was observed in NT controls, with significant moderate to strong correlations between average CReST FD and miniBEST total score (*rho* = 0.60, *pFDR* = 0.002), APA (*rho* = 0.59, *pFDR* = 0.002), and RPC (*rho* = 0.54, *pFDR* = 0.004). DG (*rho* = 0.34, *pFDR* = 0.084) showed a weak correlation that was not significant, and SO (*rho* = 0.08, *pFDR* = 0.675) demonstrated a very weak correlation and was not statistically significant in NT controls (Table 5.2).

Table 5.2. Associations Between Fiber Density and Mini-Balance Evaluation Systems Test. Spearman's rank correlation coefficients (*rho*) are presented for associations between average fiber density of the CReST and the miniBEST total score and its subcomponents. Both uncorrected *p-values* and false discovery rate-corrected values are shown. Statistically significant associations after FDR correction (*pFDR* < 0.05) are indicated in **bold**.

Abbreviations: APC – Anticipatory Postural Adjustments; RPC – Reactive Postural Control; SO – Sensory Orientation; DG – Dynamic Gait.

	Multiple Sclerosis Fiber Density			Neurotypical Fiber Density		
Variable	*rho*	*p-value*	*pFDR-value*	*rho*	*p-value*	*pFDR-value*
Mini-Balance Evaluation Systems Test						
Total Score	0.51	**0.007**	**0.023**	0.60	**0.001**	**0.002**
APA	0.42	**0.030**	**0.049**	0.59	**0.001**	**0.002**
RPC	0.49	**0.009**	**0.023**	0.54	**0.003**	**0.004**
SO	0.37	0.057	0.061	0.08	0.675	0.675
DG	0.37	0.061	0.061	0.35	0.067	0.084

For static balance, average FD in the CReST showed significant moderate correlations with CoP path length during both the eyes-open firm (*rho* = -0.40, *pFDR* = 0.041) and eyes-open compliant (*rho* = -0.49, *pFDR* = 0.027) conditions among participants with MS (Figure 5.4a-b). In NT controls, a significant moderate correlation was found for the eyes-open firm condition (*rho* = -0.49, *pFDR* = 0.020), while the eyes-open compliant condition showed a trend toward significance (*rho* = -0.38, *pFDR* = 0.053) (Figure 5.4c-d).

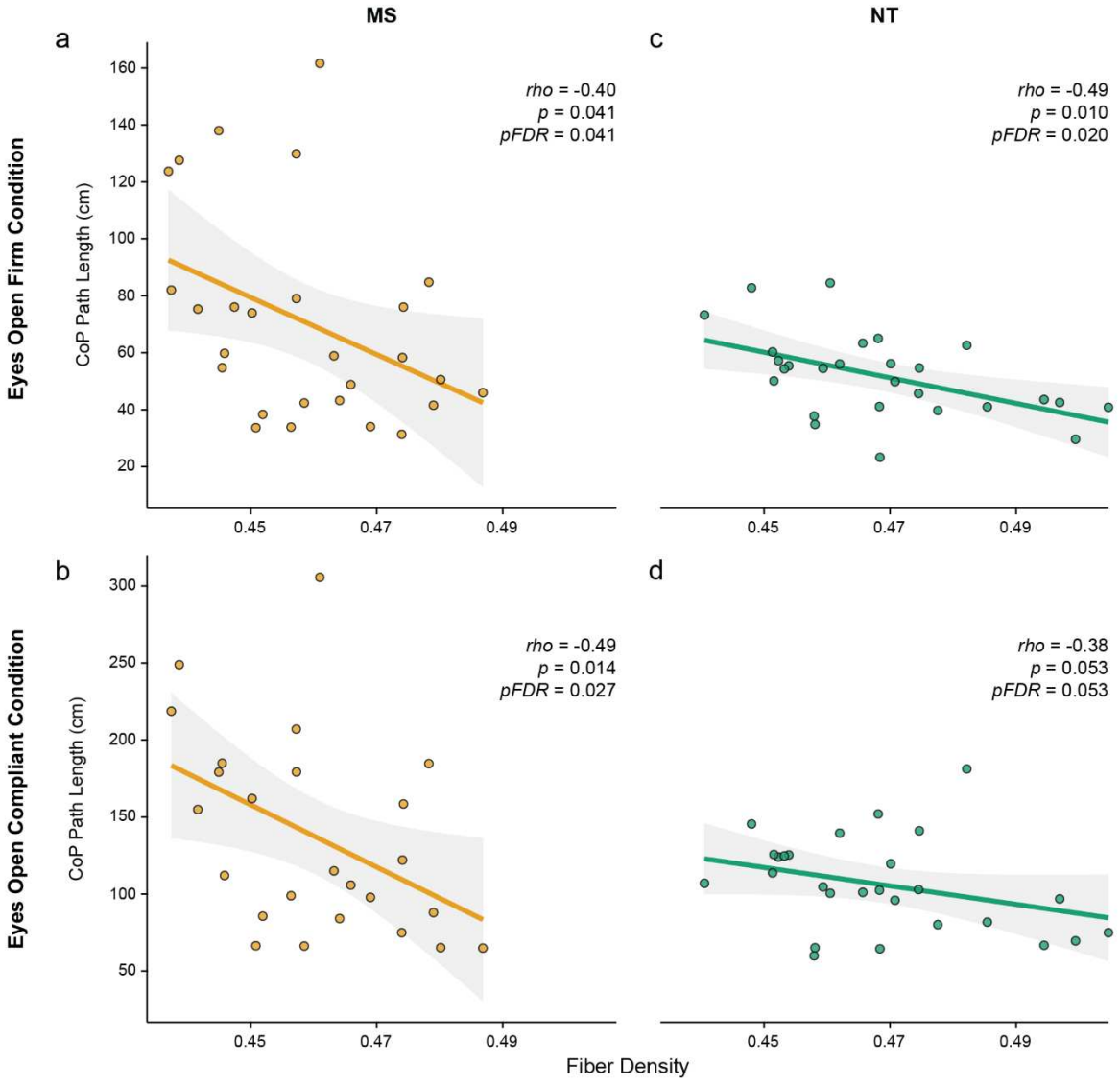

Figure 5.4. Associations Between Fiber Density and Static Balance. Spearman's rank correlation coefficients (*rho*) are presented for associations between average FD of the CReST and CoP path length during static balance assessments in participants with MS and NT controls. Both uncorrected *p-values* and false discovery rate-corrected values (*pFDR*) are reported. a) Moderate negative correlation between average FD and eyes-open firm surface condition in participants with MS. b) Moderate negative correlation between average FD and eyes-open compliant surface condition in participants with MS. c) Moderate negative correlation between average FD and eyes-open firm surface condition in NT controls. d) Weak negative correlation between average FD and eyes-open compliant surface condition in NT controls.

Associations with mobility outcomes showed participants with MS exhibited significant moderate to strong correlations between average CReST FD and both preferred walking speed (r = 0.63, $pFDR$ = 0.002) and fast walking speed (r = 0.57, $pFDR$ = 0.004), as well as a moderate negative correlation with TUG time (r = -0.50, $pFDR$ = 0.010) (Figure 5.5a-c). Additionally, a moderate negative correlation was also found between FD and MSWS-12 (rho = -0.48, $pFDR$ = 0.014) in participants with MS (Figure 5.5d). Among NT controls, no significant associations were found between average CReST FD and mobility outcomes. Correlations for preferred (r = 0.02, $pFDR$ = 0.936) and fast walking speed (r = 0.19, $pFDR$ = 0.474) were very weak, and the association with TUG time was weak (rho = -0.30, $pFDR$ = 0.336).

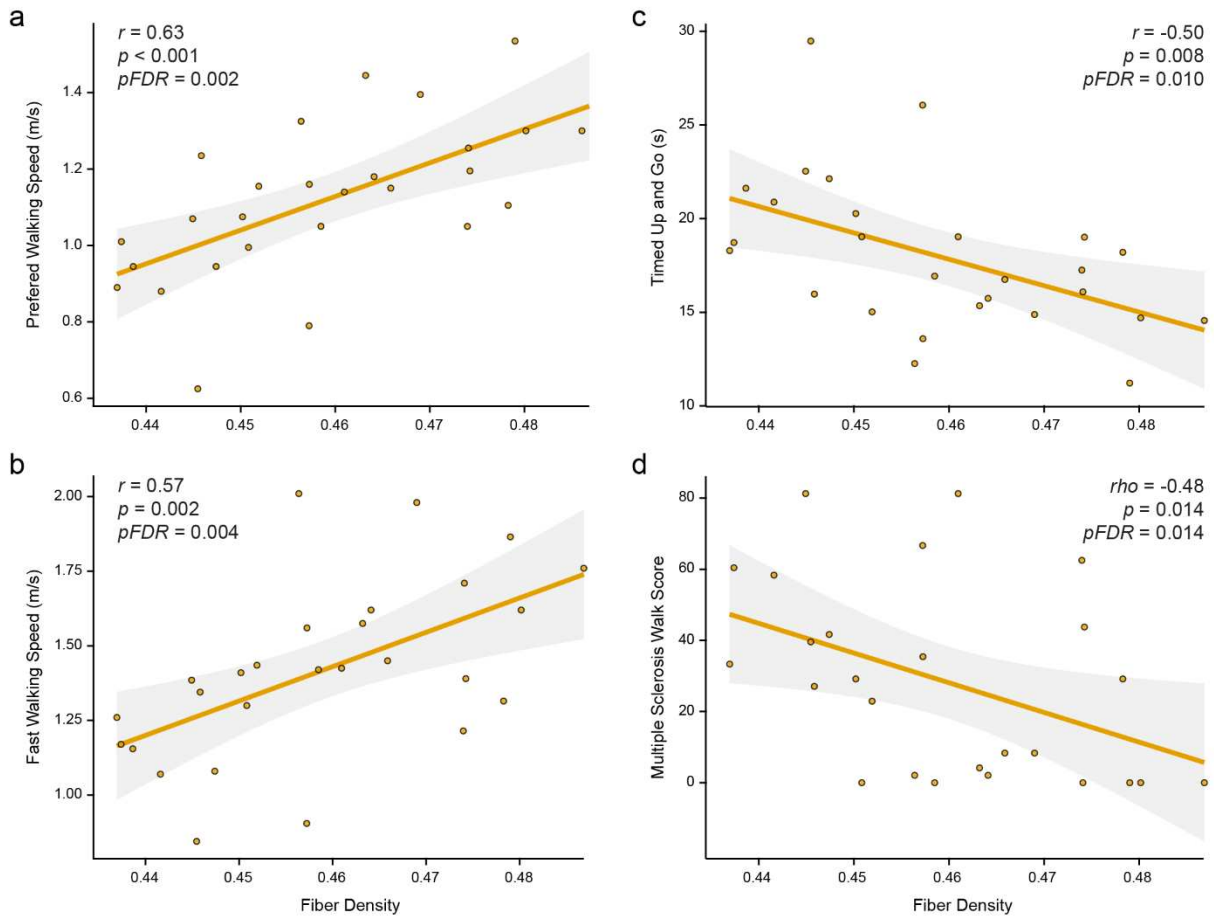

Figure 5.5. Associations Between Fiber Density and Mobility Measures in People with Multiple Sclerosis. Pearson's correlation coefficients (r) are presented for associations between

average FD of the CReST and walking speeds and TUG test performance in participants with MS. Spearman's rank correlation coefficient (*rho*) is presented for the association between average CReST FD and the MSWS-12. Both uncorrected *p-values* and false discovery rate–corrected values (*pFDR*) are reported. a) Strong positive correlation between average FD and preferred walking speed. b) Moderate positive correlation between average FD and fast walking speed. c) Moderate negative correlation between average FD and TUG test time. d) Moderate negative correlation between average FD and MSWS-12 score.

Associations Between Corticoreticulospinal Tract Fiber Density and Age

A moderate correlation was observed between age and average CReST FD in both participants with MS (r = -0.47, p = 0.013) and neurotypical controls (r = -0.59, p = 0.001).

Discussion

This study evaluated the micro- and macrostructural characteristics of the CReST in individuals with MS compared to age- and sex-matched NT controls using FBA. The results revealed significant reductions in both microstructural and macrostructural integrity within localized regions of the CReST in participants with MS compared to NT controls. Macrostructural deficits were most prominent in fibers originating from primary sensorimotor regions, whereas microstructural alterations were concentrated near the anterior limb of the right internal capsule. Average FD within the CReST was significantly associated with balance performance in both participants with MS and NT participants, and with mobility outcomes in the participants with MS. Together, these findings represent the first study to assess CReST structural integrity in individuals with MS and to link it to mobility and balance outcomes, suggesting that the CReST is a relevant neural pathway contributing to motor function in this population.

Balance and Mobility Impairments in MS Participants

Assessment of balance using the miniBEST revealed significantly poorer performance in participants with MS compared to NT controls. Significant group differences were observed for total score and across all subcomponents, APA, RPC, SO, and DG, indicating that individuals with

MS with mild to moderate disability exhibit impairments across multiple balance systems (Table 5.1). These findings are consistent with previous studies demonstrating that balance impairments can emerge early in the disease course and may even precede a formal MS diagnosis in some individuals.[8,97,98]

In contrast, no significant group differences were observed in static balance during either the eyes-open firm or eyes-open compliant surface conditions (Table 5.1). Although participants with MS exhibited longer average CoP path lengths (~20 cm in the firm condition and ~30 cm in the compliant condition), high within-group variability likely prevented these differences from reaching statistical significance. This was unexpected, particularly given the observed group differences in the SO subcomponent of the miniBEST. However, this discrepancy may be due to the SO subcomponent including more challenging conditions (eyes-closed on a compliant surface and eyes-closed on an inclined surface) that were not captured in this study's CoP path length measurements. Additionally, it was anticipated that group differences would emerge under the compliant condition, which is designed to challenge proprioceptive function, a known area of deficit in MS.[99–101] These findings contrast with previous studies, which reported significant differences in sway velocity under the same conditions in individuals with MS with low EDSS scores compared to NT controls.[102]

Notably, CoP path lengths in NT participants exceeded normative values previously reported for community-dwelling adults of similar age.[103] This may be attributable to methodological differences in this study's testing protocol, including longer trial durations and a narrower stance, feet together vs. shoulder-width, both of which may increase postural sway. Although some literature in populations with vestibular dysfunction has suggested that foot

position may influence balance performance, the reported impact was minimal and statistically insignificant.[66]

Mobility assessments also indicated apparent deficits in participants with MS compared to NT controls, consistent with the study hypotheses. Participants with MS walked significantly slower than NT controls at both self-selected preferred walking speed and fast walking speeds (Table 5.1). Additionally, performance on the TUG test was significantly slower in the MS group (Table 5.1), further supporting the presence of group differences in functional mobility. These findings align with previous studies reporting slower gait and reduced functional mobility in individuals with MS with low EDSS scores.[104–106] In addition, the MS group scored a median of 28.12 on the MSWS-12 (Table 5.1), indicating early perceived impairments that impact gait and activities of daily living.[107]

Taken together, these findings indicate that individuals with MS with mild to moderate disability exhibit measurable impairments in both clinical balance and mobility performance compared to matched NT controls.

FBA Structural Differences in the CReST

The present study revealed significant micro- and macrostructural reductions within the CReST in individuals with MS compared to matched NT controls. Although all FBA metrics demonstrated statistically significant differences, the spatial patterns and extent of these differences varied across metrics, providing insight into the nature and distribution of MS-related alterations in white matter integrity.

FDC, an integrated measure that captures both microstructural and macrostructural integrity, identified significant reductions in participants with MS compared to NT controls in 16.5% of fixels, predominantly along fibers projecting from the primary sensorimotor cortices

(Figure 5.2a). In contrast, significant group differences in FD, reflecting microscopic intra-axonal loss, were confined to a small proportion of fixels (0.6%), localized primarily in the right frontal white matter and anterior limb of the internal capsule (Figure 5.2b). LogFC exhibited the most extensive group differences, with significant reductions in MS participants compared to NT controls detected in 23.7% of CReST fixels. These reductions spanned fibers descending from the primary motor and somatosensory cortices, extending through the brainstem (Figure 5.2c). These patterns are consistent with previous FBA studies in MS, which have similarly reported spatially localized reductions in FDC, FD, and LogFC across various white matter tracts, although the CReST has not been previously examined.[24,108–110]

While FBA revealed spatially specific differences in white matter integrity across all three metrics, tract-averaged comparisons yielded a more conservative characterization of group differences. Neither FDC, FD, nor LogFC showed significant group differences when averaged across the entire CReST, suggesting that while localized differences exist near the primary motor and somatosensory pathways, these metrics are largely similar across the rest of the CReST. Taken together, these results indicate that while localized white matter disruptions are detectable across all metrics, global differences in structural integrity across the full CReST are not statistically significant in this cohort.

These findings raise the possibility of partial neural sparing within the CReST that may support preserved motor function despite evidence of localized structural damage.[45–47,53,57,111,112] The CReST is composed of widespread cortical projections, including inputs from frontal, premotor, primary motor, and somatosensory regions, potentially conferring a degree of resilience to focal injury.[53,57] Compared to the CST, which is more topographically constrained, the broader anatomical distribution of the CReST may limit the functional impact of localized lesions. For

example, a focal lesion within the CST may disrupt a larger proportion of its motor fibers, whereas a similar lesion within the CReST might affect a smaller proportion of its more diverse projections.[57] This is supported by the current study's findings, which show white matter abnormalities in specific subregions of the CReST in participants with MS. However, the absence of statistically significant group differences at the whole-tract level suggests that comparable structural integrity is maintained across the whole tract.

Further investigation is warranted to determine whether the location and extent of CReST involvement differentially influence motor outcomes in MS, and whether specific subcomponents of the tract confer greater vulnerability or potential for compensation. Identifying these patterns may improve understanding of motor reserve in clinical populations.

Associations Between Fiber Density and Balance and Mobility

The results of this study reveal that microstructural integrity within the CReST, measured by FD, is significantly associated with balance and mobility outcomes in individuals with MS. In NT controls, FD was also associated with balance outcomes. Both groups showed significant associations between the average CReST FD and the total miniBEST score, as well as between APA and RPC subcomponents (Table 5.2). The association between higher FD and improved APA and RPC performance suggests that greater microstructural integrity of the CReST supports more effective postural planning and responses in both MS and NT populations. These findings align with evidence from prior studies, which show that the reticulospinal system is involved in generating APAs, likely mediated through input from the supplementary motor area and premotor cortex. The findings also align with the CReST contributes to RPC, as the ReST is considered a key pathway mediating startle and rapid automatic responses.[29,113–115] Supporting this framework, research on people with MS has shown that white matter integrity within tracts projecting from

the pedunculopontine nucleus of the reticular formation is significantly associated with delayed tibialis anterior onset latency following perturbations, tying other areas of the reticular formation to reactive postural control,[116] Together, these converging findings highlight the relevance of the reticulospinal system, in maintaining postural stability and suggest that its disruption may contribute to impaired balance in MS.

DG demonstrated a trend toward significance in both groups but did not reach statistical significance thresholds (Table 5.2). DG tasks such as stepping over obstacles and walking with head turns likely depend on additional neural structures that influence coordination and visual input,[117,118] potentially reflecting weaker associations with CReST-specific microstructure. The lack of statistical significance may also reflect limited statistical power, and future studies with larger samples may detect significant effects. SO, which assesses balance across various surface conditions, showed a trend toward significance but was not statistically significant in the MS group. No meaningful trends or associations were observed in NT participants, likely due to a ceiling effect in this subcomponent for controls, as most scored the maximum score (Table 5.2).[65]

While the miniBEST is a clinically validated tool for assessing balance, its ordinal scoring limits the granularity of functional characterization. For example, a score of 6 on the SO subcomponent simply reflects whether a participant maintained their postural control for the entire trial, but not the degree of postural sway exhibited.[65] To address this limitation, we incorporated additional continuous measures using the mCTSIB. However, nearly 30% of MS participants (n = 8) were unable to complete the eyes-closed conditions due to loss of balance and a need for assistance, resulting in incomplete CoP path length data. Consequently, only the eyes-open conditions are reported. This high failure rate highlights a heavy reliance on visual input for postural control in some individuals with MS.[119–121]

In both eyes-open conditions, average FD in the CReST was significantly associated with CoP path length in participants with MS (Figure 5.3a-b). Among NT participants, a significant association was observed in the eyes-open firm condition, with a trend toward significance in the eyes-open compliant condition (Figure 5.3c-d). Prior research has shown that the ReST facilitates postural muscle tone and automatic adjustments via descending projections from the brainstem to spinal motor circuits.[28,114,116] Further evidence from stroke research indicates that damage to CReST fibers is associated with postural instability, highlighting the pathway's role in balance control.[122]

Altogether, the evidence suggests that damage to the CReST may impair descending motor commands, reducing the effectiveness or delaying corrective movements and resulting in increased postural sway. The present findings further establish a link between CReST microstructural integrity and balance control under conditions with visual input. Future studies should further examine its role in the absence of visual input to better delineate the tract's contribution to sensory integration during postural control.

Associations between average FD and mobility outcomes further connect CReST microstructural integrity and motor function in people with MS. In individuals with MS, higher average FD was significantly associated with better performance on mobility measures, including self-selected preferred and fast walking speeds, as well as the TUG test (Figure 5.4a-c). These findings suggest that greater integrity of the CReST supports more efficient gait and mobility. This finding is consistent with prior stroke research, which has linked the preservation of CReST to improved walking outcomes.[46–50] Similar associations have been reported in aging populations, where greater brain, gray matter, and white matter volumes are correlated with faster gait speeds.[123] Furthermore, CReST FD was significantly correlated with perceived walking impairment, as

measured by the MSWS-12 (Figure 5.4d), indicating that individuals with denser CReST microstructure not only perform better on objective functional assessments but also report fewer subjective walking limitations.

The balance-related findings in MS participants were corroborated by analyses using the mean FD from fixels that showed significant between-group differences. This suggests that microstructural degeneration unique to MS may contribute to balance impairment (Table D1, Appendix D). Notably, these fixels were localized to the right frontal white matter and the anterior limb of the internal capsule. Prior research has shown that damage to the right hemisphere disproportionately impairs balance compared to damage to the left hemisphere in stroke.[124–126] In individuals with MS, proprioceptive balance deficits have also been linked to reduced structural integrity in the right hemisphere, specifically in Brodmann area 3a.[15] These findings suggest that balance control may be more influenced by right hemisphere structural damage, aligning with the right-lateralized microstructural differences observed in the present study.

In contrast, walking outcomes were not significantly associated with these lateralized significant fixels (Table D1, Appendix D). This discrepancy may result from the limited number of locomotor-related cortical projections that pass through the anterior limb of the internal capsule. As a result, contributions from regions such as the supplementary motor area, premotor cortex, and primary sensorimotor cortices are not represented, potentially omitting information that is better reflected in the whole-tract average FD.[29] However, other studies have linked frontal cortical regions to walking performance.[54–56,127,128] It's possible that while the right frontal damage observed here may contribute to balance impairments, its unilateral nature may have a limited impact on walking performance.

Lesion segmentation analyses further support the role of the CReST in functional outcomes in MS. Lesion volume within the CReST was significantly correlated with all balance and mobility metrics (Table D1, Appendix D), indicating that a greater lesion burden along the CReST is associated with greater functional impairments. These findings are consistent with the idea that greater preservation of descending white matter pathways may support better motor and postural outcomes. Given the diverse projections of the CReST, which contain fibers from frontal, premotor, and sensorimotor regions, lesions affecting this pathway are likely to be distributed heterogeneously across individuals. This variability in lesion location may reduce the ability of group-level FBA comparisons of this sample size to detect consistent localized effects, as the lesions do not align spatially across participants.

In MS participants and NT controls, age appears to be a significant factor influencing the relationship between CReST FD and balance performance. Age was significantly associated with average FD in the CReST in both groups, suggesting that age-related microstructural changes in this tract may contribute to alterations in postural control. Given that aging is known to affect white matter integrity and is linked to declines in motor and balance function,[129–132] the CReST may play a role in maintaining postural stability across the lifespan. These findings point to the potential relevance of the CReST in MS and healthy aging and support its inclusion in future research investigating neuroanatomical contributors to age-related sensorimotor decline.

Together, this study underscores the functional relevance of CReST microstructural integrity in both balance and mobility in people with MS. The results suggest white matter integrity of the CReST supports anticipatory and reactive postural control, static balance, and gait performance, aligning with both objective and subjective functional measures in individuals with MS. These findings expand current understanding of descending motor pathways in MS and

highlight potential neural targets for intervention aimed at preserving or enhancing motor function in clinical and aging populations.

Resistance Training and the Reticulospinal System

Literature suggests that strength training can induce adaptations at both the muscular and neural levels.[133–136] While evidence for CST adaptations following resistance training remains mixed,[137] a recent study in nonhuman primates reported increased reticulospinal responses following a progressive resistance training intervention.[138] These enhancements were attributed to stronger mono- and disynaptic connections within the ReST, resulting in increased synaptic efficacy, highlighting the ReST as a potential mediator of strength adaptations.

In humans, the contribution of the ReST to strength training adaptations remains unclear, however, its role in force generation is supported by several lines of evidence. For example, studies in individuals with cortical stroke and spinal cord injury have shown that some patients can still produce forceful gross motor outputs in the affected limb despite CST damage, likely reflecting compensation via the ReST.[42,139] Additionally, the StartReact paradigm, which elicits rapid and forceful movements in response to startling stimuli, is believed to be mediated by the reticulospinal system, further linking its involvement in generating powerful, automatic motor responses.[115]

Taken together, these findings suggest that the ReST likely contributes to both strength and functional mobility and may mediate adaptations in progressive strength training. Given the present study's findings linking greater CReST microstructural integrity with better motor performance in individuals with MS, and preliminary evidence that resistance training may enhance synaptic efficacy in this pathway, progressive resistance training emerges as a promising and feasible rehabilitation approach to improve mobility in MS. Many studies have demonstrated

the functional benefits of strength training in MS,[140,141] but whether these improvements are mediated by plasticity in the CReST should be the focus of future research.

Limitations

Several limitations warrant consideration. First, the diffusion-weighted imaging protocol employed in this study included b-values lower than those typically recommended for optimal fixel-based analysis (e.g., b = 3000 s/mm²), which may have reduced the sensitivity and specificity of the FBA metrics.[85,142] Nonetheless, existing literature supports that FBA methods provide more precise outcomes than tensor models, even when using lower b-values.[143] Second, the anatomical delineation of the CReST was derived from tractography seeded from the primary somatosensory cortex extending through frontal regions. This approach was informed by retrograde tracing studies in rodents and limited behavioral data,[53] but it remains uncertain whether the human CReST extends as far anteriorly, potentially impacting the anatomical accuracy of the streamlines used in this study.

Third, a subset of participants with MS were unable to complete the mCTSIB eyes-closed conditions, resulting in no data and limiting the analysis of postural sway under visual deprivation. Future studies should consider alternative or complementary methods for capturing continuous indicators of postural control that are feasible across all conditions and participant abilities. Fourth, the study sample included only individuals with relapsing-remitting MS and mild to moderate disability (EDSS ≤ 4.5), which may limit the generalizability of findings to individuals with more advanced or progressive disease. Inclusion of a broader clinical spectrum in future work is necessary to determine whether the observed diffusion-behavior relationships are conserved across disease phenotypes and severities. Lastly, both groups had a disproportionate number of female participants, consistent with MS prevalence patterns.[144] However, potential sex-related differences

in neuroanatomy and behavior may contribute to observed variability and should be acknowledged as a possible source of bias.

Conclusion

This study provides novel evidence linking microstructural integrity of the CReST to balance and mobility function in individuals with MS. Using FBA, white matter structural integrity differences were identified between participants with MS and age- and sex-matched NT controls. The spatial distribution of group differences varied by metric, with macrostructural reductions primarily observed in fibers projecting from the primary sensorimotor cortices, and microstructural reductions localized to the right anterior limb of the internal capsule in participants with MS. Whole-tract average FD in the CReST correlated with balance and mobility performance in the MS group, highlighting a link between microstructural integrity and motor outcomes. Similar associations with balance were also observed in NT participants, suggesting that CReST microstructure may support motor function across both MS and NT populations. Future work should expand on these findings by examining the CReST's influence on motor outcomes across broader MS phenotypes and other clinical and aging populations. Collectively, these findings contribute to a growing body of literature demonstrating the role of descending motor pathways beyond the CST in sensorimotor function in MS

References

1. Walton, C. *et al.* Rising prevalence of multiple sclerosis worldwide: Insights from the Atlas of MS, third edition. *Multiple Sclerosis Journal* **26**, (2020).
2. Ghasemi, N., Razavi, S. & Nikzad, E. Multiple sclerosis: Pathogenesis, symptoms, diagnoses and cell-based therapy. *Cell Journal* vol. 19 Preprint at (2017).
3. Horng, S. & Fabian, M. The pathophysiology and clinical presentation of multiple sclerosis. in *Handbook of Relapsing-Remitting Multiple Sclerosis* (2017). doi:10.1007/978-3-319-40628-2_2.
4. Smith, K. J. & McDonald, W. I. The pathophysiology of multiple sclerosis: The mechanisms underlying the production of symptoms and the natural history of the disease. *Philosophical Transactions of the Royal Society B: Biological Sciences* **354**, (1999).
5. Criste, G., Trapp, B. & Dutta, R. Axonal loss in multiple sclerosis. Causes and mechanisms. in *Handbook of Clinical Neurology* vol. 122 (2014).
6. Green, R., Cutter, G., Friendly, M. & Kister, I. Which symptoms contribute the most to patients' perception of health in multiple sclerosis? *Mult Scler J Exp Transl Clin* **3**, (2017).
7. Peterson, E. W., Cho, C. C., von Koch, L. & Finlayson, M. L. Injurious Falls Among Middle Aged and Older Adults With Multiple Sclerosis. *Arch Phys Med Rehabil* **89**, (2008).
8. Moen, S. M., Celius, E. G., Nordsletten, L. & Holmøy, T. Fractures and falls in patients with newly diagnosed clinically isolated syndrome and multiple sclerosis. *Acta Neurol Scand* **124**, (2011).
9. Tinetti, M. E., Doucette, J., Claus, E. & Marottoli, R. Risk Factors for Serious Injury During Falls by Older Persons in the Community. *J Am Geriatr Soc* **43**, (1995).
10. Peterson, E. W., Cho, C. C. & Finlayson, M. L. Fear of falling and associated activity curtailment among middle aged and older adults with multiple sclerosis. *Multiple Sclerosis* **13**, (2007).
11. Zwibel, H. L. Contribution of impaired mobility and general symptoms to the burden of multiple sclerosis. *Advances in Therapy* vol. 26 Preprint at https://doi.org/10.1007/s12325-009-0082-x (2009).
12. Coleman, C. I., Sidovar, M. F., Roberts, M. S. & Kohn, C. Impact of Mobility Impairment on Indirect Costs and Health-Related Quality of Life in Multiple Sclerosis. *PLoS One* **8**, (2013).
13. Sutliff, M. H. Contribution of impaired mobility to patient burden in multiple sclerosis. *Current Medical Research and Opinion* vol. 26 Preprint at https://doi.org/10.1185/03007990903433528 (2010).
14. van Emmerik, R. E. A., Jones, S. L., Busa, M. A., Remelius, J. G. & Averill, J. L. Enhancing postural stability and adaptability in multiple sclerosis. *Adv Exp Med Biol* **826**, (2015).
15. Fling, B. W., Dutta, G. G., Schlueter, H., Cameron, M. H. & Horak, F. B. Associations between proprioceptive neural pathway structural connectivity and balance in people with multiple sclerosis. *Front Hum Neurosci* **8**, (2014).

16. Richmond, S. B., Whittier, T. T., Peterson, D. S. & Fling, B. W. Advanced characterization of static postural control dysfunction in persons with multiple sclerosis and associated neural mechanisms. *Gait Posture* **83**, (2021).
17. Šoda, J., Pavelin, S., Vujović, I. & Rogić Vidaković, M. Assessment of Motor Evoked Potentials in Multiple Sclerosis. *Sensors* vol. 23 Preprint at https://doi.org/10.3390/s23010497 (2023).
18. Baird, J. F., Hubbard, E. A., Sutton, B. P. & Motl, R. W. The relationship between corticospinal tract integrity and lower-extremity strength is attenuated when controlling for age and sex in multiple sclerosis. *Brain Res* **1701**, (2018).
19. Fritz, N. E., Keller, J., Calabresi, P. A. & Zackowski, K. M. Quantitative measures of walking and strength provide insight into brain corticospinal tract pathology in multiple sclerosis. *Neuroimage Clin* **14**, 490–498 (2017).
20. Hubbard, E. A., Wetter, N. C., Sutton, B. P., Pilutti, L. A. & Motl, R. W. Diffusion tensor imaging of the corticospinal tract and walking performance in multiple sclerosis. *J Neurol Sci* **363**, 225–231 (2016).
21. Cofré Lizama, L. E. *et al.* Gait stability reflects motor tracts damage at early stages of multiple sclerosis. *Multiple Sclerosis Journal* **28**, (2022).
22. Snow, N. J., Wadden, K. P., Chaves, A. R. & Ploughman, M. Transcranial Magnetic Stimulation as a Potential Biomarker in Multiple Sclerosis: A Systematic Review with Recommendations for Future Research. *Neural Plasticity* vol. 2019 Preprint at https://doi.org/10.1155/2019/6430596 (2019).
23. Kauv, P. *et al.* The corticospinal tract in multiple sclerosis: correlation between cortical excitability and magnetic resonance imaging measures. *J Neural Transm* **132**, 265–273 (2025).
24. Strik, M. *et al.* Axonal loss in major sensorimotor tracts is associated with impaired motor performance in minimally disabled multiple sclerosis patients. *Brain Commun* **3**, (2021).
25. Spampinato, M. V. *et al.* Diffusional Kurtosis Imaging of the Corticospinal Tract in Multiple Sclerosis: Association with Neurologic Disability. *American Journal of Neuroradiology* **38**, 1494–1500 (2017).
26. Brownstone, R. M. & Chopek, J. W. Reticulospinal systems for tuning motor commands. *Frontiers in Neural Circuits* vol. 12 Preprint at https://doi.org/10.3389/fncir.2018.00030 (2018).
27. Baker, S. N. The primate reticulospinal tract, hand function and functional recovery. *Journal of Physiology* vol. 589 Preprint at https://doi.org/10.1113/jphysiol.2011.215160 (2011).
28. Takakusaki, K., Takahashi, M., Obara, K. & Chiba, R. Neural substrates involved in the control of posture. *Advanced Robotics* **31**, (2017).
29. Takakusaki, K. Functional Neuroanatomy for Posture and Gait Control. *J Mov Disord* **10**, (2017).
30. Matsuyama, K. *et al.* Locomotor role of the corticoreticular-reticulospinal-spinal interneuronal system. *Prog Brain Res* **143**, (2004).
31. Takakusaki, K., Chiba, R., Nozu, T. & Okumura, T. Brainstem control of locomotion and muscle tone with special reference to the role of the mesopontine tegmentum and

medullary reticulospinal systems. *Journal of Neural Transmission* vol. 123 Preprint at https://doi.org/10.1007/s00702-015-1475-4 (2016).
32. Glover, I. S. & Baker, S. N. Both Corticospinal and Reticulospinal Tracts Control Force of Contraction. *Journal of Neuroscience* **42**, (2022).
33. MacKinnon, C. D. Sensorimotor anatomy of gait, balance, and falls. in *Handbook of Clinical Neurology* vol. 159 (2018).
34. Prentice, S. D. & Drew, T. Contributions of the reticulospinal system to the postural adjustments occurring during voluntary gait modifications. *J Neurophysiol* **85**, (2001).
35. Edgley, S. A., Jankowska, E. & Hammar, I. Ipsilateral actions of feline corticospinal tract neurons on limb motoneurons. *Journal of Neuroscience* **24**, (2004).
36. Peterson, B. W. Reticulospinal projections to spinal motor nuclei. *Annual review of physiology* vol. 41 Preprint at https://doi.org/10.1146/annurev.ph.41.030179.001015 (1979).
37. Shapovalov, A. I. Evolution of neuronal systems of suprasegmental motor control. *Neurophysiology* **4**, 346–359 (1973).
38. Lawrence, D. G. & Kuypers, H. G. J. M. The functional organization of the motor system in the monkey: I. The effects of bilateral pyramidal lesions. *Brain* **91**, (1968).
39. Lawrence, D. G. & Kuypers, H. G. J. M. The functional organization of the motor system in the monkey: II. The effects of lesions of the descending brain-stem pathways. *Brain* **91**, (1968).
40. Takakusaki, K. Neurophysiology of gait: From the spinal cord to the frontal lobe. *Movement Disorders* vol. 28 Preprint at https://doi.org/10.1002/mds.25669 (2013).
41. Akalu, Y. *et al.* Identifying the role of the reticulospinal tract for strength and motor recovery: A scoping review of nonhuman and human studies. *Physiological Reports* vol. 11 Preprint at https://doi.org/10.14814/phy2.15765 (2023).
42. Baker, S. N. & Perez, M. A. Reticulospinal contributions to gross hand function after human spinal cord injury. *Journal of Neuroscience* **37**, (2017).
43. Zaaimi, B., Edgley, S. A., Soteropoulos, D. S. & Baker, S. N. Changes in descending motor pathway connectivity after corticospinal tract lesion in macaque monkey. *Brain* **135**, (2012).
44. Paul, T. *et al.* The role of corticospinal and extrapyramidal pathways in motor impairment after stroke. *Brain Commun* **5**, (2023).
45. McPherson, J. G. *et al.* Progressive recruitment of contralesional cortico-reticulospinal pathways drives motor impairment post stroke. *Journal of Physiology* **596**, (2018).
46. Jang, S. H. *et al.* Functional role of the corticoreticular pathway in chronic stroke patients. *Stroke* **44**, (2013).
47. Jang, S. H. & Lee, S. J. Corticoreticular Tract in the Human Brain: A Mini Review. *Frontiers in Neurology* vol. 10 Preprint at https://doi.org/10.3389/fneur.2019.01188 (2019).
48. Yeo, S. S., Jang, S. H., Park, G. Y. & Oh, S. Effects of injuries to descending motor pathways on restoration of gait in patients with pontine hemorrhage. *Journal of Stroke and Cerebrovascular Diseases* **29**, (2020).

49. Jang, S. H. & Lee, H. Do. Gait recovery by activation of the unaffected corticoreticulospinal tract in a stroke patient: A case report. *Medicine (United States)* **96**, (2017).
50. Jang, S. H. & Kwon, H. G. Delayed gait recovery with recovery of an injured corticoreticulospinal tract in a chronic hemiparetic patient: A case report. *Medicine (United States)* **95**, (2016).
51. Jang, S. H. & Seo, J. P. The distribution of the cortical origin of the corticoreticular pathway in the human brain: A diffusion tensor imaging study. *Somatosens Mot Res* **31**, (2014).
52. Yeo, S. S., Chang, M. C., Kwon, Y. H., Jung, Y. J. & Jang, S. H. Corticoreticular pathway in the human brain: Diffusion tensor tractography study. *Neurosci Lett* **508**, (2012).
53. Boyne, P., Awosika, O. O. & Luo, Y. Mapping the corticoreticular pathway from cortex-wide anterograde axonal tracing in the mouse. *J Neurosci Res* **99**, (2021).
54. Crémers, J., D'Ostilio, K., Stamatakis, J., Delvaux, V. & Garraux, G. Brain activation pattern related to gait disturbances in Parkinson's disease. *Movement Disorders* **27**, (2012).
55. Boyne, P. *et al.* Functional magnetic resonance brain imaging of imagined walking to study locomotor function after stroke. *Clinical Neurophysiology* **132**, (2021).
56. Tian, Q. *et al.* The brain map of gait variability in aging, cognitive impairment and dementia—A systematic review. *Neuroscience and Biobehavioral Reviews* vol. 74 Preprint at https://doi.org/10.1016/j.neubiorev.2017.01.020 (2017).
57. Boyne, P., DiFrancesco, M., Awosika, O. O., Williamson, B. & Vannest, J. Mapping the human corticoreticular pathway with multimodal delineation of the gigantocellular reticular nucleus and high-resolution diffusion tractography. *J Neurol Sci* **434**, (2022).
58. Farquharson, S. *et al.* White matter fiber tractography: Why we need to move beyond DTI. *J Neurosurg* **118**, (2013).
59. Tournier, J. D., Calamante, F. & Connelly, A. MRtrix: Diffusion tractography in crossing fiber regions. *Int J Imaging Syst Technol* **22**, (2012).
60. Dhollander, T. *et al.* Fixel-based Analysis of Diffusion MRI: Methods, Applications, Challenges and Opportunities. *NeuroImage* vol. 241 Preprint at https://doi.org/10.1016/j.neuroimage.2021.118417 (2021).
61. Li, Y. *et al.* Fixel-based analysis reveals fiber-specific alterations during the progression of Parkinson's disease. *Neuroimage Clin* **27**, (2020).
62. Wei, Y.-C. *et al.* White matter alterations and their associations with biomarkers and behavior in subjective cognitive decline individuals: a fixel-based analysis. *Behavioral and Brain Functions* **20**, 12 (2024).
63. Kurtzke, J. F. Rating neurologic impairment in multiple sclerosis: An expanded disability status scale (EDSS). *Neurology* **33**, (1983).
64. Bowen, J., Gibbons, L., Gianas, A. & Kraft, G. H. Self-administered expanded disability status scale with functional system scores correlates well with a physician-administered test. *Multiple Sclerosis* **7**, (2001).

65. Franchignoni, F., Horak, F., Godi, M., Nardone, A. & Giordano, A. Using psychometric techniques to improve the Balance Evaluation Systems Test: the mini-BESTest. *J Rehabil Med* **42**, 323–331 (2010).
66. Wrisley, D. M. & Whitney, S. L. The Effect of Foot Position on the Modified Clinical Test of Sensory Interaction and Balance. *Arch Phys Med Rehabil* **85**, (2004).
67. Cohen, H., Blatchly, C. A., Gombash, L. L. & Di Fabio, R. P. A study of the Clinical Test of Sensory Interaction and Balance. *Phys Ther* **73**, (1993).
68. Palmieri, R. M., Ingersoll, C. D., Stone, M. B. & Krause, B. A. Center-of-pressure parameters used in the assessment of postural control. *Journal of Sport Rehabilitation* vol. 11 Preprint at https://doi.org/10.1123/jsr.11.1.51 (2002).
69. Laurie King, M. M. Mobility Lab to Assess Balance and Gait with Synchronized Body-worn Sensors. *Journal of Bioengineering and Biomedical Sciences* (2013) doi:10.4172/2155-9538.s1-007.
70. Spain, R. I. *et al.* Body-worn motion sensors detect balance and gait deficits in people with multiple sclerosis who have normal walking speed. *Gait Posture* **35**, (2012).
71. Potter, K. *et al.* Reliability, validity, and responsiveness of the mini-balance evaluation systems test in ambulatory individuals with multiple sclerosis. *Physiotherapy Canada* **71**, (2019).
72. Sebastião, E., Sandroff, B. M., Learmonth, Y. C. & Motl, R. W. Validity of the Timed Up and Go Test as a Measure of Functional Mobility in Persons with Multiple Sclerosis. *Arch Phys Med Rehabil* **97**, (2016).
73. Ramari, C., Hvid, L. G., David, A. C. de & Dalgas, U. The importance of lower-extremity muscle strength for lower-limb functional capacity in multiple sclerosis: Systematic review. *Annals of Physical and Rehabilitation Medicine* vol. 63 Preprint at https://doi.org/10.1016/j.rehab.2019.11.005 (2020).
74. Richardson, S. The Timed "Up & Go": A Test of Basic Functional Mobility for Frail Elderly Persons. *J Am Geriatr Soc* **39**, (1991).
75. Hobart, J. C., Riazi, A., Lamping, D. L., Fitzpatrick, R. & Thompson, A. J. Measuring the impact of MS on walking ability: The 12-item MS Walking Scale (MSWS-12). *Neurology* **60**, (2003).
76. Abate, C., Gromisch, E. S., Campo, M., Ruiz, J. A. & DelMastro, H. M. Predicting faller status in persons with multiple sclerosis using the Multiple Sclerosis Walking Scale-12. *Mult Scler Relat Disord* **92**, 105924 (2024).
77. Tournier, J. D. *et al.* MRtrix3: A fast, flexible and open software framework for medical image processing and visualisation. *NeuroImage* vol. 202 Preprint at https://doi.org/10.1016/j.neuroimage.2019.116137 (2019).
78. Veraart, J., Fieremans, E. & Novikov, D. S. Diffusion MRI noise mapping using random matrix theory. *Magn Reson Med* **76**, (2016).
79. Veraart, J. *et al.* Denoising of diffusion MRI using random matrix theory. *Neuroimage* **142**, (2016).
80. Kellner, E., Dhital, B., Kiselev, V. G. & Reisert, M. Gibbs-ringing artifact removal based on local subvoxel-shifts. *Magn Reson Med* **76**, (2016).

81. Andersson, J. L. R. & Sotiropoulos, S. N. An integrated approach to correction for off-resonance effects and subject movement in diffusion MR imaging. *Neuroimage* **125**, (2016).
82. Tustison, N. J. *et al.* N4ITK: Improved N3 bias correction. *IEEE Trans Med Imaging* **29**, (2010).
83. Dhollander, T., Mito, R., Raffelt, D. & Connelly, A. Improved white matter response function estimation for 3-tissue constrained spherical deconvolution. *Proc. Intl. Soc. Mag. Reson. Med* (2019).
84. Jeurissen, B., Tournier, J. D., Dhollander, T., Connelly, A. & Sijbers, J. Multi-tissue constrained spherical deconvolution for improved analysis of multi-shell diffusion MRI data. *Neuroimage* **103**, (2014).
85. Raffelt, D. *et al.* Apparent Fibre Density: A novel measure for the analysis of diffusion-weighted magnetic resonance images. *Neuroimage* **59**, (2012).
86. Raffelt, D. *et al.* Bias field correction and intensity normalisation for quantitative analysis of apparent fibre density. *Proceedings of International Society of Magnetic Resonance in Medicine* **Vol. 25**, 3541 (2017).
87. Dhollander, T. *et al.* Multi-tissue log-domain intensity and inhomogeneity normalization for quantitative apparent fibre density. *29th Proceedings of International Society of Magnetic Resonance in Medicine* 2472 (2021).
88. Raffelt, D. *et al.* Symmetric diffeomorphic registration of fibre orientation distributions. *Neuroimage* **56**, (2011).
89. Raffelt, D. A. *et al.* Investigating white matter fibre density and morphology using fixel-based analysis. *Neuroimage* **144**, (2017).
90. Torvik, A. & Brodal, A. The origin of reticulospinal fibers in the cat. An experimental study. *Anat Rec* **128**, (1957).
91. Smith, R. E., Tournier, J. D., Calamante, F. & Connelly, A. SIFT2: Enabling dense quantitative assessment of brain white matter connectivity using streamlines tractography. *Neuroimage* **119**, (2015).
92. Fischl, B. FreeSurfer. *NeuroImage* vol. 62 Preprint at https://doi.org/10.1016/j.neuroimage.2012.01.021 (2012).
93. Wiltgen, T. *et al.* LST-AI: A deep learning ensemble for accurate MS lesion segmentation. *Neuroimage Clin* **42**, (2024).
94. Raffelt, D. A. *et al.* Connectivity-based fixel enhancement: Whole-brain statistical analysis of diffusion MRI measures in the presence of crossing fibres. *Neuroimage* **117**, (2015).
95. Smith, R. E., Dhollander, T. & Connelly, A. On the regression of intracranial volume in Fixel-Based Analysis. in *International Society of Magnetic Resonance in Medicine* (2019).
96. Wuensch, K. L. & Evans, J. D. Straightforward Statistics for the Behavioral Sciences. *J Am Stat Assoc* **91**, (1996).
97. Fjeldstad, C., Pardo, G., Bemben, D. & Bemben, M. Decreased postural balance in multiple sclerosis patients with low disability. *International Journal of Rehabilitation Research* **34**, (2011).

98. Galea, M. P., Cofré Lizama, L. E., Butzkueven, H. & Kilpatrick, T. J. Gait and balance deterioration over a 12-month period in multiple sclerosis patients with EDSS scores ≤ 3.0. *NeuroRehabilitation* **40**, (2017).
99. Nilsagård, Y., Lundholm, C., Denison, E. & Gunnarsson, L. G. Predicting accidental falls in people with multiple sclerosis - A longitudinal study. *Clin Rehabil* **23**, (2009).
100. Rougier, P. *et al.* How proprioceptive impairments affect quiet standing in patients with multiple sclerosis. *Somatosens Mot Res* **24**, (2007).
101. Peterson, D. S. & Fling, B. W. How changes in brain activity and connectivity are associated with motor performance in people with MS. *NeuroImage: Clinical* vol. 17 Preprint at https://doi.org/10.1016/j.nicl.2017.09.019 (2018).
102. Kanekar, N. & Aruin, A. S. The Role of Clinical and Instrumented Outcome Measures in Balance Control of Individuals with Multiple Sclerosis. *Mult Scler Int* **2013**, (2013).
103. Goble, D. J. & Baweja, H. S. Normative data for the BTrackS balance test of Postural Sway: Results from 16,357 community- dwelling individuals who were 5 to 100 years old. *Phys Ther* **98**, (2018).
104. Özden, F., Özkeskin, M., Tümtürk, İ. & Yüceyar, N. Comparison of physical performance, gait, balance, falls efficacy, and step reaction time in individuals with multiple sclerosis. *Clin Neurol Neurosurg* **232**, (2023).
105. Allali, G. *et al.* Adapted timed up and go: A rapid clinical test to assess gait and cognition in multiple sclerosis. *Eur Neurol* **67**, (2012).
106. Remelius, J. G. *et al.* Gait impairments in persons with multiple sclerosis across preferred and fixed walking speeds. *Arch Phys Med Rehabil* **93**, (2012).
107. Goldman, M. D. *et al.* Identification and validation of clinically meaningful benchmarks in the 12-item Multiple Sclerosis Walking Scale. *Multiple Sclerosis* **23**, (2017).
108. Gajamange, S. *et al.* Fibre-specific white matter changes in multiple sclerosis patients with optic neuritis. *Neuroimage Clin* **17**, (2018).
109. Carandini, T. *et al.* Disruption of brainstem monoaminergic fibre tracts in multiple sclerosis as a putative mechanism for cognitive fatigue: a fixel-based analysis. *Neuroimage Clin* **30**, (2021).
110. Storelli, L., Pagani, E., Preziosa, P., Filippi, M. & Rocca, M. A. Measurement of white matter fiber-bundle cross-section in multiple sclerosis using diffusion-weighted imaging. *Multiple Sclerosis Journal* **27**, (2021).
111. Darling, W. G. *et al.* Hand motor recovery following extensive frontoparietal cortical injury is accompanied by upregulated corticoreticular projections in monkey. *Journal of Neuroscience* **38**, (2018).
112. Ishida, A. *et al.* Dynamic Interaction between Cortico-Brainstem Pathways during Training-Induced Recovery in Stroke Model Rats. *Journal of Neuroscience* **39**, (2019).
113. Nonnekes, J. *et al.* Startreact restores reaction time in HSP: Evidence for subcortical release of a motor program. *Journal of Neuroscience* **34**, (2014).
114. Stapley, P. J. & Drew, T. The pontomedullary reticular formation contributes to the compensatory postural responses observed following removal of the support surface in the standing cat. *J Neurophysiol* **101**, (2009).

115. Carlsen, A. N. & Maslovat, D. Startle and the StartReact Effect: Physiological Mechanisms. *Journal of Clinical Neurophysiology* vol. 36 Preprint at https://doi.org/10.1097/WNP.0000000000000582 (2019).
116. Peterson, D. S., Gera, G., Horak, F. B. & Fling, B. W. Supraspinal control of automatic postural responses in people with multiple sclerosis. *Gait Posture* **47**, (2016).
117. McVea, D. A. & Pearson, K. G. Object avoidance during locomotion. *Adv Exp Med Biol* **629**, (2009).
118. Morton, S. M. & Bastian, A. J. Cerebellar control of balance and locomotion. *Neuroscientist* vol. 10 Preprint at https://doi.org/10.1177/1073858404263517 (2004).
119. Yang, F. & Liu, X. Relative importance of vision and proprioception in maintaining standing balance in people with multiple sclerosis. *Mult Scler Relat Disord* **39**, (2020).
120. Van Emmerik, R. E. A., Remelius, J. G., Johnson, M. B., Chung, L. H. & Kent-Braun, J. A. Postural control in women with multiple sclerosis: Effects of task, vision and symptomatic fatigue. *Gait Posture* **32**, (2010).
121. Cattaneo, D. & Jonsdottir, J. Sensory impairments in quiet standing in subjects with multiple sclerosis. *Multiple Sclerosis* **15**, (2009).
122. Jang, S. H., Kim, T. H., Kwon, Y. H., Lee, M. Y. & Lee, H. Do. Postural instability in patients with injury of corticoreticular pathway following mild traumatic brain injury. *Am J Phys Med Rehabil* **95**, (2016).
123. Lee, S., Kim, E. Y. & Shin, C. Longitudinal association between brain volume change and gait speed in a general population. *Exp Gerontol* **118**, (2019).
124. Duclos, N. C., Maynard, L., Abbas, D. & Mesure, S. Hemispheric specificity for proprioception: Postural control of standing following right or left hemisphere damage during ankle tendon vibration. *Brain Res* **1625**, (2015).
125. Pérennou, D. *et al.* Postural balance following stroke: Towards a disadvantage of the right- brain-damaged hemisphere. *Rev Neurol (Paris)* **155**, (1999).
126. Andrade, S. M. & Fernández-Calvo, B. Static and dynamic impairment following stroke reflecting hemispheric asymmetry for postural control. *Acta Scientiarum - Health Sciences* **37**, (2015).
127. Yogev-Seligmann, G., Hausdorff, J. M. & Giladi, N. The role of executive function and attention in gait. *Movement Disorders* vol. 23 Preprint at https://doi.org/10.1002/mds.21720 (2008).
128. Takakusaki, K. Gait control by the frontal lobe. in *Handbook of Clinical Neurology* vol. 195 (2023).
129. Kreisel, S. H. *et al.* Deterioration of gait and balance over time: The effects of age-related white matter change - The LADIS study. *Cerebrovascular Diseases* **35**, (2013).
130. Sullivan, E. V., Rose, J., Rohlfing, T. & Pfefferbaum, A. Postural sway reduction in aging men and women: Relation to brain structure, cognitive status, and stabilizing factors. *Neurobiol Aging* **30**, (2009).
131. Moscufo, N. *et al.* Longitudinal microstructural changes of cerebral white matter and their association with mobility performance in older persons. *PLoS One* **13**, (2018).
132. Baezner, H. *et al.* Association of gait and balance disorders with age-related white matter changes: The LADIS Study. *Neurology* **70**, (2008).

133. Carroll, T. J., Riek, S. & Carson, R. G. Neural adaptations to resistance training: Implications for movement control. *Sports Medicine* vol. 31 Preprint at https://doi.org/10.2165/00007256-200131120-00001 (2001).
134. Bandy, W. D., Lovelace-Chandler, V. & McKitrick-Bandy, B. Adaptation of Skeletal Muscle to Resistance Training. *Journal of Orthopaedic & Sports Physical Therapy* **12**, 248–255 (1990).
135. Macaluso, A. & De Vito, G. Muscle strength, power and adaptations to resistance training in older people. *European Journal of Applied Physiology* vol. 91 Preprint at https://doi.org/10.1007/s00421-003-0991-3 (2004).
136. Weier, A. T., Pearce, A. J. & Kidgell, D. J. Strength training reduces intracortical inhibition. *Acta Physiologica* **206**, (2012).
137. Škarabot, J., Brownstein, C. G., Casolo, A., Del Vecchio, A. & Ansdell, P. The knowns and unknowns of neural adaptations to resistance training. *European Journal of Applied Physiology* vol. 121 Preprint at https://doi.org/10.1007/s00421-020-04567-3 (2021).
138. Glover, I. S. & Baker, S. N. Cortical, corticospinal, and reticulospinal contributions to strength training. *Journal of Neuroscience* **40**, (2020).
139. Taga, M. *et al.* Corticospinal and corticoreticulospinal projections have discrete but complementary roles in chronic motor behaviors after stroke. *J Neurophysiol* **132**, 1917–1936 (2024).
140. Kjølhede, T., Vissing, K. & Dalgas, U. Multiple sclerosis and progressive resistance training: A systematic review. *Multiple Sclerosis Journal* vol. 18 Preprint at https://doi.org/10.1177/1352458512437418 (2012).
141. Dalgas, U. *et al.* Resistance training improves muscle strength and functional capacity in multiple sclerosis. *Neurology* **73**, 1478–1484 (2009).
142. Genc, S. *et al.* Impact of b-value on estimates of apparent fibre density. *Hum Brain Mapp* **41**, (2020).
143. Calamuneri, A. *et al.* White matter tissue quantification at Low b-values within constrained spherical deconvolution framework. *Front Neurol* **9**, (2018).
144. Marrie, R. A. *et al.* Sex differences in comorbidity at diagnosis of multiple sclerosis. *Neurology* **86**, 1279–1286 (2016).

CHAPTER 6 – COMPREHENSIVE DISCUSSION, CLINICAL APPLICATIONS, AND FUTURE DIRECTIONS

Movement is a defining output of the nervous system, shaped by the continuous interplay between sensory input, neural processing, and motor execution. The brain, spinal cord, and peripheral nerves work in concert to interpret the surrounding world and transform intention into action. In multiple sclerosis (MS), an abnormal immune response causes neural injury throughout the central nervous system (CNS), interrupting these essential processes.[1,2] As a result, individuals with MS commonly experience muscle weakness, balance impairments, and limited mobility, which contribute to increased fall risk and fear of falling.[3–5] These consequences, in turn, can lead to reduced independence and diminished quality of life. [6–10] Addressing these challenges requires a clearer understanding of how MS-related neural damage alters the motor system. Such insight can support the identification of specific neural targets for assessment, monitoring, and rehabilitation.

The work presented in this dissertation pursued four central research questions:

1. How do individuals with MS perform functional transfer movements differently than their neurotypical (NT) peers?
2. What neurophysiological features are associated with these movement differences?
3. How do advanced neuroimaging measures of CNS structural integrity correspond with neurophysiological and clinical outcomes in individuals with MS?
4. Does the microstructural integrity of the corticoreticulospinal tract relate to balance and mobility function in people with MS?

Together, these questions investigate the relationship between structural and functional neural integrity and movement behavior in individuals with MS. Through a multi-modal framework that incorporates biomechanical, neurophysiological, and neuroimaging methods, this work provides insights into the neural correlates of motor impairment. The findings contribute incrementally to both scientific understanding and the refinement of clinical tools aimed at evaluating, monitoring, and addressing mobility limitations in people with MS.

Summary of Doctoral Work

Since Jean-Martin Charcot first connected sclerotic plaques in the brain to patient symptoms in 1868,[11] the structural properties of the CNS have remained a central focus of research in MS. Chapter 1 of this dissertation reviews the neuroimaging methods commonly used to characterize CNS pathology in MS, highlighting both their strengths and limitations. The chapter discusses conventional magnetic resonance imaging (MRI) techniques, such as T1- and T2-weighted imaging, which remain essential for detecting macroscopic lesions and quantifying lesion burden and brain atrophy.[12,13] The chapter also introduces advanced structural imaging methods, including diffusion tensor imaging (DTI), diffusion kurtosis imaging (DKI), and fixel-based analysis (FBA), which provide more detailed insights into white matter integrity.[14–16] These techniques are further explored in Chapters 4 and 5. Altogether, advanced structural imaging techniques hold significant promise for improving the characterization of the extent and nature of CNS damage in MS. Furthermore, ongoing advances in imaging resolution, particularly with ultra-high-field MRI, have the potential to enhance detection of neural damage, especially cortical lesions, which remain under-detected with current conventional approaches.[17,18]

Chapter 2 investigated how individuals with MS perform functional movements differently from NT controls by analyzing biomechanical measures acquired during the five times sit-to-stand

test (5XSST), a common clinical assessment of transfer ability.[19] While falls are common in transfer movements, such as the sit-to-stand,[20] few studies in MS have examined the 5XSST beyond time-based metrics.[21] This gap is notable, as prior research in older adults has demonstrated that kinetic variables, particularly lower-limb power, are more strongly associated with fall risk than task duration.[22] The results of the study indicated that individuals with MS completed the 5XSST task more slowly and with reduced force and power output compared to NT controls. Notably, lower-limb power distinguished participants with MS with a history of falls from those without, whereas time alone did not. These findings suggest that kinetic measures, such as power, may capture more nuanced aspects of motor impairment that contribute to fall risk.

Given that MS leads to neural injury within the CNS, Chapter 3 aimed to build on the findings of Chapter 2 by examining the neurophysiological correlates of altered motor function. Using transcranial magnetic stimulation (TMS), the study found that individuals with MS exhibited reduced corticospinal tract (CST) excitability, reduced intracortical inhibition, and prolonged conduction times compared to NT participants. Further, these neurophysiological measures were associated with both force production and development during isolated tibialis anterior maximal voluntary isometric contractions and the 5XSST in participants with MS. Together, the results link the biomechanical findings of Chapter 2 to differences in neurophysiology, demonstrating that motor performance during transfer tasks, such as the 5XSST, are associated with the functional status of the corticospinal system in individuals with MS.

While TMS provides valuable insight into the functional integrity of motor pathways, it does not capture spatial measures of neural architecture. Structural alterations in white matter can be examined using a variety of advanced neuroimaging techniques (Chapter 1). However, no prior study had applied multiple diffusion MRI methods in combination to assess structural integrity in

MS and explore their relationships with both clinical and neurophysiological outcomes. Chapter 4 addressed this gap by examining DTI, DKI, and FBA metrics within the CST of individuals with MS and NT controls. The results revealed reductions in structural integrity throughout the CST in individuals with MS compared to NT controls. Among the three approaches, FBA displayed the strongest correlations with clinical balance performance, disability scores, and neurophysiological measures. These findings suggest that FBA's capacity to isolate specific fiber populations and independently quantify micro- and macrostructural properties offers more detailed characterization of clinically relevant features of MS pathology.[23] Together, the findings from this study provide a structural complement to the physiological and behavioral differences observed in earlier chapters, further supporting the link between white matter structural integrity, neurophysiological function, and motor performance in individuals with MS.

Chapter 5 extended the scope of this dissertation beyond the CST, which had been the primary focus of prior chapters and much of the existing literature linking neural characteristics to motor function in individuals with MS. While the CST is essential for voluntary movement, other descending motor pathways, such as the reticulospinal tract, have been connected to balance and locomotion.[24,25] Research in stroke and spinal cord injury has highlighted the potential compensatory role of this pathway for motor recovery following CST injury,[26–28] yet its contribution to motor function in MS has not been previously investigated. To explore this understudied pathway, FBA was used to assess the microstructural integrity of the corticoreticulospinal tract, revealing that reduced microstructural integrity correlates with walking and balance performance in individuals.

Clinical Applications

One practical application that emerges across the chapters of this dissertation is strength training, commonly implemented through resistance training. A robust body of evidence demonstrates that resistance training enhances muscle strength and functional capacity across a range of populations, including individuals with MS.[29–32] This is particularly meaningful in the context of Chapter 2, which identified reduced power during sit-to-stand movements as a key identifier of fall risk. Given that lower body strength is critical for generating power during transfers, resistance training offers a practical strategy to mitigate fall risk.

Notably, the benefits of resistance training may extend beyond the musculoskeletal system. While findings are mixed, studies suggest that resistance training can induce neurophysiological changes, including reductions in CST inhibition, increases in CST excitability, and alterations in motor unit properties.[33–35] These adaptations are directly relevant to the findings in Chapter 3, where neurophysiological measures, such as CST excitability, were associated with motor performance. If neurophysiological function is modifiable through resistance training, it may offer a potential avenue for enhancing neuromuscular function.

Finally, emerging evidence suggests that improvements in muscle strength and function resulting from resistance training may, in part, be mediated by adaptations within the reticulospinal system.[36] In Chapter 5, lower fiber density in the corticoreticulospinal tract was associated with poorer balance and walking performance in individuals with MS. If resistance training can drive adaptations in this pathway, it may offer a promising avenue for enhancing motor function by strengthening the neural circuits that contribute to postural control and mobility.

Together, these connections support the hypothesis that resistance training may elicit functionally meaningful neuromuscular adaptations in people with MS. Future research should

further investigate both the muscular and neural effects of resistance training in MS to better determine its impact as a physical conditioning strategy and as a potential neurotherapeutic intervention.

Future Directions

Future research should investigate the potential of ultra-high-field MRI (7T and beyond) to improve the detection of diffuse neural damage in MS. The improved spatial resolution afforded by higher field strengths may enable more accurate identification of subtle and previously underdetected abnormalities, particularly cortical lesions, which are often missed with conventional imaging techniques.[17,18] More accurate detection of neural injury could support earlier diagnosis and strengthen associations with clinical outcomes.

Building on the transfer movement analyses in Chapters 2 and 3, future studies should continue to investigate the biomechanics of other everyday functional tasks such as stair climbing, turning, non-linear walking, and extended reaching. These weight-shifting movements may reveal additional body control strategies employed by individuals with MS not captured by the 5XSST or basic linear walking. Moreover, developing better predictive models of lower-limb power output using accessible clinical data, such as 5XSST duration and anthropometric measures, could provide clinicians with a simple and low-burden tool for accurately identifying fall risk in individuals with MS.

To build on the neurophysiological findings from this dissertation, future research should incorporate TMS during active motor tasks to assess CST function in movement-relevant contexts. Comparing responses between individuals with MS and NT controls during task execution could reveal functional differences that are not captured by baseline measures, offering insight into how CST function dynamically contributes to task performance.[37] Additionally, investigating the

distinct neural contributions to concentric and eccentric muscle contractions, particularly during full-body movements, may uncover different motor control strategies in people with MS compared to NT controls. Longitudinal studies involving resistance training or neuromodulation interventions (e.g., transcranial direct current stimulation)[38] are also warranted to determine the extent to which neurophysiological adaptations can contribute to neuromuscular function improvements.

Future neuroimaging studies should integrate both brain and spinal cord imaging to fully capture the distributed nature of motor pathway damage in MS. Additionally, research should leverage biologically informed advanced diffusion techniques such as Neurite Orientation Dispersion and Density Imaging (NODDI).[39] NODDI can provide accurate measures of structural integrity in both white and gray matter, offering a more comprehensive quantification of the extent of neural damage and its relationship to motor function.

Finally, the reticulospinal system remains an understudied yet likely contributor to motor function in individuals with MS. Future research should directly assess reticulospinal function using methods such as TMS ipsilateral motor evoked potentials[40] or the StartReact paradigm,[41] which can provide insight into the functional status of this pathway. Interventional studies investigating how the reticulospinal system responds to resistance training could clarify its role as a compensatory pathway for improved mobility in individuals with MS.

Concluding Remarks

Together, the studies in this dissertation provide a multi-modal perspective on how alterations to the nervous system in MS relate to motor function. The findings not only link structural and functional markers of CNS integrity to clinically relevant outcomes but also point to future directions for research and rehabilitation. In doing so, this dissertation contributes to a

growing body of work aimed at translating biomechanic and neuroscience research into practical strategies for improving the lives of people with MS.

References

1. Compston, A. & Coles, A. Multiple sclerosis. *The Lancet* 372, 1502–1517 (2008).
2. Lassmann, H. Multiple Sclerosis Pathology. *Cold Spring Harb Perspect Med* 8, a028936 (2018).
3. Hoang, P. D., Gandevia, S. C. & Herbert, R. D. Prevalence of joint contractures and muscle weakness in people with multiple sclerosis. *Disability and Rehabilitation* vol. 36 Preprint at https://doi.org/10.3109/09638288.2013.854841 (2014).
4. Joy, J. E. & Johnston Jr, R. B. Characteristics and management of major symptoms. in *Multiple Sclerosis: Current Status and Strategies for the Future* 115–75 (National Academies Press, 2001).
5. Kister, I. *et al.* Natural History of Multiple Sclerosis Symptoms. *Int J MS Care* 15, 146–156 (2013).
6. Peterson, E. W., Cho, C. C. & Finlayson, M. L. Fear of falling and associated activity curtailment among middle aged and older adults with multiple sclerosis. *Multiple Sclerosis* 13, (2007).
7. Peterson, E. W., Cho, C. C., von Koch, L. & Finlayson, M. L. Injurious Falls Among Middle Aged and Older Adults With Multiple Sclerosis. *Arch Phys Med Rehabil* 89, (2008).
8. Coleman, C. I., Sidovar, M. F., Roberts, M. S. & Kohn, C. Impact of Mobility Impairment on Indirect Costs and Health-Related Quality of Life in Multiple Sclerosis. *PLoS One* 8, (2013).
9. Sutliff, M. H. Contribution of impaired mobility to patient burden in multiple sclerosis. *Current Medical Research and Opinion* vol. 26 Preprint at https://doi.org/10.1185/03007990903433528 (2010).
10. Zwibel, H. L. Contribution of impaired mobility and general symptoms to the burden of multiple sclerosis. *Advances in Therapy* vol. 26 Preprint at https://doi.org/10.1007/s12325-009-0082-x (2009).
11. Lublin, F. History of modern multiple sclerosis therapy. in *Journal of Neurology* vol. 252 (2005).
12. Barkhof, F. & Koeller, K. K. Demyelinating Diseases of the CNS (Brain and Spine). in 165–176 (2020). doi:10.1007/978-3-030-38490-6_13.
13. Matthews, P. M. *et al.* A practical review of the neuropathology and neuroimaging of multiple sclerosis. *Practical Neurology* vol. 16 Preprint at https://doi.org/10.1136/practneurol-2016-001381 (2016).
14. Tournier, J. D. *et al.* MRtrix3: A fast, flexible and open software framework for medical image processing and visualisation. *NeuroImage* vol. 202 Preprint at https://doi.org/10.1016/j.neuroimage.2019.116137 (2019).
15. Zhuo, J. & Gullapalli, R. P. Diffusion Kurtosis Imaging. in *Neuroimaging Techniques in Clinical Practice* 215–228 (Springer International Publishing, Cham, 2020). doi:10.1007/978-3-030-48419-4_15.
16. Le Bihan, D. *et al.* Diffusion tensor imaging: Concepts and applications. *Journal of Magnetic Resonance Imaging* 13, (2001).
17. Kilsdonk, I. D. *et al.* Increased cortical grey matter lesion detection in multiple sclerosis with 7 T MRI: A post-mortem verification study. *Brain* 139, (2016).

18. De Graaf, W. L. *et al.* Clinical application of multi-contrast 7-T MR imaging in multiple sclerosis: Increased lesion detection compared to 3 T confined to grey matter. *Eur Radiol* 23, (2013).
19. Møller, A. B. *et al.* Validity and variability of the 5-repetition sit-to-stand test in patients with multiple sclerosis. *Disabil Rehabil* 34, 2251–2258 (2012).
20. Robinovitch, S. N. *et al.* Video capture of the circumstances of falls in elderly people residing in long-term care: An observational study. *The Lancet* 381, (2013).
21. Bowser, B., O'Rourke, S., Brown, C. N., White, L. & Simpson, K. J. Sit-to-stand biomechanics of individuals with multiple sclerosis. *Clinical Biomechanics* 30, (2015).
22. Cheng, Y. Y. *et al.* Can sit-to-stand lower limb muscle power predict fall status? *Gait Posture* 40, (2014).
23. Dhollander, T. *et al.* Fixel-based Analysis of Diffusion MRI: Methods, Applications, Challenges and Opportunities. *NeuroImage* vol. 241 Preprint at https://doi.org/10.1016/j.neuroimage.2021.118417 (2021).
24. Lawrence, D. G. & Kuypers, H. G. J. M. The functional organization of the motor system in the monkey: II. The effects of lesions of the descending brain-stem pathways. *Brain* 91, (1968).
25. Lawrence, D. G. & Kuypers, H. G. J. M. The functional organization of the motor system in the monkey: I. The effects of bilateral pyramidal lesions. *Brain* 91, (1968).
26. Baker, S. N. The primate reticulospinal tract, hand function and functional recovery. *Journal of Physiology* vol. 589 Preprint at https://doi.org/10.1113/jphysiol.2011.215160 (2011).
27. Baker, S. N. & Perez, M. A. Reticulospinal contributions to gross hand function after human spinal cord injury. *Journal of Neuroscience* 37, (2017).
28. Akalu, Y. *et al.* Identifying the role of the reticulospinal tract for strength and motor recovery: A scoping review of nonhuman and human studies. *Physiological Reports* vol. 11 Preprint at https://doi.org/10.14814/phy2.15765 (2023).
29. Hunter, G. R., McCarthy, J. P. & Bamman, M. M. Effects of resistance training on older adults. *Sports Medicine* vol. 34 Preprint at https://doi.org/10.2165/00007256-200434050-00005 (2004).
30. Brienesse, L. A. & Emerson, M. N. Effects of Resistance Training for People With Parkinson's Disease: A Systematic Review. *Journal of the American Medical Directors Association* vol. 14 Preprint at https://doi.org/10.1016/j.jamda.2012.11.012 (2013).
31. Kjølhede, T., Vissing, K. & Dalgas, U. Multiple sclerosis and progressive resistance training: A systematic review. *Multiple Sclerosis Journal* vol. 18 Preprint at https://doi.org/10.1177/1352458512437418 (2012).
32. Dalgas, U. *et al.* Resistance training improves muscle strength and functional capacity in multiple sclerosis. *Neurology* 73, 1478–1484 (2009).
33. Weier, A. T., Pearce, A. J. & Kidgell, D. J. Strength training reduces intracortical inhibition. *Acta Physiologica* 206, (2012).
34. Kidgell, D. J., Bonanno, D. R., Frazer, A. K., Howatson, G. & Pearce, A. J. Corticospinal responses following strength training: a systematic review and meta-analysis. *European Journal of Neuroscience* vol. 46 Preprint at https://doi.org/10.1111/ejn.13710 (2017).
35. Tallent, J., Goodall, S., Gibbon, K. C., Hortobágyi, T. & Howatson, G. Enhanced corticospinal excitability and volitional drive in response to shortening and lengthening strength training and changes following detraining. *Front Physiol* 8, (2017).

36. Atkinson, E. *et al.* Does the reticulospinal tract mediate adaptation to resistance training in humans? *Journal of Applied Physiology* vol. 133 Preprint at https://doi.org/10.1152/japplphysiol.00264.2021 (2022).
37. Duchateau, J. & Baudry, S. Insights into the neural control of eccentric contractions. *Journal of Applied Physiology* vol. 116 Preprint at https://doi.org/10.1152/japplphysiol.00002.2013 (2014).
38. Hendy, A. M. & Kidgell, D. J. Anodal-tDCS applied during unilateral strength training increases strength and corticospinal excitability in the untrained homologous muscle. *Exp Brain Res* 232, (2014).
39. Zhang, H., Schneider, T., Wheeler-Kingshott, C. A. & Alexander, D. C. NODDI: Practical in vivo neurite orientation dispersion and density imaging of the human brain. *Neuroimage* 61, (2012).
40. Maitland, S. & Baker, S. N. Ipsilateral Motor Evoked Potentials as a Measure of the Reticulospinal Tract in Age-Related Strength Changes. *Front Aging Neurosci* 13, (2021).
41. Tapia, J. A., Tohyama, T., Poll, A. & Baker, S. N. The Existence of the StartReact Effect Implies Reticulospinal, Not Corticospinal, Inputs Dominate Drive to Motoneurons during Voluntary Movement. *Journal of Neuroscience* 42, (2022).

APPENDIX A – CHAPTER 2 SUPPLEMENTAL MATERIAL

Chapter 2 of this dissertation examined the associations between instrumented mean power and estimated mean power values using equations from Alcazar et al. (2018) during the five times sit-to-stand (5XSST). This included the original equation (Equation 2.1, Figure A1A) and a modified version in which height was replaced by leg length (Equation 2.2, Figure A1B). Additional analyses evaluated correlations between instrumented mean power and an estimated mean power equation from Smith et al. (2010) (Figure A1C), as well as between instrumented maximum power and an estimated maximum power equation from Smith et al. (2010) (Figure A1D). Several 5XSST metrics were compared between participants with MS who reported a fall in the six months prior to the study and those who did not. Select comparisons are presented in Chapter 2, with a complete table of all exploratory comparisons provided in Table A1.

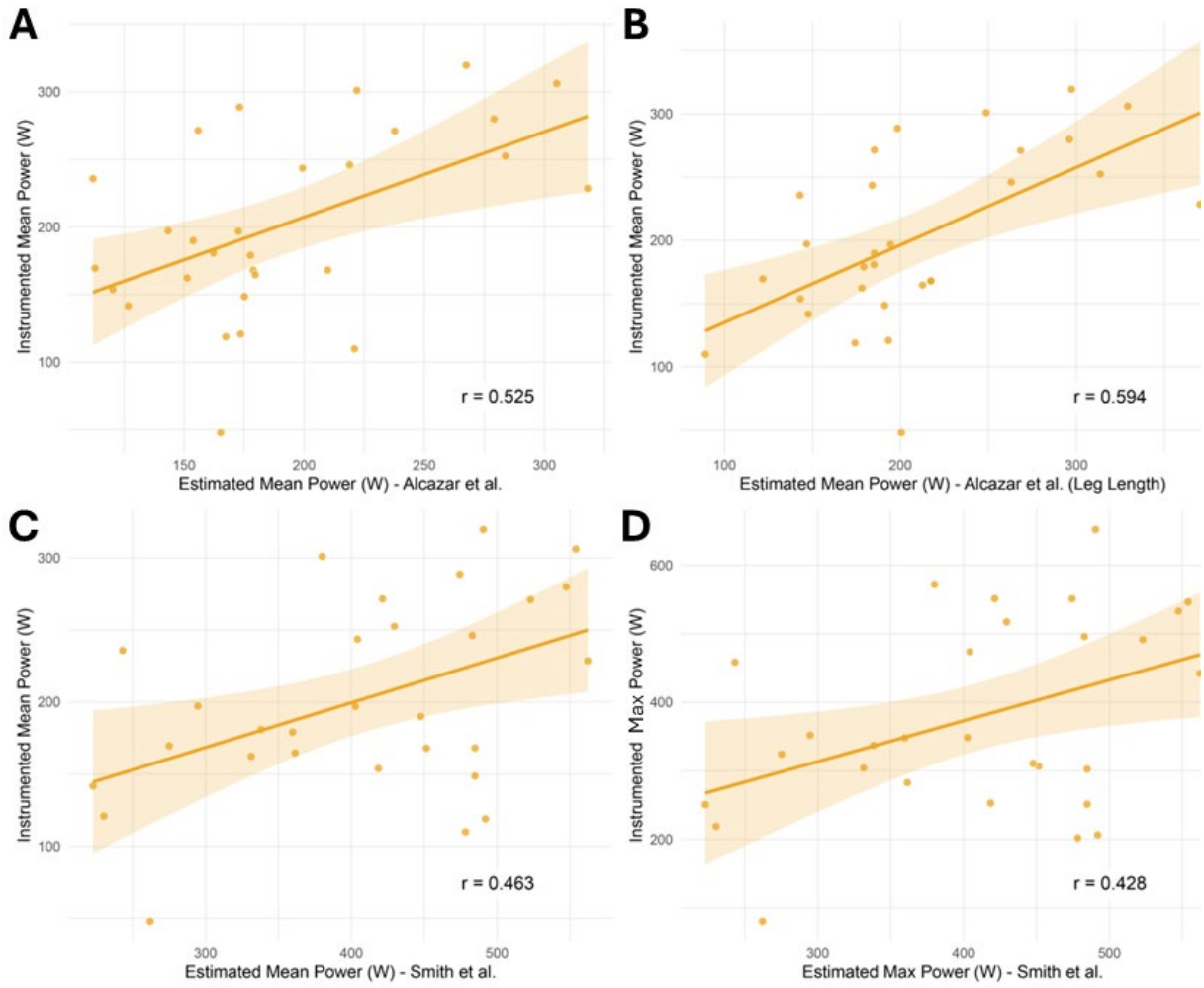

Figure A1. Correlations Between Instrumented Power and Estimated Power in People with MS. (A) Association between Equation 1 and instrumented mean power ($r = 0.525$, $p = 0.003$), (B) Association between Equation 2 and instrumented mean power ($r = 0.594$, $p < 0.001$), (C) Association between Smith et al. 2010 mean power equation and instrumented mean power ($r = 0.463$, $p = 0.011$), (D) Association between Smith et al. 2010 max power equation and instrumented max power ($r = 0.423$, $p = 0.021$).

Table A1. Comparison of 5XSST performance time, force production, and power outputs between the MS faller and MS non-faller groups.

Variable	Multiple Sclerosis - Fallers		Multiple Sclerosis - Non-Fallers		*Uncorrected p-value*	Cohen's *d*
	Mean	*SD*	*Mean*	*SD*		
Completion Time (s)	14.32	6.65	12.94	7.44	0.097	0.39
Max vGRF (%BW)	128.07	10.87	130.90	26.48	0.212	-0.28
Incline (%BW/s)	602.44	151.16	786.60	295.60	0.018	-0.72
Peak-to-Trough (%BW)	60.95	32.16	67.55	54.30	0.209	-0.30
Mean Power (W)	167.78	130.03	220.23	126.22	0.026	-0.82
Max Power (W)	315.72	275.13	410.75	267.06	0.046	-0.70
Estimated Mean Power (W) – Alcazar et al.	173.57	69.21	201.51	126.72	0.068	-0.55
Estimated Mean Power (W) – Alcazar et al. (Leg Length)	179.97	100.99	224.88	136.23	0.028	-0.75

APPENDIX B – CHAPTER 3 SUPPLEMENTAL MATERIAL

Chapter 3 of this dissertation reports that electromyography (EMG) data collected during the study exhibited powerline contamination, characterized by 60 Hz harmonics, in several participant recordings. To address this issue, a 60 Hz wavelet packet harmonic filter was applied to all participant data in addition to standard bandpass filtering. Wavelet packet filtering works by decomposing the underlying signal into components at multiple frequency bands, enabling targeted removal of specific noise, such as 60 Hz powerline interference. This technique helps suppress noise while preserving the other frequencies of the EMG signal critical for analysis. The following supplementary materials provide validation for this filtering approach, including:

- A power spectrum frequency plot from an example participant with powerline interference (Figure B1) and from one without powerline interference (Figure B4).
- EMG traces showing raw signals and signals after applying the wavelet packet harmonic filter combined with bandpass filtering, for both participants (Figures B2 and B5).
- For reference, EMG traces comparing raw signal to the results of a standard 60 Hz comb filter, a filter commonly used to reduce powerline noise, are shown in Figures B3 and B6.

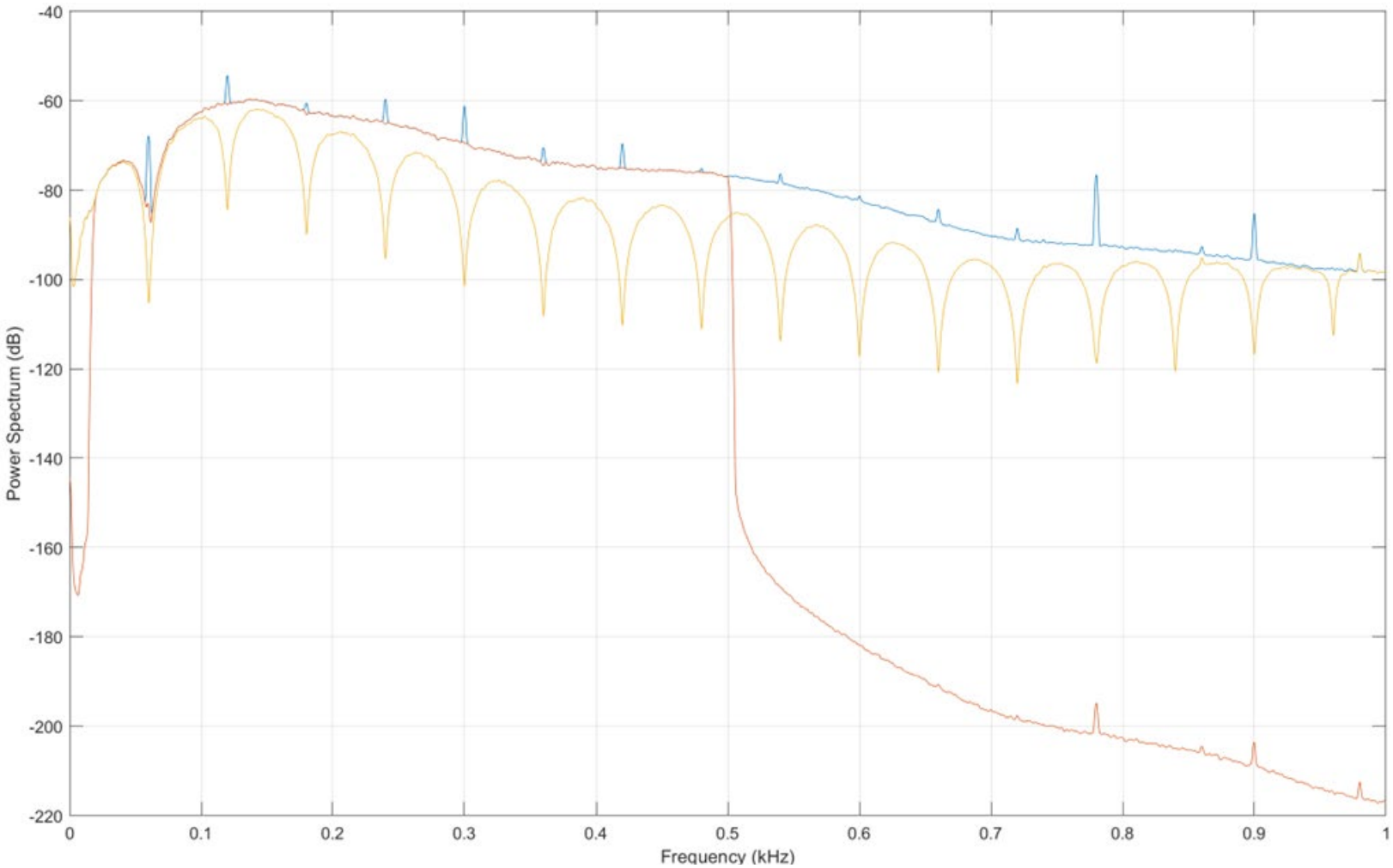

Figure B1. Power Spectrum Plot from a Participant With 60 Hz Interference. Power spectrum frequency plot from an example participant exhibiting 60 Hz powerline interference. The blue line represents the raw EMG signal, with interference visible as distinct power spikes at 60 Hz and its harmonics. The orange line shows the EMG signal after wavelet packet filtering combined with bandpass filtering, and the yellow line shows the signal after applying a 60 Hz comb filter. Both filters reduce interference, but the comb filter may excessively attenuate power at target and non-target frequencies. In contrast, the wavelet packet harmonic filter preserves more of the signal while effectively reducing interference.

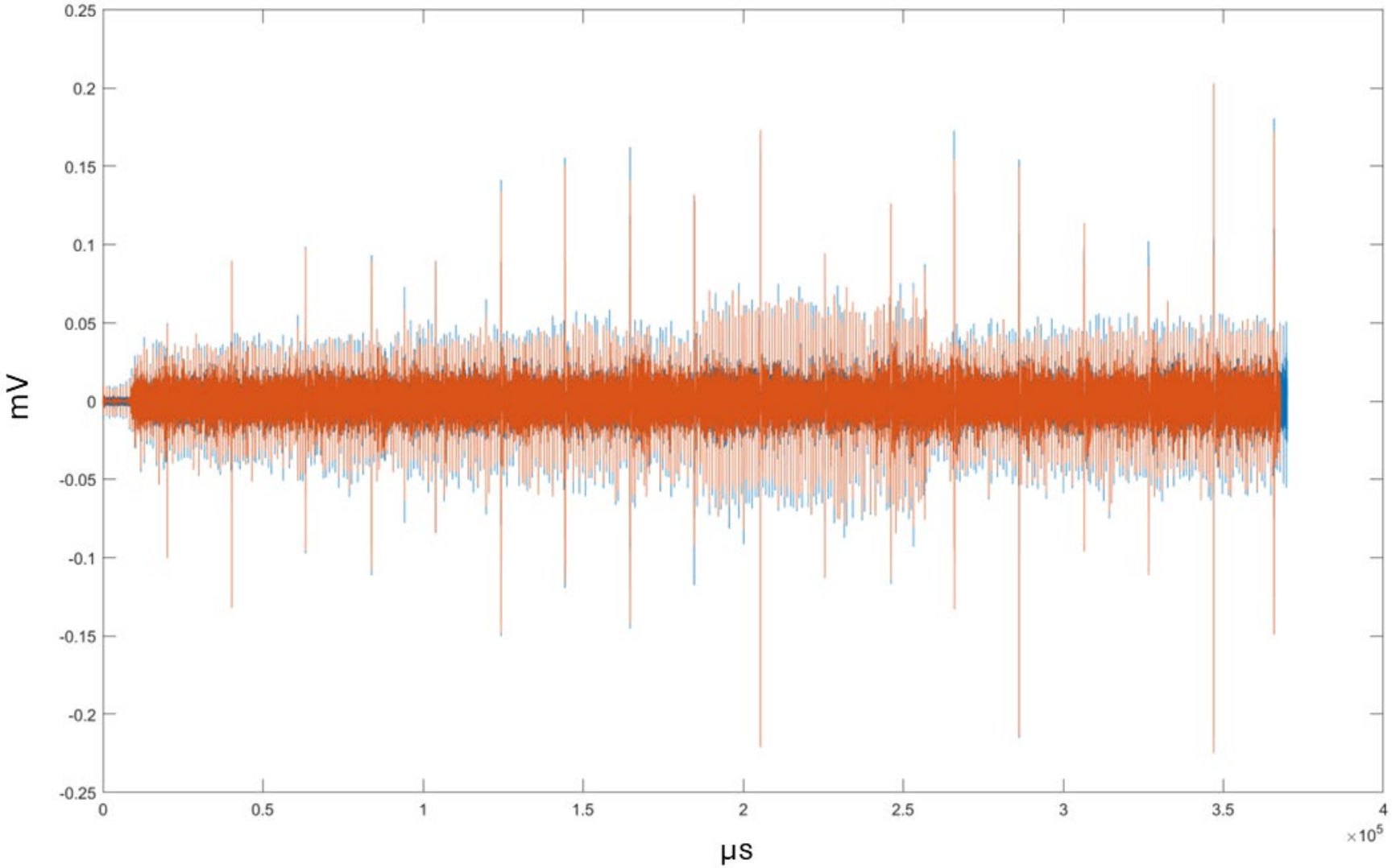

Figure B2. Wavelet Packet Harmonic Filtering of 60 Hz Interference. EMG trace from a TMS trial in an example participant with 60 Hz powerline interference. The blue line represents the raw EMG signal, while the orange line shows the signal after applying the wavelet packet harmonic filter combined with bandpass filtering.

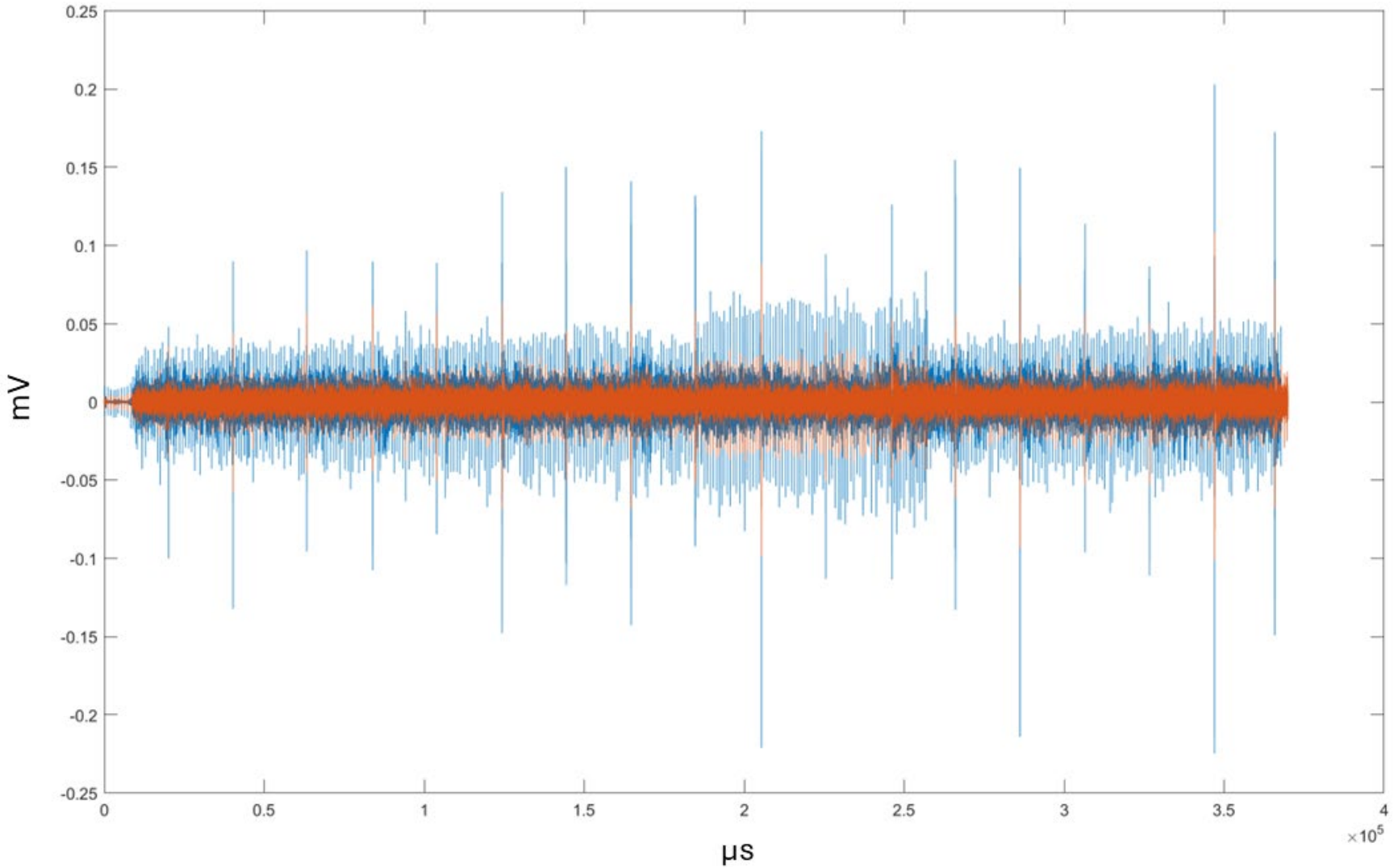

Figure B3. Comb Filtering of 60 Hz Interference. EMG trace from a TMS trial in an example participant with 60 Hz powerline interference. The blue line represents the raw EMG signal, while the orange line shows the signal after applying the 60 Hz comb filter.

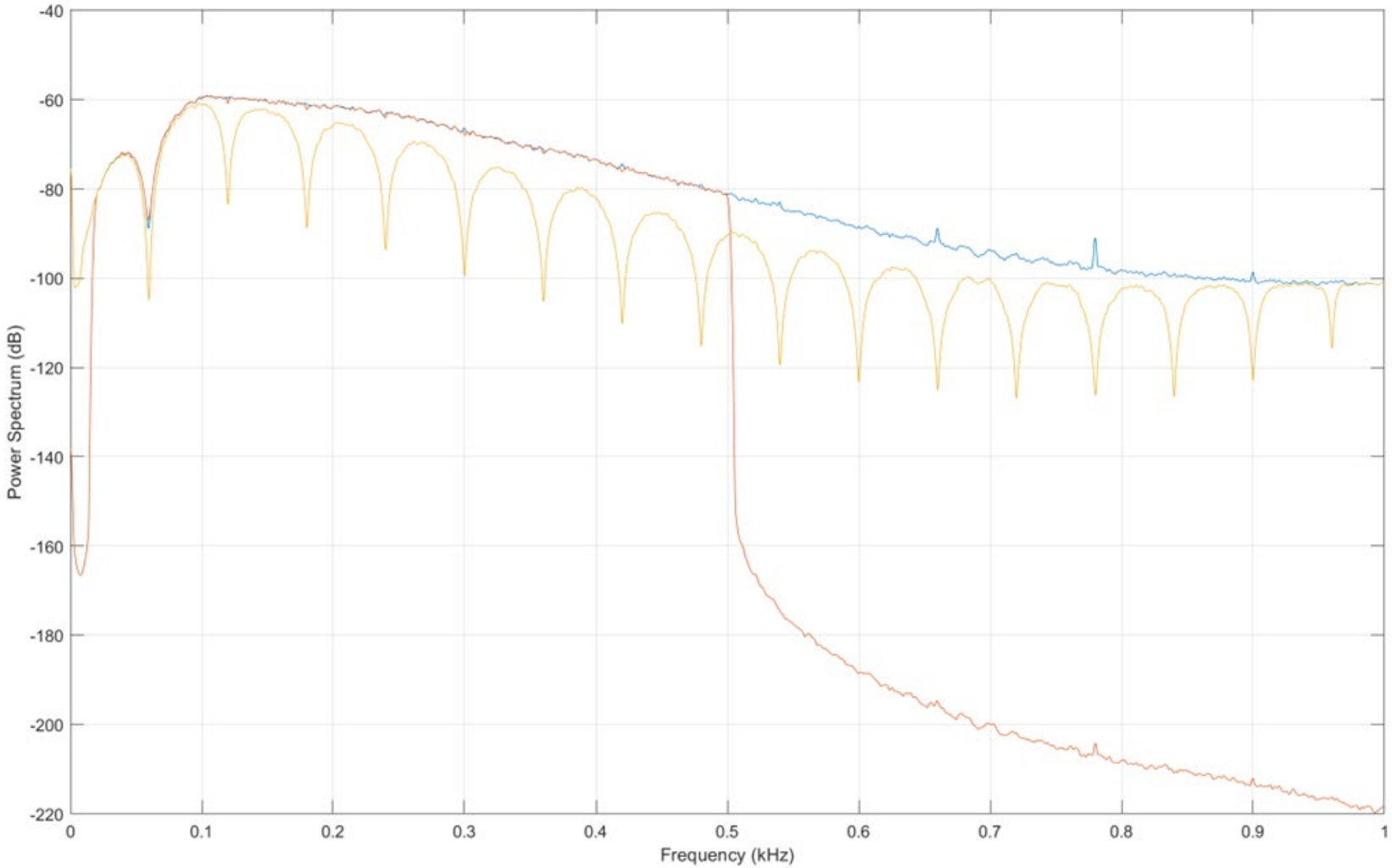

Figure B4. Power Spectrum Plot from a Participant Without 60 Hz Interference. Power spectrum frequency plot from an example participant without 60 Hz powerline interference. The blue line represents the raw EMG signal, with no visible interference at 60 Hz or its harmonics. The orange line shows the EMG signal after wavelet packet filtering combined with bandpass filtering, while the yellow line shows the signal after applying a 60 Hz comb filter. Compared to the comb filter, the wavelet packet harmonic filter more effectively preserves overall signal power and avoids unnecessary attenuation of the signal.

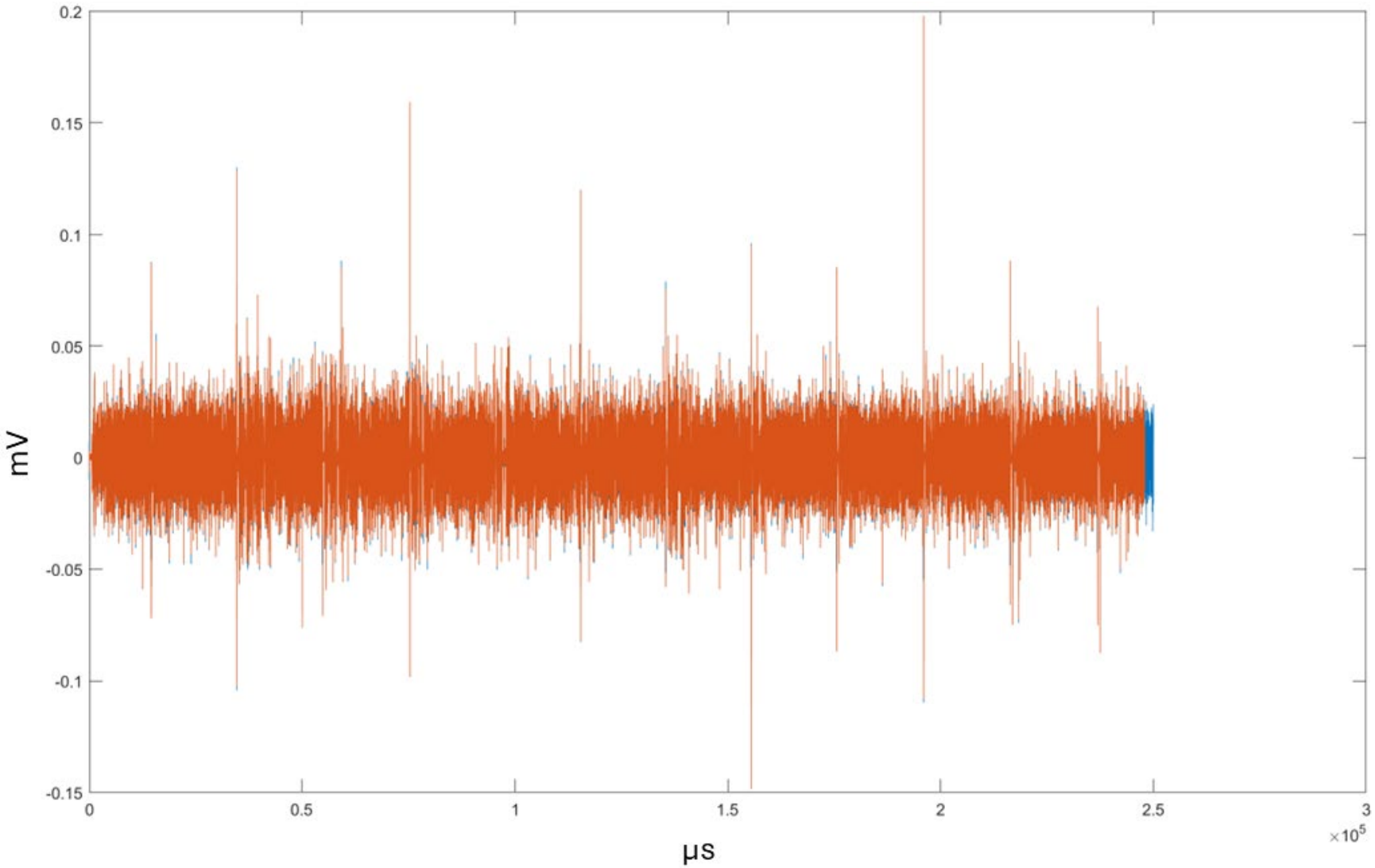

Figure B5. Wavelet Packet Harmonic Filtering Without Interference. EMG trace from a TMS trial in an example participant without 60 Hz powerline interference. The blue line represents the raw EMG signal, while the orange line shows the signal after applying the wavelet packet harmonic filter combined with bandpass filtering.

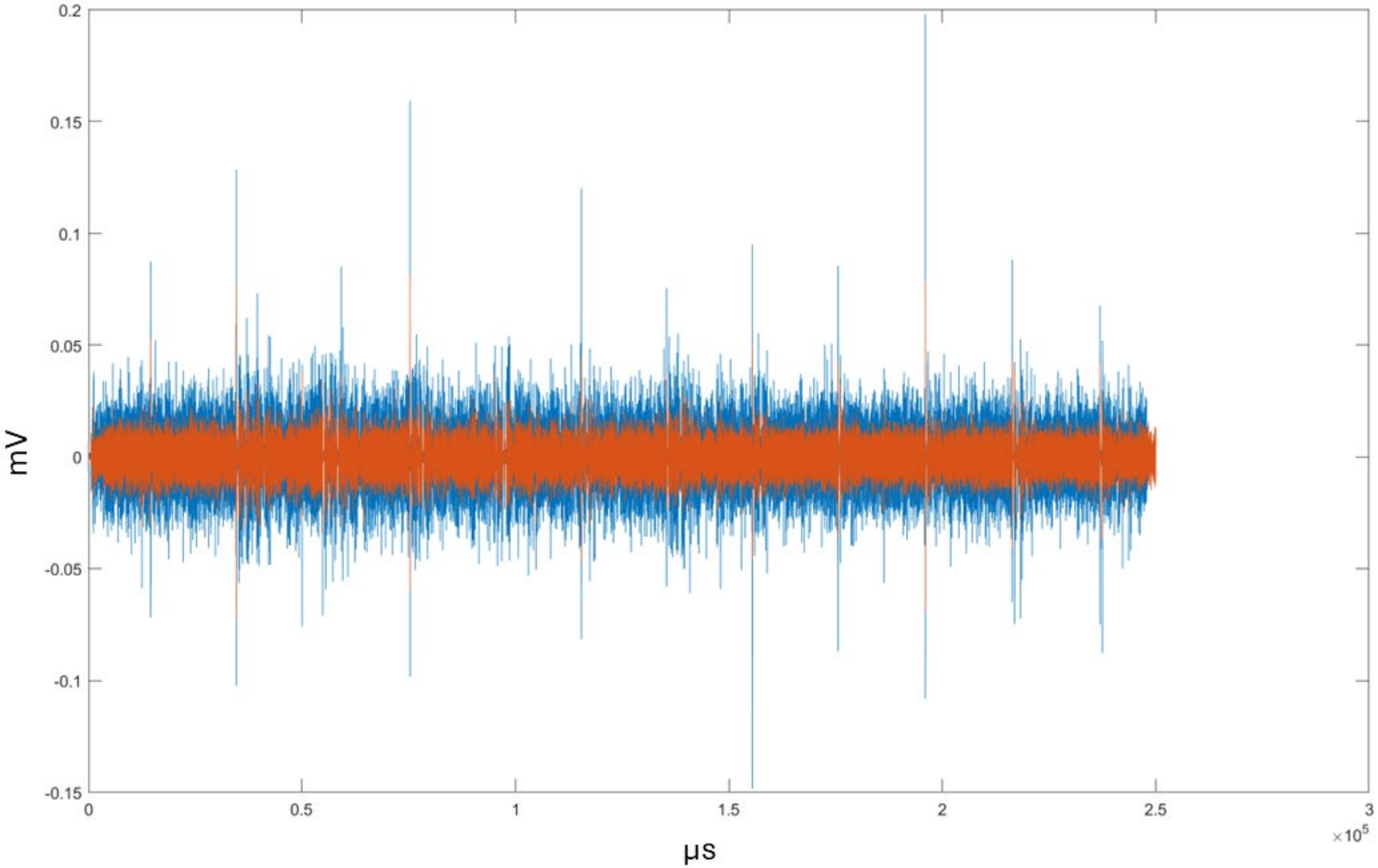

Figure B6. Comb Filtering Without Interference. EMG trace from a TMS trial in an example participant without 60 Hz powerline interference. The blue line represents the raw EMG signal, while the orange line shows the signal after applying the 60 Hz comb filter.

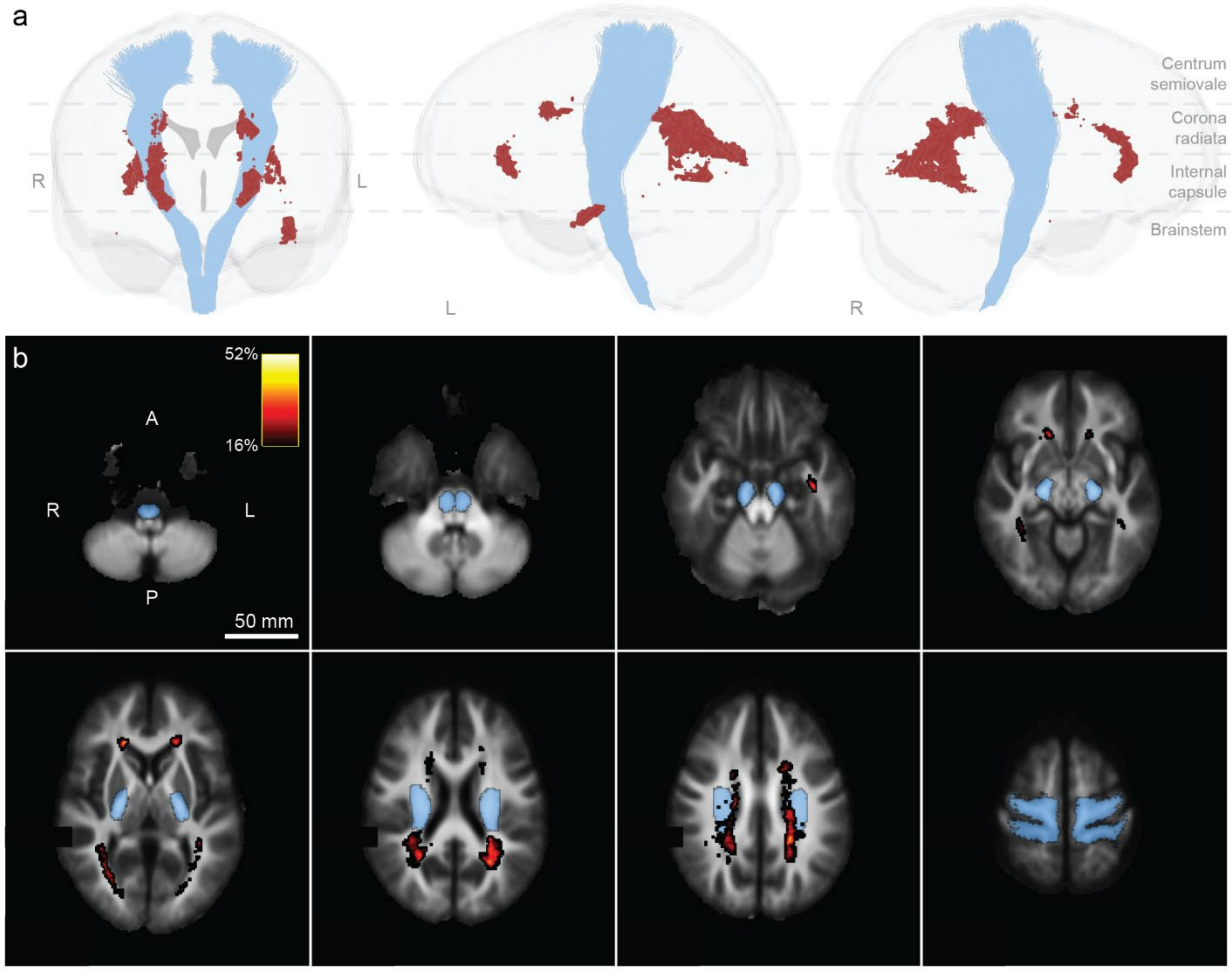

Figure C1. Lesion Probability Map for Participants with Multiple Sclerosis. Spatial distribution of lesion overlap across participants with multiple sclerosis (MS), with the corticospinal tracts (CST) visualized in blue for reference. Lesions are shown where at least 4 participants (16%) had overlapping damage. a) Volume rendering of segmented lesions from anterior, left, and right viewpoints. b) Lesion probability map overlaid on axial slices of the template brain. Slices progress inferior to superior, starting in the medulla (top left) and ascending through the brainstem and cerebrum, ending with streamlines in the precentral and postcentral gyri (bottom right). CST location is again shown in blue. The color bar indicates the percentage of overlapping segmented lesions. No region exhibited greater than 52% lesion overlap (13 participants).

Table C1. Associations Between Diffusion Metrics and Lesion Volume in the Corticospinal Tract in Participants with Multiple Sclerosis. Spearman's rank correlation coefficients (*rho*) are reported for associations between diffusion magnetic resonance imaging metrics and segmented lesion volume within the corticospinal tract (CST) in participants with multiple sclerosis (MS). Both uncorrected *p-values* and false discovery rate (FDR)-corrected values are provided. Statistically significant associations after FDR correction (*pFDR* < 0.05) are indicated in **bold**.

Abbreviations: DTI – Diffusion Tensor Imaging; MD – Mean Diffusivity; AD – Axial Diffusivity; RD – Radial Diffusivity; FA – Fractional Anisotropy; DKI – Diffusion Kurtosis Imaging; MK – Mean Kurtosis; AK – Axial Kurtosis; RK – Radial Kurtosis; FBA – Fixel-Based Analysis; FDC – Fiber Density and Cross-section; FD – Fiber Density; LFC – Log of Fiber Cross-section; CST – Corticospinal Tract.

	DTI				DKI			FBA		
Variable	*MD*	*AD*	*RD*	*FA*	*MK*	*AK*	*RK*	*FDC*	*FD*	*LFC*
CST Lesion Volume										
rho	0.81	0.277	0.82	-0.75	-0.79	-0.66	0.78	-0.54	-0.57	-0.48
p-value	<0.001	0.179	<0.001	<0.001	<0.001	<0.001	<0.001	0.006	0.003	0.016
pFDR-value	**<0.001**	0.179	**<0.001**	**<0.001**	**<0.001**	**<0.001**	**<0.001**	**0.007**	**0.004**	**0.017**

Table C2. Associations Between Balance and Clinical Disability Scores and Neurophysiologic Measures in Participants with Multiple Sclerosis. Spearman's rank correlation coefficients (*rho*) are reported for associations between the mini-balance evaluation systems test (miniBEST) total score, expanded disability status scale (EDSS), motor evoked potential (MEP) onset latency, and MEP area in participants with multiple sclerosis (MS). Both uncorrected *p-values* and false discovery rate (FDR)-corrected values are provided. Statistically significant associations after FDR correction (*pFDR* < 0.05) are indicated in **bold**.

Variable	miniBEST Total Score	*EDSS*	*MEP Onset Latency*	*MEP Area*
miniBEST Total Score				
rho	-	-	-	-
p-value	-	-	-	-
pFDR-value	-	-	-	-
EDSS				
rho	-0.61	-	-	-
p-value	0.001	-	-	-
pFDR-value	**0.002**	-	-	-
MEP Onset Latency				
rho	-0.61	0.30	-	-
p-value	0.001	0.150	-	-
pFDR-value	**0.002**	0.150	-	-
MEP Area				
rho	0.63	-0.50	-0.43	-
p-value	<0.001	0.012	0.030	-
pFDR-value	**0.002**	**0.017**	**0.036**	-

Table C3. Associations Between Full Corticospinal Tract-Averaged Diffusion Metrics and Clinical and Neurophysiologic Measures in Participants with Multiple Sclerosis. Spearman's rank correlation coefficients (*rho*) are reported for associations between diffusion magnetic resonance imaging metrics averaged across the entire corticospinal tract (CST) and clinical and neurophysiological measures in participants with MS. Both uncorrected *p-values* and false discovery rate (FDR)-corrected values are provided. Statistically significant associations after FDR correction (*pFDR* < 0.05) are indicated in **bold**.

Abbreviations: DTI – Diffusion Tensor Imaging; MD – Mean Diffusivity; AD – Axial Diffusivity; RD – Radial Diffusivity; FA – Fractional Anisotropy; DKI – Diffusion Kurtosis Imaging; MK – Mean Kurtosis; AK – Axial Kurtosis; RK – Radial Kurtosis; FBA – Fixel-Based Analysis; FDC – Fiber Density and Cross-section; FD – Fiber Density; LFC – Log of Fiber Cross-section; CST – Corticospinal Tract; miniBEST – Mini-Balance Evaluation Systems Test; EDSS – Expanded Disability Status Scale; MEP – Motor Evoked Potential.

	DTI				DKI			FBA			*CST Lesion*
Variable	*MD*	*AD*	*RD*	*FA*	*MK*	*AK*	*RK*	*FDC*	*FD*	*LFC*	*Volume*
miniBEST Total Score											
rho	-0.34	-0.33	-0.32	-0.10	0.22	0.21	0.17	0.52	0.25	0.33	-0.44
p-value	0.094	0.105	0.119	0.647	0.289	0.323	0.424	0.007	0.212	0.103	0.028
pFDR-value	0.280	0.280	0.280	0.690	0.485	0.485	0.539	**0.013**	0.231	0.154	0.065
EDSS											
rho	0.27	0.316	0.22	0.15	-0.23	-0.15	-0.14	-0.72	-0.29	-0.61	0.37
p-value	0.186	0.124	0.297	0.461	0.274	0.474	0.515	<0.001	0.162	0.001	0.065
pFDR-value	0.280	0.280	0.366	0.527	0.485	0.539	0.539	**<0.001**	0.195	**0.007**	0.075
MEP Onset Latency											
rho	0.39	0.25	0.44	-0.32	-0.47	-0.26	-0.59	-0.55	-0.55	-0.31	0.54
p-value	0.055	0.023	0.028	0.124	0.017	0.218	0.012	0.004	0.005	0.121	0.006
pFDR-value	0.280	0.304	0.280	0.280	0.099	0.485	0.099	**0.011**	**0.011**	0.162	**0.027**
MEP Area											
rho	-0.29	-0.27	-0.27	0.01	0.30	0.13	0.28	0.55	0.25	0.39	-0.40
p-value	0.155	0.192	0.192	0.978	0.114	0.539	0.170	0.004	0.233	0.06	0.049
pFDR-value	0.280	0.280	0.280	0.978	0.485	0.539	0.485	**0.011**	0.233	0.096	0.065

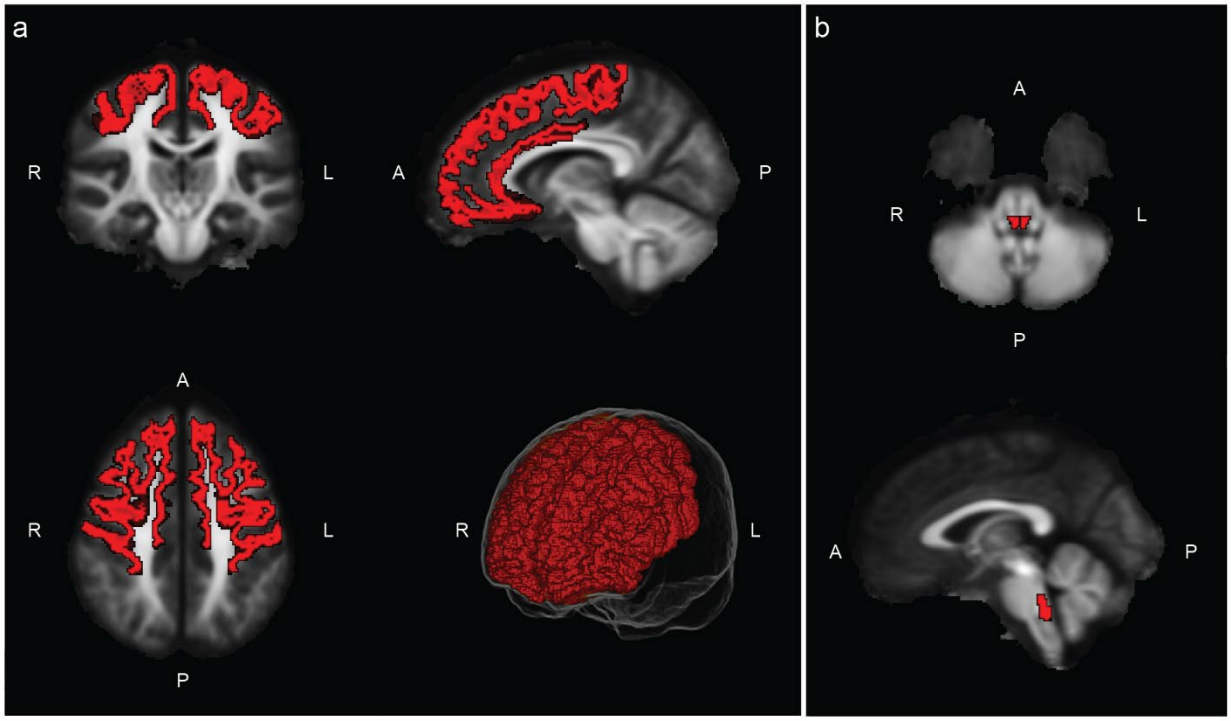

Figure D1. Corticoreticulospinal Tract Regions of Interest for Streamline Generation. Regions of interest (ROIs) used for generating streamlines of the corticoreticulospinal tract overlaid on the study template. a) Cortical ROI used as the seed region for streamline generation. Views: coronal (top left), sagittal (top right), axial (bottom left), and 3D volume rendering (bottom right). ROI sourced from Boyne et al., 2022. b) Gigantocellular reticular nucleus ROI, used as a required waypoint for CReST streamlines. Views: axial (top), sagittal (bottom). ROI sourced from Boyne et al., 2022.

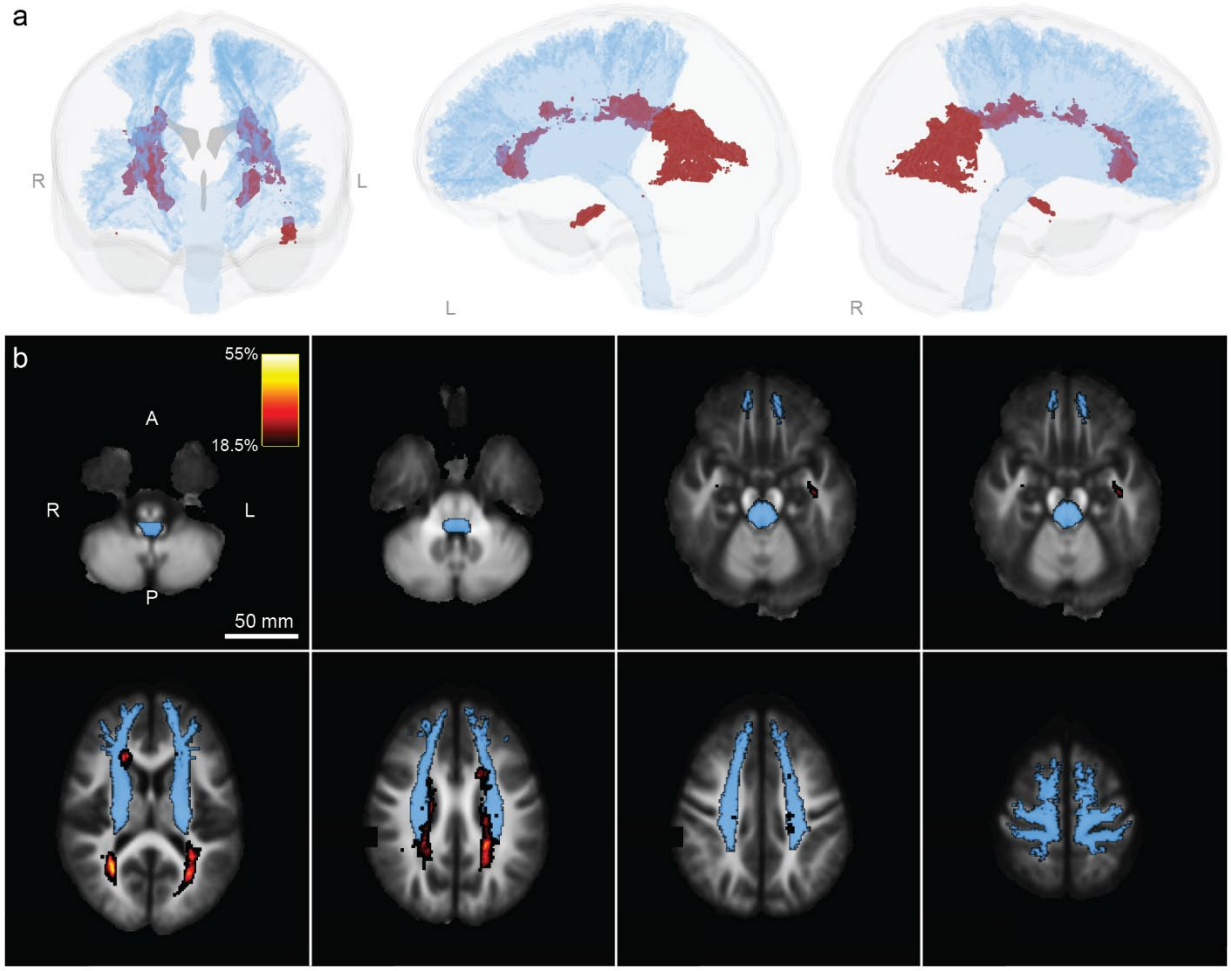

Figure D2. Lesion Probability Map for Participants with Multiple Sclerosis. Spatial distribution of lesion overlap across participants with multiple sclerosis, with the corticoreticulospinal tracts (CReST) visualized in blue for reference. Lesions are shown where at least 5 participants (18.5%) had overlapping damage. a) Volume rendering of segmented lesions from anterior, left, and right viewpoints. b) Lesion probability map overlaid on axial slices of the template brain. Slices progress inferior to superior, starting in the medulla (top left) and ascending through the brainstem and cerebrum, ending with streamlines in the cortex (bottom right). CST location is again shown in blue. The color bar indicates the percentage of overlapping segmented lesions. No region exhibited greater than 55% lesion overlap (15 participants).

Table D1. Associations Between Corticoreticulospinal Tract Fiber Density, Lesion Volume, and Functional Outcomes in People with Multiple Sclerosis. Correlations between fiber density from fixels showing significant group differences in the corticoreticulospinal tract (CReST) between participants with multiple sclerosis (MS) and neurotypical (NT) controls, and balance and mobility outcome measures in participants with MS. Correlations are also presented between lesion volume overlapping with the CReST and balance and mobility outcome measures in participants with MS. Both uncorrected *p-values* and false discovery rate (FDR)-corrected values are shown. Statistically significant associations after FDR correction (*pFDR* < 0.05) are indicated in **bold**.

Abbreviations: APC – Anticipatory Postural Adjustments; RPC – Reactive Postural Control; SO – Sensory Orientation; DG – Dynamic Gait; CoP – Center of Pressure; TUG – Timed-Up and Go; MSWS-12 – Twelve Item Multiple Sclerosis Walking Scale

	MS Fiber Density			MS CReST Lesion Volume		
Variable	*r/rho*	*p-value*	*pFDR-value*	*rho*	*p-value*	*pFDR-value*
Mini-Balance Evaluation Systems Test						
Total Score	0.52	**0.005**	**0.013**	-0.59	**0.001**	**0.003**
APA	0.44	**0.021**	**0.035**	-0.45	**0.018**	**0.018**
RPC	0.55	**0.003**	**0.013**	-0.48	**0.011**	**0.013**
SO	0.35	0.074	0.074	-0.62	**0.001**	**0.003**
DG	0.37	0.054	0.068	-0.58	**0.002**	**0.003**
Static Balance (CoP Path Length (cm))						
Eyes-open Firm	-0.45	**0.021**	**0.041**	0.57	**0.002**	**0.002**
Eyes-open Compliant	-0.41	**0.044**	**0.044**	0.60	**0.002**	**0.002**
Mobility						
Preferred Walk Speed (m/s)	0.22	0.278	0.278	-0.39	**0.045**	**0.045**
Fast Walk Speed (m/s)	0.35	0.072	0.177	-0.45	**0.020**	**0.027**
TUG (s)	-0.28	0.161	0.215	0.44	**0.020**	**0.027**
MSWS-12	-0.34	0.088	0.177	0.47	**0.016**	**0.027**